THE ANALYSIS OF ORGANIC MATTER IN OIL-SHALES

by

STEPHEN RICHARD PALMER

A THESIS SUBMITTED FOR THE DEGREE OF

DOCTOR OF PHILOSOPHY

THE UNIVERSITY OF ASTON IN BIRMINGHAM

DECEMBER 1987

The University of Aston in Birmingham.

The analysis of organic matter in oil shales.

by

Stephen Richard Palmer

A thesis submitted for the degree of
Doctor of philosophy. December 1987.

SUMMARY

The organic matter in five oil shales (three from the Kimmeridge Clay sequence, one from the Oxford Clay sequence and one from the Julia Creek deposits in Australia) has been isolated by acid demineralisation, separated into kerogens and bitumens by solvent extraction and then characterised in some detail by chromatographic, spectroscopic and degradative techniques.

Kerogens cannot be characterised as easily as bitumens because of their insolubility, and hence before any detailed molecular information can be obtained from them they must be degraded into lower molecular weight, more soluble components. Unfortunately, the determination of kerogen structures has all too often involved degradations that were far too harsh and which lead to destruction of much of the structural information. For this reason a number of milder more selective degradative procedures have been tested and used to probe the structure of kerogens. These are:

1. Lithium aluminium hydride reduction. - This procedure is commonly used to remove pyrite from kerogens and it may also increase their solubility by reduction of labile functional groups. Although reduction of the kerogens was confirmed, increases in solubility were correlated with pyrite content and not kerogen reduction.

2. O-methylation in the presence of a phase transfer catalyst. - By the removal of hydrogen bond interactions via O-methylation, it was possible to determine the contribution of such secondary interactions to the insolubility of the kerogens. Problems were encountered with the use of the phase transfer catalyst.

3. Stepwise alkaline potassium permanganate oxidation. - Significant kerogen dissolution was achieved using this procedure but uncontrolled oxidation of initial oxidation products proved to be a problem. A comparison with the peroxytrifluoroacetic acid oxidation of these kerogens was made.

4. Peroxytrifluoroacetic acid oxidation. - This was used because it preferentially degrades aromatic rings whilst leaving any benzylic positions intact. Considerable conversion of the kerogens into soluble products was achieved with this procedure.

At all stages of degradation the products were fully characterised where possible using a variety of techniques including elemental analysis, solution state ^{1}H and ^{13}C nuclear magnetic resonance, solid state ^{13}C nuclear magnetic resonance, gel-permeation chromatography, gas chromatography-mass spectroscopy, fourier transform infra-red spectroscopy and some ultra violet-visible spectroscopy.

KEYWORDS OIL SHALES KEROGENS STRUCTURAL ANALYSIS
DEGRADATION BITUMENS

Acknowledgements.

I would like to take this opportunity to express my sincere thanks to my supervisor, Dr.A.W.P.Jarvie for her constant encouragement and invaluable guidance throughout the course of my research.

I am also deeply indebted to Dr.A.F.Gaines (Birkbeck College, University of London) for his help with GC-MS data and his valuable advice and useful suggestions.

Also I would like to thank the members of the technical staff in the department of molecular sciences for their assistance, especially Dr.M.Perry for obtaining the NMR spectra, so essential to my work.

I would also like to thank Dr. H. Stephenson (Marquarie University, New South Wales, Australia) for the gift of the Australian oil shale.

Finally I would like to thank Aston University for financial support during the period October 1984 to October 1987.

CONTENTS

List of Tables

List of figures.

List of Abbreviations.

BSTFA	Bis-trimethysilyltrifluroacetamide.
CH1	Kimmeridge Clay (Clavell's Hard, Dorset, 1)
CH2	Kimmeridge Clay (Clavell's Hard, Dorset, 2)
CSRP	Chloroform soluble reduction products
DMSO	Dimethylsulphoxide
FTIR	Fourier transform infra-red
GC-MS	Gas chromatography-mass spectrometry
GPC	Gel permeation chromatography
IRP	Insoluble reduction product
JC	Julia Creek (Australia)
KC	Kimmeridge Clay (North Yorkshire)
LAH	Lithium aluminium hydride
LAD	Lithium aluminium deuteride
MAS	Magic angle spinning
MHA	Methylated humic acid
NMR	Nuclear magnetic resonance
NOE	Nuclear overhouser effect
OC	Oxford Clay
PASS	Phase altered spinning sidebands
perTFA	Peroxytrifluoroacetic acid
PSRP	Pyridine soluble reduction products
PTC	Phase transfer catalyst
SIC	Single ion chromatogram
SMEAH	Sodium bis-2-methoxy ethoxy aluminium hydride

SSB	Spinning side band
TBAH	Tetrabutylammonium hydroxide
TBAI	Tetrabutylammonium iodide
TIC	Total ion chromatogram
TMS	Tetramethylsilane
TOSS	Total suppression of spinning sidebands
UV-VIS	Ultraviolet-visible
WSRP	Water soluble reduction products.

Chapter 1.

Introduction.

1.1. Introduction.

It is well known that the incorporation of biologically derived materials into sediments over many millions of years has resulted in the formation of coal, oil and gas deposits[1]. These fossil fuels have provided sources of energy and chemical feedstocks for many years, but they are not inexhaustible and as they become increasingly depleted the search for alternative fossil fuels, and the need to utilize existing ones more efficiently, will assume great importance.

Of the total organic matter in the earths crust it has been estimated that only 0.25% is associated with the conventional fossil fuels (coal, oil, and gas)[2]. The remainder is dispersed extensively within the mineral matrix of many sedimentary rocks, a substantial proportion of which are called oil shales[3]. It is the organic matter in these oil shales which has vast potential as an alternative fossil fuel.

Oil shales are defined as sedimentary rocks which contain organic matter that produces an economic quantity of oil when destructively distilled, but not appreciably when extracted with common organic solvents. Clearly this definition is rather ambiguous because it largely depends on the fluctuations of the price of oil. In addition the term oil shale is often misleading because these rocks are rarely true shales in the geological sense and contain no oil in their native states. Nevertheless, since this term is still in common use it will be used in this thesis.

Clearly the efficient utilization of these oil shales as fossil fuels requires substantial research, especially the determination of the structure of their organic matter. Only then can processes be developed, refineries built and conditions optimised so that the maximum exploitation and conversion of these fuels may be achieved.

Thus the aims of my research were two-fold; firstly to elucidate the structure of

the organic matter in five sedimentary rocks as far as possible and secondly, and probably more importantly, to apply, test and develop methods for the determination of such structures.

The organic matter in an oil shale can be separated into that which is soluble in organic solvents (bitumens) and that which is insoluble (kerogens). Obviously the nature of the solvent and the conditions of its use have to be specified so that one can obtain an accurate definition of these two terms. Normally, kerogens are the predominant portion of the total organic matter in a sedimentary rock, the bitumens typically being no more than 5-20%. This has led to kerogen being described as the most abundant organic molecule on earth[4]. Although the definition of kerogen has shown variation in the past[5], it is becoming increasingly common to use the term to describe the insoluble organic matter in sedimentary rocks of all types[6]. It is this definition of kerogen that is used in this thesis. (The terms organic matter or organic material used throughout this thesis refer solely to the material comprised of organic molecules in monomeric or polymeric form which have been derived from the organic parts of organisms. Mineral skeletal parts such as teeth, bones and shells are not included.)

1.2 The origins of Sedimentary Organic Matter.

Like coal, oil and gas, bitumens and kerogens owe their origins to once living organic matter which became incorporated in a sediment which later formed into a rock. The production of organic matter is achieved via photosynthesis, a process whereby plants use the energy from the sun to build up organic molecules from carbon dioxide and water. The initial photosynthetic products are sugars which are then biosynthesised into more complex molecules such as polysaccharides, lipids, cellulose, lignin and proteins etc. As a result of the metabolism or the death of an organism, these materials are released and may be deposited (conditions permitting) in a sediment.

Sedimentary rocks are normally formed in an aquatic environment and if they are to contain organic matter then obviously a certain minimum amount of the total organic matter released must accumulate and survive within the sediment being deposited. This organic material may be autochthonous to the environment where it is deposited, ie. originate from the water above or within the sediment in which it is buried, or it may be allochthonous, ie. foreign to its environment of deposition. It may also be in molecular or particulate form. However, for accumulation to take place, there must be a suitable energy level in the body of water concerned. For example, if this energy level is too high then erosion of the sediment will occur instead of deposition. In addition, the organic matter must, to some degree, survive the chemical and biochemical decay processes to which it is subjected. This can be achieved by having either a high level of organic deposition, such that not all can be consumed, or through the formation of an anoxic bottom condition so that aerobic bacteria, that would normally completely consume the organic matter, cannot survive. (Some bacteria will survive anoxic conditions but normally such species act more slowly upon the organic matter).

Chemical degradation is brought about via the actions of chemicals, for example, dissolved oxygen, native to the environment. Although chemical degradation does occur, most degradation is done biologically by other organisms, especially bacteria, which use the organic matter as a source of food hence energy. It has been reported that these degradation processes may result in 99.9 to 99.99 % of all of the organic matter photosynthesised being consumed[7]. Although this leaves only a very small amount that can be incorporated into sedimentary rocks, because accumulation typically takes place over many millions of years, this level of organic deposition and preservation is sufficient for the formation of an organic rich sediment.

The most abundant chemical species making up living organisms are

carbohydrates, proteins, lipids and lignin, all of which can contribute to the organic matter eventually deposited in a sediment. However, due to the relative resistances of some of these materials towards degradation, the organic matter in a sediment is normally enriched in some of these organic materials. Carbohydrates for instance, although fairly stable to chemical degradation, can be easily broken down by the enzymes of certain bacteria[8] into saccharides and eventually hydrolysed to carbon dioxide and water. The same is true for proteins which are easily degraded via enzyme attack of their peptide linkages[8] into amino acids. In contrast both lignin and lipids show considerable (but not absolute) resistance to degradation, and it is possible therefore that they both play a major role in the formation of sedimentary organic matter. However, lignin (which is thought to be responsible for the majority of the organic matter in coals[9]), is only wide-spread in terrestrial plants, and since the majority of sedimentary rocks form in an aquatic environment, lignin will only be incorporated into a sediment where there is a significant terrestrial input, eg.in lakes and around the mouths of rivers. Lipids therefore would appear to be the most likely precursor (or the most abundant precursor) of sedimentary organic matter deposited in environments where there is little or no terrestrial influence. Lipids are wide-spread amongst organisms and can be considered to be those organism produced substances that are practically insoluble in water, but extractable by one or another of the so-called fat solvents[10]. These solvents include chloroform, carbon tetrachloride, ethers, aliphatic and aromatic hydrocarbons and acetone. Consequently lipids can encompass many materials including animal fats, vegetable oils, and the many various waxes. In turn these materials can comprise many different compound classes including fatty acids, hydrocarbons, triglycerides, alcohols, poly-isoprenoids, subin and cutin to name but a few.

Thus, lipids and lignin (to a lesser extent) can be considered as the predominant

precursors of the organic matter in sedimentary rocks. Although we know lignin originates from the terrestrial or so-called higher plants, it is less clear which organisms are responsible for the lipid precursors in such rocks. This uncertainty is because all organisms contain some lipids, and although variation between species is observed[11], these variations can be masked by the sheer number of different organisms , the geological conditions at the time of deposition, the water temperature, the nutrient flow rate and the changes that lipids undergo over the course of geological history. We also have to assume that the biochemical make-up of prehistoric organisms, and the contribution they made to the biomass, is the same as it is for modern-day organisms.

However, making these assumptions, it would appear probable that phytoplankton, such as the various strains of algae, diatoms and dinoflagellates, are the predominant species involved in the production of the organic matter which is incorporated into sediments. This can be said because phytoplankton is the basis of the food chain and as such is far more abundant than the other organisms that feed upon it. In addition chemical analysis of phytoplankton has revealed that they contain large amounts of lipid material[11] which can be deposited in a sediment. When these lipids were analysed more closely[12], it was found that they contained a high proportion of unsaturated fatty acids, which, it has been proposed, can condense and polymerise to form kerogen-like substances[13].

In addition to phytoplankton, bacteria and zooplankton also contribute to the lipids incorporated into sediments. Bacteria, the most primitive of organisms, are extremely adaptable and hence their chemical composition can vary considerably. On a dry weight basis a typical bacterium species will contain 50% proteins, 20% cell-wall membranes and 10% lipids, the rest being ribonucleic and deoxyribonucleic acids[14]. The cell-wall membranes themselves contain considerable quantities of lipid matter.

Zooplankton feed directly on phytoplankton and therefore similarities in their composition are expected. Chemical analysis of copepods (an example of a zooplankton species), shows a relatively high lipid content, to which wax esters contribute significantly[15].

Other organisms will probably contribute to the organic matter deposited in a sediment but since their relative concentration is low, so will be their input into the sediment. As mentioned before, decomposition products from terrestrial plants may find their way into an aquatic environment and subsequently be deposited. Apart from this, the organic matter in the majority of sedimentary rocks can be considered to have been derived mainly from the lipids of phytoplankton, bacteria and zooplankton, in that order.

1.3 The Evolution of Sedimentary Organic Matter.

Even when organic matter finds its way into a sediment, its modification, reaction and transformation is not complete. There are three main stages in the evolution of such organic matter;

a) diagenesis

b) catagenesis

c) metagenesis or metamorphism.

Diagenesis is a process whereby the organic matter in a young sediment is transformed into a more stable form (kerogen)[16]. The depth of burial, over which diagenesis occurs, is normally in the order of the first few hundred metres. Therefore increases in temperature and pressure experienced by the buried organic matter are small and thus diagenetic transformations can be considered to occur under relatively mild conditions. Diagenesis results in the formation of kerogens (geopolymers) from the breakdown products of biopolymers (lipids, carbohydrates, proteins etc) and can be

considered to take place in three stages. Firstly, buried organic matter, up to a depth of a few metres, can be further acted upon by bacteria and burrowing organisms which facilitate its continued biodegradation into lower molecular weight compounds. Secondly, these initial breakdown products are then condensed together to form relatively high molecular weight compounds called fulvic and humic acids[17]. This polycondensation or polymerisation leads to a loss of some functional groups (usually carboxylic acid groups), which enhances the insolubility of these materials. This process can be demonstrated by the condensation of acid- and base-soluble fulvic acids into humic acids which are only soluble in base. Thirdly the polycondensed humic acid-like material will continue to condense further producing material that is more and more insoluble. Soil scientists refer to this material as humin, whereas geochemists use the term kerogen. This stage of diagenesis normally occurs at greater burial depth than the polycondensations that form the fulvic and humic acids.

At the end of this diagenesis stage in the evolution of sedimentary organic matter, nearly all of the buried organic matter has been converted to insoluble kerogens. As the burial depth increases the temperature and pressure also increase and at a depth of about 1000m, the buried organic matter is transformed again. This process in called catagenesis. During catagenesis temperatures may range from 50 to 150°C and pressures from 300 to 1500 bars. Under these conditions, the kerogens start to produce liquid petroleum products and later wet gas and condensate. At some point in their evolution no more oil or condensate can be produced from the kerogens, which are then considered to have entered their metagenesis stage of evolution. During this stage, which is reached only at great depth, the remaining kerogen residues are converted predominantly to graphite which may even crystallise to some extent. No oil or condensate is formed during this stage of evolution and only very little gas. The organic

matter remaining after metagenesis is very stable and resistant to further change. This stage in the evolution of sedimentary organic matter can be regarded as equivalent to the anthracite-forming stage in coal evolution.

These evolutionary stages of sedimentary organic matter are summarised in figure 1.1

1.4 The Nature of the Organic Matter in Oil Shales.

It should be obvious from the preceding text that the organic matter in sedimentary rocks is exceedingly complex. As we have seen the nature of the organic matter in these rocks is dependent on a number of factors including the type of source organisms and their composition, the deposition conditions and the geological history after deposition. All of these variables have combined to create a diverse array of organic matter that varies not only between different deposits but within the same deposit as well. This complexity and heterogeneity of these materials complicates their chemistry and has resulted in their analysis being conducted in a similar fashion to that of coal. Despite this variation in sedimentary organic matter it has been noted that kerogens can be classified into three broad types which differ in their elemental composition and their evolution trends. These three types are discussed more fully in chapter 2 section 2.

1.5 Analytical Strategy.

The analysis of sedimentary organic matter presents a number of intriguing problems. As discussed above the organic matter is often intimately mixed with a large quantity of inorganic mineral matter which complicates the structural investigation (see chapter 2). In addition the organic materials are extremely complex and cannot be

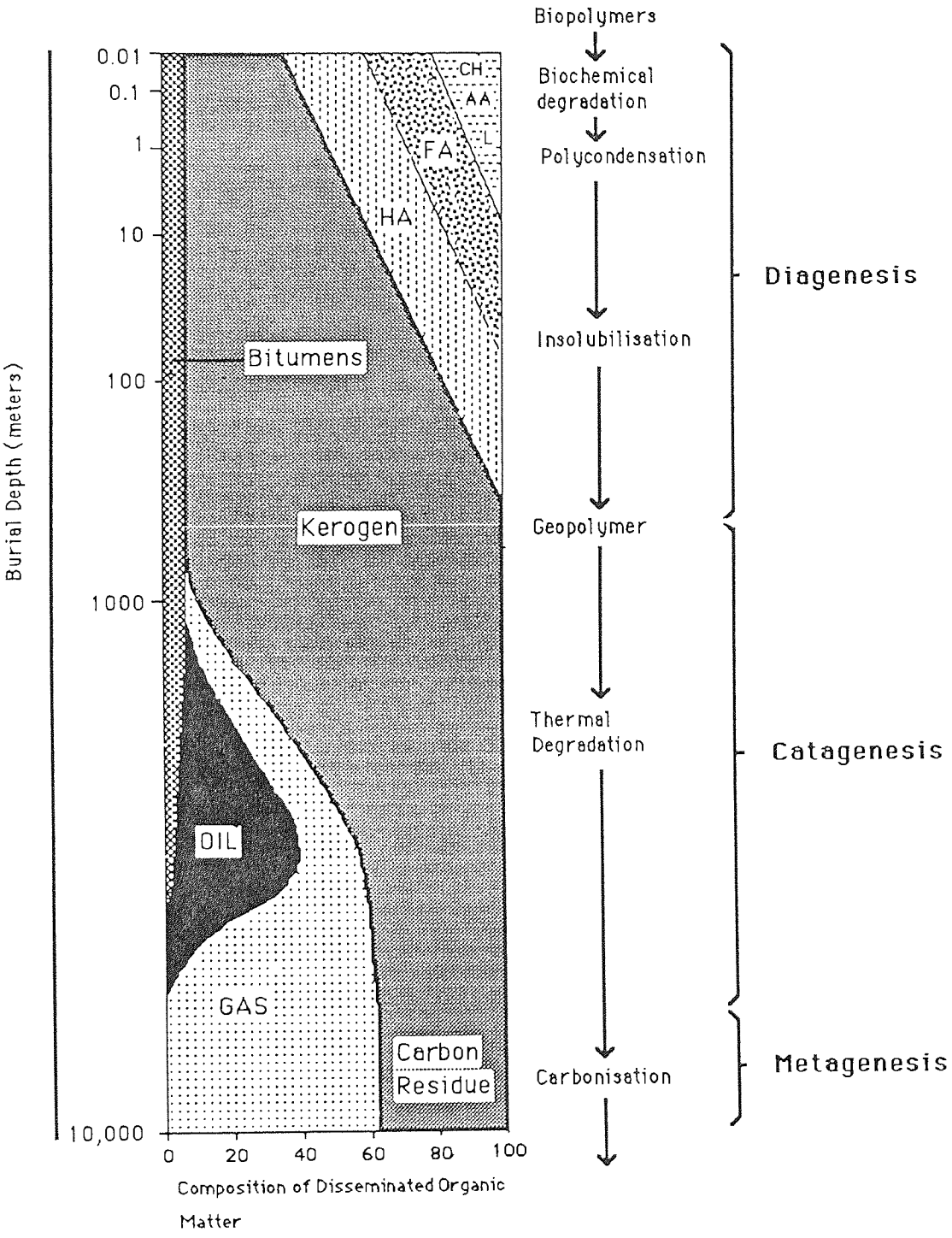

Figure 1.1 The Evolution of Sedimentary Organic Matter.[16]

CH =Carbohydrates

AA = Amino acids

L = Lipids

FA = Fulvic acids

HA = Humic acids

described as uniform molecules, but rather as assemblages of units with varying molecular structure. Furthermore a large portion of the sedimentary organic matter is insoluble and is therefore not amenable to routine chemical analysis. A variety of approaches have been used to overcome these various problems including microscopical investigations, pyrolytic degradation, the effect of various chemical reagents, and the application of physical methods of analysis. These have served either to break down the organic matter into lower molecular weight, hence more soluble products, or to characterise the whole organic matter without degradation.

Previous workers have concentrated mainly on the determination of the structure of the oils that are produced by the distillation of the organic matter in the sedimentary rock[18,19]. Although this type of analysis provides rapid results, the products that are produced bear an uncertain structural relationship to the organic matter from which they are derived. Consequently, analysis of these oils cannot provide accurate structural information on the original materials. Methods used for this type of analysis will only be useful if they do not change the structure of the organic matter or if they change it in a known and controlled way. In consequence physical methods of analysis and mild, specific chemical ones are the only methods that will provide useful information. Chemical methods must be mild and specific otherwise the structural relationship between the kerogen and its degradation products may be lost.

Before these methods of analysis can be applied however, it is first necessary to isolate the organic matter from its mineral matrix. Methods currently available for this, and the method of choice, are discussed in chapter 2. Once the organic matter has been isolated it can then be separated into its kerogens and bitumens by extraction with organic solvents. This separation is advantageous because it produces simpler fractions

(albeit still very complex), fractionation and simplification are constant goals in the analysis of these materials. The isolated bitumens can be analysed by a variety of physical techniques that include solution state NMR, GPC, and GC-MS as well as FTIR, elemental analysis and UV/VIS spectroscopy etc. Such solution state analytical techniques are not applicable to kerogens because of their insolubility and hence bitumens are far easier to characterise. Despite this, kerogens can be analysed by solid-state physical methods such as FTIR, elemental analysis, pyrolysis mass spec, TGA, ESR spectroscopy, microscopy and solid state NMR etc, however, these techniques can only generate an average molecular structure for these materials. For a detailed chemical analysis to be carried out the kerogens must be rendered soluble, and as discussed earlier, this solubilisation must be achieved in a mild, selective and controlled way. Only then can individual components of the kerogen be separated out, analysed (especially by GC-MS), and then hopefully reassembled to give some idea of the original kerogen structure.

Many of the early methods used to solublise kerogens were rather severe. The commonly used methods were oxidation with nitric acid, potassium permanganate, or chromic acid. Such methods lead to the near total destruction of the kerogens into carbon dioxide, water and a few water soluble, low molecular weight carboxylic acids. Clearly very little structural information could be obtained from such products. Recently, more selective oxidation reactions have been introduced. For example, potassium permanganate has been used in a step-wise fashion with isolation of oxidation products between permanganate additions. This approach has led to improved yields of long chain fatty acids and other products. Since this step-wise procedure appeared to give better structural information we decided to use this procedure in our studies. This will be dealt with in more detail in Chapter 6.

This permanganate oxidation together with other methods for the chemical

degradation of kerogens have been reviewed[20]. In addition to the methods discussed in this review a wide variety of other chemical reagents have been used to investigate the structure of kerogens. These include perchloric acid[21] p-toluenesulphonic acid[22], methyl iodide with tetrabutyl ammonium hydroxide, lithium aluminium hydride/deuteride, hydrogen bromide with tetraphenyl phosphonium bromide, sodium hydroxide with ethane-1,2-diol, nitrobenzene with sodium hydroxide[23], trimethylsilyl iodide(TMSI) and sodium bis-2-methoxyethoxy aluminium hydride[24] and sodium dichromate in glacial acetic acid[25]

These reagents were usually employed because of their relative mildness and specificity. The chemical reactions that I have employed, include lithium aluminium hydride/deuteride reduction, O-methylation, potassium permanganate oxidation and peroxytrifluoroacetic acid oxidation. These procedures follow from our previous work on kerogen structures[23] and are discussed later in this thesis.

From the results of a large number of studies it has been possible to develop structural models for complex organic materials such as coal[26,27], asphaltenes[28], humic acids[29], lignite[30] and kerogens[2,31,32,33,34,35,36] (especially those of the Green River Formation). These models, for example figures 1.2 and 1.3, are only average molecular structures which fit the chemistry and behaviour of those substances as far as we currently understand them. Thus these models do not represent the structure of any actual component of the organic material concerned, only their combined average. Although this is true at present, by continued investigation and modification, these models will begin to approximate to actual structures present within these materials.

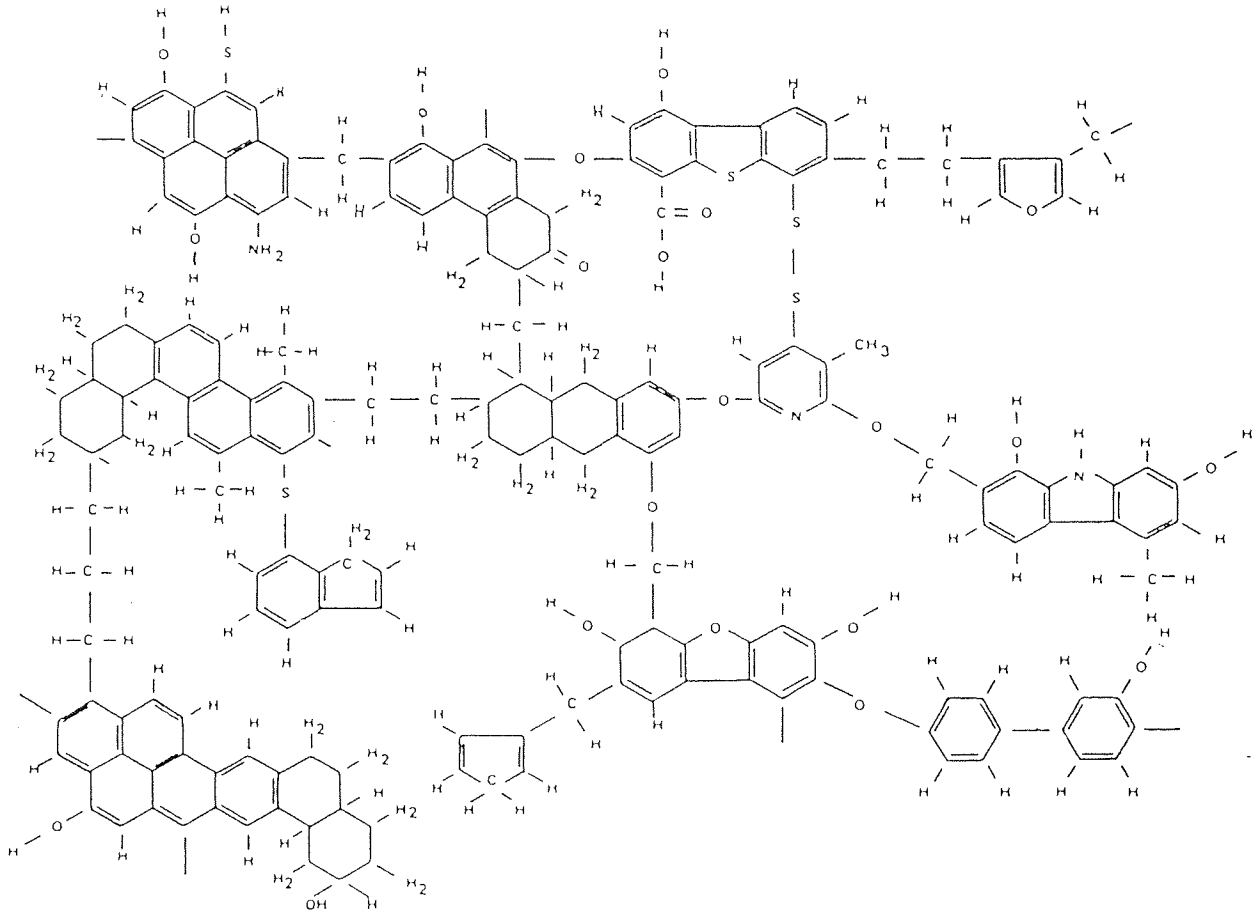

Figure 1.2 Model of a sub-bituminous coal proposed by Given.[26]

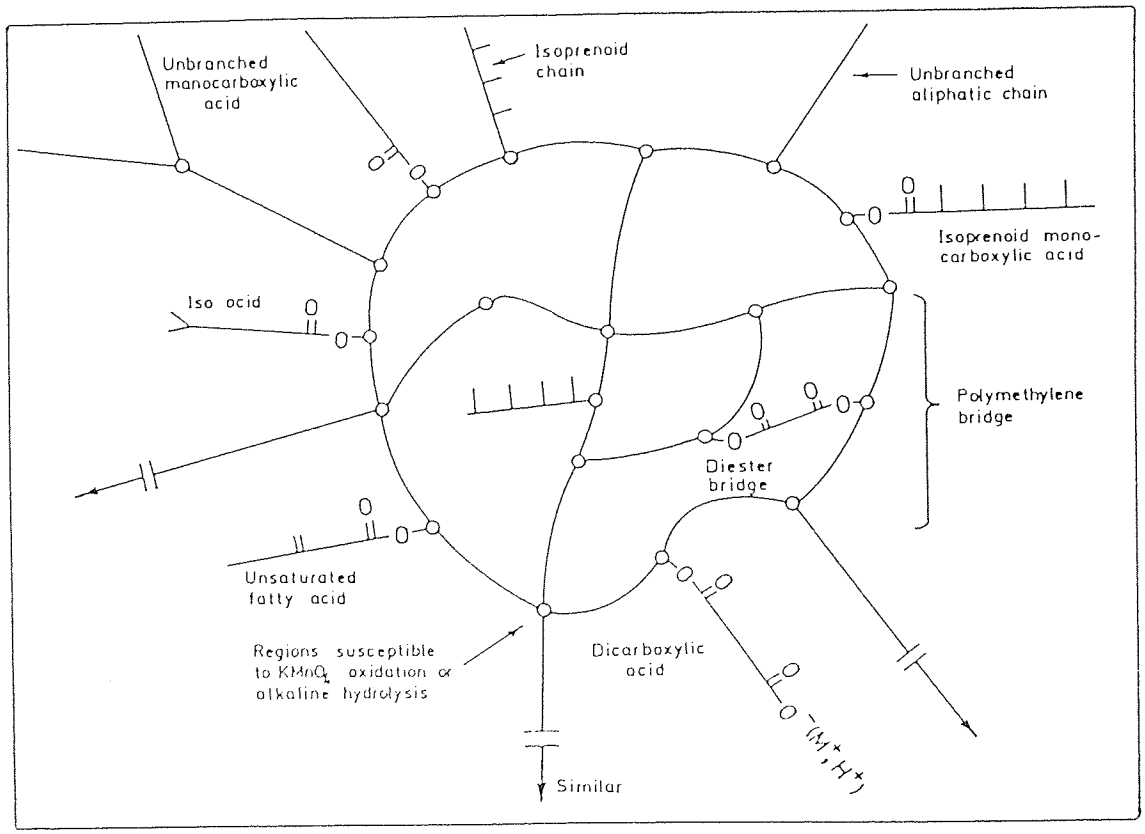

Figure 1.3 Model of the Green river oil shale kerogen.[2]

1.6 The Samples Studied.

Throughout this work we have concentrated on five samples of oil shale which contain various quantities of organic matter. We have studied three from the British Kimmeridge Clay formation, one from the British Oxford Clay formation and one from the Julia Creek deposits in Queensland Australia. For a more detailed account of the origins of these samples refer to the experimental section (Chapter 8).

The British Kimmeridge Clay formation is of Upper Jurassic age (125-136 million years) and comprises a series of more or less silty mudstones and shales, some rich in organic material, with occasional argillaceous limestones. The rhythmic alternation of bituminous laminated shale, lacking a benthos fauna, and bioturbated shale suggests a very low-energy depositional environment, with variation from aerobic to anaerobic bottom conditions. The Kimmeridge Clay attains a considerable thickness, some 500 metres in the south, of which some 350 metres is exposed at the Kimmeridge Bay area outcrop. A detailed account of the geology of the Kimmeridge Clay sequence is available[37,38].

The Oxford Clay formation is also of Upper Jurassic age (136-139 million years) but is slightly older than the Kimmeridge Clay which overlays it. The Oxford Clay deposit is one of the most uniform of the European Jurassic system. The lower Oxford Clay is bituminous at certain horizons and its deposition environment appears to have been fairly aerobic[39]. The mudstones of the Middle and Upper Oxford Clay are more calcareous and plastic, and less bituminous, than those of the lower division, but nonetheless were probably deposited in shallow-water marine shelf conditions, below normal wave base. The Oxford Clay sample studied was a greenish grey, shaly, bituminous mudstone of the Upper Oxford Clay deposits, which had in part weathered to a

tenacious brown clay. A number of excellent texts exist which give the detailed geology of the Oxford Clay sequence[40,41,42].

The Julia Creek oil-shale sample had the appearance and texture of a bituminous mudstone and came from the deposits of the same name which are one of a number of shales that make up the Toolebuc Formation of the Eromonga and Carpenturia Basins of Queensland, Australia. The Julia Creek oil-shales were deposited in the Cretaceous period, (75-135 million years ago).

Very little previous work has been done on any of these samples, especially on the Oxford Clay and Julia Creek deposits, and of the work that has been done little has involved the structural determination of their total organic matter. Therefore, much less is known about their constitution than for example the widely studied Green River Formation, the Estonian Kukersite or the Aleksinac shale organic matter[43]. Most of the work carried out on Kimmeridge samples has involved the analysis of the shale oils that they produce upon distillation[44,45,46], although some work has also been carried out on the analysis of their bitumens[47]. In an early study Kimmeridge Clay kerogens were oxidised with potassium permanganate in an effort to determine their structure[48]. Due to the use of over harsh conditions very little structural information was obtained from this study. Apart from our studies[23], the organic geochemistry of the Oxford Clay has been largely overlooked. However, some limited work has been performed on the Julia Creek deposits. Again these have largely concentrated on shale oil analysis[49,50,51], but there have been some structural investigations of the whole organic matter by solid state NMR[52,53].

The work recorded in this thesis concerns the study of the structure of the whole organic matter in the five oil shales mentioned above via the application of both physical and chemical methods of analysis.

Chapter 2.

Analytical methods.

2 ANALYTICAL TECHNIQUES.

2.1 Isolation of organic matter.

- 2.1.1 Solvent extraction.
- 2.1.2 Physical methods.
- 2.1.3 Chemical methods.

2.2 Elemental analysis.

2.3 Infra-red analysis.

2.4 NMR analysis.

- 2.4.1 Solution state NMR.
- 2.4.2 Solid state NMR.

2.5 GC and GC-MS spectroscopy.

2.6 Gel-permeation chromatography.

2. Analytical Methods.

This chapter is concerned with the techniques that we have used to characterise the organic matter in the oil shales. In order that these materials may be fully characterised it is necessary for them to be isolated. For this reason procedures used to isolate the organic matter are also discussed.

2.1 Isolation of Organic Matter.

There is a tendency for inorganic minerals to interfere with the analysis of kerogens and bitumens and therefore it is necessary to separate them from these organic materials. Minerals normally found in oil shales include quartz, feldspars, clays, carbonates, pyrite and saline minerals. Numerous isolation methods have been tried[54,55,56,57,58] and it is apparent that there is no universally accepted procedure for the separation and characterisation of sedimentary organic matter.

For any subsequent physical and chemical analysis to be worthwhile it is of paramount importance that any isolation technique yield organic matter as unaltered as possible. This requirement therefore rules out the distillation of organics out of the rock by pyrolysis because of the severe chemical and physical changes that it produces. It is also necessary to isolate the organic matter totally so that average molecular structures determined by analytical methods are representative of the whole organic matter, not just some fraction of it.

Isolation techniques in common use can be broken down into three groups. These are:

a) Solvent extraction.

b) Physical methods.

c) Chemical methods.

2.1.1 Solvent Extraction.

Extraction of sedimentary organic matter is necessary for the separation of bitumens from kerogens. Solvent extraction can be performed on the powdered rock (in which case only the bitumens are separated from the minerals) or the isolated organic concentrate (where minerals have already been removed). The latter extraction is preferred if total separation of bitumens and kerogens is required.

The nature of the isolated kerogens and bitumens depends on the nature of the solvent and the conditions under which it is used. Therefore, in all reports involving solvent extraction studies it is very important to record the solvent and the conditions of its use. In most cases, almost complete extraction can be achieved by ultrasonic agitation at room temperature or by Soxhlet extraction at the boiling point of the solvent[57,58,59]. The amount of extractable material increases with extraction temperature and with polarity and chemical reactivity of the solvent. Vitorovic and Pfendt[60] have investigated the extractability of Aleksinac oil shale in a wide range of solvents and have found extractability ranging from 0.53% in petroleum ether to 11.44% in dioxane and 52.63% in aniline. Oxidation and chemical alteration were responsible for the high extractability obtained with aniline. It has also been reported[61] that high extractability of kerogens can be achieved with tetralin at 400°C, although this result too is probably due to chemical degradation.

In this study pyridine was used extensively for extraction since this can dissolve considerable amounts of sedimentary organic matter. The pyridine extract was then extracted with chloroform to yield a fraction more amenable to analysis.

2.1.2 Physical Methods.

There are a selection of physical processes available for the separation of sedimentary organic matter from its inorganic mineral phase. These processes mainly

rely upon floatation and centrifugation in pure or mixed dense liquids or on differences in wettability in water and liquid hydrocarbons[57]. Other physical techniques involving ultrasonics, electrostatics and magnetism have been used.

Physical methods of isolation allow for an organic concentrate to be prepared which has not been chemically altered. Although this is a clear advantage, there are three main reasons why these techniques are not normally used. These are:

1.) A general method for isolation does not exist and often many repeated separations are required to give a satisfactory separation.

2.) Much of the organic matter is lost during the separation and normally only a small quantity of mineral-free organic concentrate is obtained.

3.) Fractionation of the organic matter on the basis of size, density or mineral association is very likely, leading to a concentrate that does not represent the actual organic matter in the rock.

These problems severely limit the application of physical methods of isolation especially when we wish to determine the structure of the whole organic matter. For these reasons these techniques were not used in our work.

2.1.3 Chemical Methods.

Chemical treatment is the method of choice for isolating all of the organic matter from rocks. Normally the ground and extracted rock is subjected to the action of concentrated acids, hydrochloric acid (HCl) to remove carbonates, sulphates, sulphides, oxides and hydroxides, and hydrofluoric acid (HF) to remove silica and silicates[56]. This acid demineralisation can give a more or less mineral-free organic concentrate but there are three main problems associated with this method of isolation. These are:

1.) Some minerals do not dissolve in these acids. Pyrite (FeS_2) is a particular problem especially when its concentration is high in relation to that of the organic

matter.

2.) HF can form insoluble fluorides such as CaF_2, $MgAlF_6.xH_2O$, $NaAlF_4.xH_2O$ and $Fe(II)[Al.Fe(III)]F_5.xH_2O$ during the demineralisation process.

3.) Reactions may take place between the organic matter and the acids used.

The first two problems can be largely overcome. Pyrite can be dissolved by nitric acid, sodium borohydride, powdered zinc with HCl, 10% aqueous sodium hydroxide, aqueous ferrous salts and lithium aluminium hydride (LAH)[57]. Indeed the use of LAH to remove pyrite and its effect on the organic matter are discussed in detail in Chapter 4 and will not be dealt with here. Insoluble fluorides need not be a problem since their influence on the analysis of the organic matter is small. Nevertheless the formation of these fluorides can be minimised if dilute HF is used in an excess of HCl.

The third problem, that of reaction and therefore modification of the organic matter cannot be eliminated. The functional groups which can be affected by these acids are listed in table 2.1.

The effects of HCl and HF on sedimentary organic matter have been studied by a number of groups[57,58]. Although some workers have shown that slightly evolved organic matter is affected by HCl and HF, there is general agreement that mature organic matter is left largely unaltered so long as the temperature during demineralisation is kept below 70°C. For instance there was no major change in the elemental analysis of mature organic matter after acid treatment, only minor increases in chlorine and fluorine contents[62]. IR analysis , ESR analysis, electron microscopy and other techniques all suggest the organic matter to be predominantly unaltered by these acids. Thus it can be concluded that the advantages gained by isolating all of the organic matter by acid attack more than compensate for any possible modification of the organic matter that might have occurred. This method was our method of choice.

Table 2.1 Possible effects of HF and HCl on organic functional groups.

Acid	Type of reaction	Functional group affected.
HCL	hydrolysis	R-COOR (ester)
		$R\text{-}CONH_2$ (amide)
		polysaccharide
		$(\text{-}NHCHR\text{-}CO\text{-})_n$ proteins, polypeptides
		$(\ R\text{-}COO)_2M(II)$ (metal salts)
	addition	$R_2C{=}CR_2$ (alkenes)
	quaternisation	R_3N (amines)
	alkyl halide formation	R-OH (alcohols)
HF	hydrolysis	as for HCl
	addition	as for HCl
	condensation*	$R_2C{=}CR_2$ + R-H, R-X + R(arom)-H, R-OH + R(arom)-OH.

* normally under anhydrous conditions.

2.2 Elemental Analysis.

Determination of the elemental composition of kerogens or organic concentrates normally involves combusting them in oxygen and then separating out the CO_2, H_2O and nitrogen etc, before measuring the quantities of each. Direct analysis of carbon, hydrogen, nitrogen, sulphur and oxygen is only possible when an ash-free organic concentrate or kerogen is available. In the presence of mineral matter, oxygen must usually be determined by difference. This can lead to significant errors in the oxygen content because a knowledge of the minerals present and their behaviour under the ashing conditions is required before an accurate figure for the oxygen content can be

obtained. Clearly these errors will increase with increased mineral content. Errors may also arise due to the variable moisture contents of the samples and their inherent heterogeneity. Variation in the moisture contents can be reduced by careful drying and the effects of heterogeneity minimised by repeated analysis. (Each of our samples was analysed ten times and the average taken).

Data obtained from elemental analysis can be used to calculate an empirical formula for the kerogen, eg. $C_{215}H_{330}O_{12}N_5S$ has been calculated for the Green River formation kerogen. In addition the data can be plotted on various compositional diagrams and the differences between various samples observed diagrammatically. One particularly useful diagram was developed by Van Krevelen for the analysis of coals[63]. This diagram is a plot of H/C ratio vs O/C ratio and can reflect changes in the composition of kerogens as they evolve or react.

It was found that when the elemental compositions of many kerogens were plotted on the same Van Krevelen diagram, certain regions were more populated than others. When kerogens from the same source but different degrees of burial (hence evolution) were compared, this trend became even clearer. It is now evident that as burial depth increases (ie. as maturity increases) the O/C and H/C ratios fall, and an evolution pathway is displayed on the Van Krevelen diagram. (See Figure. 2.1.). It also appears that there are three main evolution pathways which coalesce at high levels of maturity. This led to classification of kerogens into type I, II or III , depending upon which evolution pathway they belonged to. The three kerogen types are as follows:

Type I is typified by the organic matter from the Green River Shales of Uinta Basin USA. This material is highly aliphatic and has a similar elemental composition to the alginite maceral of coals.

Type II is typified by the organic matter from the Lower Toarcian Shales in the Paris

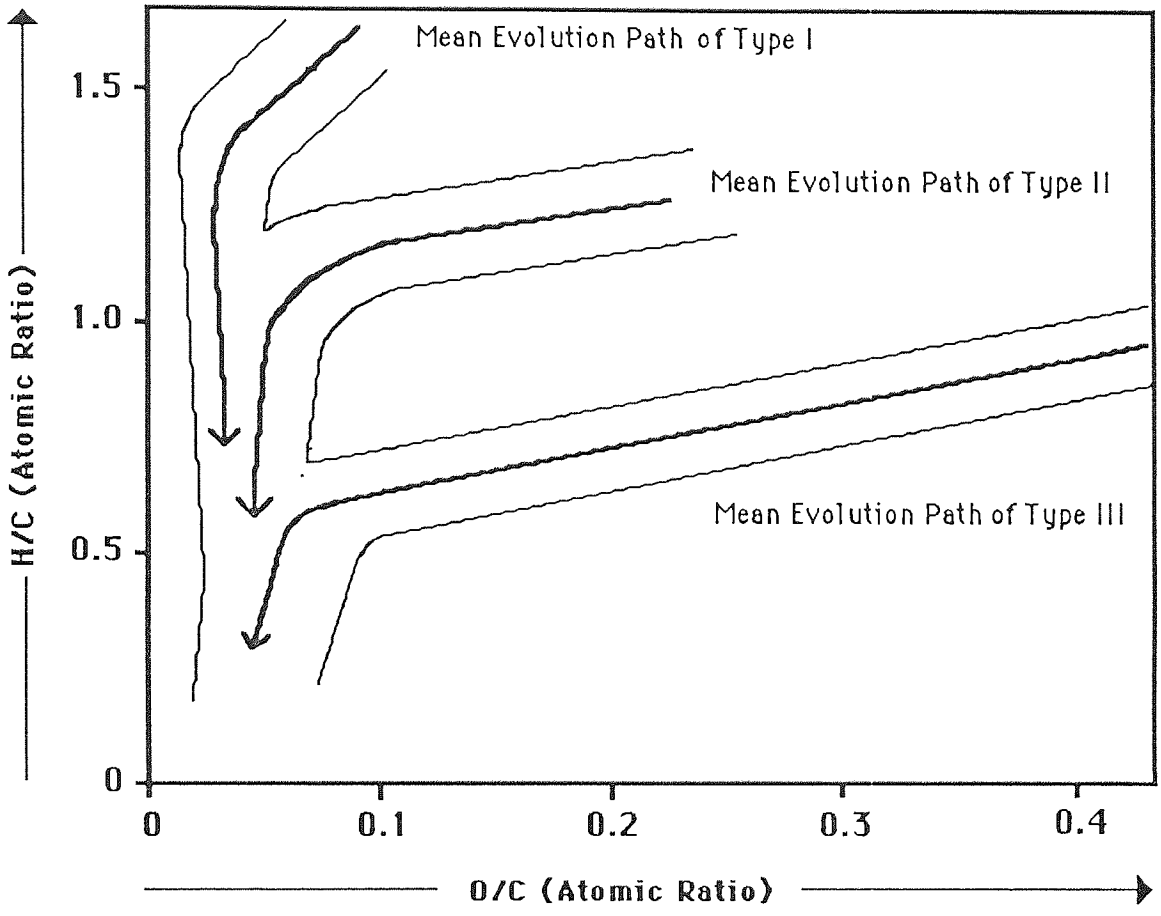

Figure 2.1 Van Krevelen diagram showing the evolution trends Of type I,II and III kerogens.[64]

Basin, France. Its composition is consistent with that of saturated polycyclic rings and is comparable to the exinite maceral of coals.

Type III is typified by the Upper Cretaceous Shales from the Doucxila Basin, Cameroon. The kerogen structure is consistent with a high proportion of aromatic entities and is comparable to the vitrinite maceral of coals[65].

Thus elemental analysis can be used to follow the behaviour of kerogens under natural evolution or chemical attack. It serves to monitor the changes that occur in a global way so that overall structural changes, not detailed molecular changes, can be seen. The distinction of three types of kerogen may not always be seen from a Van Krevelen diagram simply because at some stage all three types coalesce. In addition weathering has a significant effect on the position of a kerogen in a Van Krevelen diagram, this complicates the classification further.

2.3 Infra-red Analysis.

Infra-red (IR) analysis is a non-destructive technique which is applicable to whole, fractionated or chemically altered samples. It can provide an insight into the functionality and the overall or average structure of these materials. Infra-red radiation is absorbed by molecules, indeed parts of molecules, which subsequently vibrate at the frequency of the absorbed radiation. This intensity of absorption is measured and then plotted against wavenumber (cm^{-1})absorption. The frequency of absorbance depends on the masses of the atoms vibrating and on the strength of the bonds between them. Thus different functional groups and structures give different absorption bands which can then be used to identify them in unknown compounds.

Infra-red spectra of complex organic solids such as coals, kerogens, humic substances and other natural polymers have been presented in various

publications[66,67,68,69,70,71]. These spectra show a number of rather broad bands which are due to common chemical groups and which reflect the complexity and diversity of the molecular structures making up these materials[72,73,74].

The spectra of coals are very similar to those of kerogens[69] and humic substances[70] and therefore the data available for coals [66,67,68,71] can be used to identify the absorption bands of kerogens. Although all of these carbonaceous solids essentially give the same absorption bands, different samples can be easily distinguished because the intensity of these bands varies from sample to sample. For instance, the intensities of the bands in the spectra of coals change regularly according to rank and reflect the main chemical modifications occurring as the burial depth increases. A valuable use of IR spectroscopy for the characterisation of these solids thus requires considering the intensities of these bands. If this is done, the infra-red spectra provide a sort of 'empirical' functional analysis of the complex solid.

IR analysis cannot be quantitative because the extinction coefficients of individual groups, (for example the OH group) vary from one organic structure to another. Since the contribution that each structure makes to the whole is unknown, a simple measure of the OH absorption can not be correlated to an OH content. Nevertheless the presence of a band indicates that certain types of structure are present and conversely the absence of a band indicates the absence of certain types of structure.

The introduction of computerised Fourier transform infra-red (FT-IR) spectrometers has made the analysis of carbonaceous solids much easier. In general the spectra can be generated far quicker and are of much better quality. This is due to the greater throughput, resolution and hence noise reduction capabilities of these instruments. There is also available specifically designed software for the manipulation of IR spectra so that undesirable effects such as drifting baseline and noise can be

removed. Use of these techniques has helped with the assignment of the absorption bands commonly found in these materials.

Although there still remains some controversy as to the origins of some bands, especially the one at 1600-1630cm^{-1}, most of the common absorbance bands have now been assigned with a fair degree of certainty. These are:

a) Bands due to molecular water.

Water will contribute to the broad OH stretching band around 3400cm^{-1} and its bending mode will appear at 1630cm^{-1}. Experiments on coals have found that incorporation of water increases with sample preparation time[67] and it is therefore necessary to dry prepared KBr discs before IR analysis is performed. The moisture content of kerogen and coal is related to their oxygen content and not to their surface area[69,71]. This is because water associates with their hydroxyl groups[76] and therefore the contribution from water will vary with the OH content of the sample.

b) OH stretching band.

The OH stretch vibration produces the broad band below 3600cm^{-1}, giving a maximum at around 3400cm^{-1}. Because the baseline is frequently sloping and because of the overlap with C-H bands between 3000 and 2800cm^{-1}, the low wavenumber end of this band is not always obvious, but frequently extends below 3000cm^{-1}. The extension of the OH band towards low wavenumbers reflects the presence of stronger hydrogen bonding, possibly due to carboxylic acids. This is normally more pronounced in shallow samples where a separate maximum around 3200cm^{-1} is often seen.

c) Bands due to alkyl groups.

The stretching vibrations of alkyl groups generally occupy the 3000 - 2800

cm^{-1} region. Peaks around 2930 and 2860cm^{-1} are due to asymmetric and symmetric stretches of alkyl CH_2 groups. Methyl groups absorb at about 2960 and 2870cm^{-1} and are responsible for the broadening of the CH_2 band at higher wavenumbers. This methyl absorption often shows as a shoulder at 2960cm^{-1} in the spectra of coals and kerogens.

The band at 1455$cm^{-1}$is due to asymmetric bending of CH_2 and CH_3 groups, whereas the band at 1375cm^{-1} arises mainly from the symmetric bending of CH_3 groups. (some CH_2's close to oxygen atoms absorb in this region). The relative concentration of methyl vs methylene groups can be determined from the relative intensities of the bands at 1375 and 1455cm^{-1}. Since IR spectroscopy is not quantitative such measurements can only be used as a rough guide and to follow trends among a series of samples.

In some samples a small peak at 1395-1400cm^{-1} may appear. This is due to the C-H deformation of isopropyl or isobutyl groups. Also some kerogens or coals have an absorption at 720cm^{-1}, which has been attributed to the skeletal vibrations of alkyl chains with more than 4 carbon atoms.

d) CH vibrations of unsaturated groups.

The C-H stretching of aromatic and alkene groups absorbs in the region 3100-3000cm^{-1}. Normally this band is weak and largely obscured by the OH peak. Bands at 870, 820 and 750cm^{-1} have been assigned to out-of-plane deformation vibrations of aromatic C-H groups. These bands only appear in mature kerogens and coals and their appearance may depend on the degree of aromatisation undergone by the sample. Bands below 1000cm^{-1} in the spectra of immature kerogens may be due to C-H deformations of alkene groups but further work is needed to substantiate this.

e) Carbonyl absorptions.

Frequently one observes an absorption at around 1700-1710 cm^{-1} in the spectra of kerogens, coals, and especially humic acids. The absorptions in this region arise from the carbonyl stretching mode of aldehydes, ketones and carboxylic acids. Ester absorptions occur at higher wavenumbers and may be seen as a broadening of the 1700-1710 cm^{-1} band or as a shoulder on this band. The carbonyl peak is usually fairly intense in immature samples but as the degree of evolution or burial increases the carbonyl peak becomes weak or even lost. This band is more intense in kerogen samples that have been exposed to air. This is due to the formation of carboxylic acids by oxidation[67]. Some carbonyl absorptions[74] can appear as low as 1540cm^{-1} which has led to confusion over the assignment of other bands (especially the one at 1600cm^{-1}).

f) Band at 1630-1600cm^{-1}.

The assignment of this band has been the subject of some controversy and many publications[76]. It has been suggested that the bending vibrations of water, the C=O stretching vibrations of quinones bridged to acidic hydroxyls (H-bonding) and the C=C stretching vibrations of alkenes, aromatic rings and polyaromatic layers may all make some contribution to this band. There have been conflicting reports concerning the effects of LAH reduction of coals on the 1630-1600cm^{-1} band. In some cases reduction appeared to have no effect[77] indicating no carbonyl contribution to this band, whereas other workers observed a drop in the intensity of this band upon reduction, indicating that there was a carbonyl contribution[78]. The intensity of this band increases sharply with rank as does the aromaticity, which has led to the assignment of this band, at least in part, to aromatic structures. Indeed two recent reports conclude that aromatic structures are responsible for the predominant portion of this band, although there may may be some contribution from carboxylate ($-COO^-$) groups in the case of low rank

materials[79,80].

g) Unresolved absorptions between 1800 and 930cm^{-1}.

The spectra of coals and kerogens show unresolved absorptions extending from the 1710-1630cm^{-1} bands to 930cm^{-1}, with a maximum around 1200cm^{-1}. The high wavenumber region (above about 1400cm^{-1}) is presumably due to extension and overlap of the bands already described and attributed to C=O and C=C stretching, and to C-H deformation. The low wavenumber region may be attributed to C-C skeletal vibrations of aliphatic and aromatic fragments, to C-O stretching of ether and alcohol groups and to C-OH deformation of alcohols.

The spectra of immature materials such as peat always show intense absorptions between 1000 and 1100cm^{-1}. These absorptions accompany an intense OH stretching band and may be attributed to alcoholic functions. The spectra of mature products often show a small peak or shoulder at around 1030cm^{-1} which may be due to to C-O vibrations of aryl-alkyl ethers; the C-O absorption of aryl-aryl ethers is expected to occur at higher wavenumbers.

h) Bands of foreign substances.

Sedimentary organic matter which has been isolated by acid demineralisation frequently contains some inorganic mineral, especially pyrite. Pyrite can be recognised by its sharp absorption bands at 425 and 350 cm^{-1}. These peaks are not too troublesome because they occur in regions of the spectra largely devoid of organic peaks.

A summary of these IR absorptions is shown in table 2.2

Table 2.2 Infra-red correlation chart for coals and kerogens.

Wavenumber	Band assignment
3000 - 3600	OH and NH bonds
3000 - 3080	aromatic C-H bonds
2800 - 2950	aliphatic C-H bonds
1680 - 1745	C=O bonds
1580 - 1650	C=C bonds, H_2O deformations, aromatic and graphitic structures, carboxyl salts, conjugated C=O bonds.
1500 - 1520	aromatic rings
1400 - 1460	aliphatic CH_2 and CH_3 groups
1370 - 1380	CH_3 groups + some CH_2 bonded to oxygen
1090 - 1250	C-O bonds
890 - 980	C=C bonds
740 - 850	condensed aromatic rings
720 - 725	aliphatic chains greater than C_4

It should be noted that the presence of mineral matter can obscure many of these bands.

2.4 NMR Spectroscopy.

Like electrons, the nuclei of certain atoms can be considered to be spinning charge particles. This circulation of charge generates a magnetic moment along the axis of spin and consequently these nuclei can be thought of as acting like tiny bar magnets. Two of the most important nuclei which display this property are the proton (nucleus of the hydrogen atom) and the nucleus of the carbon l3 isotope, both of which have a spin of a 1\2. These nuclei are very useful in NMR spectroscopy because they are prevalent throughout organic molecules.

If these nuclei are placed in an external magnetic field, then these tiny bar magnets, according to quantum mechanics, can either align with or against the external field. Alignment with the field is more stable and energy must be absorbed to 'flip' the tiny bar magnet so that it aligns against the field. This is the basic principle behind nuclear magnetic resonance spectroscopy.

The energy required to flip the alignment of the nuclear magnetic moment (tiny bar magnet) depends on the strength of the external field; the stronger the field the greater is the amount of energy required, ie the radiation required has to be of higher frequency. However, not all nuclei of the same atomic species require the same amount of energy to flip to the higher energy level. This is because nuclei, or more correctly each set of equivalent nuclei, have different chemical environments which largely depend on their local electron density. This variable chemical environment shields the nuclei from the external magnetic field to a variable degree and consequently this external field is not the same as the effective field experienced by the nuclei. As a result nuclei in different chemical environments need to absorb radiation of a slightly different energy. This phenomenon is called the chemical shift.

Thus NMR can reveal the number of different (non-equivalent) protons or ^{13}C

nuclei in a molecule, the chemical environment of these nuclei (by reference to known compounds), and since the intensity of the NMR signal can often depend on the number of each nuclei present, NMR may provide a quantitative analysis of each set of nuclei.

Until recently it was only possible to study samples in the solution-state but recent developments have broadened the scope of NMR to include the study of solid samples as well. This has allowed the study of unfractionated and non-degraded coal/kerogens in a most direct way. Two excellent reviews on the application of NMR to fossil fuel research have recently been published[81,82].

There are a number of very good publications which cover the basic theory of NMR[83,84], and therefore we shall not deal with it here, but concentrate our attention on the use of NMR in the study of coals and kerogens.

2.4.1 Solution-State NMR of Kerogens/Coals.

Many solvents can be used in solution-state NMR, some of the more common ones include chloroform, carbon tetrachloride, acetone, methanol, benzene, pyridine, DMSO and water. The choice of solvent depends on the solubility of the material to be analysed and the degree to which the solvent interferes with the desired spectrum. For instance, if one is interested in the aromatic region of a ^{13}C NMR spectra the use of either benzene or pyridine is ruled out.

Common chemical shifts have been measured for both ^{1}H and ^{13}C nuclei and tables produced. Tables 2.3 and 2.4 show the common organic structures identified in coal derived products by ^{1}H [85,86,87] and ^{13}C [88] NMR respectively. Table 2.3 illustrates one problem with ^{1}H NMR. There is considerable overlap of chemical shifts from many different structures and therefore accurate assignment of particular absorptions to particular protons is not always possible. This problem can be overcome in part by the use of ^{13}C NMR, because the range of chemical shifts occupied by ^{1}H NMR

is 10 ppm whereas in ^{13}C NMR it is 600 ppm. Consequently, there is much greater resolution of peaks in ^{13}C NMR spectra, and therefore these peaks are more easily distinguishable.

Table 2.3 ^{1}H NMR Chemical shifts.[82]

ppm range	hydrogen type	Ref.
9.0 - 8.3	hydrogen on aromatic nitrogen	85
9.2 - 6.2	aromatic hydrogen	87
9.0 - 6.0	aromatic hydrogen	86
9.0 - 5.0	phenolic hydroxyl	86
8.3 - 7.7	phenolic hydroxyl	85
7.15	benzene hydrogens	85
6.65 - 6.5	olefinic H next to ring	85
6.0 - 4.5	olefinic H	87
5.0 - 3.4	ring-joining methylene	86
4.2 - 3.2	methylene α to two rings	85
4.4 - 1.7	aliphatic: α-CH_2, O-CH_2, α-CH_3, αα-CH_2, β-CH_2-tetralin, β-CH_2-indans	87
3.4 - 1.9	CH_3, CH_2 and CH α to aromatic rings	86
2.6 - 1.85	H on C atoms α to aromatic rings.	85
1.95	cyclohexane	85
1.90 - 1.0	β-CH3, CH2 and CH-β from aromatic ring, paraffinic CH2 ,CH	86
1.85 - 1.05	H on C atoms β to aromatic rings	85
1.7 - 1.0	β-CH_3, remote CH_2, β-CH_2 alicyclics.	
1.05 - 0.5	H of paraffinic methyl groups and methyl groups δ to aromatic rings.	85
1.0 - 0.7	remote CH_3	87
1.0 - 0.5	CH_3 δ or further from an aromatic ring, paraffinic CH_3.	86

Table 2.4 NMR chemical Shifts For ^{13}C Nuclei.[82]

ppm range	Carbon type.
170 - 210	carbonyl
148 - 168	aromatic C-O eg. phenol
129.5 - 148	mainly substituted aromatic and aromatic C-NH
100 - 129.5	mainly aromatic C-H with aromatic C-H ortho to C-OH between 100 and 115 ppm
100 - 60	aliphatic carbon atoms bonded to oxygen
50 - 60	methoxyl
37 - 60	ring joining methylene (23-44ppm), CH in alkyl group (except iso-alkyls) and naphthenic rings: CH_2 in alkyl group adjacent to CH
27.5 - 37	CH_2 in alkyl groups not adjacent to CH (except some α-CH_3 and CH_2 adjacent to terminal CH_3 in alkyl groups $>C_4$). CH_2 in ring-joining ethylene groups, α-CH_2 and CH, β-CH_2 in hydroaromatic rings; naphthenic CH_2.
24 - 27.5	naphthenic CH_2; shielded α-CH_2 groups; β-CH_2 in indan and propyl groups; β-CH_3 in isopropyl.
22.5 - 24	CH_2 adjacent to terminal CH_3 in alkyl groups > C_4; β-CH_2 in un-substituted tetralin structures; CH_3 on hydroaromatic and naphthenic rings (18-24 ppm).
20.5 - 22.5	α-CH_3 not shielded by any adjacent rings or groups.
18 - 20.5	α-CH_3 shielded by one adjacent ring or group
15 - 18	β-CH_3 in ethyl groups
11 - 15	CH_3 δ or further from an aromatic ring, α-CH_3 shielded by two adjacent rings or groups.

It is also possible by ^{13}C NMR to determine non-protonated carbon environments which are of course invisible in ^{1}H NMR. Thus ^{13}C NMR shows the carbon backbone of the sample regardless of whether it is protonated or not. This is an obvious advantage over ^{1}H NMR. Unlike ^{1}H NMR however, normal ^{13}C NMR cannot be regarded as wholly

quantitative. This is because in order to remove line broadening effects in ^{13}C NMR it is necessary to decouple the ^{1}H - ^{13}C spin-spin coupling. This produces sharper ^{13}C signals but alters the way that ^{13}C nuclei can relax. This produces relative signal enhancement for some ^{13}C nuclei over others and is known as the Nuclear Overhauser Effect (NOE). Attempts have been made to overcome NOE using relaxation agents such as $Cr(acac)_3$ (acac = acetylacetone) and a technique called gated decoupling. These methods give quantitative results and can be used if quantitative analysis is required.

Although solution-state NMR provides reasonably accurate structural information, it is restricted to that portion of the coal or sedimentary organic matter which is soluble. This problem has now been substantially eliminated through the advent of solid-state NMR.

2.4.2 Solid State Carbon 13 NMR of Kerogens.

Since the introduction of the solid state ^{13}C NMR techniques there has been a steady increase in the application of these procedures to the study of fossil fuels. Indeed some of the earliest measurements illustrating the use of the techniques were applied to coals[89,90] and oil shales[91,92]. The main impetus for this was that solid state techniques provide structural information through measurements that are direct, non-destructive and which can be applied to whole coal or oil-shale samples, thereby eliminating the need to solubilise them.

The Theory Behind Solid State Carbon 13 NMR.

There are three main factors which make it difficult to obtain high resolution NMR spectra from carbonaceous solids by normal Fourier Transform techniques.

These are: a) anisotropic dipole and quadrupole interactions,

b) chemical shift anisotropy,

c) extremely long ^{13}C spin-lattice relaxation times.

a) Anisotropic dipole and quadrupole interactions are due to neighbouring nuclei generating local magnetic and electrical fields which alter the externally applied magnetic field experienced by the nucleus under observation. This results in extensive line broadening of the NMR resonance frequencies of the observed nucleus.

b) Chemical shift anisotropy is a result of the different orientations of molecules in a solid. The external magnetic field causes circulation of electrons in atoms and chemical bonds which then give rise to magnetic moments. These magnetic moments affect the chemical shift of nuclei in the molecule. Since the hindrance to the circulation of electrons is dependent on the orientation of the bond axis to the external field, the chemical shift is anisotropic and very broad resonances result. These problems do not arise in liquids because Brownian Motion randomises the chemical shift anisotropy to zero.

c) Long spin-lattice relaxation times for ^{13}C nuclei in a solid sample are a major problem. After a nucleus has been perturbed (irradiated with an radiofrequency (rf) field) its magnetisation returns to equilibrium within a certain time characterised by a constant called the spin-lattice relaxation time (T_1). This nucleus can not be perturbed again until it has returned to its equilibrium state and it is necessary to wait $5xT_1$ before perturbation can be repeated. Thus the shorter the T_1 the more perturbations can be performed in unit time and therefore a better signal to noise ratio achieved.

Unfortunately T_1's for ^{13}C nuclei in solids are in the range of minutes or hours rather than seconds as they are in liquids. This difference is due to reduced molecular mobility in solids. Consequently an ordinary FT ^{13}C solid state NMR experiment requires extremely long instrument time which puts severe limitations on the technique.

The Solutions to the Problems.

These three main obstacles to obtaining high resolution spectra of solids can now be removed by the application of a number of sophisticated techniques.

These are: a) High power decoupling,

b) Magic angle spinning (MAS)

c) Cross polarisation (CP) (proton enhancement).

a) High power decoupling:- In ^{13}C NMR we are dealing with dilute nuclei in a 'sea' of abundant nuclei - usually protons. It is these abundant nuclei which produce most of the dipolar broadening. This effect can be eliminated by what is called high power decoupling. By irradiating all of the protons with a rf field of sufficient frequency range all of the protons can be brought into resonance. At resonance the magnetic moment of the proton rotates and is time-averaged to zero. Therefore this magnetic moment has no effect on the ^{13}C nuclei which are now said to be decoupled. This double resonance technique gives considerable sharpening of resonance lines.

It should be noted that this technique can only remove the dipolar interactions of heteronuclear systems. Homonuclear dipolar interactions can only be removed by magic-angle spinning.

b) Magic-angle spinning (MAS):- Homonuclear dipolar interactions, quadrupole interactions and chemical shift anisotropy effects can only be removed by ' magic-angle spinning'. All of these interactions or effects depend on the angle between the applied magnetic field and the axis joining the two interacting centres. It just so happens that for a particular angle $\emptyset$ = 54°44' no interaction is experienced. Thus by spinning the sample at this angle all anisotropic effects are eliminated and solid state resonances are sharpened considerably.

c) Cross-Polarisation:- In order to circumvent the long relaxation times of ^{13}C nuclei the method of cross-polarisation was developed. Without going into the details of

this technique too far, it can be said that it relies on the transfer of energy or polarisation between ^{1}H and ^{13}C nuclei. This thermal contact (Hartmann-Hahn condition) enables ^{13}C nuclei to relax via the protons which have much shorter relaxation times(T_{1H}). Thus the protons can be considered as a 'heat sink' for hot ^{13}C nuclei. Measurement of these proton relaxation times is therefore necessary so that a sufficiently long repetition rate is used such that saturation of the carbon nuclei does not occur. Thus cross-polarisation allows for higher repetition rates to be used thereby reducing instrument time and improving the signal to noise ratio.

The Dipolar Dephasing Technique.

Dipolar dephasing is a technique by which ^{13}C NMR spectra of solids can be simplified by removing the methylene (CH_2) and methine (CH) carbon species from the spectra. This is accomplished using a pulse sequence which introduces a delay after the cross-polarisation contact time and before data acquisition. During this delay the high power decoupling between the ^{1}H and the ^{13}C nuclei is removed and therefore the ^{13}C spins that are strongly coupled to the ^{1}H spins, (CH_2) and (CH), dephase. We are left with quaternary carbons which are not affected as much because they are not directly bonded to a hydrogen atom. Methyl groups also remain but this is due to their molecular motion. By comparing the normal CP spectrum with that obtained using dipolar dephasing, we can resolve the broad resonances obtained for coals and kerogens into more well-defined chemical structures.

Application of Solid State Carbon 13 NMR to Coals and Kerogens.

As mentioned earlier solid state NMR opened-up a new and very important way of analysing the organic structure of coals and kerogens without the need to solubilise or chemically alter them. Subsequently, kerogens and especially coals, have been extensively studied using this technique.

The determination of coal aromaticity (fa values) in coals of different rank has been a frequent use of the solid state technique[93,94,95,96]. Results show that there is a relationship between fa values and carbon content[93]. Such determinations have also been applied to kerogens[97,23] and proposed as a method of classifying them[98] Also a correlation has been found between the fa values of kerogens and their potential oil yield upon pyrolysis[99].

Several workers[100,101,102]have studied individual coal macerals[103] and found structural differences between them. Comparison of the three different types of kerogen have also been made[98].

Other work[104,105] has suggested that coals consist of both a mobile and a rigid phase. This two phase system was used to explain why the measured T_1's had fast and slow components, the fast T_1's being due to the mobile phase and the slow T_1's to the rigid phase. Mobile CH_2 groups were discovered in a Blair Athol vitrain but not in Illinois No.6 Coal [106]. It has also been noted that aliphatic and aromatic protons had different relaxation times[107]. This led to suggestions that the mobile phase of coals resides in the aliphatic structure alone, and that aliphatic and aromatic units are not chemically joined[108].

Two of our kerogens have already been analysed by solid state NMR and the results published[23]. In our present study these have been analysed again along with the three other samples.

A Word of Warning.

Ever since the introduction of cross-polarisation to the study of carbonaceous solids serious doubts have been expressed regarding the quantitative accuracy of this technique[109,110,111].

These doubts mainly arise from speculation that not all of the ^{13}C nuclei will be enhanced equally by cross-polarisation. This is because the efficiency of cross-

polarisation depends upon the proximity of the carbon and the hydrogen atoms transferring energy[110]. Thus non-protonated carbon atoms cannot cross-polarise as effectively as a methine, methylene or methyl group and subsequently their signal may not be enhanced to the same degree. This effect is expected to be largely biased against aromatic systems, especially ones with fused rings because of their lack of protonated carbon atoms. In addition it is possible that some protons relax before cross-polarisation takes place, once again leading to the ineffective transfer of energy. This process is governed by the spin lattice relaxation time of the proton in the rotating frame ($T_{1\rho}$) and results in the decay of the 'spin-locked' ^{1}H magnetisation. If the $T_{1\rho}$'s vary for different chemical structures within the coal or kerogen then the spectra produced by the cross-polarisation experiment may not be quantitative. Thus, in addition to measuring T_{1H}'s (which govern the pulse repetition rate) it is necessary to measure the $T_{1\rho}$'s so that the extent of this possible error can be determined. The optimum cross-polarisation experiment would only be possible when the time required to cross-polarise was much shorter than the contact time which in turn was much shorter than the $T_{1\rho}$'s. Experiments in which the CP contact time was varied showed how important this factor is in determining the spectral shape[107].

Many workers have considered these quantitative aspects of solid state ^{13}C NMR[1,2]. Some have concluded that the results are quantitative[107] but there still remains sufficient evidence for some uncertainties to remain[82]. Thus at present there are still some limitations to the solid-state ^{13}C NMR techniques. There are considerable advances to be made in the optimisation of spectrometer conditions and pulse sequences, especially the contact times and repetition rates. If one is considering aromaticity values then it would appear that the best policy is to regard the values obtained by solid-state NMR as minima[111]. This technique however, is still a very useful tool in the structural

analysis of our materials, especially when it is used in comparative studies where the need for absolute quantities becomes unnecessary.

2.5 GC and GC-MS Analysis.

The detailed analysis of sedimentary organic matter at the molecular level usually requires such material to be in solution. However as we have seen most of this organic matter is insoluble. This insolubility can be overcome to some extent by degrading the insoluble kerogens. (Some degredation techniques are discussed in later chapters of this thesis). The soluble material, no matter how derived, is a very complex mixture of individual compounds. Clearly if these are to be identified then they must be separated from each other. One of the most useful techniques for this is gas chromatography[112].

Gas chromatography, like other forms of chromatography, involves both a stationary phase and a mobile phase. The mobile phase is a gas such as helium or nitrogen which is used to carry the complex mixture over the stationary phase. For this reason it is called the carrier gas. The stationary phase consists of a high boiling liquid, for example a polymethylsiloxane, which is absorbed onto a suitable support material (packed columns) or coated onto the wall of a thin column (capillary column).

On introduction of the sample (usually in solution and by syringe) it is vaporized and swept into the column and over the stationary phase by the carrier gas. Separation of the individual components of the mixture is brought about by repeated absorption and desorption of these components from the stationary phase. The rate of absorption and desorption is governed by the relative volatilities of each component, their solubilities in the stationary phase and whether they interact further with the stationary phase. Because of differences in these properties different compounds travel along the column at different rates and if the column is of sufficient length individual compounds emerge

separately in the effluent stream and are detected.

If the conditions of the analysis are kept constant, for example the column temperature and carrier gas flow rate, an individual component will take the same time to be eluted from the column in many repeated analyses. This time is called the retention time and is a characteristic of that compound. By calibration with pure authentic compounds the unknown compounds in the complex mixture may be identified and quantified. This can only be done if separation is complete, ie if there is no overlap of unknown compounds, and if no two or more pure samples have the same retention time.

To overcome these restrictions one can replace the normal flame ionisation detector with a mass spectrometer to give a combined gas chromatograph - mass spectrometer (GC-MS)[113]. The structure of each component can then be determined as it is eluted from the column without having to refer to authentic samples and retention times (although this is often very useful). Many different geochemical samples, for instance crude oils[114,115,116], bitumens[117,118,119,120], shale oils[46,121] and degradation products[24,122,123] are now analysed using this GC-MS technique.

Mass spectroscopy can determine the molecular weight of a compound (assuming that a molecular ion can be seen). The determination of empirical formulae from molecular weights is possible so long as the mass spectrometer has sufficiently high resolution. Even with low resolution instrumentation it is often possible to obtain sufficient information to assign molecular structures with a high degree of certainty.

When a component reaches the source of the mass spectrometer it is ionised by an electron beam (usually 70eV) to give the molecular ion and a series of fragment ions which are then separated out according to their mass to charge ratio (m/z). Fragment ions are very important because they are produced by the cleavage of bonds in the molecule. They are therefore characteristic of certain molecular entities and can give an indication of the structure of the molecule. For example alkyl chains can be

recognised by the fragment ions which arise from the successive loss of CH_2 groups. Likewise phenyl derivatives can be recognised because they give an intense fragment ion at m/z 77, corresponding to the $C_6H_5^+$ ion[124]. This property of the fragment ions allows many classes of compounds to be detected and their structures assigned. Table 2.5 shows some of the common compound classes and their characteristic fragment ions.

Modern instruments with advanced data handling facilities can produce plots of elution time vs the intensity of any specific ion of interest, for instance the fragment ions in table 2.5.

Table 2.5 Common compound classes and their characteristic fragment ions.

Fragment ion (m/z)	Compound Class
71, 85, 99	n-Alkanes, branched alkanes
77, 91, 105, 106, 119, 120	Benzene and substituted benzenes
82, 83	Cyclohexanes
93	Phenoxy derivatives
97	n-Alkenes
113, 183, 197	Acyclic isoprenoids
109, 123, 194, 208, 222, 236	Bicyclic sesquiterpenoids
109, 123, 163, 191	Diterpenoids
123, 163, 191	Tricyclic and tetracyclic terpanes
143	Naphthoxy derivatives
149, 163, 177, 191, 205, 219	Pentacyclic hopanes
177	Demethylated hopanes
189, 231	Certain hopenes
243	Fernenes
217	Regular steranes (14α(H), 17α(H)
218	Regular steranes (14β(H), 17β(H)
231	Methylsteranes
232, 259	Rearranged steranes (diasteranes)
273	Methyl diasteranes
253	Monoaromatic steranes
231, 245	Triaromatic steranes
154	Diphenyl
156, 141	Dimethyl naphthalenes (141<156)
	Ethyl naphthalenes (156<141)
170, 155	Trimethyl naphthalene (155<170)
	Methyl ethyl naphthalene (155>170)
178	Anthracene, phenanthrene
202	Pyrene, Fluoranthene
228	Chrysenes

These plots (chromatograms) only show those components of the mixture which contain structures of the type characterised by this fragment ion. These chromatograms are called single ion chromatograms (SIC's). This type of treatment has been used extensively in the analysis of geochemical samples particularly in the identification of biomarkers (biologically derived molecular fossils having a structure characteristic of a particular source material)[125,126].

Despite the useful information that can be provided by GC and GC-MS analysis, there are still a number of problems that arise in the analysis of complex mixtures. Firstly, there is no guarantee that absolute separation will be achieved and therefore there is still the possibility of having to analyse a mixture, albeit much simpler. Secondly, many compounds give unstable molecular ions which are not detectable by GC-MS. This can lead to errors in structural assignment. Thirdly, both GC and GC-MS are restricted to the fraction of the injected sample which is volatile under the conditions used. Practically, this usually limits the analysis to compounds with boiling points below 500-550°C. However it is possible to increase the volatility of some compounds by removing their intermolecular attractions (eg hydrogen bonding) by derivatisation. This is normally achieved by silylating alcohols, amines and phenols[127] and methylating carboxylic acids[128]. Nonetheless high molecular weight compounds (MWt >500-600) will still be involatile and must be detected by means other than GC or GC-MS. One such method is gel-permeation chromatography.

2.6 Gel Permeation Chromatography.

Gel permeation chromatography (GPC)[129,130,131] or size exclusion chromatography is a method by which components in the liquids derived from sedimentary organic matter may be fractionated according to their molecular weights.

Fractionation is achieved by passing the sample through a column packed with beads of a cross-linked polymer gel (stationary phase) under a positive solvent pressure of 500-3000psi (mobile phase). As the sample passes along the column smaller molecules can enter the beads of polymer gel and are slowed down, whilst the larger molecules flow around the beads largely unrestricted. This results in the high molecular weight material eluting before the low molecular weight material and thus a molecular weight distribution is obtained. In addition, the number average molecular weight (Mn), the weight average molecular weight (Mw) and the polydispersity (PD) or heterogeneity index can be determined. These terms are defined by the equations:

The number average molecular weight is defined:

$$Mn = \frac{\sum N_i M_i}{\sum N_i}$$

Where Mn = Number average molecular weight

N_i = number of molecules of species i

M_i = molar mass of species i

The weight average molecular weight is defined:

$$Mw = \frac{\sum w_i M_i}{\sum w_i}$$

Where Mw = weight average molecular weight

w_i = Weight fraction of species i

M_i = molar mass of species i

The polydispersity or heterogeneity index is given by the quotient Mw/Mn and as its name implies measures the spread or heterogeneity of molecular weights. Because of the way Mn and Mw are calculated values of Mn are biased towards lower molecular weights whereas the values of Mw are biased towards high molecular weight components. This explains why Mw values are usually greater than Mn values.

In effect it is not really the molecular weight which determines the rate of elution, but molecular size. Size is a rather vague concept because it depends on a number of factors including; molecular weight, solvated molecular volume and hence solvent, actual molecular orientation and the presence of functional groups within the molecule[132]. Such functional groups may also interact with the column packing to produce other non-size dependent effects. These variables make it necessary to calibrate the GPC column with a host of different compounds in order to determine the molecular weight vs elution volume relationship for each type of compound[133]. For example straight chain alkanes and polycyclic aromatics of the same molecular weight will not have the same elution volume and therefore calibration with both types of compound is necessary. However samples derived from sedimentary origin are far too complex for an accurate calibration by one or even a series of simple molecules[134,135] to be obtained. Other problems arise from the methods used to detect the amount of material eluted from the column throughout the experiment. It is customary to use either an ultra-violet (UV) and/or a refractive index detector, neither of which can accurately quantify the eluting material. This is because the UV detector only registers an eluting compound if that compound has a chromophore that absorbs at the wavelength at which the detector is set. Thus many compounds may pass undetected. Even if they are detected the UV response depends on their extinction coefficients as well as their amount. The refractive index detectors suffer from the same type of problem. They measure the refractive index difference between the eluting solution and the pure solvent. Since the refractive indices of organic molecules vary, the refractive index detector response does not solely measure the amount of material in solution. However, the refractive indices of organic molecules do not vary that much (no-where near as much as UV extinction coefficients do) and the RI detector response is preferable. The only way to quantify the eluting

material is to use preparative GPC equipment so that you can actually weigh the material eluting at different elution volumes. Unfortunately this apparatus was not available to us. Apart from calibration and detection difficulties other errors are introduced by the adsorption of certain molecules onto the column packing. Also it is possible for some molecules to aggregate together thereby giving a falsely high molecular weight[133]. In spite of this GPC has received constant use in the analysis of coal liquids[136,137,138].

Thus GPC can not produce absolute molecular weight values for liquids of geological origin. However the values obtained can be quoted in terms of calibrant equivalent molecular weights (polystyrene was used in our work) which can then be used in comparative studies. It is possible therefore to get some indication of molecular weight variations between samples and the effects of certain chemical reactions upon them.

Chapter 3.

The Isolation and Instrumental Analysis of the Whole Organic Matter in Oil Shales.

Chapter 3

The isolation and Instrumental Analysis of the whole organic matter in Oil shales.

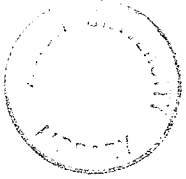

3.1 Introduction.

As mentioned in chapter two it is necessary to isolate the organic matter in a sedimentary rock before its structure can be determined. Once this has been achieved separation into the kerogens and bitumens by solvent extraction is required so that each can be analysed independently.

3.2 Isolation and Separation of Organic matter.

Details of the procedures used in the acid demineralisation of the rock samples are given in the experimental section (Chapter 8) of this thesis. The effects of the combined HF and HCl treatment on the dissolution of the minerals are given in table 3.1 below.

Table 3.1 Organic content of acid demineralised organic concentrates.

	Organic Content Wt%				
	KC	JC	OC	CH1	CH2
Untreated Rock	4	19	8	41	31
After acid demineralisation	40	70	69	88	72

As can be seen from table 3.1 the initial organic content of the oil shales varied from about 4% in KC to about 41% in CH1. (These figures are calculated on the actual amount of organic matter isolated from 100g of ground rock by acid demineralisation and lithium aluminium hydride reduction). The effect of the acids can be clearly seen. For each of the five samples the organic content of the demineralised product is much higher than that of the original oil shale. However the organic content is still fairly low, especially in the case of KC which still contained 60% mineral. Despite repeated HF and HCl treatments very little improvement in the mineral/organic ratio could be achieved. It was therefore concluded that the remaining minerals were either pyrite (a

notoriously difficult mineral to dissolve) or neoformed complex fluorides. To see if the remaining mineral was pyrite the combustion ashes were tested for the presence of iron. A positive test was obtained for each sample. In addition, each acid demineralised sample was subjected to sulphur analysis using both the Eschka method (see experimental chapter) and the Carlo Erba auto analyser. If pyrite (FeS_2) were the offending mineral, then there should be a correlation between sulphur contents and mineral content in the acid demineralised organic concentrates. The results of the sulphur determinations are given in table 3.2.

Table 3.2 Sulphur and mineral contents of acid demineralised organic concentrates.

	Acid demineralised sample				
	KC	JC	OC	CH1	CH2
Sulphur Content	31.4	9.7	17.0	7.7	7.1
Mineral Content	60	30	31	12	28

When the sulphur content is plotted against the mineral content for corresponding organic concentrates, Figure 3.1, we can see that the plots for KC, OC and CH1 are very close to the expected correlation, ie all mineral in these samples is pyrite. Both JC and CH2 fall well below the expected correlation whilst KC falls only very slightly below. These results can be explained by the presence of minerals other than pyrite in the acid demineralised organic concentrates, which of course leads to a sulphur content that is too low (that is if these other minerals have no sulphur). These minerals are likely to be neoformed complex fluorides. Both CH1 and OC have slightly more sulphur than can be explained by pyrite alone, which is probably due to organic sulphur that is present in the organic concentrates. It is likely that organic sulphur functions are present in all five samples, but with the KC, JC and CH2 samples, due to the presence of minerals other than pyrite, this is not apparent from the graph in figure 3.1.

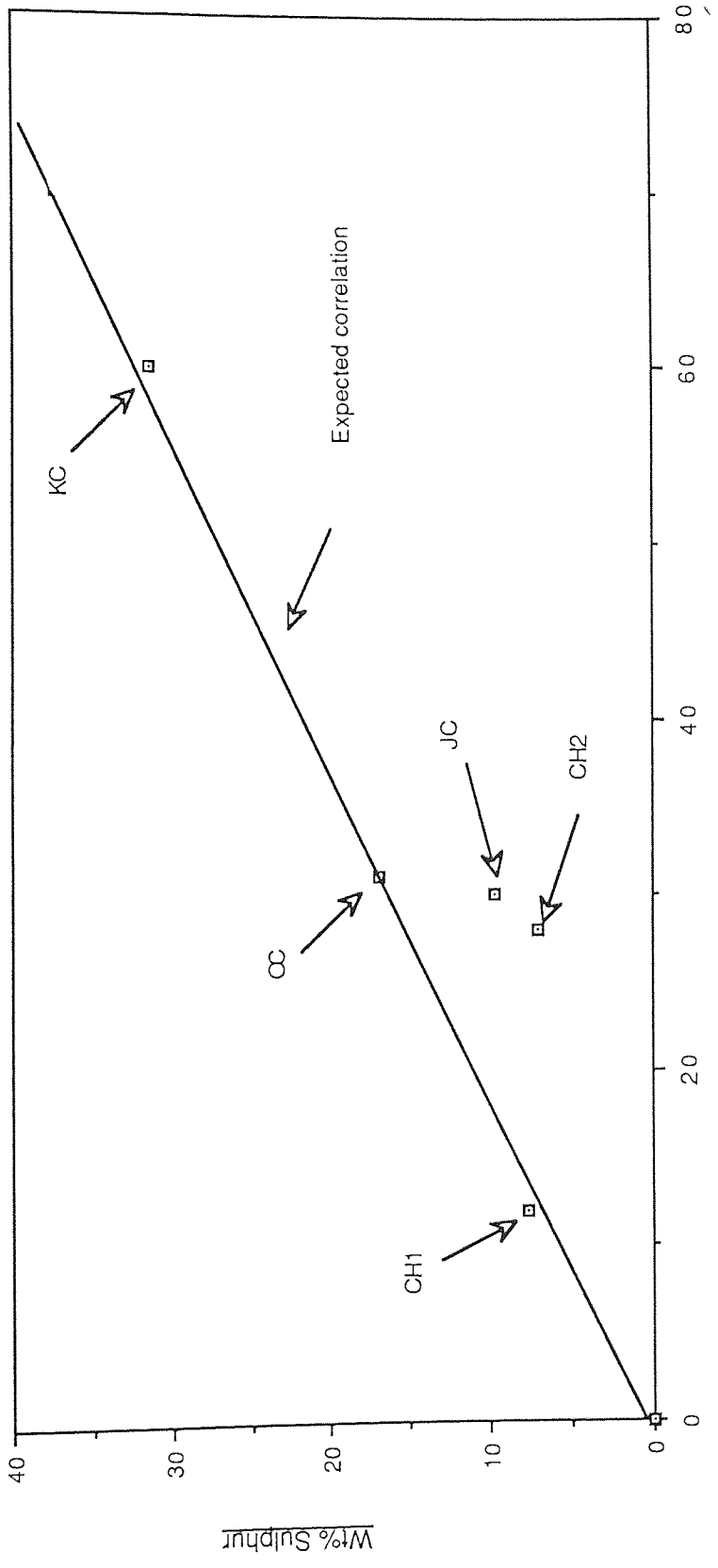

Figure 3.1 Wt% Sulphur vs Wt% Mineral for Acid Demineralised Organic Concentrates

Pyrite was subsequently removed by lithium aluminium hydride reduction. The organic matter would also be partially degraded by this reagent, this problem is dealt with in chapter 4.

The acid demineralised organic concentrates were extracted with pyridine as described in the experimental chapter. The unfractionated pyridine extracts proved difficult to analyse because residual pyridine interfered in all spectral determinations. For example pyridine absorbs in the aromatic region of an NMR spectrum and therefore obscures any aromatic signals that may arise from the bitumen. This is true also of UV-vis spectral analyses. IR analysis also showed residual pyridine contamination. Finally pyridine was found to tail very badly on the GC columns thus interfering with GC-MS analysis. Thus it was found necessary to fractionate the pyridine extracts into chloroform solubles and insolubles to facilitate their routine analysis.

Once this fractionation had been achieved the physical properties of the residual pyridine extracts (those fractions not soluble in chloroform) were found to be improved and it was possible to characterise them by FTIR and some NMR spectroscopy. From here on the two fractions produced by this fractionation, the chloroform soluble and the pyridine soluble but chloroform insoluble fractions, will be described as the chloroform bitumens and the pyridine bitumens respectively.

The results of the pyridine extraction of the organic concentrates and the subsequent fractionation of the pyridine extracts are given in table 3.3 overleaf. As can be seen from table 3.3 solubility varied from sample to sample. Also slightly more than half of each pyridine extract dissolves in chloroform. Total solubility of the pyridine extract in chloroform was not expected since pyridine is the stronger solvent (more polar/basic) and therefore it would be anticipated that some of the pyridine soluble material would not be sufficiently solvated to dissolve.

The separated bitumens and kerogens were then analysed independently.

Table 3.3 Solubility of acid demineralised organic concentrates.

	Solubility*				
	KC	JC	OC	CH1	CH2
pyridine	17.0	10.5	7.4	6.0	6.5
$CHCl_3$ soluble py ext	11.1	7.2	4.0	3.0	3.5

* Values correspond to Wt% solubilities based upon a dry mineral free basis.

3.3 The analysis of Bitumens.

As we have seen, bitumens are soluble in organic solvents and are therefore amenable to analysis by a great number of analytical techniques. Bitumens are mainly the products of the natural degradation of kerogens, ie. those products formed during the burial of a kerogen and its exposure to the geothermal gradient. The physico-chemical processes that occur during burial, take place at relatively low temperatures, and therefore it is very probable that the structures found in bitumens represent structures that were once an integral part of the kerogen. For this reason the study of bitumens leads not only to their own eventual characterisation, but can also give an insight into the structure of their associated insoluble kerogens. From such information it is possible to postulate the possible source organisms for these materials, the conditions under which deposition occurred and the relative maturity of the deposit.

The chloroform bitumens were analysed by FTIR, ^{1}H and ^{13}C NMR, GC-MS, UV-vis spectroscopy, GPC and elemental analysis. Pyridine bitumens were analysed by FTIR, NMR and elemental analysis. The results of these analyses are presented in the following sub-sections.

3.3.1 Elemental Analysis of Bitumens.

Elemental analyses were carried out and empirical formulae calculated for both the chloroform and pyridine bitumens from each of the five organic concentrates. The results are shown in table 3.4

The chloroform bitumens all have high hydrogen to carbon (H/C) ratios with the exception of those from the KC sample. Such ratios have also been noted for chloroform solubles obtained from a pyridine extract of a bituminous coal[139] and are indicative of the presence of highly aliphatic structures, especially long paraffinic chains. The H/C ratio of 1.03 for the KC chloroform bitumens is suggestive of a higher aromatic contribution to the structure. The oxygen contents are seen to vary considerably from sample to sample and this may reflect the degree of weathering undergone by each sample.

Table 3.4 Elemental composition of chloroform and pyridine bitumens.

		Elemental composition				
Bit class	Sample	C	H	N	O	Empirical Formulea
$CHCl_3$	KC	84.9	7.3	ND	7.8	$C_{100}H_{103}O_7$
	JC	74.7	9.6	ND	15.7	$C_{100}H_{154}O_{16}$
	OC	68.4	9.0	0.5	22.1	$C_{100}H_{158}O_{25}N_1$
	CH1	68.2	11.6	0.7	19.5	$C_{100}H_{204}O_{21}N_1$
	CH2	80.0	14.4	0.5	5.1	$C_{100}H_{217}O_5N_1$
pyridine	KC	52.0	3.1	1.5	43.5	$C_{100}H_{72}O_{65}N_2$
	JC	69.7	4.7	4.0	21.6	$C_{100}H_{82}O_{28}N_5$
	OC	62.9	3.8	3.1	30.2	$C_{100}H_{72}O_{40}N_4$
	CH1	68.9	4.8	4.6	21.7	$C_{100}H_{84}O_{29}N_6$
	CH2	66.9	5.0	2.5	25.6	$C_{100}H_{90}O_{31}N_3$

ND = Not detected above background

The pyridine bitumens have lower H/C ratios than their chloroform soluble counterparts. This may indicate that they are more aromatic than the chloroform soluble materials. In addition these pyridine bitumens contain more oxygen and less carbon than the chloroform bitumens but the significance of this is not immediately obvious. It should also be noted that the pyridine bitumens have higher nitrogen contents than the chloroform bitumens. This may be due to retention of pyridine by the bitumens[140] or it may reflect the true nitrogen contents of these bitumens.

3.3.2 Infra-red Analysis of Bitumens.

The FTIR spectra of the chloroform and pyridine bitumens are presented in figures 3.2 and 3.3 respectively. All of the chloroform and pyridine bitumens show the bands expected from a product derived from a fossil fuel. (See chapter 2 section 2.3). Differences between each bitumen spectrum are not in absorptionthe presence or absence of bands, but differences in the relative intensities of bands. In general the spectra of the chloroform bitumens show strong absorptions arising from aliphatic structures whilst in the pyridine bitumen spectra, these are of lower intensity and are accompanied by stronger aromatic and carbon-oxygen absorptions.

The most prominent absorptions in all five of the chloroforrn bitumen spectra are due to C-H stretches of aliphatic groups (2800 - 2950 cm^{-1}). C = O stretches (1680 - 1745 cm^{-1}) and C - H bends from aliphatic groups at 1400 - 1460 cm^{-1} and 1370 - 1380 cm^{-1}. This absorption pattern indicates long aliphatic chains or extensive aliphatic ring systems which possess carbonyl functions at various sites in their structures. A rough guide to the relative average length of alkyl chains or their degree of branching can be determined from the ratio of the peak intensities of the methyl and methylene groups. Thus by ratioing the 2920 cm^{-1} peak (methylene stretch) with the 2960 cm^{-1} peak (methyl stretch) or the 1455 cm^{-1} peak (methyl and methylene asymmetrical bends) with the 1375 cm^{-1}peak (methyl symmetrical

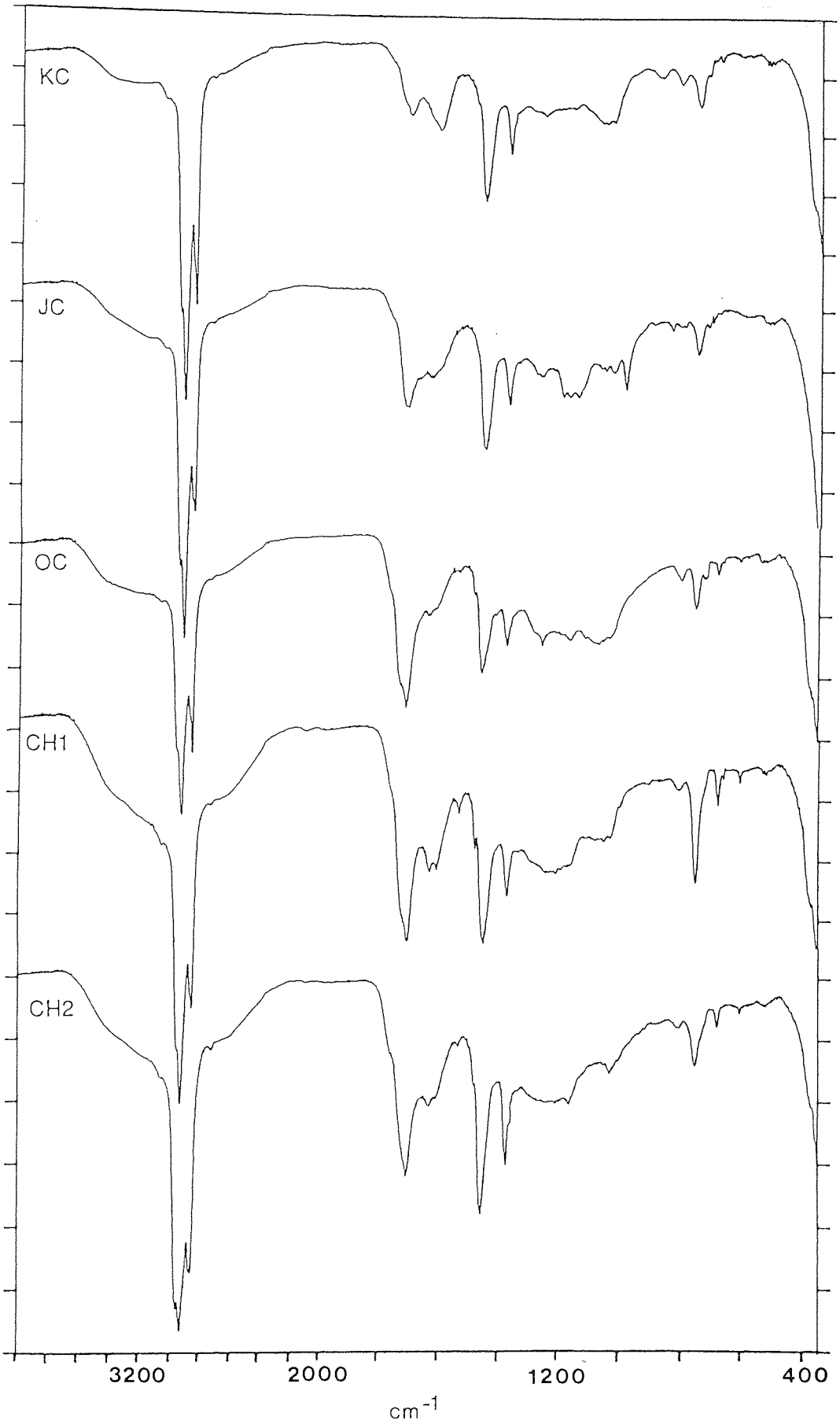

Figure 3.2. FT-IR Spectra of Chloroform Bitumens.

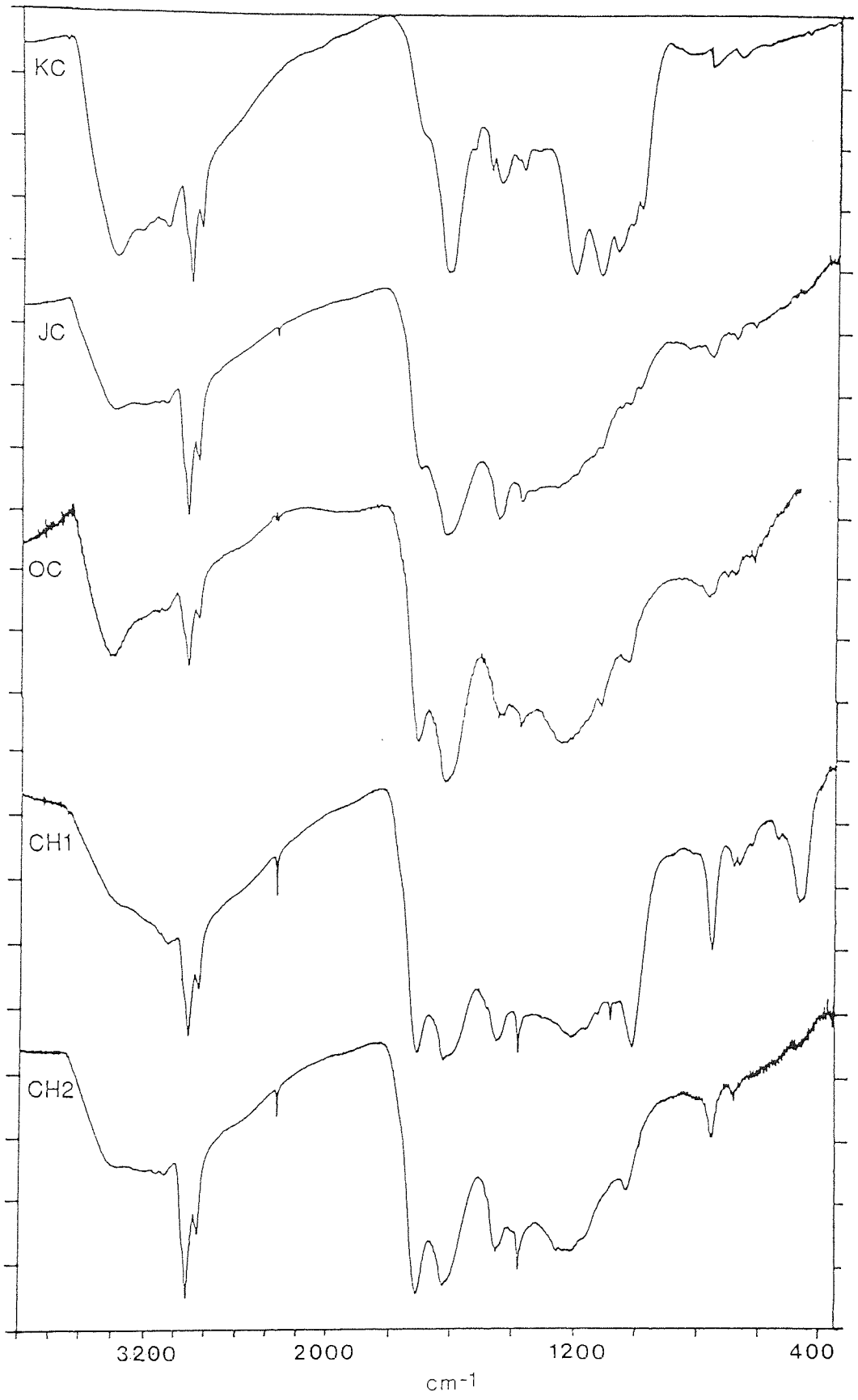

Figure 3.3. FT-IR Spectra of Pyridine Bitumens.

bends), the relative chain length or degree of branching can be measured. Of course this depends upon the assumption that the extinction coefficients of the groups absorbing in these regions do not vary a great deal from sample to sample. If we are dealing with mainly aliphatic chains then this will be true. These ratios were calculated and are shown in (Table 3.5).

The lower the ratio the shorter or more branched is the average alkyl chain. Although there is not a perfect correlation between the two methods used to calculate the average chain length/ degree of branching, it is clear from Table 3.5 that the CH2 chloroform bitumens have the shortest or most branched alkyl chains of the five samples examined. Although it is more difficult to repeat this treatment on the pyridine bitumens, the ratios obtained indicate that average alkyl chain lengths are longer or the degree of branching less in these bitumens compared with their chloroform counterparts.

Table 3.5 CH_2 and CH_3 peak intensities from FTIR analysis of chloroform bitumens.

$CHCl_3$ Bitumen	peak intensity ratios	
	I 2920/2960	I 1455/1375
KC	1.38	2.00
JC	1.31	2.00
OC	1.42	2.00
CH1	1.24	2.13
CH2	1.08	1.72

Where I = intensity

The relative intensities of both the carbonyl and the OH peaka are seen to increase from top to bottom in the spectra of the chloroform bitumens (Figure 3.2). The

increases in these two peaks are strong evidence for an increased carboxylic acid content as we proceed from the KC to CH2 samples. Closer examination of the carbonyl region of the chloroform bitumen spectra reveals some fine structure in each of the five samples. In each case the main absorption occurs at 1705-1715 cm^{-1} but in addition there are two shoulders at 1735 cm^{-1} and 1770 cm^{-1}respectively. Due to the overlap of various carbonyl groups these peaks cannot be assigned absolutely, but it seems likely that the main absorption is due to saturated carboxylic acids. The shoulder at 1770 cm^{-1} is not due to common ketones, aldehydes or carboxylic acids and therefore may be due to esters of some kind. (Some anhydrides absorb in this region but are unlikely to be present in our extracts since they are very easily hydrolysable). If esters are present it is somewhat surprising because one would have expected them to have been cleaved during the acid demineralisation of the rock samples. There is no fine structure observed for the carbonyl absorptions of the pyridine bitumens- the only absorption taking place at 1705 - 1715 cm^{-1} and assignable, as we have seen, to carboxylic acids.

The pyridine bitumen spectra show weaker aliphatic peaks than the corresponding chloroform bitumens. The OH and carbonyl absorptions are stronger in the pyridine bitumens than in the chloroform bitumens which indicates the presence of a higher proportion of carboxylic acids in the former. Other major differences in the IR spectra of the chloroform and pyridine bitumens occur in the aromatic regions. All of the pyridine bitumen spectra exhibit stronger aromatic C-H stretches at 3000-3080 cm^{-1} and C = C ring deformations at 1650 - 1580 cm^{-1} than the corresponding chloroform bitumens.

Thus, from IR analysis it is apparent that the chloroform bitumens are predominantly aliphatic with varying carbonyl contents of which carboxylic acids appear to be the major form. The CH2 chloroform bitumens seem to contain either shorter or more branched aliphatic chains than the other four similarly derived

bitumens. Pyridine bitumens appear to be more aromatic than the chloroform bitumens and possess more carboxylic acid groups. This observation may help to explain why pyridine bitumens only dissolve in pyridine and not chloroform - the strongly basic pyridine being necessary to disrupt the hydrogen bonding between carboxylic acids.

3.3.3 NMR Analysis of Bitumens.

As we mentioned previously there are problems in analysing pyridine bitumens so the bulk of the NMR analysis was concentrated on the chloroform bitumens. The spectra obtained by ^{1}H and ^{13}C NMR of the five chloroform bitumens (KC, JC, OC, CH1 and CH2) are presented in Figures 3.4 - 3.8 respectively. Some pyridine bitumens were redissolved as far as possible in d^{6}-DMSO but these semi-solutions produced only crude ^{1}H NMR spectra. Two such spectra, those from OC and KC, are presented in Figure 3.9 a and b respectively.

3.3.3.1 ^{1}H NMR

The ^{1}H NMR spectra of the chloroform bitumens show two large absorptions in the aliphatic region. These occur at 0.8-1.0 and 1.1-1.4 ppm and are due to methyl groups on aliphatic chains/rings and methylene groups of aliphatic chains/rings respectively.(See chapter 2 section 2.4). The ratio of the methylene peak to the methyl peak in each spectrum can be considered to be a measure of the average chain length or degree of branching along the alkyl chain. Bearing this in mind it is apparent from examination of the CH2 sample spectrum that this particular sample contains either highly branched or comparatively short alkyl chains.

Generally the methylene peak does not show any fine structure (CH2 sample excepted), but examination of the methyl absorptions reveals at least two and possibly three distinct methyl absorptions. This is most pronounced in the ^{1}H NMR spectrum of the CH2 chloroform bitumens where three methyl absorptions can be clearly seen at 0.827, 0.876 and 0.895 ppm respectively. The observation of three absorptions indicates

Figure 3.4. 1H and 13C NMR Spectra of KC Chloroform Bitumen.

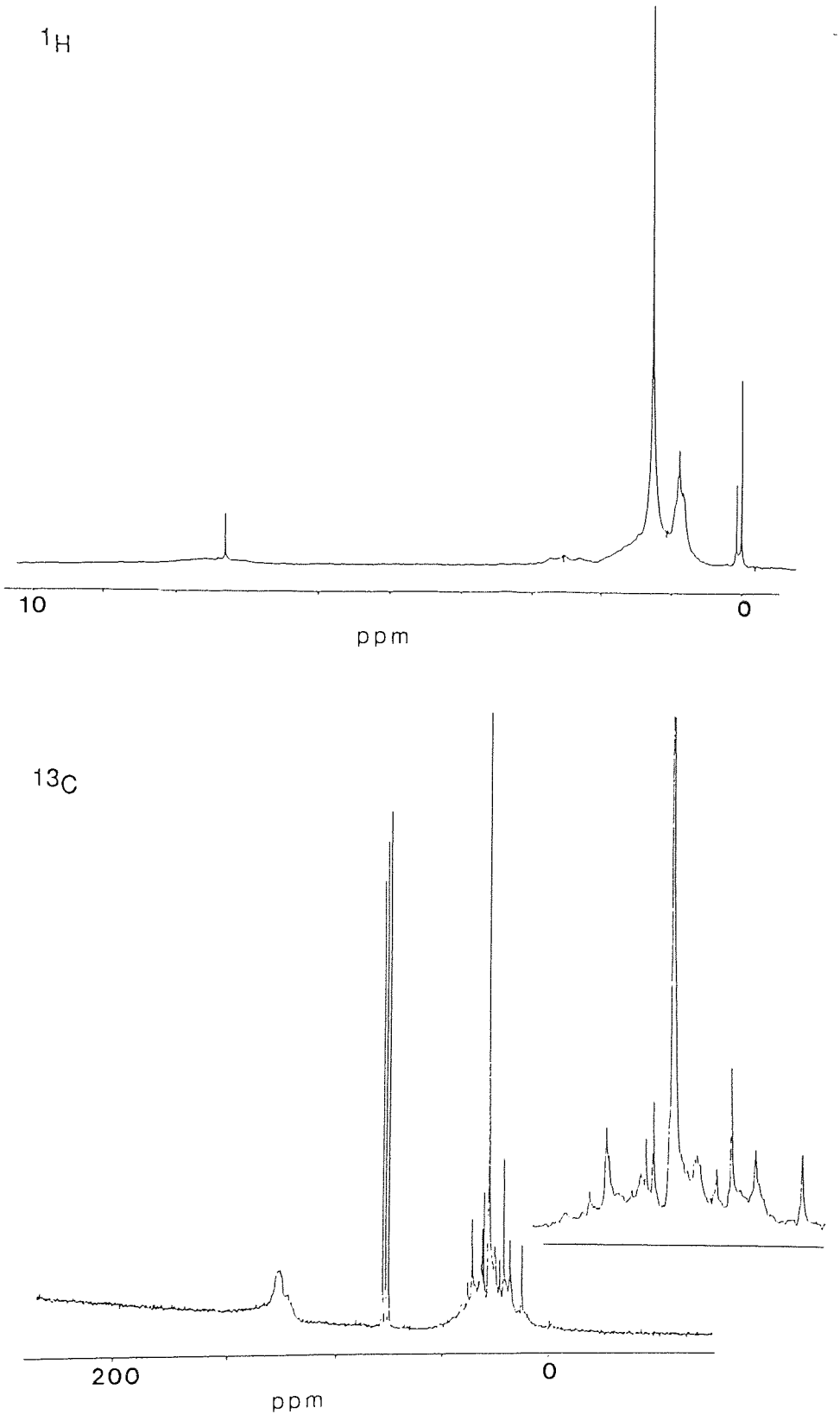

Figure 3.5. 1H and 13C NMR Spectra of JC Chloroform Bitumen.

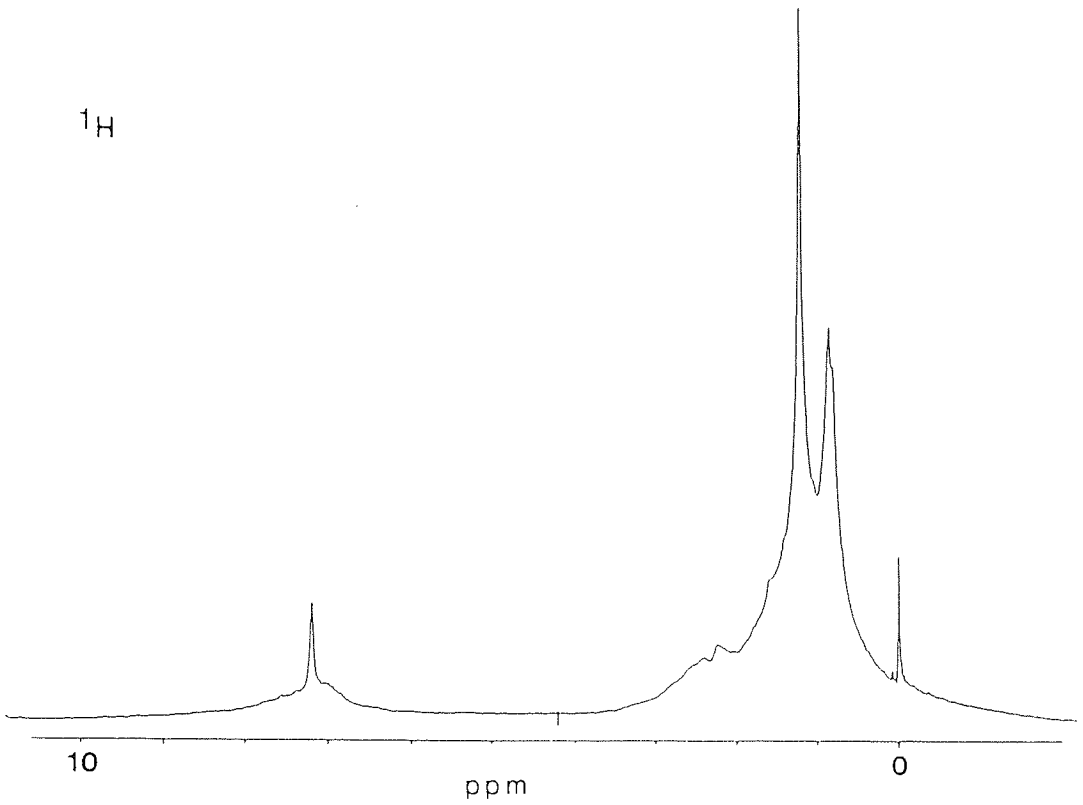

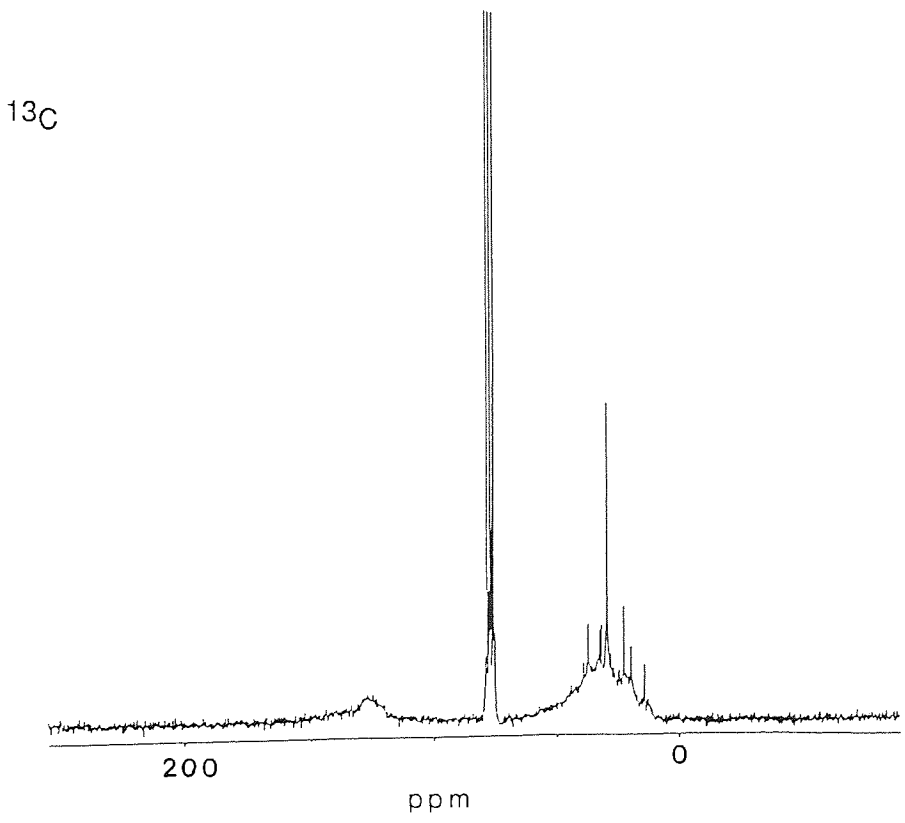

Figure 3.6. 1H and 13C NMR Spectra of OC Chloroform Bitumen.

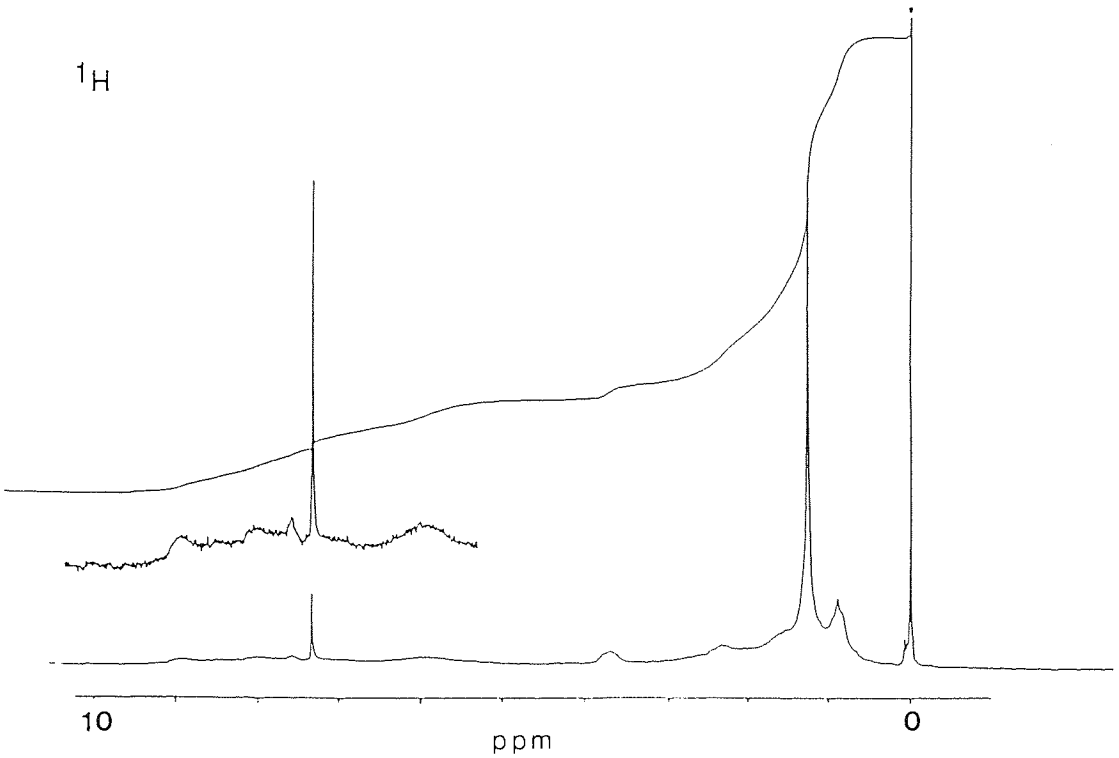

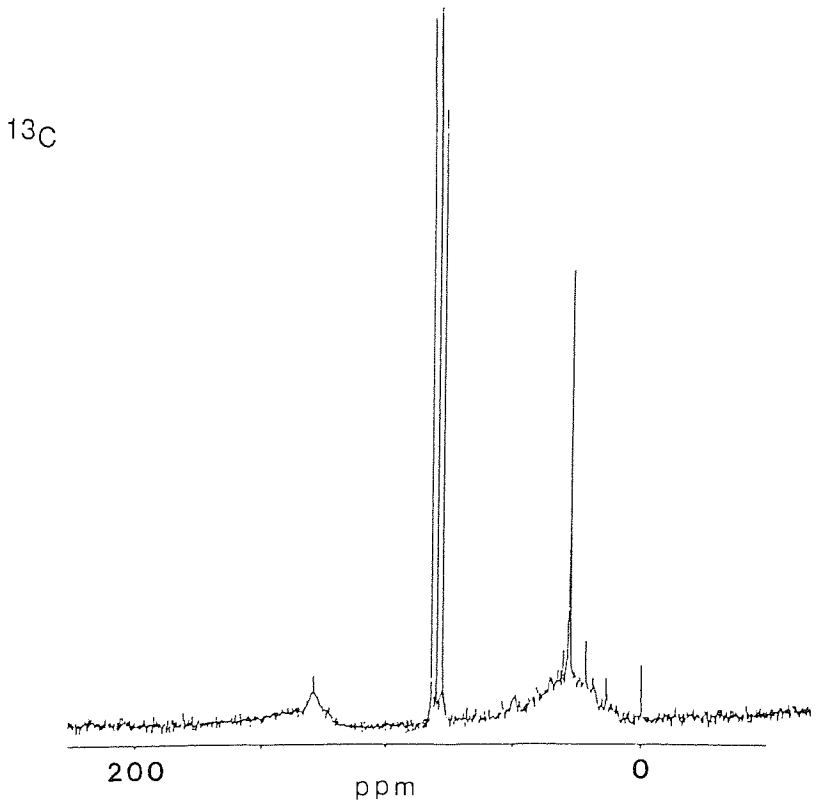

Figure 3.7. 1H and 13C NMR Spectra of CH1 Chloroform Bitumen.

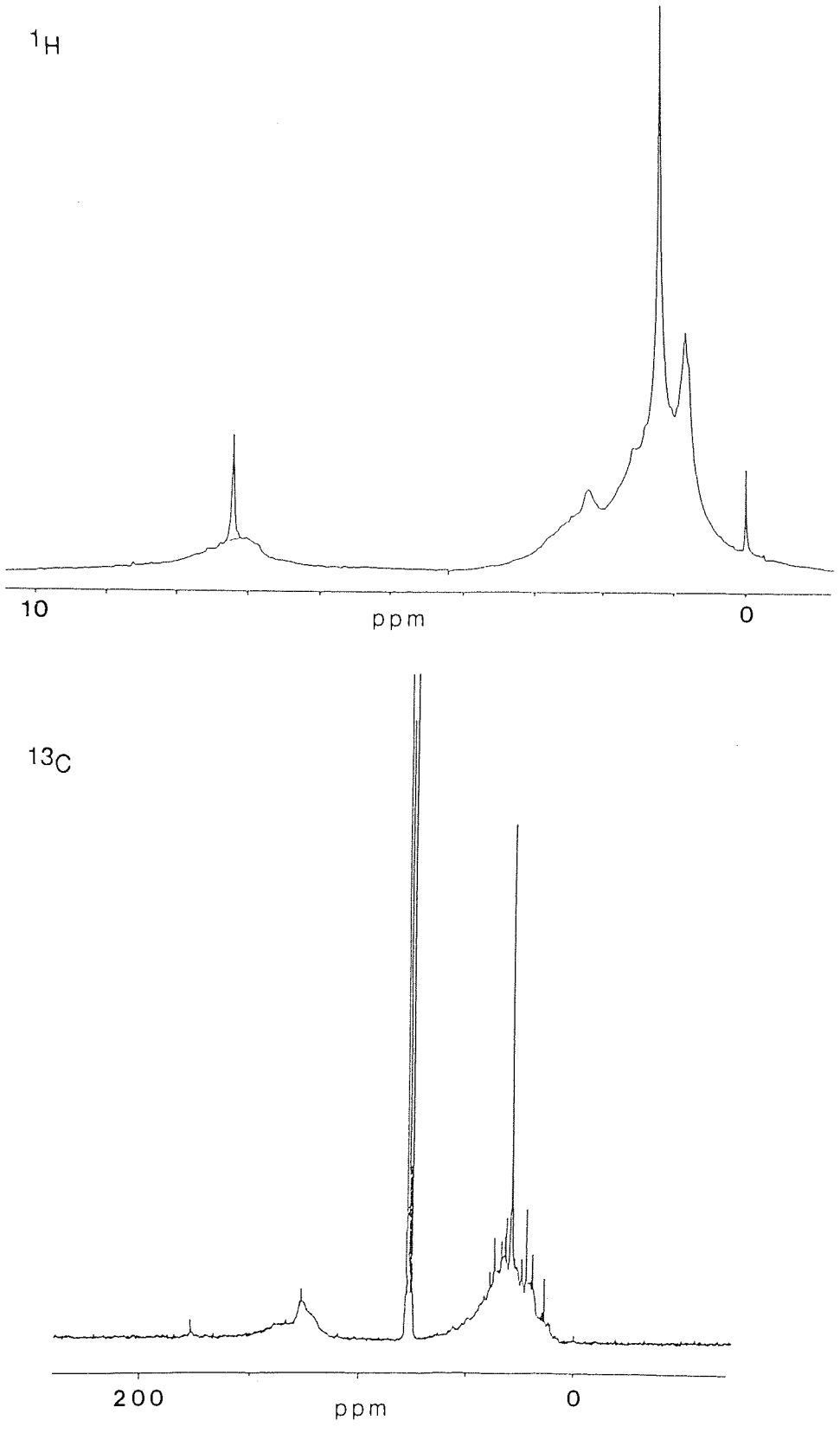

Figure 3.8. 1H and 13C NMR Spectra of CH2 Chloroform Bitumen.

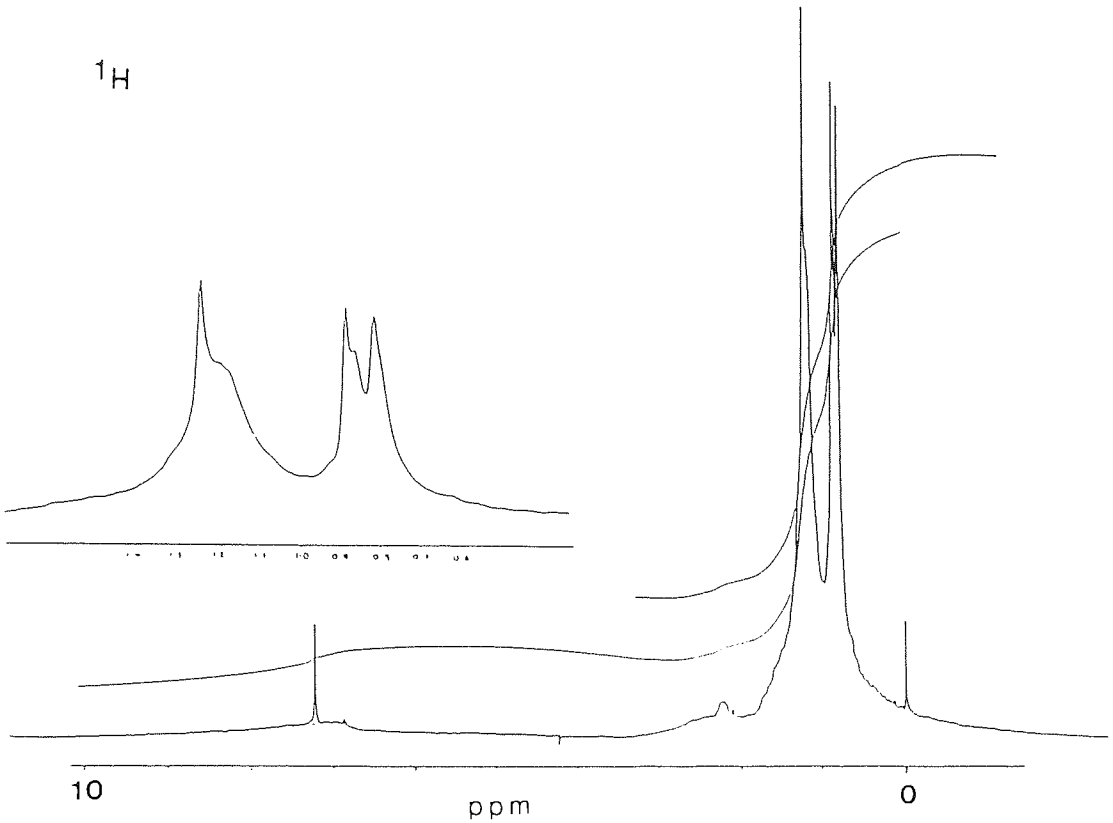

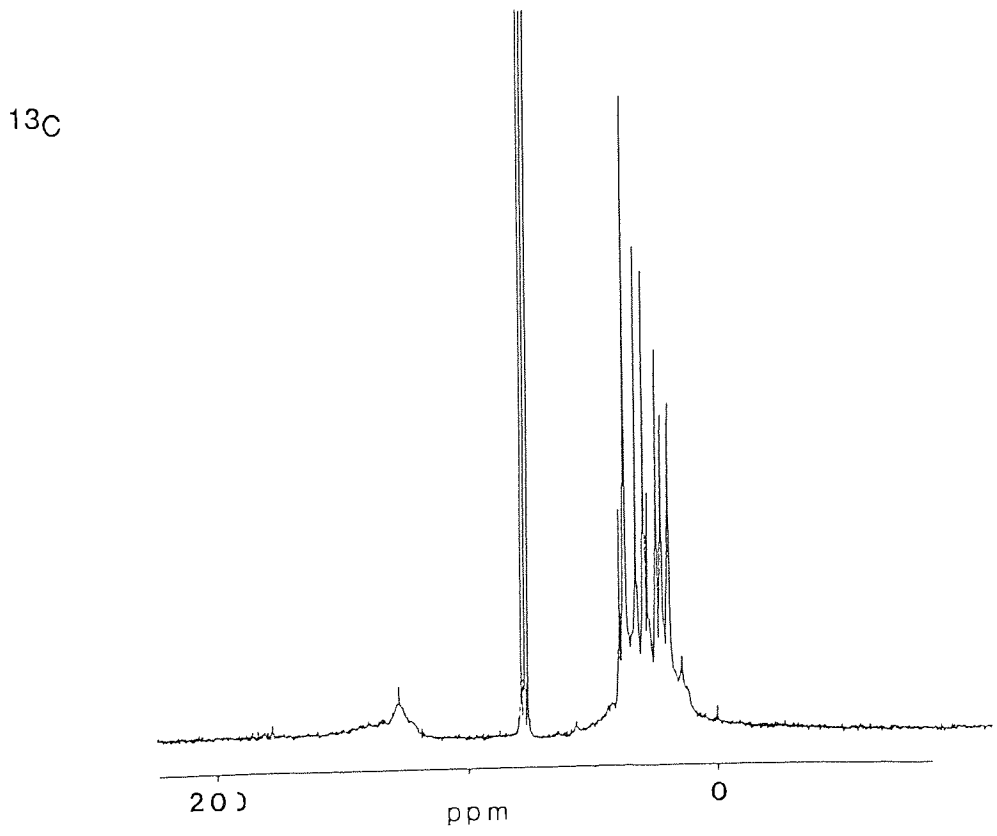

Figure 3.9. 1H NMR Spectra of a) OC Pyridine Bitumens and b) KC Pyridine Bitumens.

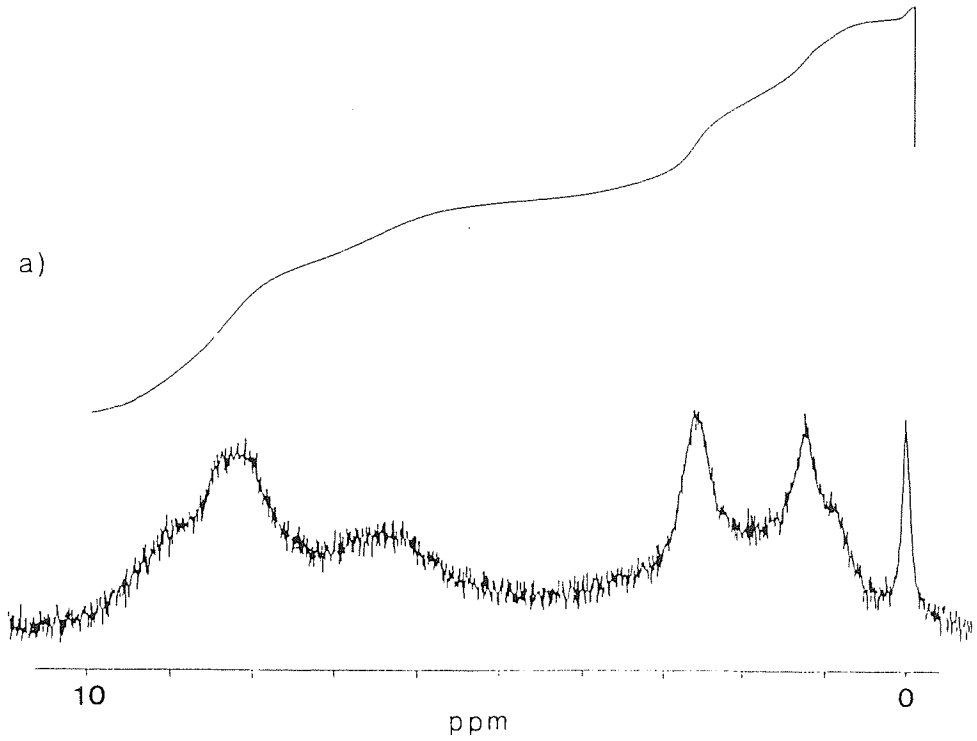

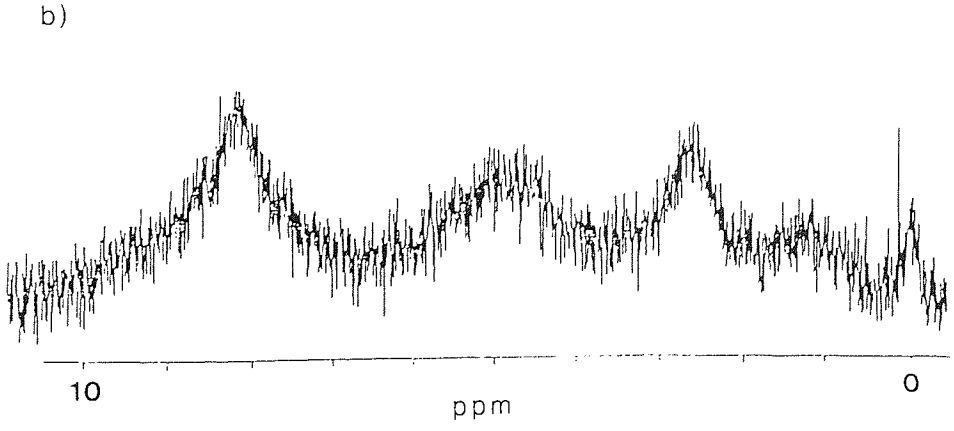

that there are three types of methyl group in this sample which would therefore appear to be a highly branched aliphatic system.

Other peaks in the ^{1}H NMR spectra of the chloroform bitumens are very weak in comparison to these methyl and methylene peaks. There are weak absorptions in the aromatic region (6 - 9 ppm) but one must be careful to take into account the residual proton absorption from the deuterated chloroform solvent which absorbs at 7.3 ppm. Also there are weak absorptions in the 2.2 - 2.3 ppm region which can be attributed to a number of groups including CH_2-O groups and H on carbons α to aromatic rings and $CH_3C{=}O$ groups.

The ^{1}H NMR spectra of the pyridine bitumens (Fig 3.9 a+ b) are of comparatvely poor quality. However we see a significant increase in the aromatic proton absorptions indicating that these materials are much more aromatic than the corresponding chloroform bitumens. This supports the IR data. These spectra are very similar to those published for a SRC asphaltene[141].

3.3.3.2 ^{13}C NMR

Examination of the five chloroform bitumens by ^{13}C NMR spectroscopy reveals two major absorption areas besides that due to the solvent ($CDCl_3$) at 77.7 ppm. These absorptions occur in the ranges 0 - 50 ppm and 110 - 150 ppm and are due to the aliphatic and aromatic carbon atoms respectively. The greater intensity of the aliphatic peaks over the aromatic peaks indicates that these materials are predominantly aliphatic. The aliphatic region is better resolved than the aromatic region, with distinct resonances being easily distinguishable. In the KC, JC, OC and CH1 chloroform bitumens the major aliphatic peak is at 29.8 (+- 0.2) ppm and is due to methylene groups of long linear alkyl chains. Other peaks in the aliphatic region are at 14.1, 19.8, 22.6, 24.4, 31.9, 32.7, 34.0, 37.4 and 39.4 (+-0.2)ppm . These absorptions are much weaker than the 29.8 ppm peak and are due to various methyl, methylene and methine groups in

straight or branched aliphatic chains or rings. The only sample that does not conform to this pattern is the CH2 bitumen. In the ^{13}C NMR spectra of this particular sample the peak of greatest intensity is the aliphatic peak at 37.6 ppm. In general the aliphatic resonances at high ppm values are of greater intensity in this sample than in the others. As can be seen from comparing all five ^{13}C NMR spectra, this is a most striking difference.

The intense 37.6 ppm peak can be attributed to the methylene groups neighbouring the carbon atoms bearing the methyl groups in long isoprenoid chains [142]. These methylene groups are shown below marked *.

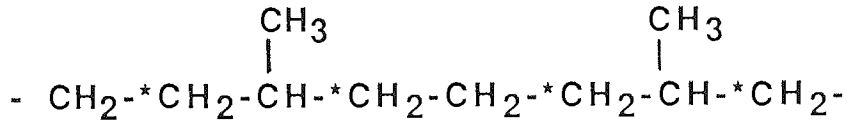

A chemical shift of 39.7 ppm has been assigned to a CH_2 near the terminus of an isoprenoid chain, which explains why a fairly intense peak at 39.7 ppm is also seen in this particular sample. There is another intense peak in the ^{13}C NMR spectrum of the CH2 sample at 33.0 ppm and this is attributed to the methine group of an isoprenoid chain. This assignment is confirmed by some recent NMR analysis of shale oils derived from the Green River Deposits[143]. Thus it would appear that the CH2 chloroform bitumens have a high proportion of isoprenoid alkyl chains when compared to the other four samples, which explains the intense methyl absorptions in the ^{1}H NMR of this sample and supports the IR data discussed previously.

Apart from the aromatic and aliphatic peaks already mentioned, the only other identifiable peaks in these spectra occur in the regions 178-180 ppm and 50-65 ppm. Peaks in these regions can be attributed to carbonyl and methoxy groups respectively.

3.3.3.3 Structural Parameters from NMR Analysis of Bitumens.

The previous section was devoted mainly to the qualitative description of the ^{1}H and ^{13}C NMR spectra, although some brief mention was made of methylene / methyl ratios. This section is concerned with the calculation of further structural parameters.

Although ^{13}C NMR is the most common method for the determination of the carbon atom distribution, ^{1}H NMR can also be used for this purpose and the ^{1}H NMR data, combined with elemental analysis and a few assumptions, are often used to generate structural parameters. For example f_a values can be obtained using the Brown-Ladner equation[144]:

$$f_a = \frac{C/H - H_\alpha/x - H_0/y}{C/H}$$

Where C = Mole % carbon

H = Mole % hydrogen

H_α = mole fraction hydrogen α to aromatic rings

H_0 = mole fraction of aliphatic hydrogen not α to aryl ring

x = average ratio of hydrogen to carbon on carbons α to aryl rings

y = average ratio of hydrogen to carbon on aliphatic carbons not α to aryl rings

C/H is obtained from elemental analysis and H_α and H_0 from the spectral data. The x and y in the equation are assumed to be 2, which is the same as saying that all non-aromatic carbons are predominantly methylene groups. The f_a values can also be determined from the ^{13}C NMR data by simply dividing the peak area for the aromatic carbons by the total area for all carbon atoms. Using both these procedures the following results were obtained. (Table 3.6).

Table 3.6 Brown-Ladner structural parameters for chloroform bitumens.

Bitumen	Sample	C/H	$(H_\alpha/x + H_0/y)$	$f_a{}^1H$	$f_a{}^{13}C$
$CHCl_3$	KC	0.97	0.43	0.55	0.27
	JC	0.65	0.44	0.32	0.18
	OC	0.51	0.40	0.22	0.20
	CH1	0.49	0.44	0.10	0.18
	CH2	0.46	0.46	0.00	0.14
pyridine	KC	1.26	0.23	0.81	-
	OC	1.20	0.24	0.80	-

Although there are large variations between the f_a values calculated for the same bitumen using the ^1H and ^{13}C methods, the trends in the f_a values between the bitumens are consistent. Both methods indicate aromaticity decreases from KC to JC to OC to CH1 and finally CH2. Also the higher aromaticity of the pyridine bitumens compared with the chloroform bitumens is clearly indicated.

The discrepancies between the f_a values calculated by the two methods are probably due to errors in assuming x and y to be equal to 2, and as a result of the nuclear overhauser enhancement (NOE) in the ^{13}C NMR spectra. The NOE depends upon the relaxation mechanism of each individual ^{13}C nucleus. Consequently an uneven enhancement of some ^{13}C nuclei over others is produced and therefore ^{13}C NMR data cannot be considered as wholly quantitative. Methods for the removal of the NOE were not available.

3.3.4 GC-MS Analysis of Bitumens.

No volatile components analysable by GC-MS were detected in the pyridine bitumens. Therefore only the chloroform bitumens, which contained large numbers of volatile species were analysed by GC-MS. The traces produced (called total ion chromatograms (TIC's) from the KC, JC, OC, CH1 and CH2 chloroform bitumens are presented in Figures 3.10 to 3.14 respectively. Also the individual components

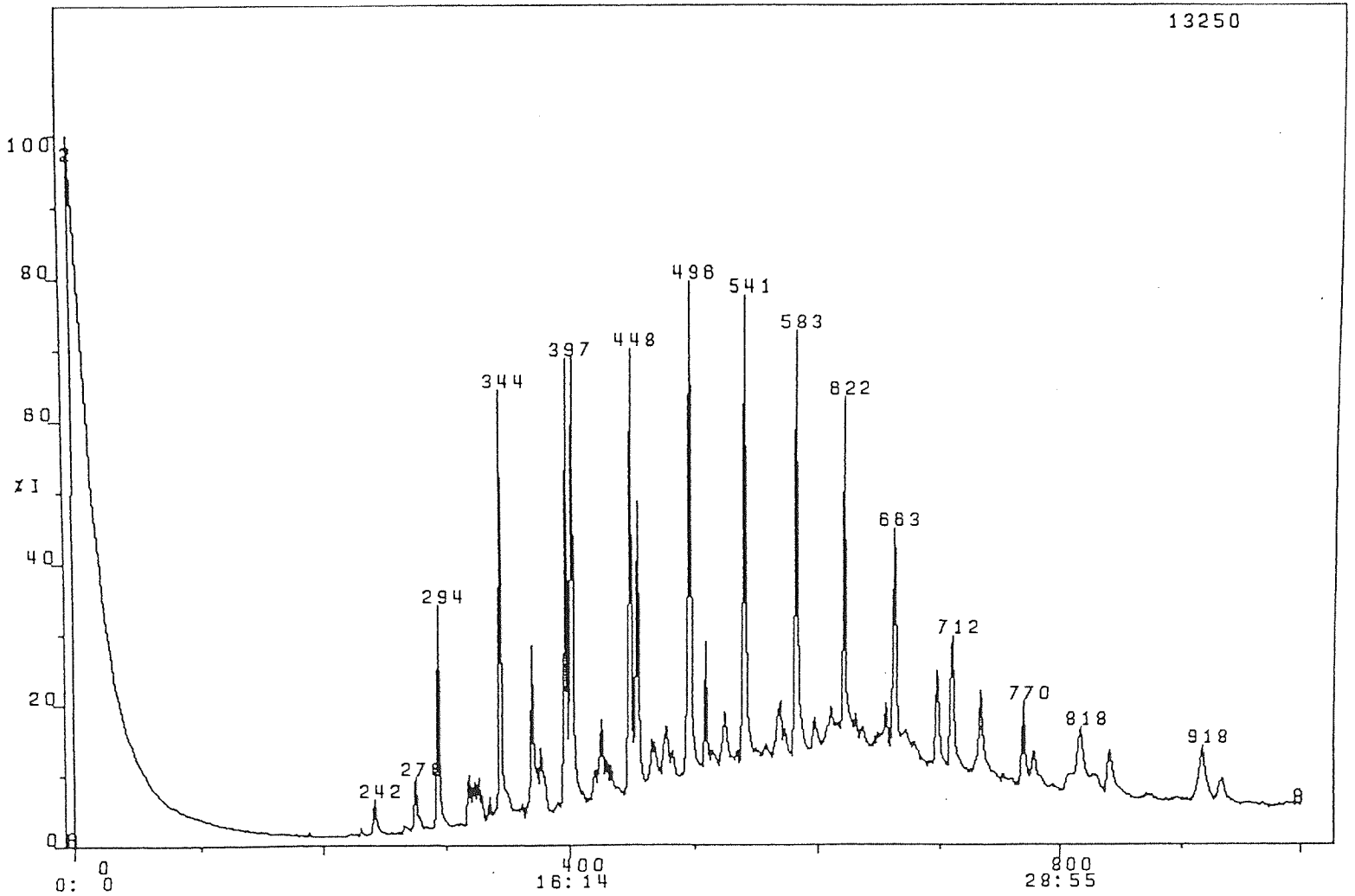

Figure 3.10. GC-MS TIC From KC Chloroform Bitumens.

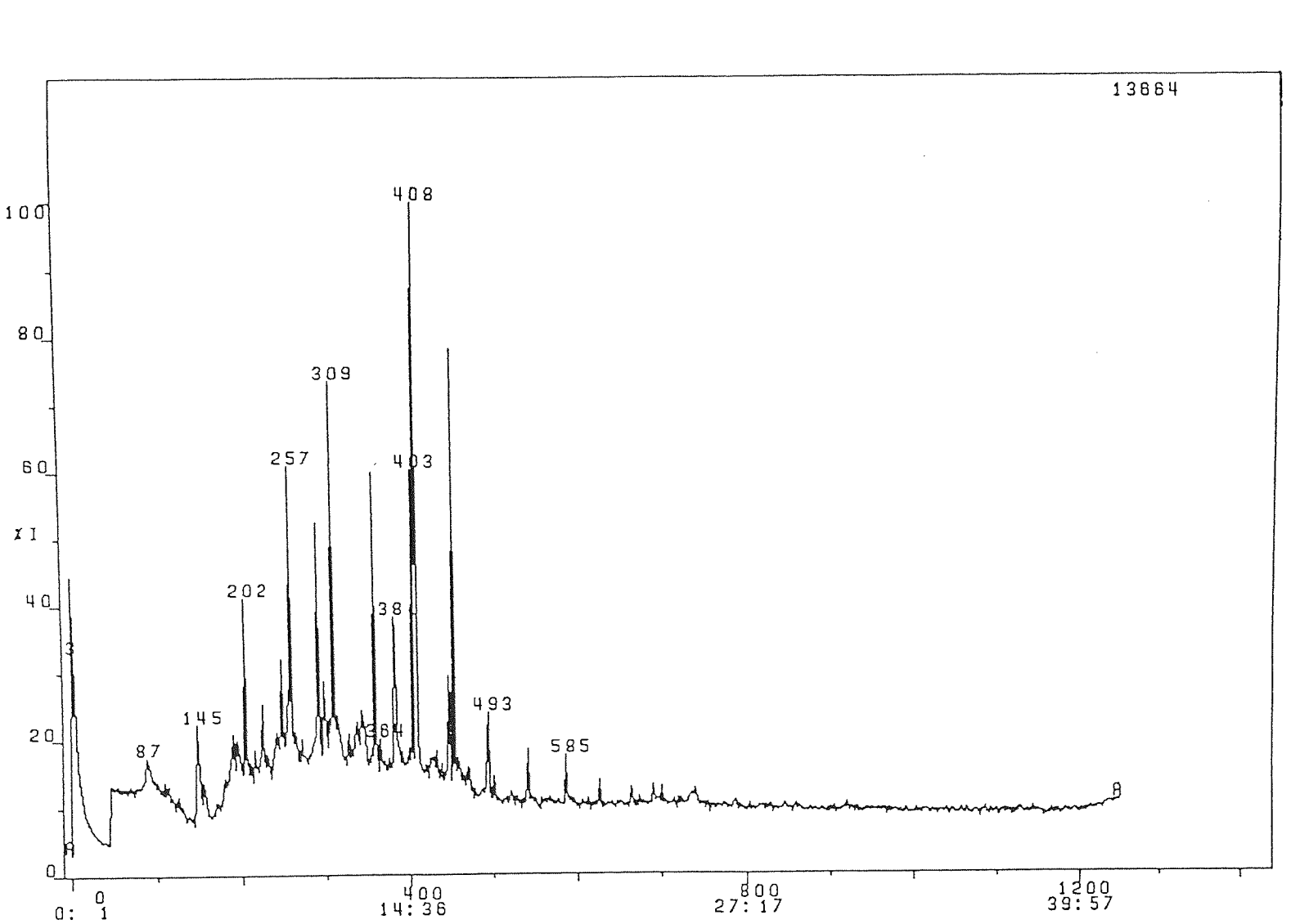

Figure 3.11. GC-MS TIC From JC Chloroform Bitumens.

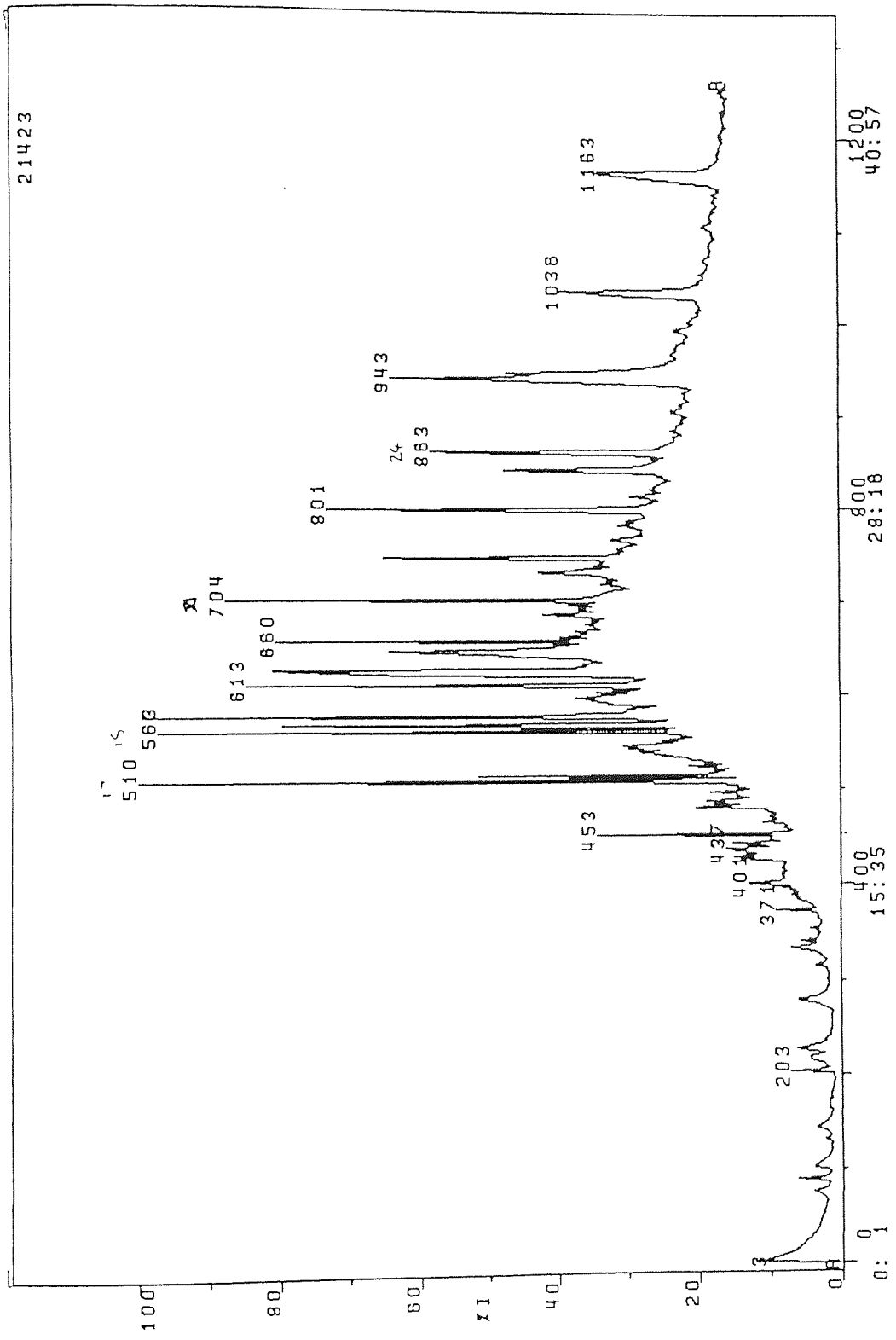

Figure 3.12. GC-MS TIC From OC Chloroform Bitumens.

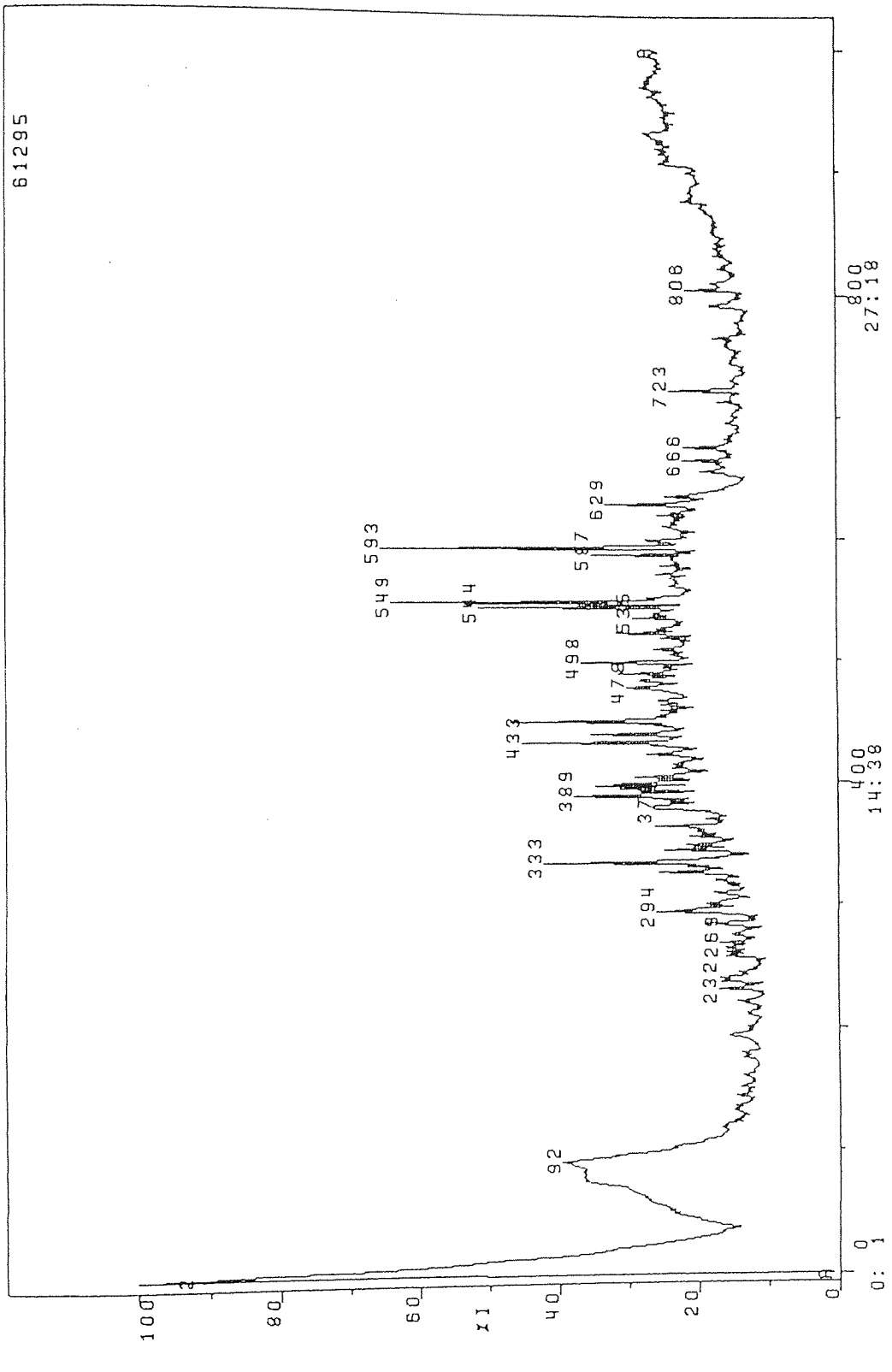

Figure 3.13. GC-MS TIC From CH1 Chloroform Bitumens.

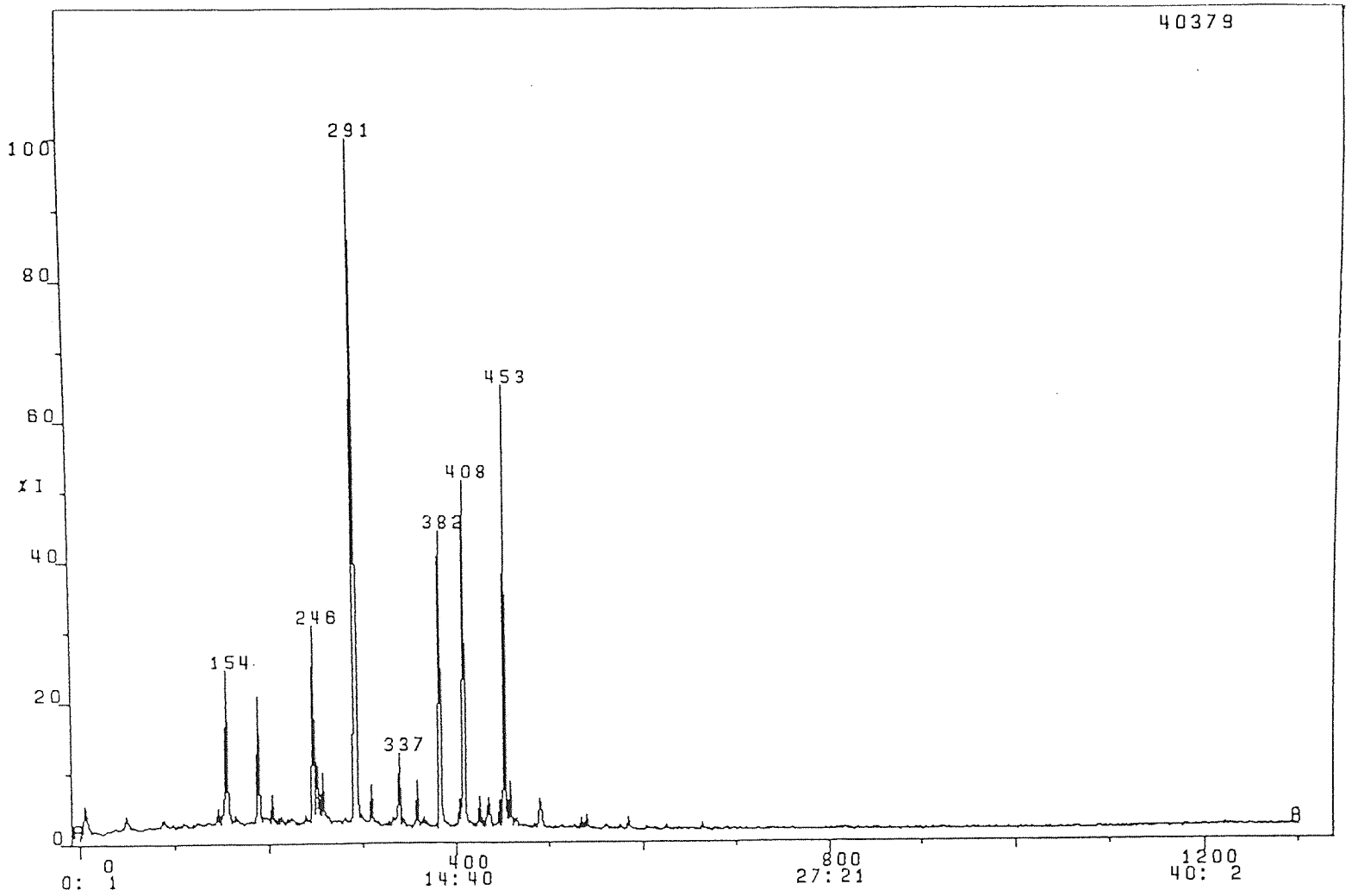

Figure 3.14. GC-MS TIC From CH2 Chloroform Bitumens.

(identified by examination of their mass spectra), from the five samples are recorded in appendix 1 (a-e). The analysis of all five chloroform bitumens is summarised in table 3.7.

Table 3.7 shows a number of parameters which can be used to characterise bitumens and indeed their origins. These parameters include the pristane/phytane ratio, the n-alkane distribution and the n-alkane maxima within those distributions. In addition to these parameters others may be generated from single ion currents for particular ions. (See chapter 2 section 2.5 for the common characteristic fragment ions used). Single ion currents are those currents produced in the detector of the mass spectrometer from that ion specified, and only that ion. The values shown in table 3.7 were obtained from single ion chromatograms (SIC's) of the specified ion and therefore are the sums of all of the single ion currents in all mass scans recorded. In addition the values have been normalised by dividing them by their respective total ion current(the currents produced from ions of all masses and summed over all mass scans). This is explained more clearly by equation 1.

Equation 1.

$$\text{Normalised } SICT_x = \frac{\sum_n \text{Current of ion x}}{\sum_n \text{Current of all ions}}$$

Where x = ion of interest (usually characteristic of a compound class)

n = total number of mass scans

$SICT_x$ = Single ion current for ion x.

This treatment allows for comparisons between samples to be made and the monitoring of their relative composition. Also it enables further parameters to be calculated. For example, the ratio of aliphatic molecules to aromatic molecules (Al/Ar) can be calculated from equation 2 using the derived SICT values for ion characteristic of

Table 3.7. Summary of GC-MS Analysis of Bitumens.

Sample	Normalised Single Ion Currents* x10^3												
	TIC	71+85	77	91	93	141	143	149	191	iso-alkane / n-alkane	n-alkane distrib^n	n-alkane max.	pristane / phytane	aliphatic / aromatic
KC	13250	160	2.6	2.8	4.2	2.6	0	83.7	0	0.26	C_{11}-C_{27}	C_{19}	1.60	13.1
JC	13664	314	6.8	4.6	2.4	18.3	4.1	26.6	1.2	0.81	C_{11}-C_{28}	C_{15}, C_{17}	1.28	11.4
OC	21423	274	9.5	7.3	15.6	4.3	2.1	191	1.6	0.22	C_{14}-C_{27}	C_{17}, C_{23}	0.65	7.1
CH1	61295	133	8.0	6.3	2.7	39.2	6.2	24.5	0.6	0.65	C_{11}-C_{28}	C_{15}, C_{17}, C_{21}	0.91	2.1
CH2	40379	202	0.7	0.7	0	18.5	0	1.5	0	6.67	C_{11}-C_{24}	C_{14}	0.75	10.2

aliphatic and aromatic molecules.

Equation 2.

$$\frac{\text{Aliphatic}}{\text{Aromatic}} = \frac{\text{Al}}{\text{Ar}} = \frac{\sum \text{SICT}_{71+85}}{\sum \text{SICT}_{x} \text{ (where } x = 77,91,93,141,143)}$$

This ratio can be used to monitor the relative aromaticity of the volatile components of each sample. These ratios do not measure actual aromatic contents but enable trends to be observed between samples. Using equation 2 the order of increasing aromatic content was found to be KC < JC < CH2 < OC < CH1. This of course only measures the volatile components of the bitumens and therefore does not characterise the bitumens as a whole.

As we can see from Appendix 1 , table 3.7 and indeed Figures 3.10 to 3.14, the predominant volatile species in all five chloroform bitumens are saturated alkanes. In addition various alkyl benzenes, alkyl naphthalenes, naphthoxy derivatives, phenoxy derivatives, hydroaromatics, cyclohexyl derivatives and other compound classes were detected in varying amounts in each sample. Also a series of carboxylic acids or their ethyl esters were detected in the OC and CH1 chloroform bitumens, but not in any of the others. Detailed lists of components detected are given in Appendix 1. Alkyl phthalates were found in all of the samples analysed and it is suspected that these may be impurities derived from plastics containing these molecules as plasticizers.

Steranes and terpanes were detected only infrequently and then only in trace quantities. These compounds are known to be present in Kimmeridge Clay deposits[47,120,145], and our failure to detect them may be due to their low concentration in our samples. In those cases where these compounds were detected, the bitumens had been extensively fractionated in order to concentrate the sterane/terpane fractions. This study was not concerned with biological marker analysis but the analysis

of the major components of these systems, since these have greater overall relevance to the structure of the materials.

It was pointed out previously that saturated paraffins were the predominant volatile species in all five chloroform bitumens. Although this is true there was considerable variation in the distribution of these saturated alkanes in the five samples. This is demonstrated by the differences in the n-alkane distribution, the n-alkane maxima within that distribution, the ratio of isoprenoid alkanes to n-alkanes and the pristane to phytane ratio in all five samples.

The distribution of n-alkanes, and the maxima in their distribution, are used as indicators of the origins and maturity of sedimentary deposits[146]. The n-alkanes are widely distributed in various plants and other organisms and are probably the most commonly used biomarkers. In all of our samples the distribution of n-alkanes is approximately C_{11}-C_{27} and this together with maxima at C_{15} - C_{19} suggests a lower plant (cyano bacteria or algae) origin for the organic matter in these deposits[147,148,149,150]. A higher plant input, ie. land plants, would normally give rise to a n-alkane distribution[151] between C_{25} and C_{35}, with maxima in that distribution[152] at C_{27}, C_{29}, or C_{31}. We see weak n-alkane peaks up to C_{27} or C_{28}, with no maxima at these carbon numbers. Therefore we can conclude that the organic matter in our samples did not originate from land plants. However, we do see maxima at C_{21} and C_{23}, as well as at C_{17}, in the OC and CH1 samples which creates a bimodal n-alkane distribution by superposition over the unimodal n-alkane distribution displayed by the remaining samples. Maxima at these carbon numbers are harder to explain but some work has indicated that these alkanes originate from lower land plants such as mosses[153,154]. Such bimodal n-alkane distributions have been noted for other Kimmeridge Clay samples and explained in a similar fashion[47].

Isoprenoid alkanes were also detected in each of our five samples. These

molecules are the result of a 'head to tail' biosynthesis of isoprene units. One common source of these hydrocarbons is likely to be the isoprenoid side chain of the chlorophyll molecule[155]. The relative abundance of these branched alkane chains in relation to the n-alkanes is given for each sample in table 3.7. It can be seen that in four of the samples the n-alkanes predominate over the isoprenoid alkanes. However, the CH2 sample shows the opposite with a large predominance of isoprenoids over normals.(See Fig. 3.14). This may reflect a different source input in this particular sample, but it may also be due to biodegradation. It is well known that contact between crude oils and certain bacteria will lead to a depletion of the n-alkanes in the crude oils[156,157]. Isoprenoid alkanes are also biodegraded but at a slower rate. This may have happened to the CH2 sample, with the n-alkanes being preferentially depleted by biodegradation. However, the possibility of a different source input cannot be eliminated, even though it has been reported that the organic input into the Kimmeridge Clay deposits remained more or less constant throughout the sequence[120].

Two of the isoprenoid alkanes, pristane (2,6,10,14-tetramethylpentadecane) and phytane (2,6,10,14-tetramethylhexadecane), are commonly used to indicate whether the conditions of deposition were oxidative or reducing[158]. The use of the pristane to phytane ratio for this is based upon the premise that pristane is formed from phytol (the side chain of chlorophyll) by various oxidative and decarboxylation reactions. On the other hand phytane is formed by hydrogenation and dehydration of phytol. It is therefore proposed that the formation of pristane occurs in oxidising environments whereas phytane is produced by more reducing deposition environments. Thus samples with pristane/phytane< 1 are likely to have been deposited in a reducing environment and samples with pristane/phytane>1 in an oxidising environment. From this we can say that the pristane/phytane ratios of our five samples indicate that KC and JC were deposited in oxidising environments and that OC,CH1 and CH2 were deposited in

a reducing environment. The pristane/phytane ratios for CH1 and CH2 are 0.91 and 0.75 respectively and are in the range expected for Kimmeridge Clay samples of the Dorset area[47,145]. The North Yorkshire Kimmeridge Clay sample, KC, has a pristane/phytane ratio of 1.6 which is much higher than for any Dorset sample. Although this has been noted for Northern Kimmeridge Clay samples[120], a satisfactory explanation of why there is such a difference between these and the Dorset samples has not been forthcoming. It may well be due to the greater maturity of these samples since it has been observed that as coalification proceeds the pristane/phytane ratios increase, possibly via the cracking of phytane to pristane.

3.3.5 GPC Analysis of Bitumens.

Each of the chloroform bitumens was analysed by gel permeation chromatography as described in the experimental section. The GPC traces obtained are shown in Figure 3.15. The GPC column was calibrated with polystyrene calibrants with molecular weights ranging from 1,400,000 to 1,240. Both the ultraviolet (UV) and the refractive index (RI) detector traces were used to measure the molecular weight distribution, the number average molecular weight (Mn), the weight average molecular weight (Mw) and the polydispersity (PD) or heterogeneity index. (See chapter 2 section 2.6). These values obtained from both detectors from each bitumen are presented in table 3.8.

Table 3.8 GPC data from analysis of chloroform bitumens.

Sample	Detector	Mn	Mw	PD	Mwt Range
KC	RI	930	6760	7.2	140,000 - 20
	UV	650	6960	10.5	80,000 - 12
JC	RI	1350	4300	3.1	50,000 - 60
	UV	930	4450	4.7	50,000 - 60
OC	RI	600	8370	13.9	230,000 - 12
	UV	420	18940	44.6	1,800,000 - 12
CH1	RI	660	9950	14.9	700,000 - 12
	UV	630	7170	11.4	230,000 - 12
CH2	RI	1710	9640	5.6	230,000 - 60
	UV	1200	10570	8.8	230,000 - 30

where RI = refractive index

UV = ultra violet.

Table 3.8 shows the chloroform bitumens to contain material having a wide molecular weight distribution (equivalent to the polystyrene calibrant). Although we

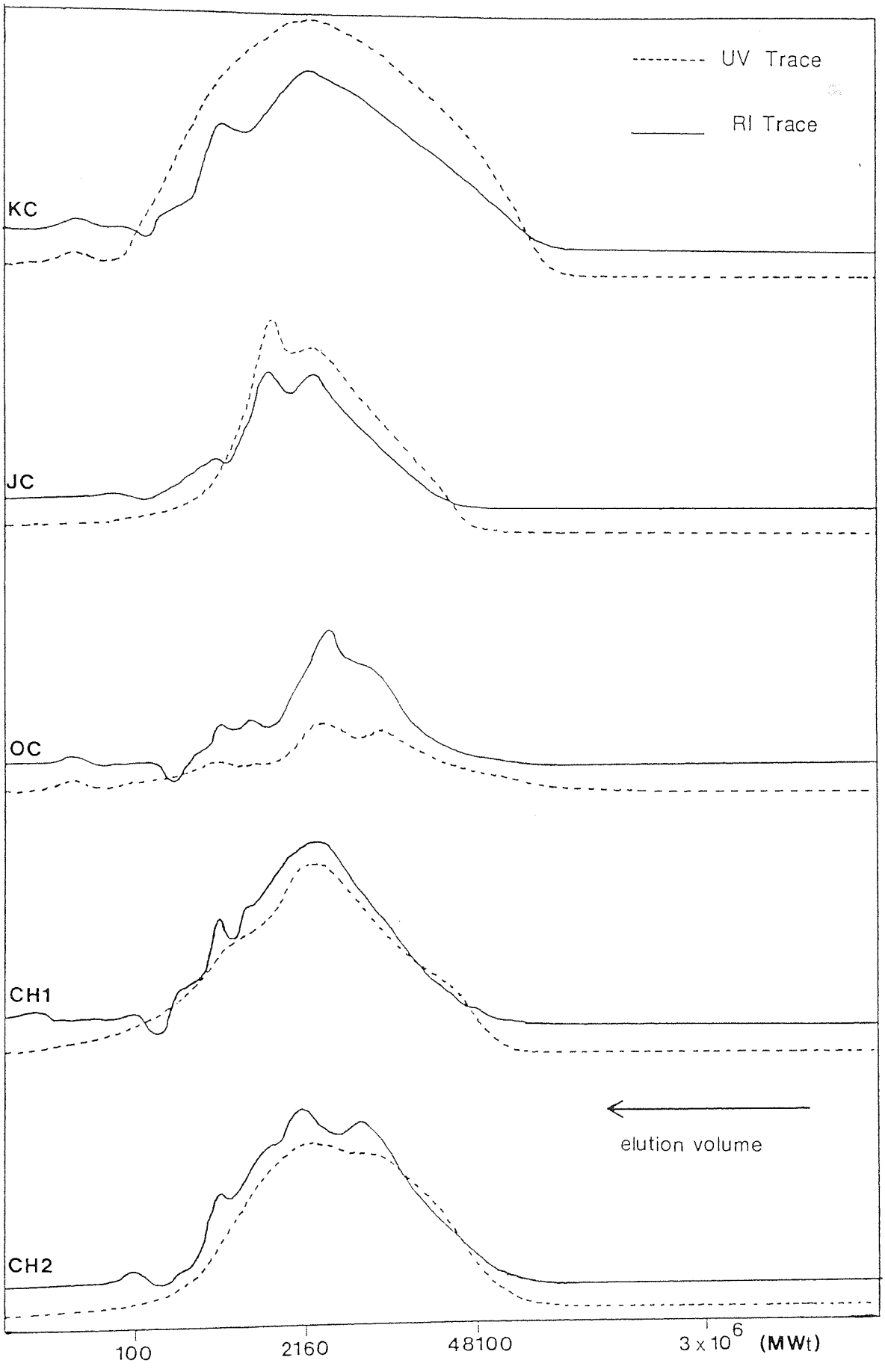

Figure 3.15. GPC Traces of the Chloroform Bitumens.

cannot be precise about the actual molecular weights of the materials in the bitumens, table 3.8 indicates that substantial quantities of high molecular weight material exist. This material will be involatile and therefore not detected by GC-MS. In general the molecular weights ranged from several hundred thousand to 12 with Mn's ranging from 420 - 1710 and Mw's from 4300 - 18940. Obviously the low end of the molecular weight distribution (Mwt 12) is in error and illustrates the problems that arise from not having a suitable calibrant for bitumens. In the case of the OC sample, a bitumen component having a molecular weight as high as 1,800,000 was detected by the UV detector. This molecular weight was much higher than than any other found in the remaining samples and may be due to aggregate formation. However, the RI detector did not detect this component and therefore there cannot be much of it.

The values of Mn and Mw calculated for each bitumen by the RI and UV detectors generally show good agreement. The one exception to this was the Mw values calculated for OC. The Mw for OC calculated from the UV trace is exceptionally high and accounts for the high polydispersity (PD) value of 44.6. As we mentioned earlier these figures may result from aggregate formation. More common values for the polydispersity are in the range 3 - 15 but they still indicate a high heterogeniety between the components of each bitumen. This is not surprising considering the nature of bitumens. Comparing the PD values of the five samples indicates that the order of heterogeneity increases from JC to CH2 to KC to CH1 and finally to OC. There are differences in the Mn and Mw values between the five bitumens but they are relatively small and we have not been able to relate these to any major trends.

Although it is more apparent in some samples than others, it can be seen from Figure 3.15 that all the GPC traces show some partially resolved peaks. This apparent non-unimodal molecular weight distribution can be explained in terms of some molecular weights being more populated than others. However, as was discussed in

chapter 2 section 2.6. separation or resolution of components may not occur on a molecular weight basis but rather on the basis of size or the possession of certain functional groups. Thus, although some bitumens do show resolution into a number of different component types, the difference between them remains uncertain. This problem would be overcome if preparative GPC were available, then each resolved component could be separated and characterised independently. This would obviously add to our understanding of the composition of bitumens.

3.3.6 UV-VIS Spectra of Bitumens.

absorption of light in the ultraviolet and visible regions of the electromagnetic spectrum produces changes in the electronic energies of molecules associated with the excitation of an electron from a stable to an unstable orbital[159]. This absorption of radiation can be used to detect certain types of molecules present in bitumens and other fossil fuel derived liquids[160]. This technique when used with such complex systems gives broad, poorly resolved peaks and the information which can be obtained is limited to the determination of the proportions of various types of aromatic species in the sample. The spectra obtained are presented in Figure 3.16.

The spectra from KC,OC,CH1 and CH2 are very similar. Each has a very broad absorption extending from 200nm right through into the visible end of the spectrum, and which maximises at 250-260 nm. This is attributed to the absorption of substituted benzene rings. Other smaller maxima or points of inflection on the main absorption occur at about 300 and 380 nm respectively and are probably due to alkyl naphthalenes and anthracenes/phenanthrenes respectively. Conjugated polyalkenes also absorb in this region but it is very unlikely that such compounds would be produced by the burial and evolution of sedimentary organic matter. The overall broadness of these absorptions indicates that the aromatic ring systems concerned have a large number of different substituents.

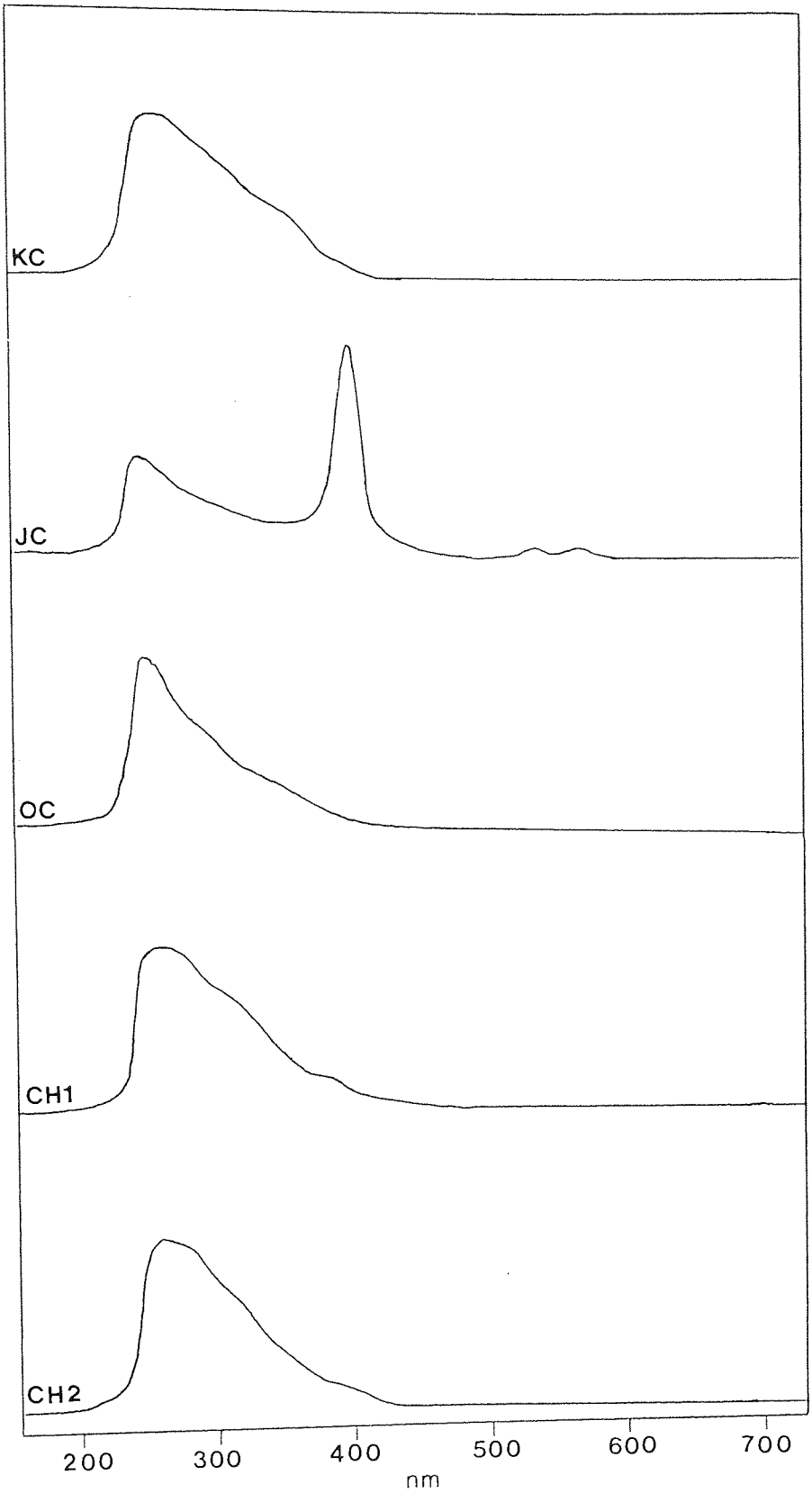

Figure 3.16 UV-VIS Spectra of the Chloroform Bitumens.

The UV-vis spectrum of the JC sample has all of these features but in addition there is a very intense absorption at 409 nm and two smaller ones at 535 and 575 nm . These peaks are due to a petroporphyrin[161] which is responsible for giving this bitumen its bright red colour.

3.4 Analysis of Kerogens.

The structural analysis of kerogens by methods other than chemical or physical degradation is limited to solid-state techniques. This restriction is due to the insolubility of kerogens.

Kerogens make up the predominant part of the total organic matter in sedimentary rocks and therefore their analysis assumes great importance. Unfortunately those methods that are suitable to the study of kerogens without their degradation can only generate an average or global structure. Nonetheless significant information can be obtained which is very useful if subsequent degradation products from the kerogen are to be correlated with its initial structure. Only through such a comparison or correlation can the degradation reactions be understood. Thus the analysis of the starting kerogens assumes paramount importance.

In this work we have used elemental analysis, infra-red spectroscopy and solid state NMR to characterise and identify the organic structures present in our five kerogens.

3.4.1 Elemental Analysis of Kerogens.

Each of the five kerogens, prepared as described earlier in this chapter, were analysed ten times. The results of these analyses are plotted on a van Krevelen diagram (Fig. 3.17). As can be seen from comparison with figure 2.1 (page 40), these kerogens fall roughly on the evolution pathway expected for a type II kerogen.

H/C ratios are reasonably reliable but not the O/C ratios. This is because the oxygen contents of these kerogens were obtained by difference, ie. subtracting the wt% carbon, the wt% hydrogen, the wt% nitrogen and the wt% ash from 100%. Clearly if the mineral content is high then this will lead to errors in the oxygen contents. This is because the behaviour of the mineral under ashing conditions is not well understood, ie, does the mineral lose or gain weight under combustion, and if so to what degree? In some

Figure 3.17 Van Krevelen Plots for the five Untreated Kerogens

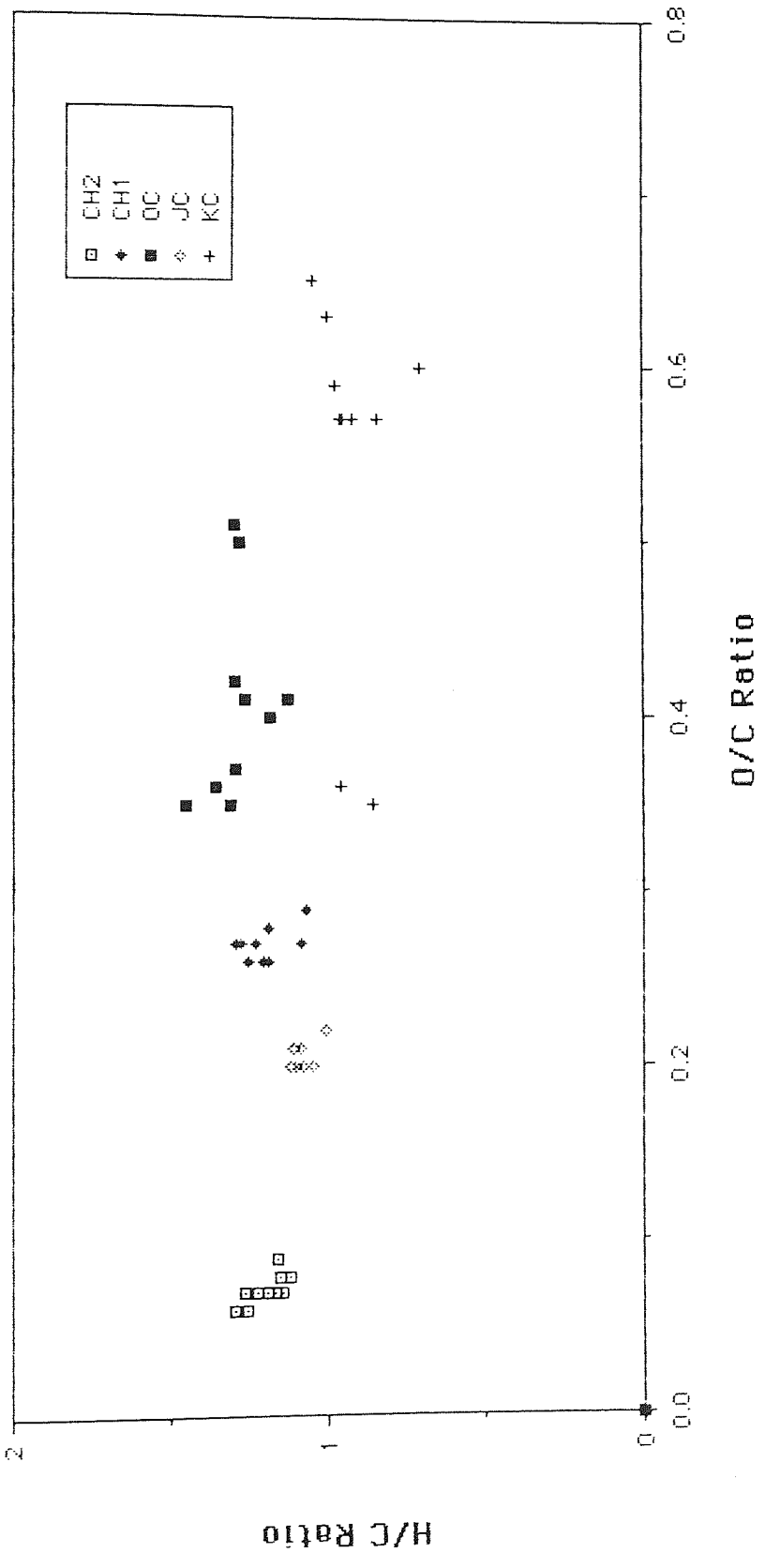

cases pyrite is known to be the only predominant mineral remaining after acid demineralisation, but this is not true for all of our samples. Thus the data presented here should be treated with some caution. The elemental analyses of lithium aluminium hydride reduced kerogens are presented in chapter 4. These reduced kerogens have very little mineral matter and therefore their elemental analyses should be far more reliable.

As can be seen from figure 3.17 there is considerable spread in the ten data points for each kerogen, especially for the KC and OC kerogens. The range or spread of points for each kerogen is a measure of its heterogeneity. This heterogeneity is a result, not only of the local variation in the structure of the organic components, but also of the variable degree of association of these organic components with the remaining mineral matter. Obviously if larger sample sizes were used for elemental analysis then these heterogeneity influences would be substantially eliminated. However, the apparatus required for such determination was unavailable and hence it was necessary to analyse each sample ten times so that a reasonable average could be obtained. Once this had been done an empirical formulae could be calculated, (table 3.9).

Table 3.9 Elemental composition of kerogens.

	Average Elemental Composition (wt%)					
Sample	C	H	N	O	Ash	Empirical Formulae.
KC	30.5	2.6	0.6	26.3	40.0	$C_{100}H_{91}O_{59}N_1$
JC	58.6	5.3	0.8	15.4	19.9	$C_{100}H_{109}O_{21}N_1$
OC	44.5	4.8	0.8	23.3	26.6	$C_{100}H_{129}O_{41}N_2$
CH1	59.0	5.8	0.7	20.9	13.6	$C_{100}H_{119}O_{27}N_1$
CH2	67.9	6.7	0.5	6.1	18.8	$C_{100}H_{119}O_7N_1$

The oxygen values appear to be high but this is to be expected considering the assumptions used to calculate them. Nonetheless the H/C ratios suggest that there is a

trend in the aromatic character of these kerogens. Although elemental analysis is not conclusive proof for this, when this information is taken in conjunction with other results from different techniques, this seems a reasonable suggestion.

3.4.2 FT-IR Spectroscopy of Kerogen.

Each kerogen was analysed by FT-IR spectroscopy. The spectra are shown in Figures 3.18 - 3.22. As we can see all five kerogen spectra share similar absorption bands. However, the kerogens are distinguishable because the intensities of the absorption bands are seen to vary from kerogen to kerogen.

Most bands in these kerogen spectra can be attributed to aliphatic, aromatic , carbonyl, hydroxyl and various ether groups and have been described earlier in section 3.3.2. In general the kerogens appear to be predominantly aliphatic in character. This is shown by their large methyl and methylene absorptions. As with the bitumen spectra it is possible to measure the relative alkyl chain length/degree of branching for the five kerogens. Using the same peaks as before we can obtain a relative methyl/methylene ratio. The results of this treatment are shown in table 3.10.

Table 3.10 CH_2 vs CH_3 peak intensities from FTIR analysis of kerogens.

Kerogen	peak intensity ratio	
	I 2920/2960	I 1455/1375
KC	2.50	2.75
JC	1.49	3.60
CC	1.42	2.25
CH1	1.39	2.16
CH2	1.28	2.15

As previously the lower the ratio the shorter or more branched is the average alkyl chain. Once again there is not a good correlation between the two methods used to

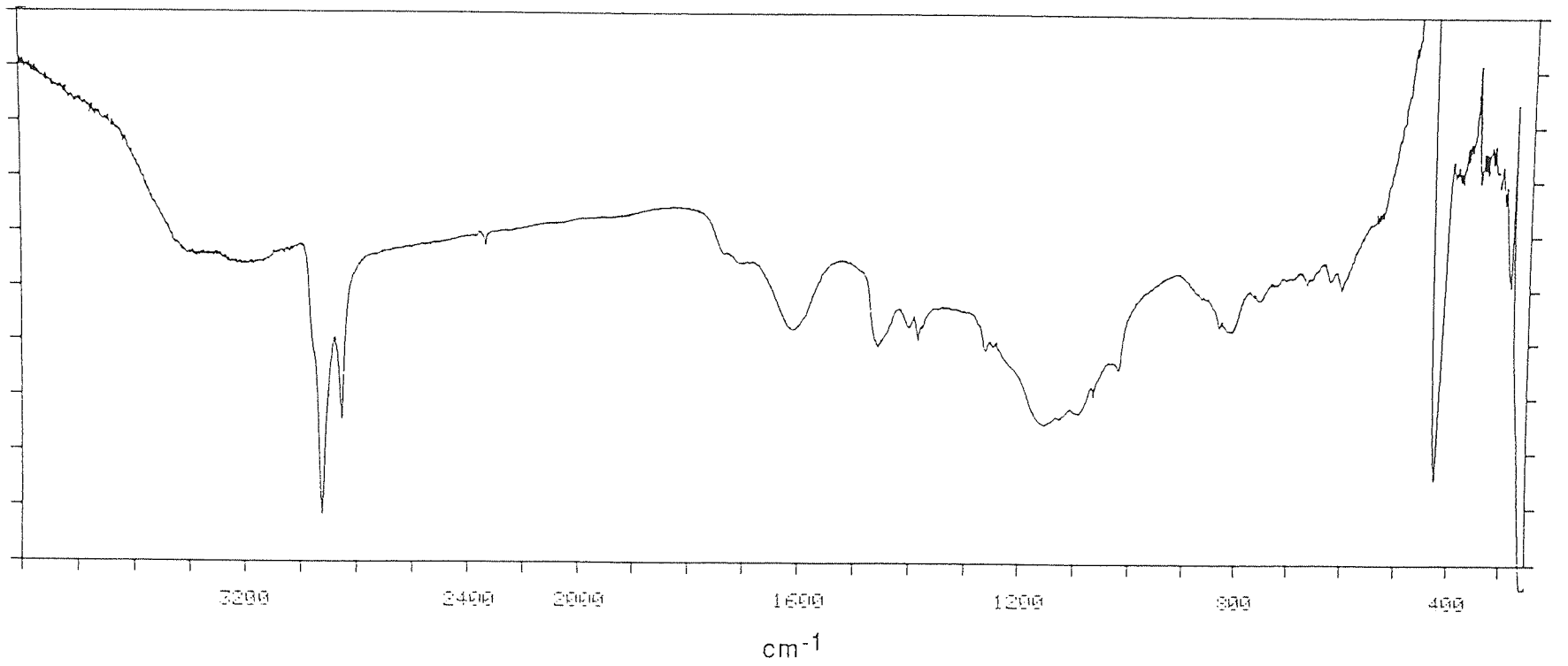

Figure 3.18 FT-IR Spectra of Acid Demineralised KC.

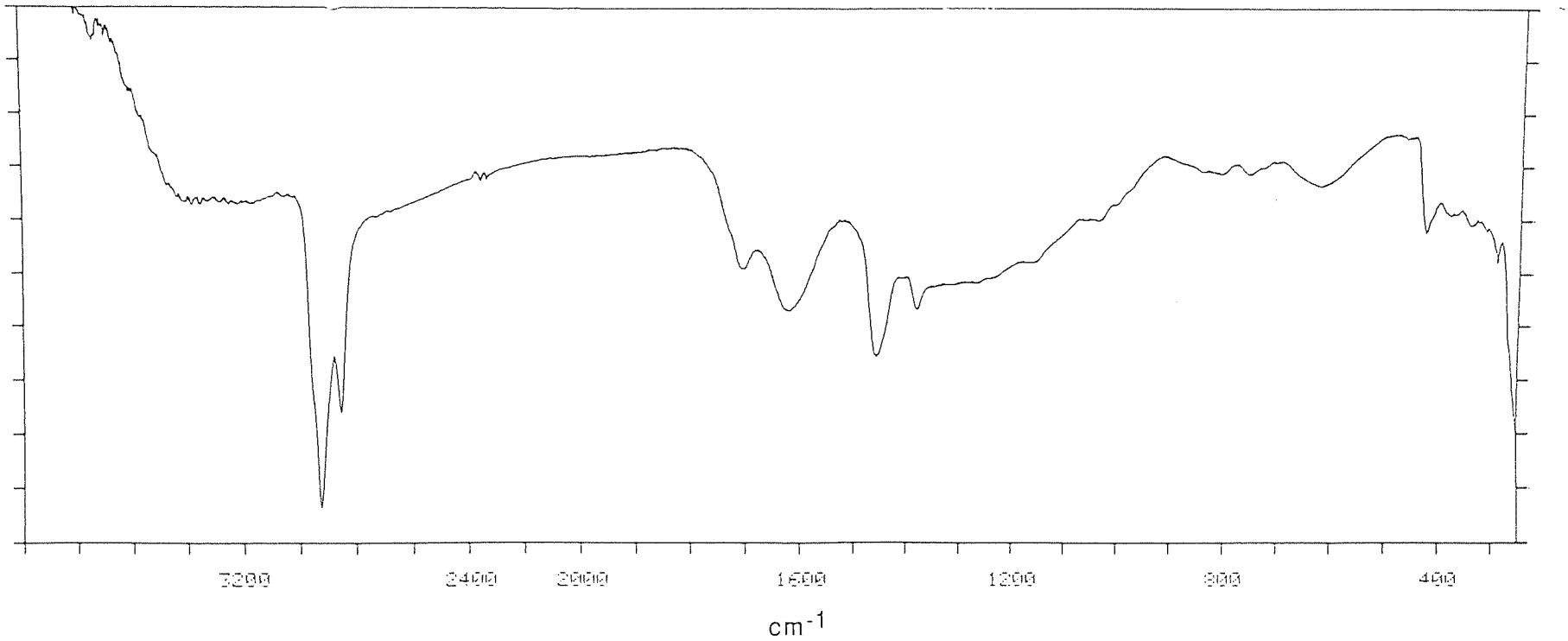

Figure 3.19 FT-IR Spectra of Acid Demineralised JC.

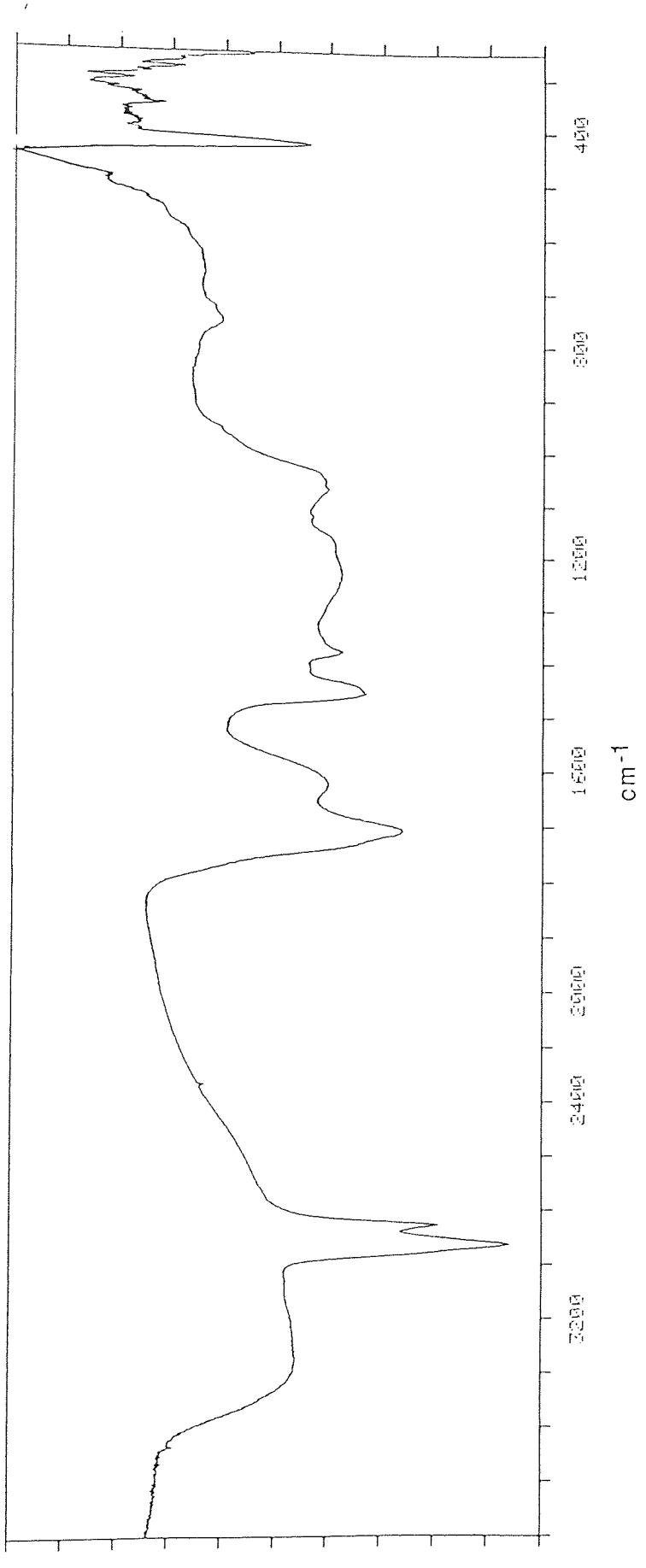

Figure 3.20 FT-IR Spectra of Acid Demineralised OC.

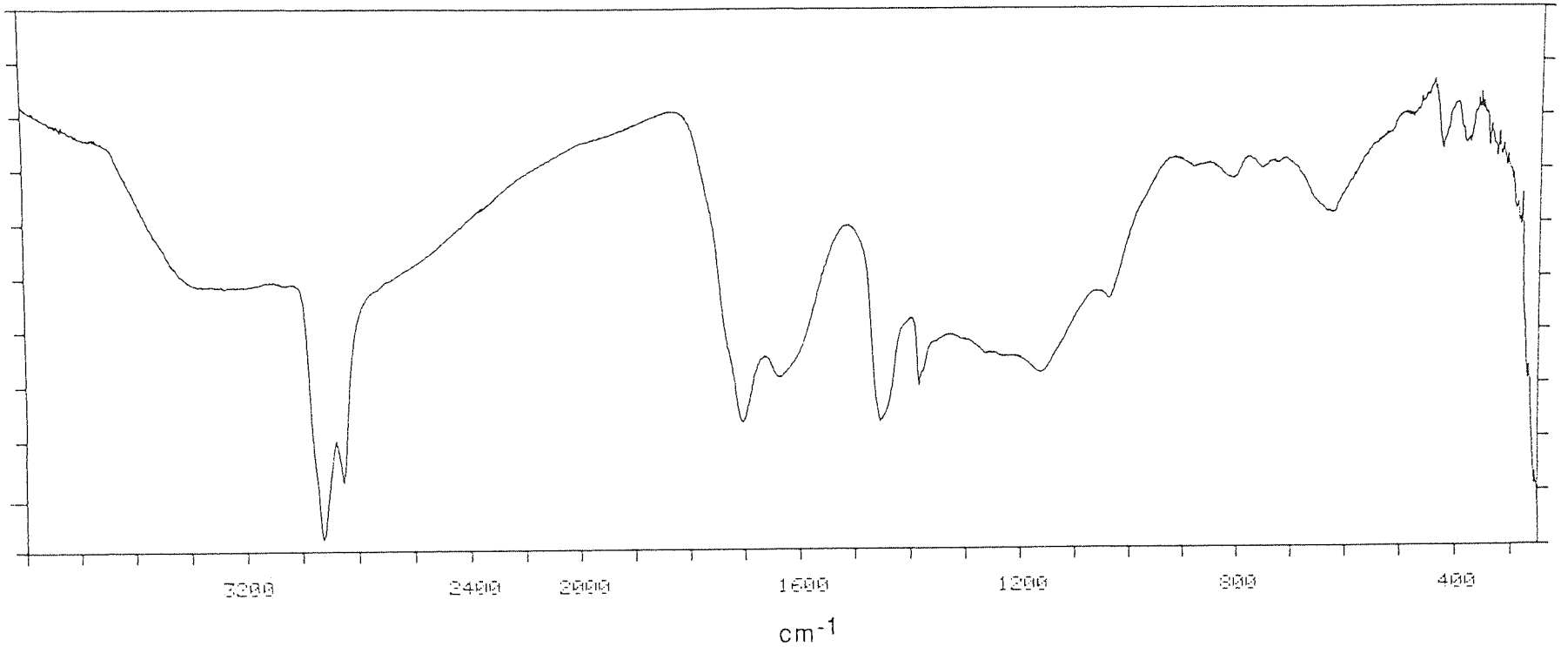

Figure 3.21 FT-IR Spectra of Acid Demineralised CH1.

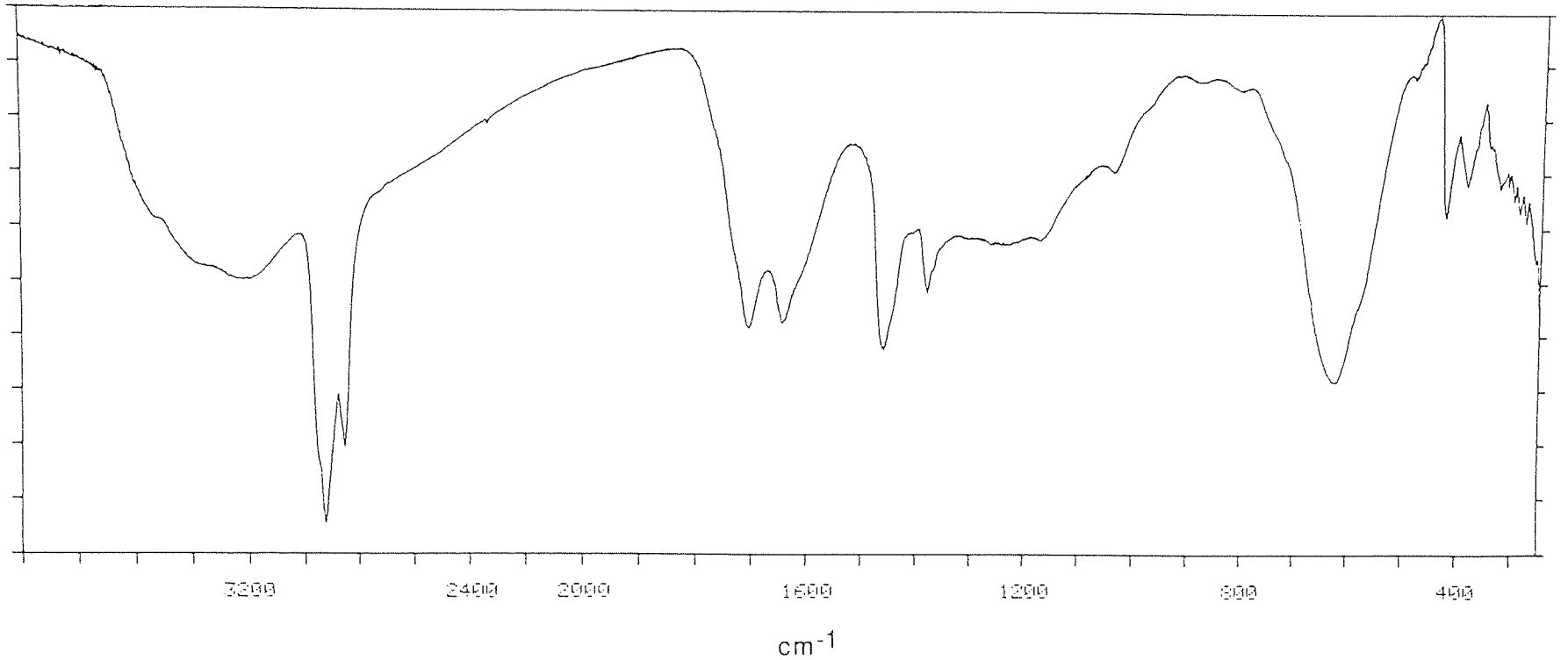

Figure 3.22 FT-IR Spectra of Acid Demineralised CH2.

calculate this parameter, but it is clear that, as with the bitumens, the CH2 kerogen has the shortest/most branched average alkyl chain.

The relative intensities of the carbonyl absorptions from these kerogens increase in the order KC>JC>CH2> OC>CH1, and as we can see from Figures. 3.2 and 3.3 (page 75 and 76), this is a repeat of the trend observed in both the chloroform and pyridine bitumens. There is some fine structure associated with the kerogen carbonyl absorptions but it is not well defined and it appears, as with the bitumens, that the main absorption at 1700-1715 cm^{-1} is due to carboxylic acids. This explains the presence of the broad hydroxyl absorption in these spectra.

The kerogen spectra also show absorptions due to aromatic structures, especially at 1650 - 1580 cm^{-1}. However, due to the overlap with the neighbouring carbonyl absorptions, it is not possible to ascertain the order of aromaticity for the five kerogens. (This is possible however after the kerogens have been reduced, ie. when there is no further carbonyl interference. See the FT-IR analysis of reduced kerogens in chapter 4.)

Comparing each kerogen spectrum with those of their corresponding chloroform and pyridine bitumens more closely, we find that the kerogen spectra can be considered hybrids of their corresponding chloroform and pyridine bitumen spectra. In other words, the structures of the kerogens (as indicated by FT-IR analysis) appear to be somewhere in between those of their corresponding chloroform and pyridine bitumens. This can be illustrated by the FT-IR spectra of the CH1 kerogen, chloroform and pyridine bitumen. If we take the peaks in the 2000-1500 cm^{-1} region, it is clear that the relative intensities of the peaks in the kerogen spectra are in between those observed in the chloroform (weaker intensity) and pyridine (stronger intensity) bitumens.

Significant peaks which appear in the kerogen spectra but not in the bitumen spectra occur at 425 cm^{-1}. These peaks are attributable to pyrite. Naturally the

relative size of this peak measures the relative pyrite content of the kerogen, and therefore it is no surprise that the spectrum of KC kerogen (which is approximately 60 % pyrite by weight) has a very sharp and intense peak in this area. A large peak centering at 615 cm^{-1} in the spectrum of the CH2 kerogen remains uncharacterised, but it is probably due to some residual mineral of some kind (since few organic groups absorb significantly in this region).

3.4.3 Solid State NMR of Kerogens.

Using the pulse sequences outlined in the experimental section, solid state ^{13}C NMR spectra for the five acid demineralised kerogens were generated. These are presented in figures 3.23 - 3.27. These spectra show good separation of the aromatic and aliphatic carbon signals and some additional resolution of individual carbon environments, especially in the aliphatic region. The overall broadness of the spectra may result from the interference of paramagnetic species such as free radicals but we believe that it reflects the complexity of these materials.

Interpretation of the spectra is hampered by the presence of spinning side bands (SSB) which result from the dephasing and rephasing of magnetisation vectors as the sample rotates[162]. SSB are worst for carbon environments that have large chemical shift anisotropies and therefore they usually occur symmetrically displaced about the aromatic peak only. This is observed in our spectra. The position and intensity of a SSB is also a function of spin speed, and under our operating conditions the regions occupied by these SSB are 210 - 170 and 100 - 60 ppm. Consequently we cannot quantify with accuracy carbonyl, ether, alcoholic and other carbon types that resonate in these regions. We can however, to some extent, relieve this problem. We have noticed that the peaks in the 210 - 170 ppm region do not change significantly when the sample is reduced with lithium aluminium hydride. This suggests that these peaks have little carbonyl contribution and therefore are predominantly SSB. Using this information we

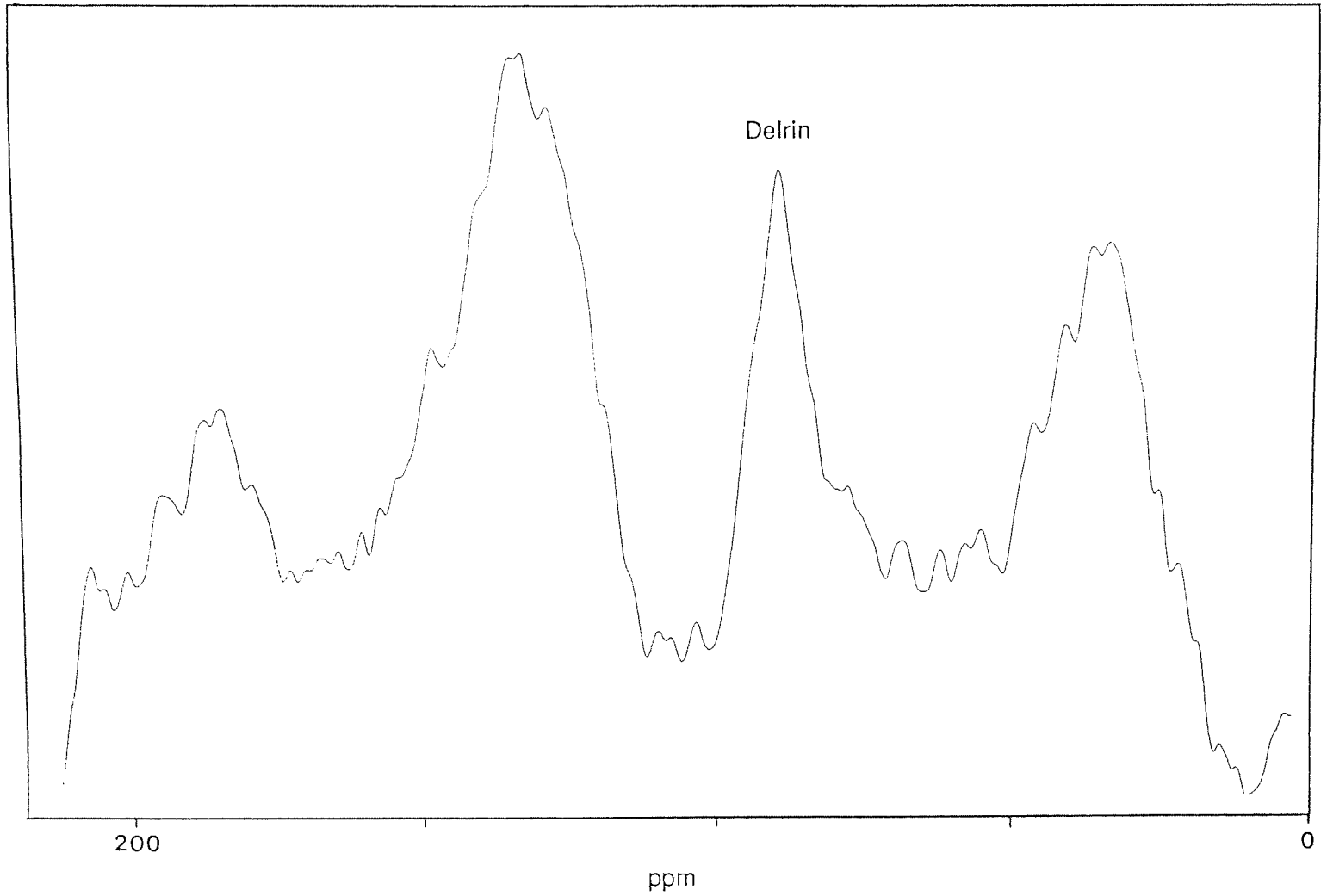

Figure 3.23 Solid state ^{13}C NMR spectra of acid demineralised KC.

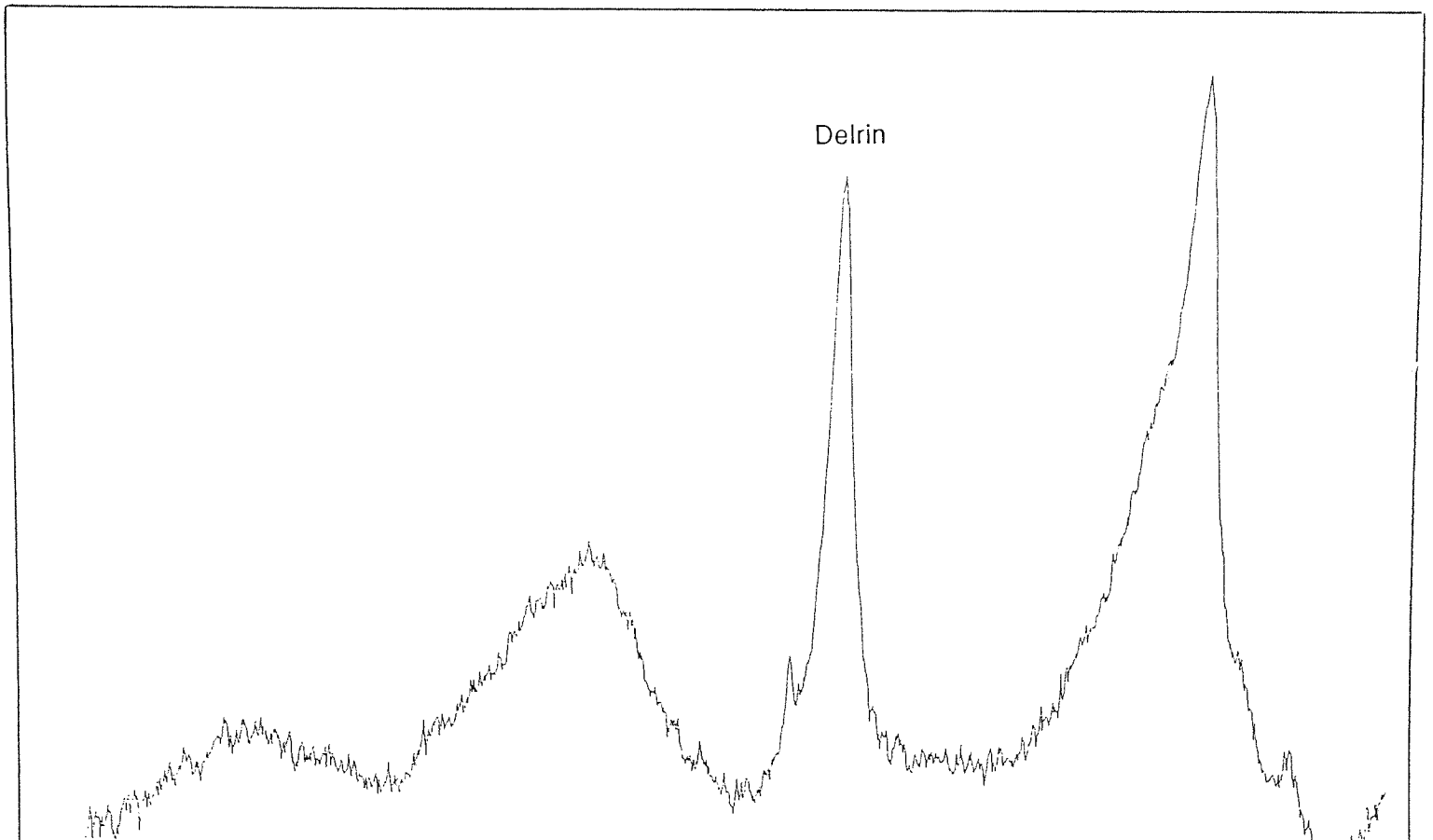

Figure 3.24 Solid state ^{13}C NMR spectra of acid demineralised JC.

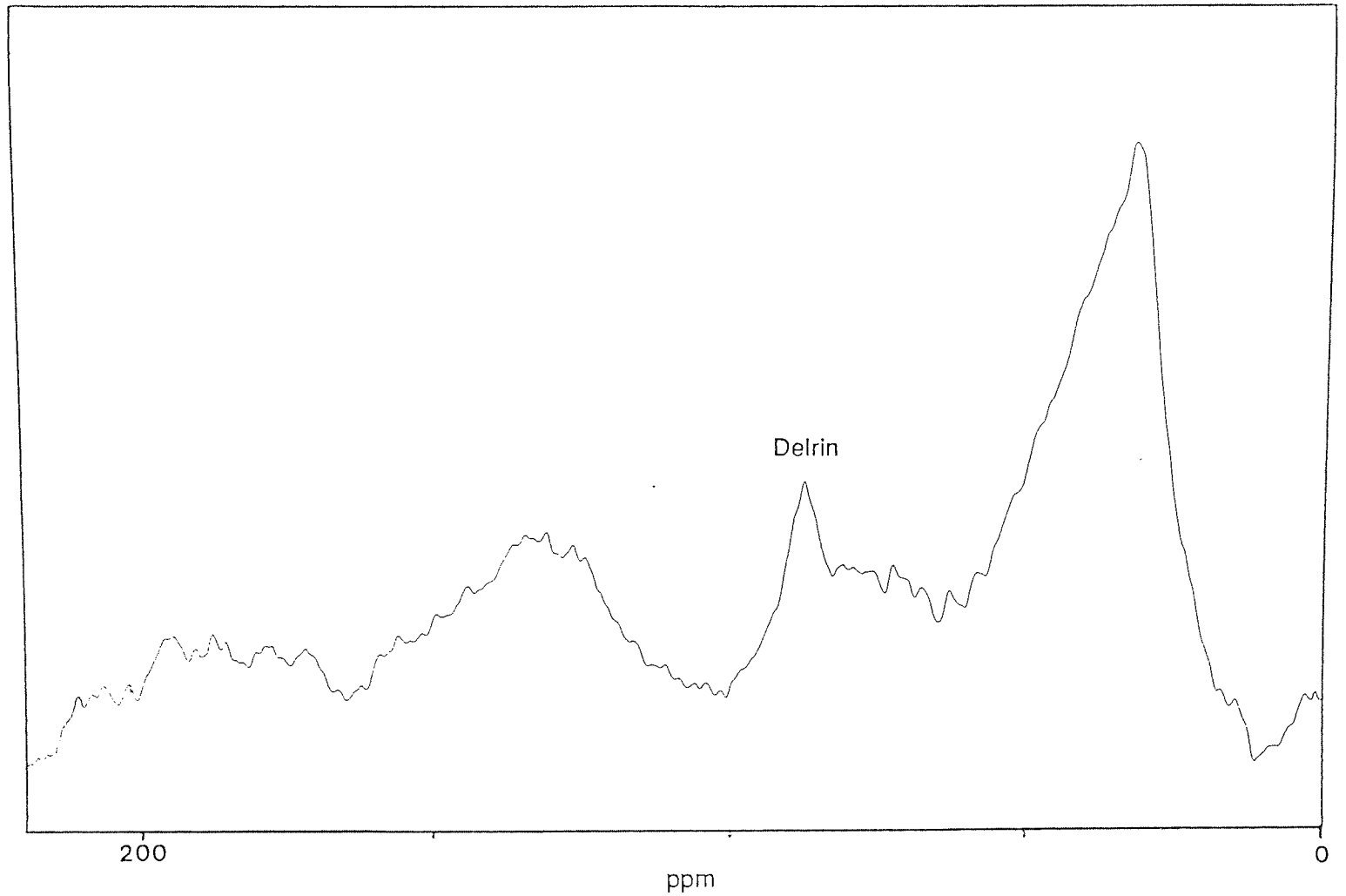

Figure 3.25 Solid state ^{13}C NMR spectra of acid demineralised OC.

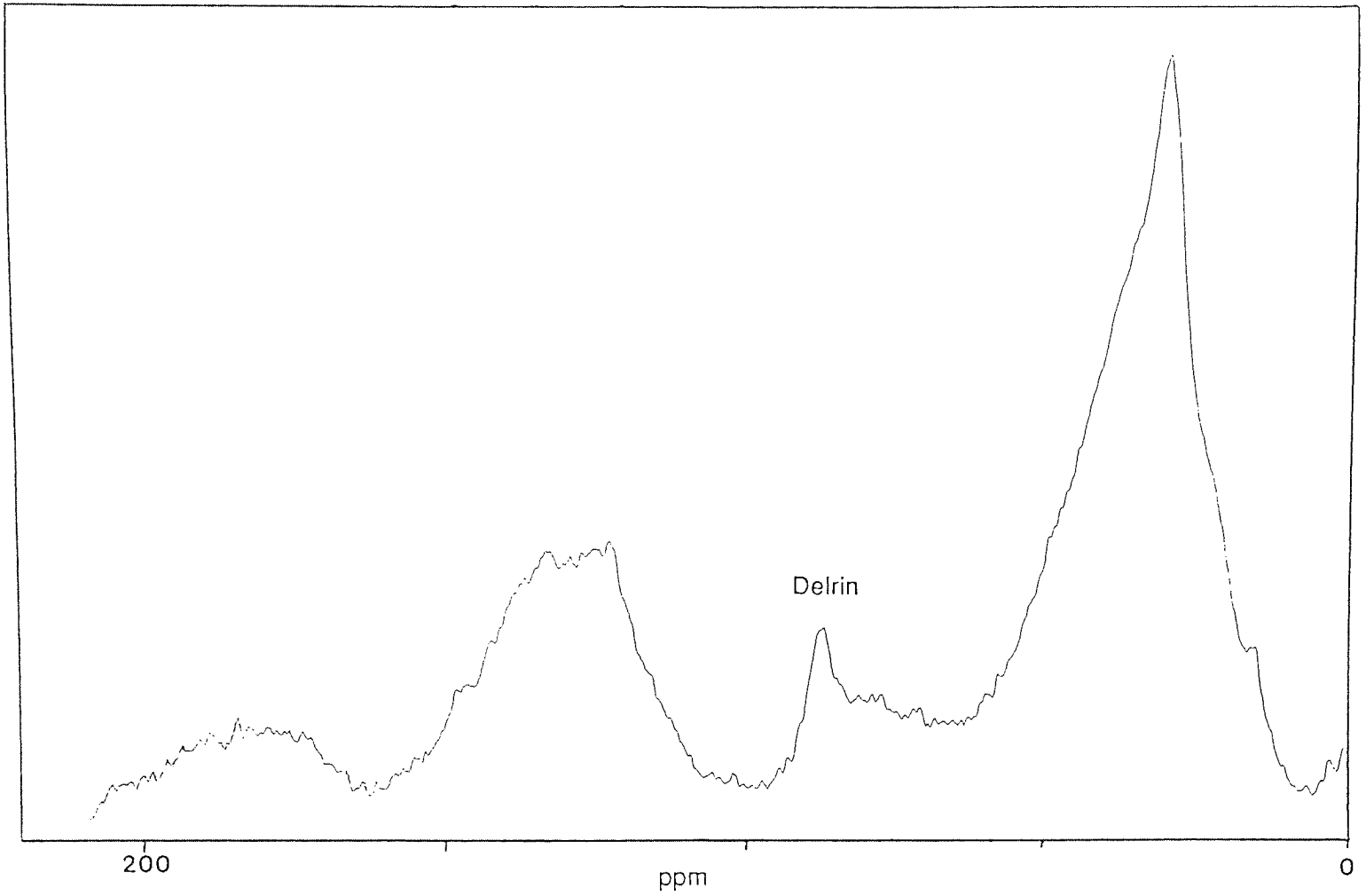

Figure 3.26 Solid state ^{13}C NMR spectra of acid demineralised CH1.

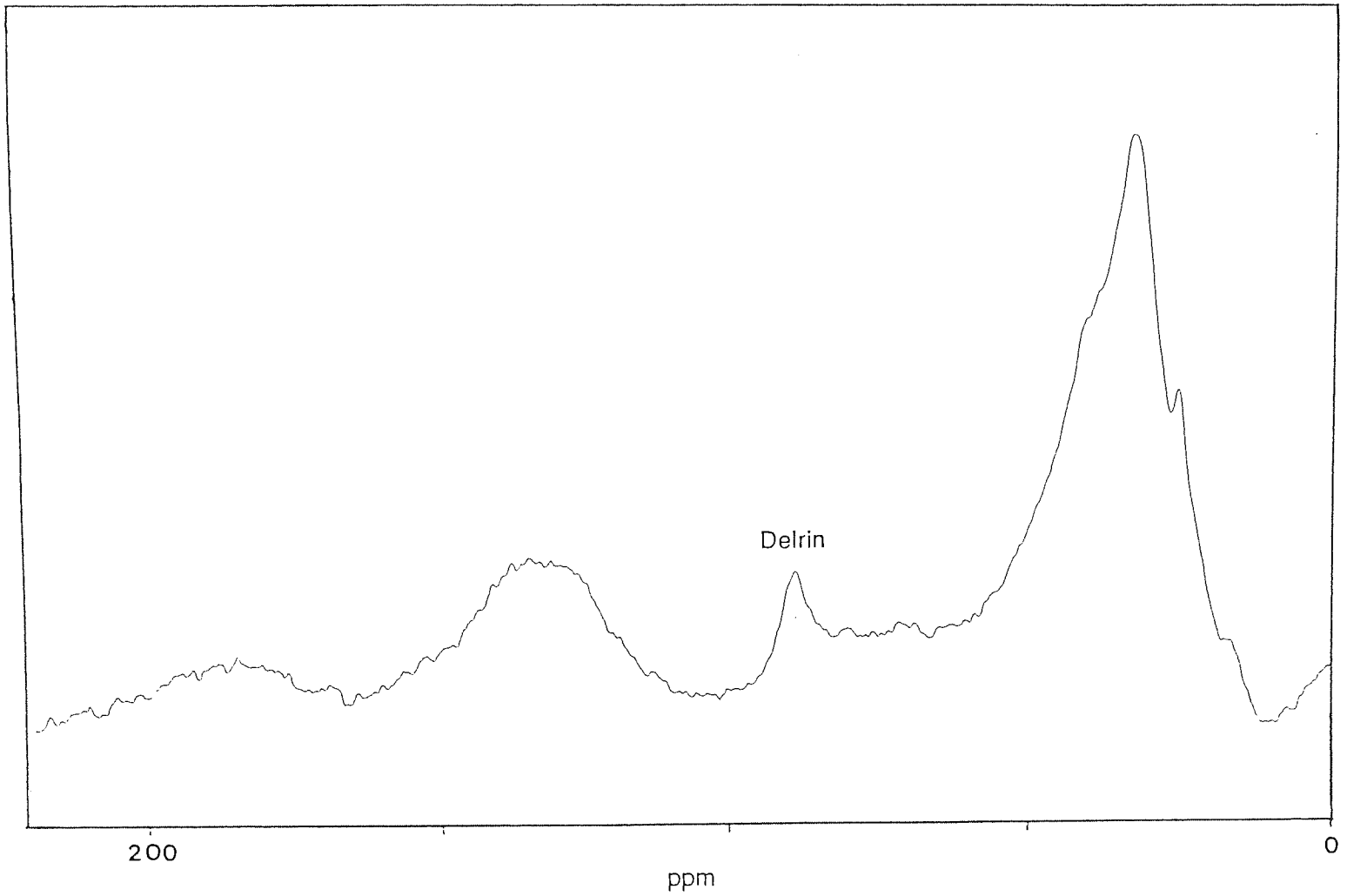

Figure 3.27 Solid state ^{13}C NMR spectra of acid demineralised CH2.

can subtract the SSB peaks in the region 210 - 170 ppm from those in the 100 - 60 ppm region thereby obtaining a measure of the carbon environments which had been obscured. This may not be a completely satisfactory answer to this problem but without the SSB suppression pulses (TOSS[163] and PASS[164]) we have no other choice.

There is another peak at 90 ppm (of variable intensity throughout our spectra) which is due to a background signal from the Delrin rotor base. This peak is reasonably sharp and symmetrical and therefore can be subtracted from the underlying sample resonances quite easily. The Delrin subtraction and that for the SSB were performed so that the different carbon environments in the sample could be measured.

Using the information in chapter 2, Section 2.4, each spectrum was divided into seven regions which represent different chemical environments. The intensities of the peaks in these regions and their contributions to the whole spectra were measured. The results of this are reported in table 3.11.

Table 3.11 Distribution of carbon environments in the kerogens.

			% contribution of each carbon environment				
Region	Range	Carbon Environment	KC	JC	OC	CH1	CH2
1	210-170	carbonyl *	-	-	-	-	-
2	170-129	subs +b'head Arom.	34	25	20	17	17
3	129-100	protonated Arom.	19	20	14	14	11
4	100-60	alcohols/ethers	1	3	9	2	6
5	60-50	methoxy	5	4	8	6	7
6	50-24	methylene/methine	35	41	42	49	47
7	24-0	methyl	6	7	7	12	12
fa		Aromatic signal / Total carbon signal	0.53	0.45	0.34	0.31	0.28

* Carbonyls could not be determined because of the SSB subtraction.

This table together with Figures 3.23 - 3.27 shows that there is considerable variation in the structure of these kerogens. As we can see, fa values (the fraction of the carbon atoms that are aromatic) increase in the order CH2<CH1<OC<JC<KC which is 52% aromatic. This trend is in good agreement with that obtained from solution state NMR analysis of the corresponding bitumens, see table 3.6 (page 89). The greater fa value for the KC sample (North Yorkshire) as compared with the other two Kimmeridge Clay samples (CH1 and CH2 from Dorset) indicates that it is much more mature. Since these oil shales were all deposited at more or less the same time, this result suggests that the northern Kimmeridge Clay has been buried deeper and hence exposed to higher temperatures. This may well explain the higher pristane/phytane ratio that was observed for this sample.

It is interesting to note that the fa values for OC, JC and KC reported here are considerably higher than those previously reported[23,53] for the same samples (0.20, 0.34 and 0.40 respectively). This follows the trend towards higher fa values as improvements are made towards the optimisation of spectrometer conditions. Although a different spectrometer was used to obtain these earlier values (thus a direct comparison is made difficult), it would appear that increasing the recycle time from 0.75 to 4 seconds may be responsible for the increases in fa values. The contact time (so important in determining the spectra shape), was kept constant (3ms) in both experiments and therefore the variation in fa values cannot be attributed to this.

From table 3.11 we can see that, apart from the various aromatic, methyl, methylene and methine resonances, there is little else. In general methoxy, alcoholic and other ethereal carbon functionalities are not abundant. As mentioned earlier carbonyl resonances could not be determined because of SSB interference, but reduction studies (see chapter 4) show there to be only a few anyway.

The resolution of the aliphatic region into methyl and methylene peaks is only

partially achieved. However, as with the solution state ^{13}C NMR of the chloroform bitumens (CH2 bitumens excluded), the predominant aliphatic resonance occurs at 29.8 ppm. As we have seen this can be attributed to long polymethylene chains. The presence of these methylene chains in both the kerogens and their corresponding bitumen extracts suggests that a degree of structural similarity exists between them. This is supported by the closer examination of the CH2 kerogen spectrum (Fig. 3.27) which reveals partially resolved methyl and methylene peaks at 22.4, 37.6 and 39.7 ppm . These peaks can be attributed to isoprenoid structures which, it has been shown, are also abundant in the CH2 chloroform bitumen. However, since the bitumens show little aromatic character in their NMR spectra (unlike the kerogens), we must conclude that the kerogen/bitumen structural similarity must be restricted to the aliphatic portion of the kerogens.

N.B. It should be remembered that there are doubts as to the quantitative accuracy of solid state ^{13}C NMR spectra. As mentioned earlier (see chapter 2 section 2.4.2) it is necessary to measure T_{1H} and $T_{1\rho}$ for each sample so that the cross-polarisation experiment can be optimised. Since neither the instrument time or sophistication was available to determine these relaxation times, the values in table 3.10 should be treated with some caution. Indeed in a previous examination of OC and KC kerogens by solid state ^{13}C NMR[23] it was found that $T_{1\rho}$'s of a significant proportion of the protons in each sample were less than 1 millisecond and consequently many of the ^{13}C nuclei would be unable to absorb energy by cross-polarisation. However, so long as this loss of carbon magnetisation does not discriminate between different chemical environments the values in table 3.10 may not be that far out. This point has been demonstrated[254].

3.5 Conclusions.

Treatment of each rock sample with HF and HCl failed to remove all minerals but resulted in considerable enrichment of their organic matter. The residual mineral was found to be predominantly pyrite in most cases. Kerogens and bitumens were separated by pyridine extraction. The pyridine extract was then separated into chloroform solubles (chloroform bitumens) and chloroform insolubles (pyridine bitumens).

Analysis of the chloroform bitumens by elemental analysis, FTIR, NMR and GC-MS revealed that they consisted predominantly of aliphatic structures. GC-MS analysis revealed long aliphatic chains (M.Wt.< 400) as the predominant volatile species and although variation was found between the different samples, the distribution of the n-alkanes suggested that algea were important source organisms for these materials. The CH2 bitumen was particularly interesting because it was found to contain more isoprenoids than n-chain material. This was detected not only by GC-MS analysis but was confirmed by the IR and NMR data for this sample. This phenomenon may be due to the preferential biodegradation of n-alkanes but may well indicate a significant structural difference in this particular sample. Not surprisingly, GPC analysis of the bitumens revealed a much higher molecular weight distribution than GC-MS with Mw typically in the 10000 - 4000 range and Mn in the 2000 - 400 range. Pyridine bitumens were more difficult to analyse but appear to have a stronger aromatic character than their corresponding chloroform bitumens.

Analysis of the kerogens was restricted to solid state techniques of which ^{13}C NMR was probably the most useful. Although some problems with spinning side bands were encountered it was possible to determine not only f_a values but further structural parameters also. From these results it was apparent that the structures of the kerogens varied considerably. This was most striking when comparing the Kimmeridge Clay kerogen from North Yorkshire (KC) with those from Dorset (CH1 and CH2). The much

greater aromaticity of the KC sample indicates its much greater maturity. This indicates that this particular sample has been buried deeper and exposed to higher temperatures than the others. Elemental analysis was hindered by the residual mineral content (mainly pyrite) but showed the heterogeneous nature of these materials. FTIR spectroscopy provided a functional group analysis of each kerogen, which together with the NMR data showed the kerogens to be predominantly aliphatic materials with varying amounts of aromatic, carboxylic, alcoholic, phenolic and ether units. As shown by both FTIR and NMR, the CH2 kerogen showed evidence of containing more isoprenoid structures than the other kerogens. This was also a significant feature in the CH2 bitumens and suggests a structural similarity exists between bitumens and certain portions of their associated kerogens.

Chapter 4.

Reduction of Kerogens with Lithium Aluminium Hydride.

4.1. Introduction.

As mentioned in chapter 3, treatment of the five oil shale samples with HF and HCl significantly reduced their mineral contents. However this treatment did not remove pyrite and as a result this mineral was still present (in very high concentrations in some of the kerogen samples). Lithium aluminium hydride (LAH) reduction was adopted to dissolve this pyrite. Despite the frequent use of LAH for this purpose, very little has been published regarding its use as a degradant for kerogens. Thus the aims of this piece of work were: 1). To obtain pyrite-free, low ash organic concentrates, and 2). To determine the effects of LAH on our kerogens and thus to evaluate its potential as a degradant in structural studies.

Removal of Pyrite.

There are three principal methods for the elimination of pyrite from organic concentrates:

1. Physical separation in dense liquors.

2. Destruction by oxidising agents; dilute nitric acid [165,166], aqueous solutions of soda[167] or ferric iron salts[168].

3. Destruction by reducing agents; nascent hydrogen (formed by the action of hydrochloric acid on zinc)[169,170], sodium borohydride[171,172] or lithium aluminium hydride[170,171,173,174].

Physical separation usually results in fractionation of the organic matter whilst chemical reagents, except for LAH and dil HNO_3, usually require many repeated treatments to have the desired effect. Dil. HNO_3 dissolves pyrite but also oxidises/nitrates the organic matter. Therefore LAH is normally the method of choice for the removal of pyrite.

Pyrite reacts with LAH through the formation of a complex which can be subsequently decomposed by water[57].

$$FeS_2 \xrightarrow[ii)\ H_2O]{i)\ LiAlH_4} FeS + S^{2-} \xrightarrow{H+} Fe^{2+} + 2H_2S\uparrow$$

The organic matter is also reduced but it has been reported that there is only slight modification to the kerogens[57,58,171,173,174]. Despite these reports we investigated in some detail the use of LAH as a degradant.

LAH Reduction.

Previous studies of kerogen reduction have followed the existing procedures already developed for coals and related materials, eg. humic acids. The most common of these reduction procedures are; reductive alkylation[175,176], reduction with hydrogen and a catalyst[177], HI[178], alkali metals in liquid ammonia[179], alkali metals in ethylenediamine[173], zinc dust distillation[180] and sodium amalgam (Na/Hg)[181]. These procedures all result in significant reduction and solubilisation of the substrate, but they all have the disadvantage of involving rather harsh reagents or conditions. This raises the question; are the structures of the soluble products representative of the structures in the original materials?

To overcome this problem, milder more specific reductants such as sodium borohydride ($NaBH_4$) and LAH have been introduced. Although widely used for the removal of pyrite these reagents have not been extensively applied to the degradation of kerogens. SMEAH (Sodium bis-2-methoxyethoxy aluminium hydride), a hydride whose chemistry is similar to that of LAH, has been used as a specific degradative reagent in the analysis of the Green River kerogens[24]. However, it was not very effective and only about 0.6% (wt%) of the kerogen was solubilised. Sodium borohydride was found to be

too mild to reduce substrates adequately[182] so attention was turned to the more powerful reductant LAH.

In normal synthetic organic chemistry, LAH is regarded as a very strong reducing agent which reacts with a variety of functional groups but under relatively mild conditions[183]. Table 4.1 lists the common functional groups which may be reduced with ethereal solutions of LAH. LAH will react with any compound having acidic protons, hence alcohols, phenols and amines will all form salts with LAH. However, when these salts are hydrolysed the original substrate in regenerated and the net result in just consumption of the LAH. Thus, the most synthetically important reactions of LAH are reductions of unsaturated polar groups, especially (C=O). Some reduction (addition of hydrogen) will occur to normally non-polar unsaturated groups eg. (C=C) if they are conjugated with a polar unsaturated group. Normally single C-C and C-O bonds are largely unaffected by this reagent. It should be noted that LAH reacts explosively with water and mineral acids which should be absent from the reduction medium. LAH can only be quenched with water in the presence of a large excess of moderating solvent and with extreme caution. LAH dust is also pyrophoric and should be treated accordingly.

From table 4.1 we can see that fragmentation of the parent molecule can occur from the LAH reduction of some functional groups. These are esters, disulphides, some tertiary amides and the sulphone/sulphonate derivatives. Reduction of the other functional groups just results in the conversion of the functional group concerned with no breakdown of the parent molecule into smaller fragments. Thus in addition to removing pyrite, LAH reduction may also provide a way to probe the contribution esters, disulphides etc make towards the kerogen structure. However, it must be remembered that these kerogens have already been in contact with HF and HCl. Therefore many of these groups may have already been cleaved by these acids.

In this study we determined the increase in solubility of the kerogens in both

chloroform and pyridine as afforded by LAH reduction. Both the insoluble and solubilised reduction products were analysed using the same techniques as used to characterise the original kerogens and bitumens. Reduction products that were soluble in the water used to quench the excess LAH were extracted and analysed by FTIR and GC-MS.

Table 4.1. Common functional groups reduced with lithium aluminium hydride.

Fuctional Group	Product
$-CHO$	$-CH_2OH$
$>C=O$	$>CHOH$
$-COCl$	$-CH_2OH$
$-\overset{|}{C}-\overset{|}{C}-$ $\quad\diagdown O \diagup$	$-CH_2CH_2OH$
$-CO_2R$	$-CH_2OH + ROH$
$-CO_2H$	$-CH_2OH$
$-CO-N(R_2)H_2$	$-CH_2-N(R_2)H_2$ or $\left[\begin{matrix}CH_2NR_2\\ \vert \\ OH\end{matrix}\right] \longrightarrow CHO + R_2NH$
$-CO-NHR$	$-CH_2NH-R$
$-C\equiv N$	$-CH_2NH_2$
$-C=NOH$	$-CH-NH_2$
$-C-NO_2$	$-C-NH_2$
$-CH_2-OSO_2-C_6H_5$	$-CH_3$
$-CH-OSO_2-C_6H_5$	$=CH_2$
$R-S-S-R$	$R-SH$
$-CH_2X$	$-CH_3$
$-CHX$	$=CH_2$

In some cases lithium aluminium deuteride (LAD) was substituted for LAH. Our reason for using LAD was to incorporate deuterium into the kerogen as a label via the reaction shown below. (Since LAD is expensive these reductions were carried out on a smaller scale).

$$R\text{-}\underset{\underset{O}{\|}}{C}\text{-}X \xrightarrow[ii)\ H_3O+]{i)\ LiAlD_4} RCD_2OH$$

where X = OH, OR, Cl, $NR_2(H_2)$, etc.

Thus by using LAD it was possible to estimate the distribution of the incorporated deuterium (hydrogen) between the soluble and insoluble products.

4.2. Results and Discussions.

The procedures used to reduce the kerogens, isolate and characterise the products are outlined in the experimental chapter of this thesis.

4.2.1. Removal of pyrite.

Table 4.2 below shows the ash contents of each kerogen before and after LAH reduction.

Table 4.2. Ash contents of reduced vs unreduced kerogens.

	Ash Contents (Wt %).				
	KC	JC	OC	CH1	CH2
Before reduction	40.0	19.9	21.0	7.9	18.8
After reduction	2.0	4.3	2.0	1.2	1.6

As can be seen, LAH reduction produced an almost ash-free organic residue, which can be explained by the dissolution of the residual pyrite mineral (section 3.2).

4.2.2. Extraction of Reduced kerogens.

Each reduced kerogen was extracted with pyridine and the resulting pyridine extract fractionated into chloroform solubles and insolubles as described in the experimental chapter(8). The results of this are shown in table 4.3.

Table 4.3. Solubility of reduced kerogens.

	% Solubility				
Solvent	KC	JC	OC	CH1	CH2
Pyridine	18.1	1.2	10.1	1.0	1.0
Chloroform	9.8	1.1	4.4	0.9	0.9

As we can see solubility of the pre-extracted reduced kerogens in pyridine and chloroform varies considerably. This increase in solubility as we mentioned in the introduction to this chapter, may be due to the reduction of esters, disulphides and the other functional groups which give rise to molecular fragmentation. It may also be due to the reduction of carboxylic acid groups to alcohols, thereby reducing the strength of any hydrogen bonds that might have contributed to the insolubility of these materials. However, it must not be overlooked that pyrite has been removed from the kerogens and this removal may result in easier access of solvents into the kerogens thereby increasing their extractability. Indeed, if we take the sulphur contents of the unreduced kerogens as a measure of their pyrite content (section 3.2) and plot these S% against the solubility of the reduced (pyrite-free) kerogens (either pyridine of chloroform) we obtain a very good correlation. (Figure 4.1). In other words it would appear that most of the increase in solubility provided by LAH reduction is due to the removal of pyrite and

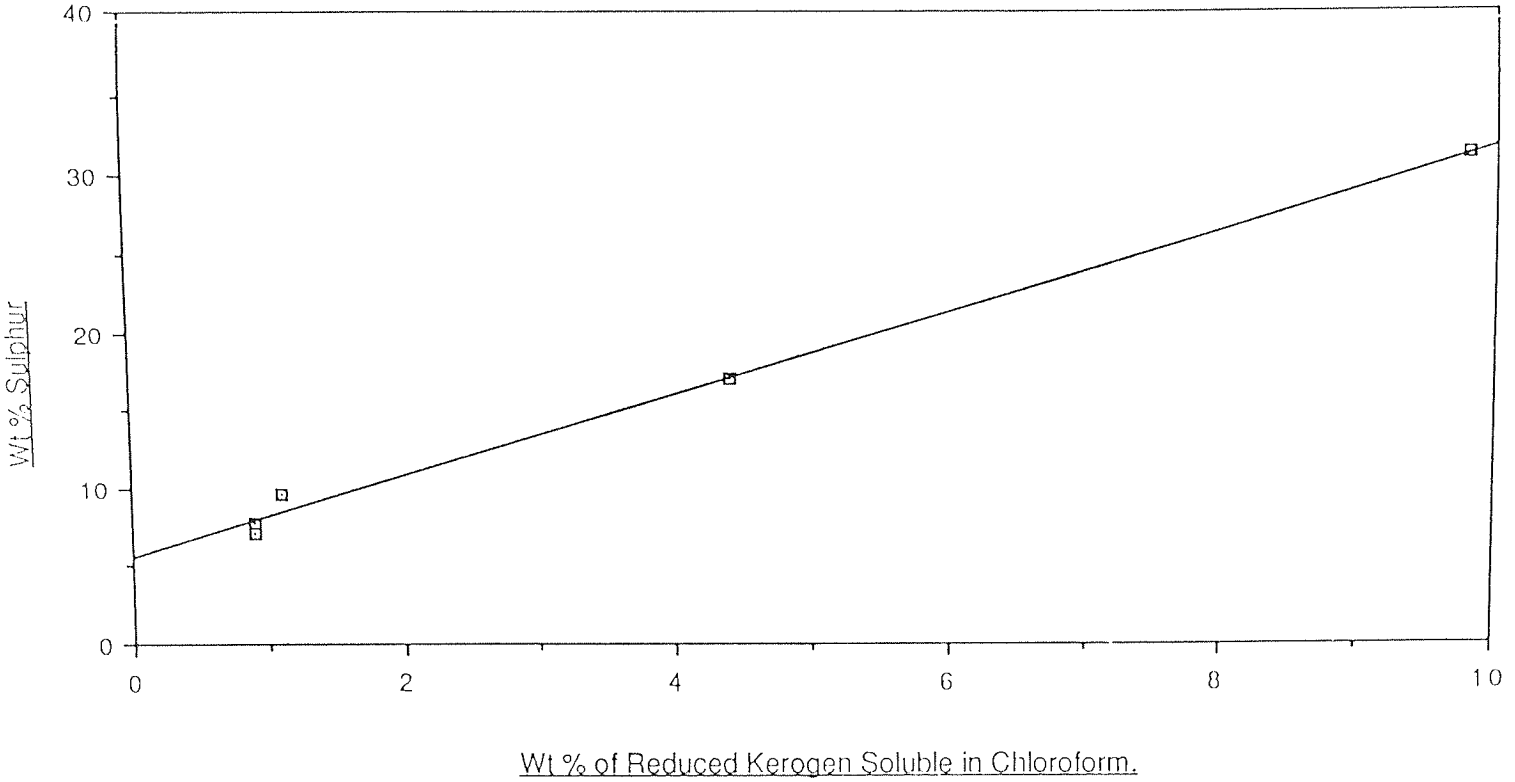

Figure 4.1 Plot of Wt% S of unreduced kerogens vs % solubility in $CHCl_3$ of reduced kerogen.

not the cleavage of labile functional groups within the kerogen. Although this may be true to a large extent, the reduction of these groups, (if they exist within the kerogens prepared by via HF and HCl), will undoubtedly result in some solubilisation. Thus it is still worthwhile to search for their cleavage products.

The fact that pyrite has such an influence over the solubility of kerogens suggests a very intimate association between it and the organic matter of kerogens. Indeed, electromicrographs have revealed such an association[184] and the intimacy of the pyrite/organic association is well documented[185].

4.2.3 Analysis of Soluble Reduction Products.

a) Water-Soluble Reduction Products.(WSRP).

It was found that the aqueous media resulting from the quench of excess LAH with water, contained some organic matter in solution. However, only a few milligrams of this material was isolated from each reduction reaction, so quantitatively it is not very important and analysis was restricted to FTIR and GC-MS analysis. Unfortunately no WSRP could be isolated from the reductions involving LAD. This is probably due to the small scale of the reactions and the small amounts of material being produced anyway.

FTIR analysis of the WSRP revealed peaks characteristic of alcohols (see Figure 4.2a). These include the O-H stretch peak at 3500-3000 cm^{-1} and the C-O stretch/OH deformation peaks at 1060, 1100 and 1300 cm^{-1}. Other peaks present in these spectra are attributable to the CH_3/CH_2 stretches and deformations of aliphatic groups. No thiols could be detected by FTIR but this might be due to their very weak absorptions (2600-2550 cm^{-1}).

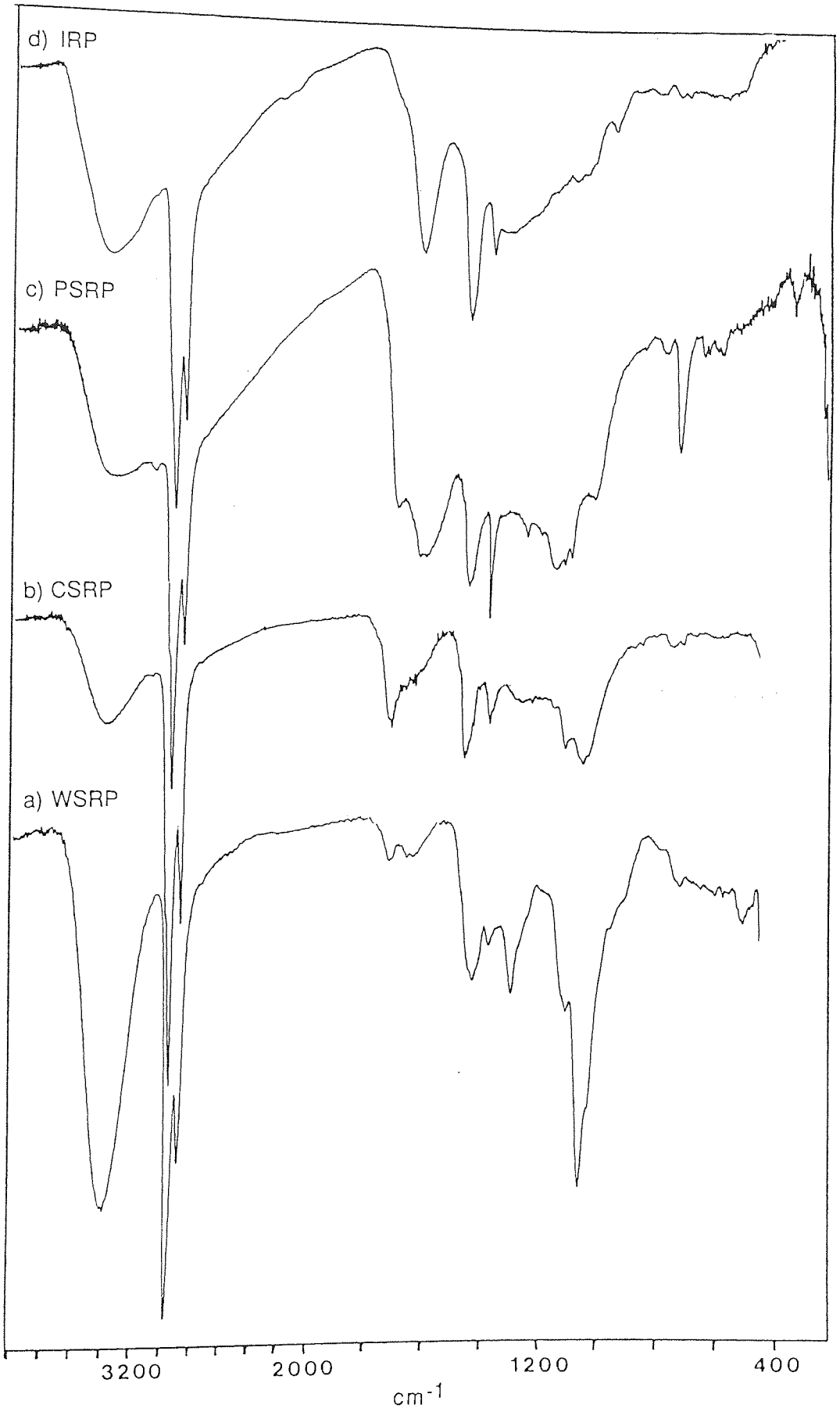

Figure 4.2 FTIR spectra of the reduction products from the JC kerogen.

GC-MS analysis of these WSRP fractions showed a series of components which had the characteristics of alcohols. This was determined by examination of their mass spectra which showed the characteristic alcohol peaks at m/z 31 and 45 which correspond to the CH_2OH^+ and the $CH_2CH_2OH^+$ ions respectively. However, the absence of molecular ions (a common feature of the mass spectra of alcohols) prevented their absolute characterisation. To help with the determination of these compounds they were derivatised with a silylating agent (BSTFA) which should increase their volatility and help identification of their molecular ions. Examination of these derivatised samples by GC-MS showed increased numbers of volatile components (see Figure 4.3), illustrating that involatile alcohols had failed to 'show-up' before derivatisation. Examination of individual mass spectra of these derivatised components however, did not show molecular ions and hence it was not possible to determine their molecular weights. Nonetheless by generating single ion chromatograms (SIC's) for m/z 73 and 147 it was possible to detect both a series of alcohols and diols (as their trimethyl silyl ethers) in each of the samples analysed. These compounds are presumably formed from the reduction of labile functional groups which gives rise to molecular cleavage and therefore solubilisation. To support this idea, alcohols and especially diols were detected from the SMEAH reduction of the Green River kerogen and explained in terms of the reductive cleavage of esters[24]. (The m/z value of 73 is due to the $^+Si(CH_3)_3$ ion whilst the m/z value of 147 corresponds to the $(CH_3)_3SiO^+{=}Si(CH_3)_3$ ion which is formed by migration of one trimethylsilyl group to the other in derivatised diols when they are ionised)[186]. Some evidence for the presence of thiols was also found in our samples.

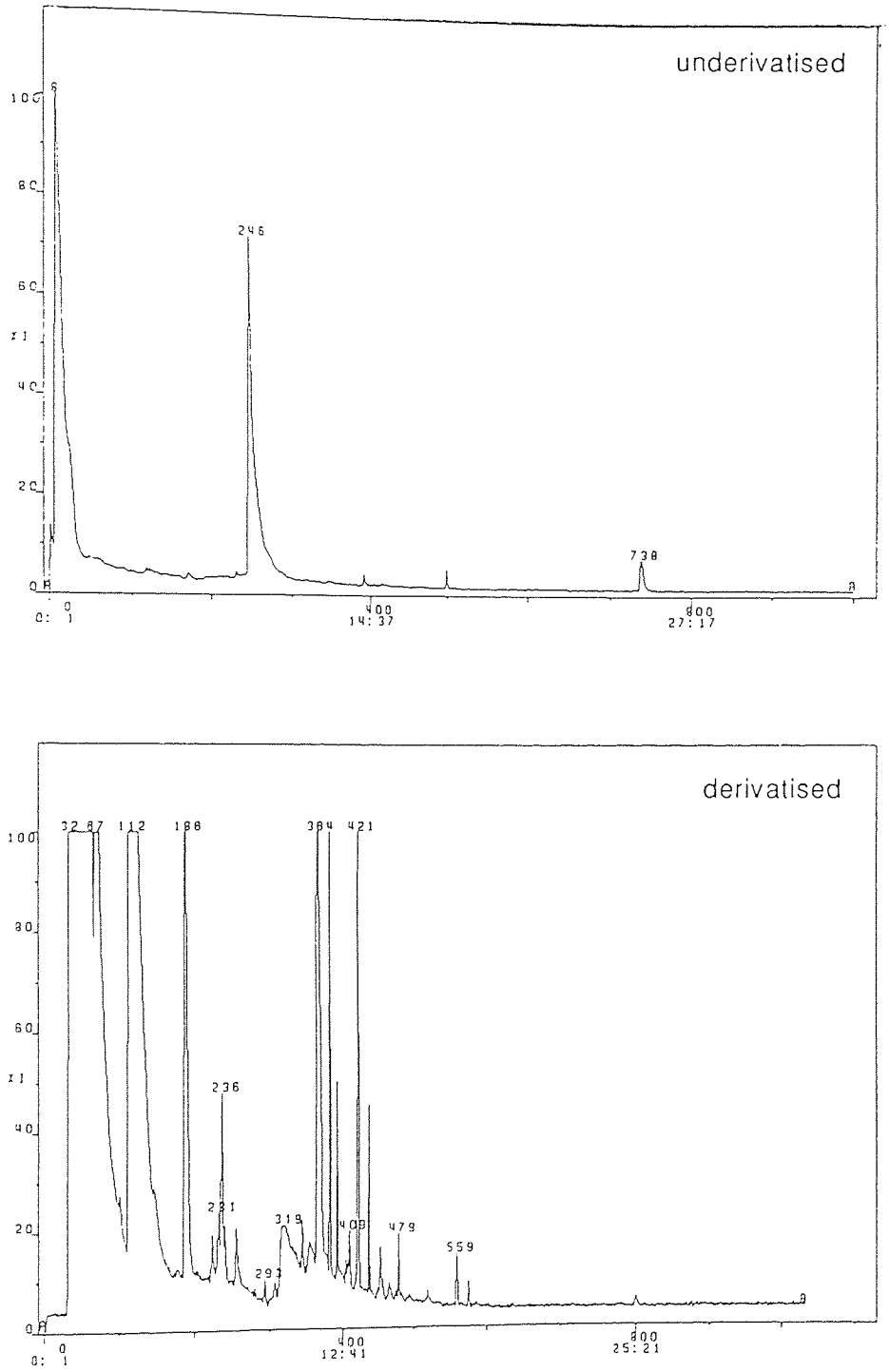

Figure 4.3 GC-MS TIC traces for derivatised and non-derivatised WSRP isolated from the CH1 kerogen.

b) Chloroform-Soluble Reduction Products. (CSRP).

FTIR analysis of the chloroform soluble reduction products gave spectra similar to those obtained for the chloroform bitumens isolated from these kerogens prior to their reduction. (See Figure 4.2b cf. Figure 3.2 (page 75)). There are some differences however. In the reduced products the OH peaks are slightly stronger and sharper whilst the carbonyl peaks are weaker. This is to be expected from the reduction of carbonyl groups to the alcohol by LAH. The carbonyl peaks are not completely absent in these spectra indicating either, 1). incomplete reduction by LAH or, 2). oxidation of the samples during their work-up. We believe the second process applies here because we feel it is unlikely that soluble materials would resist reduction under the conditions employed. CSRP resulting from the use of LAD instead of LAH showed only very weak C-D bond absorptions in their IR spectra. This indicates that the number of reduced functional groups present in these solubilised fractions is low. This is not surprising in the light of the evidence we have which suggests solubilisation of the kerogens is not a function of their reduction, but of pyrite dissolution.

^{1}H and ^{13}C NMR analysis of the five CSRP gave spectra which, to a large degree, are similar to those of their corresponding bitumens. In other words the CSRP appeared largely aliphatic in nature with abundant polymethylene chains. Figures 4.4 and 4.5 show the spectra (both ^{1}H and ^{13}C) obtained for the CSRP derived from the CH1 and CH2 kerogens respectively. (Cf. Figures 3.7 and 3.8 (pages 83 and 84) for comparison with their bitumens). It is interesting to note that once again the material isolated from the CH2 kerogen, this time by reduction, appears to contain a high level of isoprenoid chain structures.

Despite the similarity of these spectra with those of their corresponding original bitumens, there are a number of differences worthy of note. In general the CSRP spectra

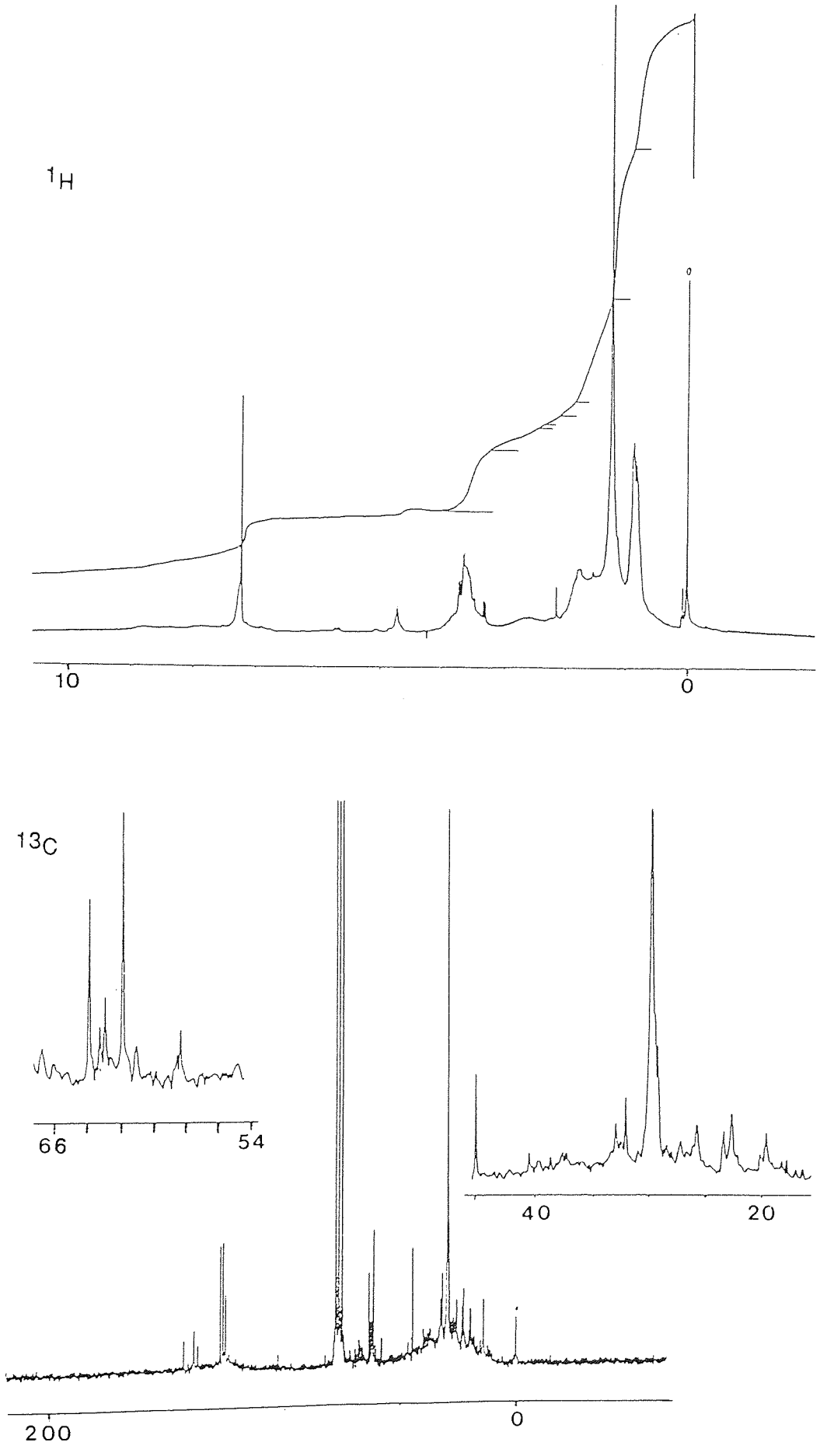

Figure 4.4 ^{1}H and ^{13}C NMR spectra of the CSRP isolated from the reduced CH1 kerogen.

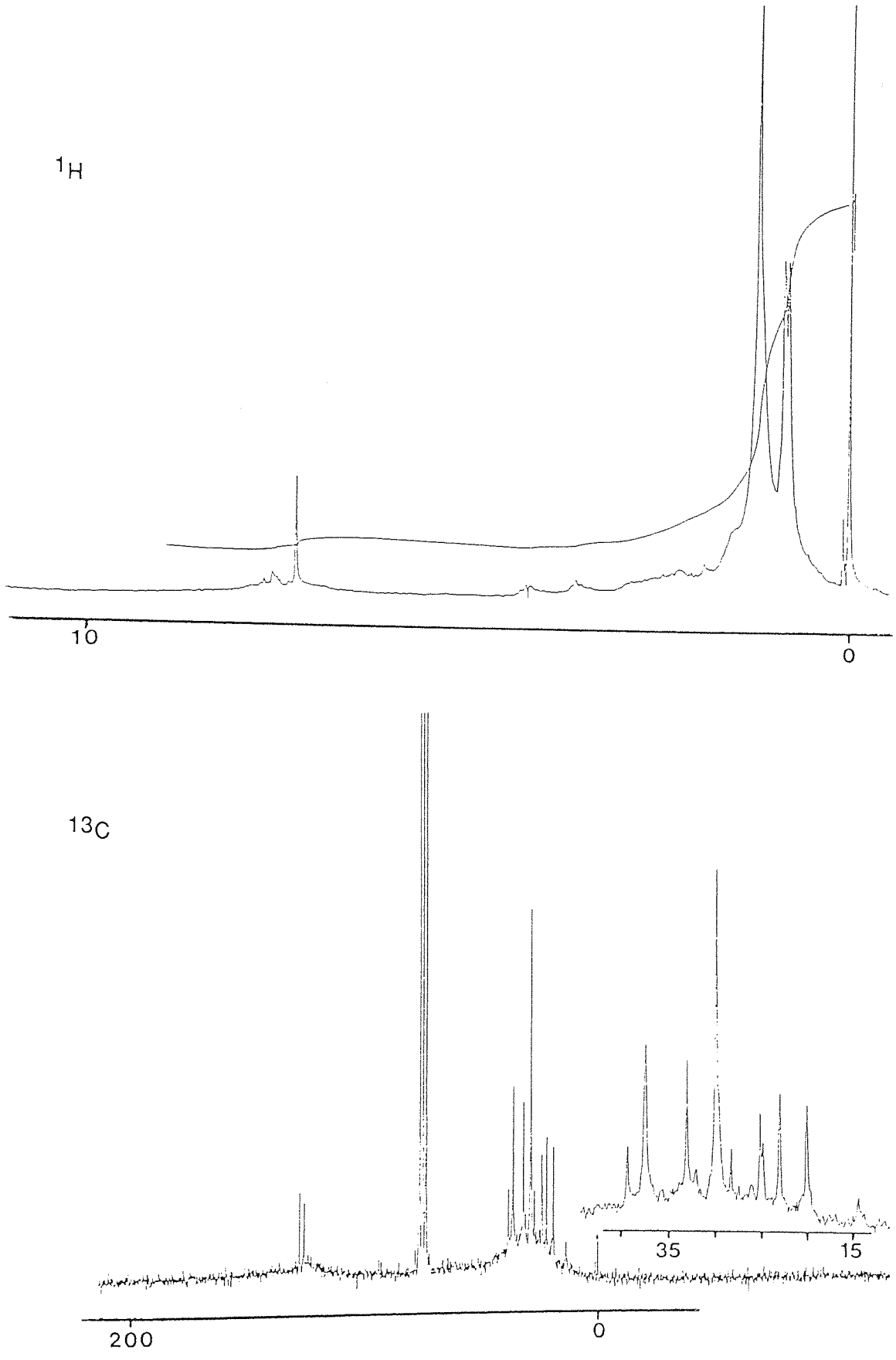

Figure 4.5 ^{1}H and ^{13}C NMR spectra of the CSRP isolated from the reduced CH2 kerogen.

show greater resolution in the aromatic regions. This is especially evident in the ^{13}C spectrum of the CSRP from the CH1 kerogen (Figure 4.4). Here we can clearly see two sets of three carbon resonances. The first set has resonances at 129.7, 128.4 and 127.2 ppm respectively whilst the second has resonances at 145.7, 141.3 and 139.6 ppm. Having established that these resonances were not due to pyridine contamination, the first set was attributed to unsubstituted benzene ring carbon atoms whilst the second set, being shifted on average by about 11-15 ppm downfield, can be attributed to aromatic positions substituted with a CH_2OH group. This therefore suggests the reduction of benzoic acid groups in the kerogens to benzyl alcohols, as shown below:

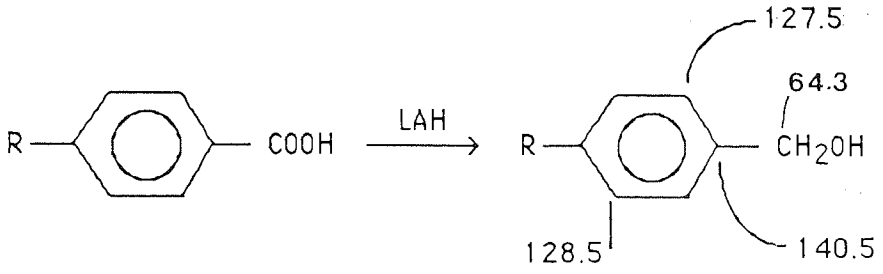

Literature ppm values are shown for benzyl alcohol.

The observation of a peak at 64.0 ppm which can be attributed to the carbon atom of the CH_2OH group, provided further evidence that this reduction had taken place. Obviously the precise position of resonance of these carbon atoms depends on the substitution of the aromatic ring system. This explains the minor variations of our resonance positions from those given in the literature for benzyl alcohol. Other resonances in the ^{13}C spectrum that can be attributed to the CH_2OH group of alcoholic structures occur at 63.4, 63.1, 62.0, 61.1 and 58.4 ppm. (See Figure 4.4). At first it was thought that some of these peaks may be due to contamination from THF. However the only THF resonance that occurs in this region is at 67.9 ppm and therefore THF was ruled out as a contaminant. It was therefore concluded that the CSRP from the CH1 kerogen contained a

considerable alcoholic character with a significant contribution from benzyl alcohol structures.

Further evidence for this conclusion was obtained from the ^1H NMR spectrum of this sample. This spectrum showed a peak at 4.7 ppm, which can be attributed to the methylene groups of benzyl alcohols. Unfortunately the aromatic protons of these compounds resonate at 7.3 ppm and therefore are not distinguishable from the residual proton resonances in the deuterated chloroform solvent. In addition the OH proton resonance occurs at 1.8 ppm and is obscured by other peaks. Addition of D_2O to facilitate a deuterium exchange failed to change the spectrum. Other peaks in the ^1H NMR spectrum which indicate alcohols occur at 3.4 - 3.8 ppm. These can be attributed to the methylene protons in the CH_2OH group of aliphatic alcohols. It should be noted that the relative size of the peaks due to alcoholic structures as determined by NMR varied from sample to sample. In general the CH1 CSRP appeared to have the highest alcoholic character of the five samples followed by CH2, JC, OC and KC CSRP in that order.

GC-MS analysis of the five CSRP gave the TIC traces shown in Figure 4.6. As can be seen reduction with LAH gives rise to a considerable number of volatile components the distribution of which varies from one sample to another. N-chain alkanes are prominant volatile species in all but the CSRP from the CH1 kerogen. In the latter case they occur only in low concentrations. It is interesting to note that the distributions of the n-alkanes in the CSRP differ from those in the corresponding original chloroform bitumens. (See table 4.4 cf. table 3.7, page97).[The parameters in table 4.4 were derived in the same way as those in table 3.7]. Other compound classes detected in these extracts were alkyl benzenes, alkoxy benzenes, branched and cyclic alkanes and small quantities of alkyl naphthalenes. The observed concentrations of these species were low when compared with those of the n-alkanes. (CH1 kerogen excepted). The formation of

Figure 4.6

GC-MS TIC traces for the CSRP.

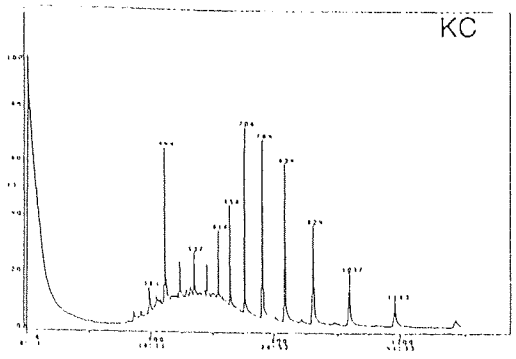

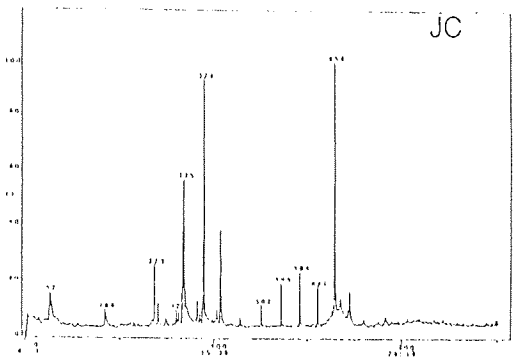

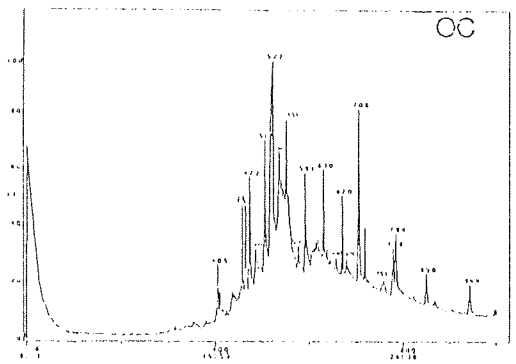

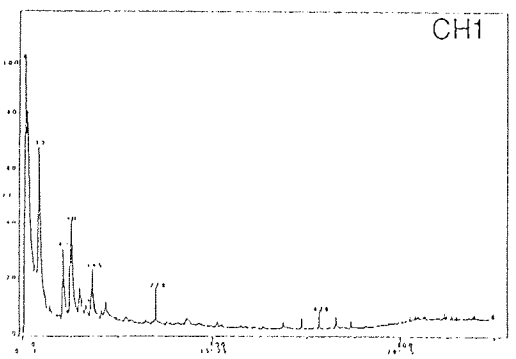

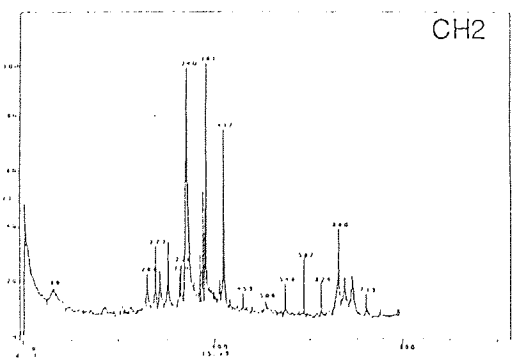

Table 4.4. Summary of GC-MS Analysis of CSRP.

CSRP Sample	TIC	Normalised Single Ion Currents x10^3 71+85	77	91	93	141	143	149	191	Iso-alkane / n-alkane	n-alkane distrib^n	n-alkane max.	pristane / phytane	aliphatic / aromatic
KC	29593	175	1.3	3.2	0.8	4.2	0	0.4	0	-	C_{16}-C_{30}	C_{25}	-	18.4
JC	36571	68	112	24	12	112	0.8	223	3.6	0.09	C_{14}-C_{30}	C_{16}, C_{23}	1.07	0.26
OC	19717	356	7.0	60	7.3	3.3	0.2	484	0	0.13	C_{17}-C_{28}	C_{19}	0.31	4.57
CH1	28265	144	6.5	18	6.2	1.3	1.1	5.9	3.9	-	C_{19}-C_{32}	C_{24}	-	4.35
CH2	25739	82	159	36	9.1	159	27	159	2.6	0.50	C_{16}-C_{28}	C_{23}	0.44	0.21

these compounds and the n-alkanes is hard to envisage by the normal reduction reactions of LAH. Therefore, it is suggested that they result from the release of trapped materials within the kerogen matrix upon pyrite dissolution. Alkyl phthalates were found in high concentrations in the CSRP derived from the JC, OC and CH2 kerogens, and are thought to be contaminants. In addition, CSRP samples derived from JC and CH2 both contained significant quantities of two components that could not be fully identified. The first of these is a benzene derivative since it yields a very strong m/z 77 peak in its mass spectrum. Consultation of the eight peak index plus a computer search yielded only diphenyl ether as the best, yet poor fit. The second component had a molecular weight of 350 and a base peak of 251 but could not be identified by either computer search or from the eight peak index. The CSRP from the CH1 kerogen alone were found to contain significant quantities of components having very strong m/z 71 base peaks. These compounds did not show the characteristic alkane fragmentation patterns which suggested that they might be alcohols, perhaps methyl cyclohexanols which are known to give strong m/z 71 peaks. However, derivatisation of this sample with BSTFA (as with the other CSRP samples) did not reveal the presence of any alcoholic material. Also, as far as we could tell, GC-MS analysis of the CSRP formed by the use of LAD instead of LAH, did not reveal any compounds containing deuterium.

Thus IR and NMR analysis show alcoholic moieties to be present in the CSRP, yet GC-MS failed to detect any. This can be explained by the alcoholic structures being attached to high molecular weight and/or involatile materials which are soluble in the NMR solvents, but yet not volatile enough for GC-MS analysis.

UV-vis spectroscopy of the CSRP gave spectra very similar to those recorded for their corresponding original bitumens. The only exception to this was the UV-vis spectra obtained for the CSRP derived from the JC kerogen, which showed only weak

peaks due to the petroporphyrin identified in its original bitumen. This indicates that in the CSRP of the JC kerogen the relative concentration of this petroporphyrin is much lower.

c) Pyridine Soluble Reduction Products. (PSRP).

FTIR analysis of the PSRP showed them to be very similar to the original pyridine bitumens isolated from each kerogen. (See Figure 4.2c cf. Figure 3.3). The only significant differences are slight sharpenings of the OH stretch absorptions and the development of C-O and OH deformation absorptions at 1100 - 1200 cm^{-1} in the spectra of the PSRP. Both these differences are consistent with the reduction of carbonyl groups to alcohols. However, there is no discernable change in the carbonyl peaks of these PSRP spectra when compared to the original pyridine bitumen spectra. This it is felt is due to air oxidation of the samples during their extraction and work-up. FTIR analysis of the PSRP produced via reduction with LAD showed the extra absorptions due to C-D bonds, but once again these were relatively weak.

NMR analysis of the PSRP was found to be very difficult. No ^{13}C spectra could be obtained, for reasons unknown, and only very poor ^{1}H NMR spectra could be obtained. However these ^{1}H NMR spectra did suggest that once again, pyridine soluble materials (PSRP) were much more aromatic than their chloroform soluble counterparts (CSRP). This follows the trend observed with the original chloroform and pyridine bitumens.

As found for the original pyridine bitumens, the PSRP were found to contain no volatile components identifiable by GC-MS analysis, even after derivatisation with BSTFA.

4.2.4. Analysis of Insoluble Reduction Products, (IRP).

Elemental analysis of the five IRP gave the compositions and empirical formulae shown in table 4.5.

Table 4.5 Average elemental composition of IRP.

	Average Elemental Composition (wt%)					
IRP	C	H	N	O	Ash	Empirical Formula.
KC	71.8	5.9	1.0	19.3	2.0	$C_{100}H_{98}O_{21}N_1$
JC	71.7	7.8	1.1	15.1	4.3	$C_{100}H_{131}O_{17}N_1$
OC	67.6	7.2	0.6	22.6	2.0	$C_{100}H_{130}O_{27}N_1$
CH1	73.5	8.0	1.2	16.1	1.2	$C_{100}H_{131}O_{18}N_1$
CH2	76.3	8.4	0.6	13.1	1.6	$C_{100}H_{132}O_{13}N_1$

The ten analyses used to calculate these average elemental compositions for each IRP are plotted in the form of a van Krevelen diagram (Figure 4.7). If this is compared with the similar diagram for the unreduced kerogens (Figure 3.17, page 108) it is clear that treatment with LAH reduces the heterogeneity of each sample. (The spread of the data points is reduced). This is probably due to the removal of pyrite and hence the variable association of this mineral with the organic matter.

If the data in table 4.5 are compared with those in table 3.9, it is clear that LAH reduction increases the H/C ratio whilst reducing the O/C ratio of these materials. This is to be expected if reduction of the functional groups of the type shown in Table 4.1 takes place. Unfortunately it is not possible to correlate the drop in the H/C ratio that occurs upon reduction with the number of functional groups reduced for two main reasons. Firstly, as we can see from table 4.1, different functional groups give rise to different products with differing H/C ratios, and secondly these elemental

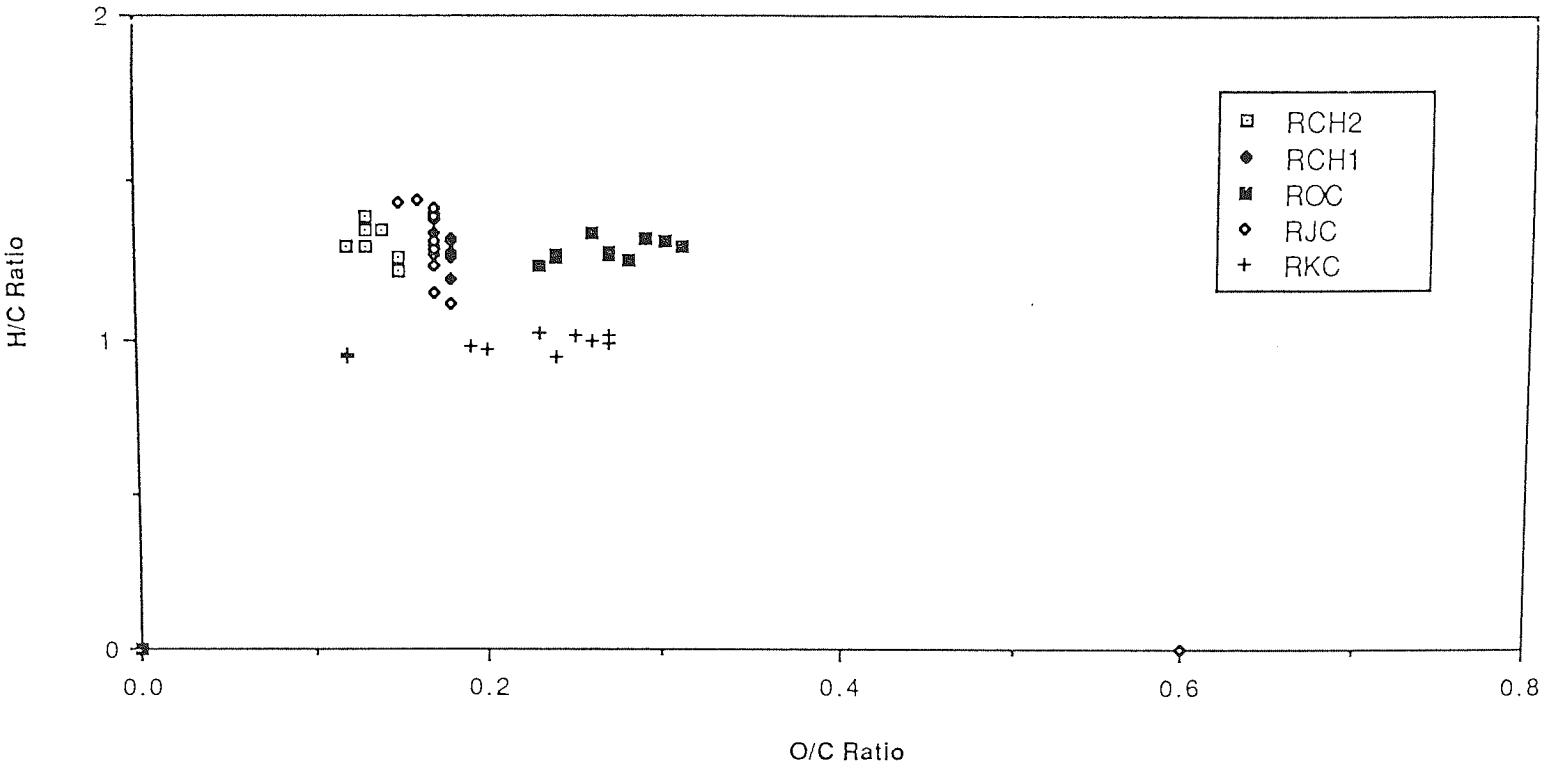

Figure 4.7 Van Krevelen plots for the IRP.

determinations only represent part of the reduction products, ie. the solubilised materials were not included in the analysis.

FTIR analysis of the IRP gave spectra similar to those of their corresponding original kerogens. (See Figure 4.2d cf. Figure 3.19, page 112). However, as with the soluble reduction products, there are a number of marked differences. As we might expect, the spectra of the IRP show enhanced OH absorptions and decreased carbonyl absorptions, when compared with their corresponding parent kerogens. It was also noted that upon reduction the shape of the aromatic ring deformation absorption at 1630-1600 cm^{-1} changed, it became much sharper. This suggests that there is at least some contribution to this peak from certain carbonyl groups. Since the carbonyl contribution is removed by reduction it is now possible to obtain an indication from FTIR of the order of relative aromaticities of these samples. The order suggested is JC>CH1>KC>OC>CH2, but this does not agree with the order obtained from solid state NMR (page 117). Reductions with LAD yielded IRP whose spectra contained the additional C-D stretch peaks at 2200-2000 cm^{-1}. (See Figure 4.2d) The size of this C-D absorption relative to the C-H absorptions was small in each of the IRP but similar to that found in the soluble reduction products. This indicates that the incorporation of deuterium via reduction did not discriminate between the material solubilised and that which remained insoluble. This in turn suggests that the reduced functionalities are evenly distributed between the various product fractions (IRP,CSRP and PSRP).

Solid state ^{13}C NMR analysis of the IRP produced spectra more or less identical to those obtained for the parent kerogens. This is especially interesting in the cases of the OC and KC kerogens for it means that the extraction of 10.1% and 18.1% of their organic material respectively, did not change their overall structure (as indicated by the solid state NMR analysis.) Thus , within experimental error, it appears that the

material solubilised by reduction must be of similar composition to that which remains insoluble - otherwise the spectra would have changed after reduction and extraction.

Also it was noted that the 210 - 160 ppm region of the spectra did not change appreciably upon the reduction. This indicates either; 1.) There are few carbonyl groups in the original kerogens or , 2.) LAH reduction did not reduce the carbonyl groups. However, we know from FTIR analysis that reduction of carbonyl groups took place and therefore we are left with the conclusion that our kerogens posses relative few carbonyl groups. From this observation it is clear that the peaks which are present in this region of the spectra must be spinning side bands of the aromatic peaks. It is this piece of information that made the partial resolution of the 100-50 ppm region in the NMR spectra of the original kerogens possible (See section 3.4.3).

4.3 Conclusions.

LAH was successfully employed to eliminate pyrite from the kerogens prepared by acid demineralisation. This reductant was also found to have a favorable solubilising effect on the kerogens, the degree of solubilisation was found to parallel their pyrite content. The dissolution of the kerogens therefore is explained , not by the cleavage of labile functional groups in the kerogen backbones, but by the increased penetration of solvents into the kerogen matrix which is facilitated by the removal of pyrite. This idea is substantiated by the detailed analysis of the soluble reduction products which were found to contain n-alkanes and other compounds which are not the products expected from the cleavage of functional groups. These compounds are thought to have been trapped within the kerogen network until the removal of pyrite allowed their extraction.

Reduction of the kerogens is confirmed by the attenuation of the carbonyl absorptions and enhancement of the OH absorptions in the FTIR spectra of all reduction products, as compared to the original kerogens. In addition deuterium can be seen to be

incorporated into the reduction products when LAD is used as the reductant. These observations are consistent with the reduction of the various carbonyl groups to their alcoholic products. Despite the increased alcoholic character of all the reduction products, only very small quantities of volatile alcohols and diols could be detected. Evidence was found from NMR analysis to suggest that in the CH1 kerogen especially, reduction of benzoic acid structures to their benzyl alcohols was taking place. However GC-MS analysis of this product did not show any volatile benzyl alcohols and we must conclude that this is due to their attachment to larger involatile substituents. Although the reduction products have a higher alcoholic character, it would appear that they have much the same composition as their corresponding original bitumens and kerogens. Indeed analysis of the CH2 reduction products shows a very high contribution from isoprenoid structures as compared with the other samples. This was a strong feature of the original bitumens and kerogens isolated from this sample. Solid state NMR of the insoluble reduction products suggests that carbonyl groups are in a relatively low concentration in the kerogens, as compared with, for example, a humic acid.

Thus, we have shown that LAH reduction can lead to considerable enhancement in the solubility of kerogens. This leads to more of the organic material being characterised by the more powerful solution state techniques and hence to a better understanding of the structure of these complex materials. Hence we feel that LAH reduction is a very useful process for the analysis of our and similar materials.

Even if solubility enhancement by LAH reduction is low, the treatment may be of benefit since it simplifies the kerogen structure by reducing a whole host of different functional groups into just a few common ones. Hence any subsequent treatment or reaction involving a reduced kerogen is likely to be simpler and the products less varied, simply because the number of different functional groups that may react or interfere has been reduced.

Chapter 5

The O-Methylation of Kerogens

5. O-Methylation of Kerogens.

O-methylation is a highly specific reaction by which the secondary structure or hydrogen bonding within kerogens or coals can be substantially disrupted. It therefore provides a means whereby the contribution that H-bonding makes towards the insolubility of kerogens can be determined. To highlight the benefits of this type of alkylation over others the following introduction contains a short survey of other alkylation reactions which are, or have been, used in the study of coals and similar materials.

5.1 Introduction.

One of the more common techniques used to increase the solubility of coals or kerogens is alkylation. There are several methods currently available for the alkylation of such substrates and they all have their own advantages and disadvantages.

The alkylation of coals or kerogens can be divided into three main categories:

a) Friedel Crafts alkylations and transalkylations,

b) Reductive alkylation

c) O - Alkylation (O - Methylation is the method we adopted).

a) Friedel Crafts Alkylations and Transalkylations.

The common feature of these reactions is the use of strong Lewis acids. The Friedel Crafts alkylation is the reaction of an alkyl halide or alkene with an aromatic molecule in the presence of a Lewis acid such as $AlCl_3$ or BF_3 to give alkyl aromatics[187]. This can be represented as shown below:

$$Ar\text{-}H + RX \xrightarrow{AlCl_3\ cat.} Ar\text{-}R + HX$$

where X = halide.

Due to their aromatic character, both coals and kerogens readily undergo Freidel Crafts alkylations. Extensive studies have been made on coals[188,189], but in contrast there are few recorded studies on kerogens[190].

The transalkylation reaction uses low molecular weight aromatic compounds such as phenol, toluene, xylene or diphenyl ether etc, which act as acceptor molecules for fragments of the coal or kerogen which have been cleaved by the Lewis acid[191]. These fragments of the coal/kerogen are therefore acting as alkylating agent. This can be represented as shown below:

$$\text{Coal-R} + \text{xylene} \xrightarrow{AlCl_3 \text{ cat.}} \text{Coal-H} + \text{R-Xylene}$$

Where R = Coal fragment.

Acid catalysed reactions of this type produce large increases in solubility. For example a transalkylated Texan lignite coal[192], where m-xylene and $AlBr_3$ catalyst were used, had a solubility in pyridine of up to 38% compared with only 12% before alkylation.

Although at first sight this increase in solubility seems very encouraging, it has since been shown that the nature of these reactions is much more complex than the simple alkylation, initially thought to take place[193]. Lewis acids readily cleave aliphatic bridges in the coal structure and initiate a series of isomerisation reactions. For example the Lewis acid can react with aliphatic bridge carbons to produce benzyl type carbonium ions. These carbonium ions can then undergo aromatic electrophilic substitutions on aryl positions in the coal structure. By such a series of cleavage and condensation reactions the primary structure or the original covalent backbone of coal is drastically altered and the reaction products may be much more aromatic than the

original coal.

Other problems associated with these reaction include the way acceptor molecules can associate and adsorb tenaciously to the coal residues. This hinders the analysis of the reaction products because the extent of association or adsorption needs to be known before interpretation of elemental analysis, solid state NMR and IR results can be made.

In view of these problems and despite the attractive increases in solubility afforded by this reaction, we decided not to pursue studies of this kind on our kerogens.

b) Reductive Alkylation.

More recently reductive alkylation (introduced to coal research by Reggel and co-workers in 1958)[194] has received attention as a way of rendering coals[195] and kerogens[196] more soluble. It involves the treatment of a coal or kerogen with an alkali metal in THF or other suitable solvent, in the presence of a 'transfer agent', commonly naphthalene. This reaction has recently been reviewed by Stock[174].

This mixture generates anions of the transfer agent by electron transfer from the metal. These then donate their charge to receptive centres within the coal to form a coal anion. Upon completion of this reduction of the coal an alkyl halide is added which subsequently alkylates the sites of negative charge in the coal anion. These steps can be shown by the following equations:

$$\text{Coal} + nK \xrightarrow[\text{naphthalene}]{\text{THF}} \text{Coal}^{n-} + nK^{+}$$

$$\text{Coal}^{n-} + nRX \longrightarrow \text{Coal}(R)_n + nX^{-}$$

Some coals have had their pyridine solubility enhanced to 97% by reductive

alkylation, however, 50-80% would be more common.[197]. This high solubility is due to the instability of certain anionic sites produced within the reduced coal. These negatively charged sites decompose by carbon-oxygen[198] or carbon-carbon[199] bond cleavage to yield new, lower molecular weight compounds which when subsequently alkylated are soluble in organic solvents.

However, it is now clear that the reaction is much more complex than initially thought[200,201]. Reductive alkylation of a sample of the Illinois No. 6 seam was accompanied by incorporation of both naphthalene and tetrahydrofuran in the products[202]. Also, it was found that other reactions such as eliminations and reduction of carbonyl functionalities took place as well as the carbon-oxygen and carbon-carbon bond cleavages[203].

Even though there is very little in the literature regarding reductive alkylation of kerogens we decided not to perform this reaction on our kerogens primarily as a consequence of these difficulties.

c) **O-Alkylation.**

In view of the problems mentioned above we concentrated our efforts on the milder and more selective O-alkylation of our kerogens. This follows from our previous work on kerogens[23]. O alkylation is more specific than the other types of alkylation because it only takes place at acidic functional groups. These are normally the hydroxyl group of the phenol and carboxylic acid but reaction at alcoholic, amine and thiolic sites will also take place if they are sufficiently acidic. The O-alkylation reaction can be shown as follows:

$$\text{Coal-OH} + \text{RX} \xrightarrow{\text{Base}} \text{Coal-OR} + \text{HX}$$

where X = halide

As with the other alkylation procedures one of the main aims of O-alkylation is to increase the solubility of the coal or kerogen so that more of it becomes amenable to solution state spectroscopic and chromatographic analysis. Since no C-C or C-O bonds are broken in these reactions, solubility can only be enhanced via the disruption of secondary bonds in which the acidic functional groups participate. These bonds are normally referred to as hydrogen bonds (H-bonds). It was hoped that by derivatising the acidic sites the H-bonds would be broken and thus cause a subsequent increase in substrate solubility.

The selective reaction of acidic functional groups in coals is not new; O-silylation[204] and O-acetylation[205] reactions for instance are known to produce derivatised oxygen functionalities. However these reactions have limitations. All published conditions for the silylation and acetylation reactions require the use of pyridine which acts as both base and good swelling solvent for the coal. However pyridine is notoriously difficult to remove from the alkylated products and therefore leads to difficulties in their analysis.

Methods for the O-methylation of carboxyl and hydroxyl functions in humic acids have been studied in some detail by Briggs and Lawson[206]. The methods studied were:

i) Methanol with concentrated sulphuric acid

ii) Methyl iodide and silver oxide in dimethylformamide

iii) Methyl iodide and barium oxide or hydroxide in dimethylformamide

iv) Methyl iodide and solid sodium hydroxide

v) Dimethylsulphate and aqueous sodium hydroxide

vi) Dimethylsulphate and solid sodium hydroxide

vii) Dimethylsulphate and anhydrous potassium carbonate in acetone.

They found that methods (ii-vi) were unsuitable because methylation was slow or incomplete or for other reasons, eg. silver oxide appears to cause some oxidation and

barium compounds gave products with high ash contents. Diazomethane was not tested because previously it had been found that its use always led to products with increased nitrogen contents. The first method (methanol/sulphuric acid) only esterifies carboxylic acids and is therefore of little use in the methylation of reduced kerogens. The last method (vii) was found to methylate both hydroxyl and carboxyl groups but it required repeated treatments before reaction was complete.

Recently a highly selective O-alkylation procedure for coals and kerogens has been developed by Liotta[207] which involves the use of a basic phase transfer catalyst (PTC) to aid the alkylation process. This phase transfer reaction proceeds quantitatively under very mild conditions and is specific to the acidic proton sites. It generates products in which the integrity of the covalent backbone is preserved. Since the introduction of this reaction many coals have been O-alkylated and subjected to analysis. This reaction has found application in the modification of physical properties of coals[208,209] and has assisted studies involving the swelling and therefore the macromolecular structure of coals[210,211].

The PTC serves two purposes throughout the reaction. Firstly it serves as a strong base which abstracts the acidic protons from the coal thus facilitating the reaction between the coal alkoxide anion and the alkyl halide. Secondly it serves to swell the coal allowing the penetration of the alkylating agent into the coal.

The use of PTC's in this fashion is different from their normal role. Normally they are used to transfer lipophobic (hydrophilic) species from an aqueous phase into a lipophilic (hydrophobic) organic phase which contains the other reactant. A typical example is the catalytic conversion of 1-chlorooctane into 1-cyanooctane shown schematically below:

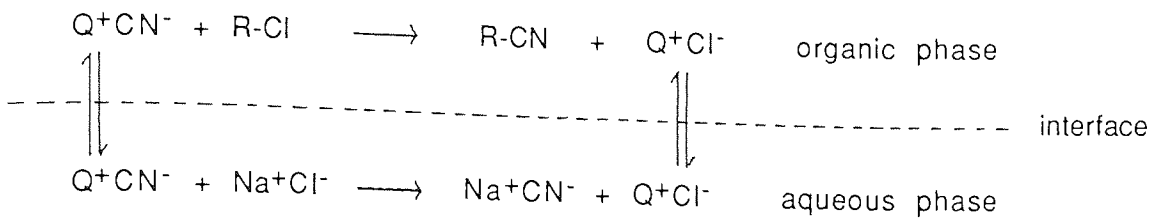

Q^+ = quaternary ammonium cation (PTC)

Such reactions only require catalytic amounts of PTC but our reaction upon coals/kerogens uses the PTC in reagent rather than catalytic quantities. This is to facilitate the swelling of the coal/kerogen and to allow for a much faster reaction than would otherwise be possible. On completion of the reaction the PTC becomes free to 'pick-up' further reagent from the aqueous phase. Excellent reviews on the use of PTC's in organic synthesis are available[212,213,214].

The most common PTC used in the O-alkylation reaction of coals is tetrabutylammonium hydroxide (TBAH). Others have been used, but usually the only difference from TBAH is the length of the alkyl groups. These basic PTC's are more effective than pyridine for swelling coals[215]. They are thought to do so by association with the acidic protons in the coal thereby isolating them from each other and releasing the coal from its secondary or H-bonding. PTC's can also be regarded as wedges holding apart the coal/kerogen matrix[216]. Thus the PTC-assisted alkylation of coals or kerogens can be represented as:

$$\text{(Coal)-OH} + (C_4H_9)_4NOH \longrightarrow \text{(Coal)-ON}(C_4H_9)_4 + H_2O$$

and

$$\text{(Coal)-ON}(C_4H_9)_4 + RI \longrightarrow \text{(Coal)-OR} + (C_4H_9)_4NI$$

The kinetic reactivities of the acidic hydroxyl groups in coal towards PTC-assisted O-methylation have been measured[217]. The reactivities of the acidic functional

groups in the coal were correlated to the reactivity of acidic groups in model compounds. It was discovered that the activation energy associated with the nucleophilic displacement determined the rate of the O-methylation of the coal. Thus the rate of this reaction is not limited by the mass transport of the chemical reagents into the coal structure. This surprising result supports the proposed mechanism whereby the coal is swollen by the PTC thus allowing the free access of reactant molecules into the coal matrix.

Many alkyl halides have been used for the purpose of coal alkylation. In general the iodides are the best because they possess the most labile leaving group of the halogens. Also the size of the alkyl group was found to affect the rate of coal O-alkylation. Studies using methyl iodide, n-butyl iodide, benzyl iodide, n-heptyl iodide and n-octadecyl iodide showed that as the length of the alkyl chain was increased so it took longer for reaction to take place[215]. As mentioned earlier this is not a mass transport problem and merely reflects the usual decrease in the rate of S_N2 substitution reactions as the size of the alkyl group is increased. In addition, it was also found that the longer the alkyl chain introduced upon O-alkylation, the more soluble was the alkylated product. This is to be expected since larger alkyl groups increase the non-polar character of a substance and therefore increase its solubility in certain solvents. Also the larger the alkyl group introduced the more physical distortion of the alkylated coals occurs. This holding apart of the coal matrix could result in the easier extraction of trapped materials.

In our study we have used TBAH and methyl iodide in an attempt to discover the chemistry involved in the O-methylation of our five reduced and pyridine extracted kerogens. In some cases perdeuterated methyl iodide was also used. This allows for the O-methylation reaction to be more easliy followed. The nature of the methylated products and the extent to which solubility was enhanced have been determined. Comments are

made regarding the role of secondary or H-bonding in our five kerogens. Material made soluble or extractable by O-methylation is explained in terms of the release of trapped compounds by the opening up of the insoluble kerogen matrix.

5.2 Results and Discussion.

The O-methylated and O-perdeuteromethylated kerogen derivatives were extracted with pyridine. Both insoluble residues and the soluble materials were analysed using a variety of techniques. The results of these actions are reported below.

52.1. Solvent Extraction.

Each of the O-methylated kerogens was extracted with pyridine and then fractionated into chloroform and pyridine extractables as described in the experimental section 8.6.1. The results of this treatment are given in table 5.1.

Table 5.1. Solubility of O-methylated kerogens in chloroform and pyridine.

	solubility%*	
O-Meth sample	Chloroform	Pyridine
CH2	0.5	1.4
CH1	0.4	1.0
OC	0.3	1.3
KC	1.2	3.6
JC	0.4	2.3

*Because the methyl groups that are added to the kerogen upon O-methylation only make a small contribution to the weight of the products, it was not necessary to correct for this weight change when calculating % extractabilities.

As mentioned earlier, the kerogens had been reduced with $LiAlH_4$ and exhaustively extracted with pyridine prior to O-methylation. Thus the material extracted after O-methylation should be due to the solubilising effect of O-methylation. To make sure that this was the case blank pyridine extractions were carried out on the reduced and extracted starting kerogens. This produced only very small yields of soluble extract (<0.1%) and confirmed that O-methylation was responsible for the increase in

solubility.

As can be seen from table 5.1 the quantity of soluble extract produced by O-methylation of our five kerogens is small. However this is in agreement with recent work by Mallya and Stock[218] in which six high rank bituminous coals were O-methylated and then extracted with pyridine. Their results showed that pyridine solubility was enhanced by no more than 4% by O-methylation. With one particular coal it was not enhanced at all. This rather modest solubilising effect of O-methylation has also been reported for a Cero Negro asphaltene[219]. The solubility of this asphaltene in n-heptane was only improved by 1%.

These later results are in sharp contrast to earlier work by Liotta, Rose and Hippo[215] on Illinois No.6 and Rawhide coals. These O-methylated coals were extracted with THF, benzene and chloroform. Solubility was enhanced significantly in all solvents and reached a maximum of 21.7% (for Illinois No.6 coal) using chloroform. Why there should be such a large discrepancy between these results and those of other workers is not clear. One could argue that it is due to the fact that different coals were used and that the variation in solubility reflects differences in the structures present in these coals. Although this is likely to contribute to the large variation observed, it has recently been shown that TBAH is very difficult to wash out of the coal[220] and therefore any subsequent solvent extraction of coals treated with this reagent would yield TBAH or its salt in the extract. We are therefore suspicious that TBAH may have contributed significantly to the solubility figures quoted in these earlier papers.

Indeed our initial O-methylation reactions using TBAH gave solubility figures of between 5-10%. This was found to result from the failure of the work-up procedure, used by Liotta[207] and Liotta, Rose and Hippo[215], to remove the TBAH and its salt from the alkylation products. Subsequently we found it necessary to develop methods for the removal of the TBAH and its salts. In the first method the alkylation mixture was

exhaustively extracted with pyridine. This gives a TBAH/salt free extraction residue and a pyridine extract containing all of the TBAH/salt and the material extracted from the kerogen. Subsequent treatment of this pyridine extract as described in experimental section 8.6.1 and 8.4 gave a TBAH/salt-free pyridine extract. The second method involved the use of a strong cation exchange resin and graded THF/water solutions[221]. FTIR and GLC analysis of the extracts treated in these ways showed the absence of TBAH/salt.

5.2.2 Analysis of the O-Methylation Residues.

5.2.2.1 Elemental Analysis of O-Methylation Residues.

Treatment of the five reduced and pyridine extracted kerogens as described in the experimental section 8.6.1 gave O-methylated kerogens having the empirical formulae given in table 5.2. These are compared with the empirical formulae of the kerogens before O-methylation.

Table 5.2. Empirical formulea of kerogens before and after O-methylation.

	Empirical Formulae	
Sample	Before O-Meth	After O-Meth
CH2	$C_{100}H_{132}O_{13}N_1$	$C_{100}H_{129}O_{16}N_1$
CH1	$C_{100}H_{133}O_{18}N_1$	$C_{100}H_{132}O_{20}N_1$
OC	$C_{100}H_{130}O_{29}N_1$	$C_{100}H_{128}O_{24}N_1$
JC	$C_{100}H_{131}O_{17}N_1$	$C_{100}H_{114}O_{12}N_1$
KC	$C_{100}H_{99}O_{23}N_1$	$C_{100}H_{92}O_{35}N_1$

As we can see from table 5.2, in all but the JC sample, O/C ratios increase while H/C ratios fall as a result of the O-methylation procedure. This is a sure sign that oxidation has taken place. Since the O-methylation reaction itself took place in a sealed

vessel under nitrogen, it must be concluded that oxidation occurred during the work-up procedures. This is despite the normal precautions being taken (eg the passage of N_2 over the extraction apparatus and storage in a vacuum desiccator). This oxidation prevented the observation of the the slight increase in H/C ratio which we might have expected upon methylation. It is therefore impossible to determine the relative number of methyl groups added to the kerogens from these elemental analysis results. Solid state NMR is best suited for this.

5.2.2.2 FTIR Analysis.

In addition to elemental analysis each O-methylated/perdeuteromethylated kerogen residue was subjected to FTIR examination. The spectra obtained from two representative samples, JC and CH1, are shown in Figures 5.1 and 5.2 respectively. The other samples all gave very similar spectra. In each figure part a) represents the reduced extracted kerogen prior to O-methylation, part b) represents the extracted O-methylated kerogen and part c) represents the extracted O-perdeutero methylated kerogen.

As can be seen from these spectra the broad and intense band attributed to the absorption of the hydroxyl group stretch (3600-3000 cm^{-1}) is significantly reduced and sharpened upon O-methylation/ O-perdeutero methylation. However, as expected it is not completely removed. The residual OH absorption is due to alcoholic OH groups which are insufficiently acidic to be methylated by methyl iodide under the conditions used. Carboxylic acids and phenols have pKa values in the ranges 3-5 and 8-10 respectively. The pKa values of alcohols are typically 15-18. This represents a significant difference in the acidity between alcohols and phenols/carboxylic acids of about 10^5-10^{10} times. This is why alcoholic OH groups are not methylated whereas the others are.

Since the residual OH absorptions in the IR spectra are due to alcoholic OH's

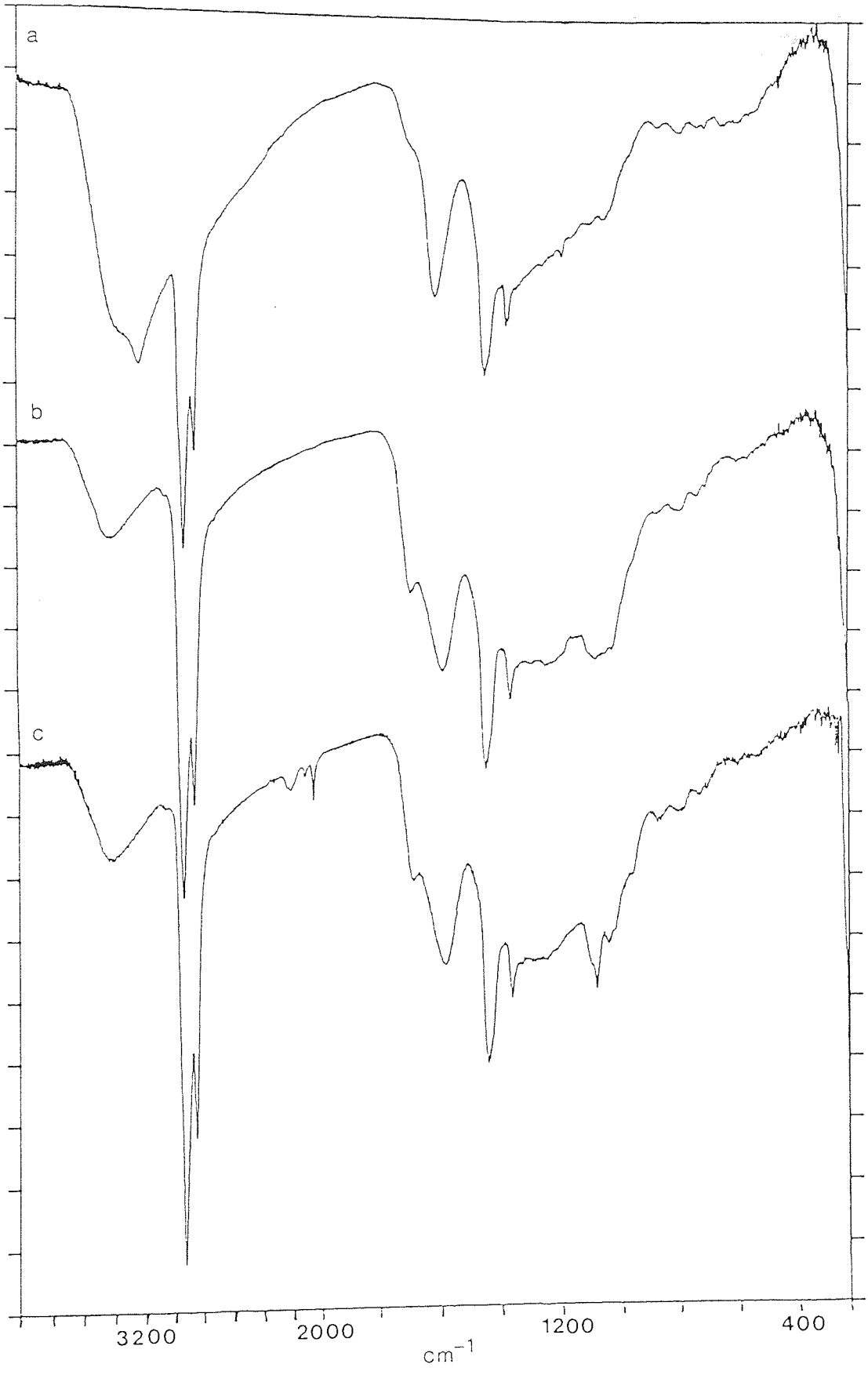

Figure 5.1 FTIR spectra of O-methylated JC kerogen.

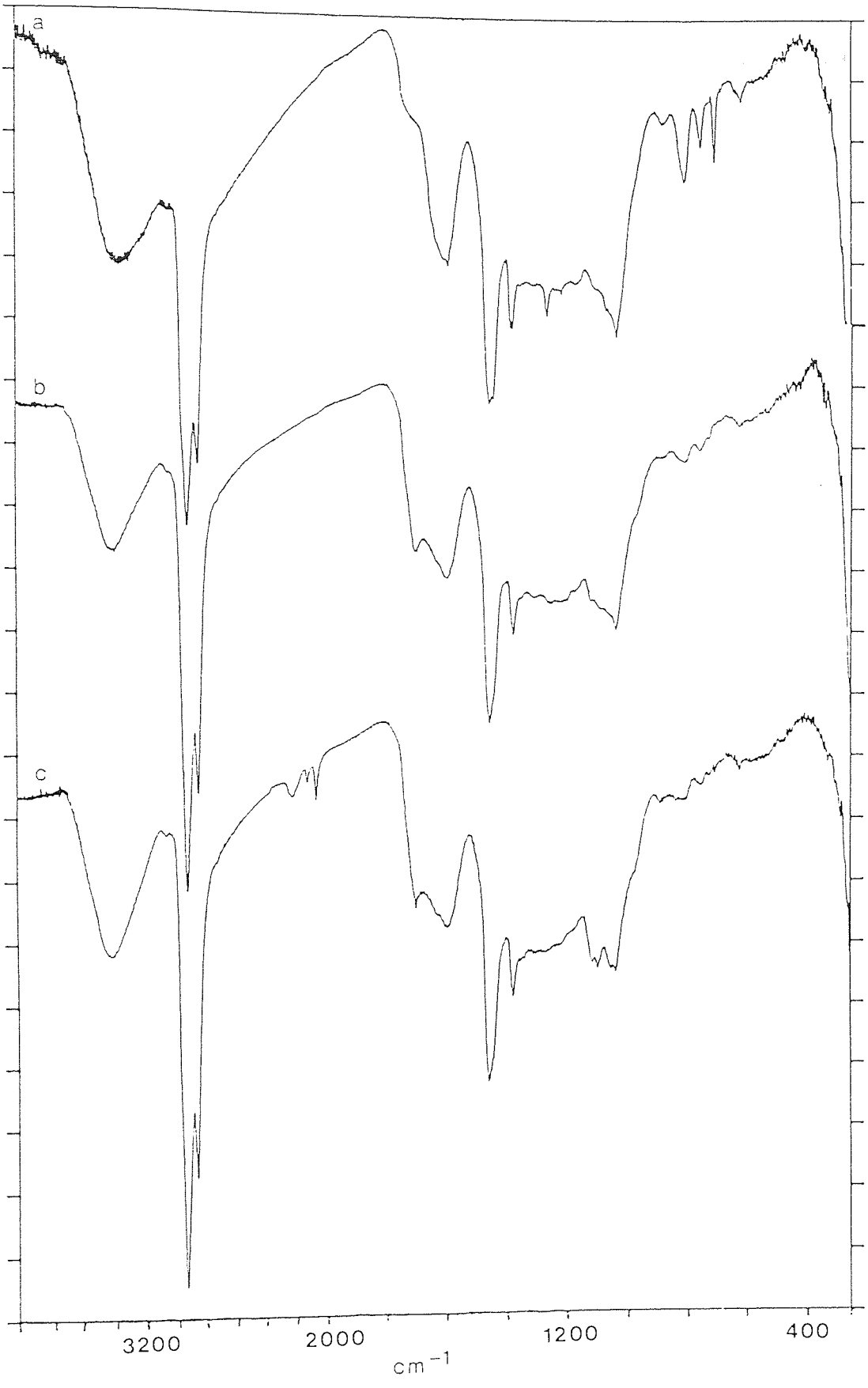

Figure 5.2 FTIR spectra of O-methylated CH1 kerogen.

alone, they can be used as a relative measure of the alcoholic nature of the reduced kerogens. Using the ratio of the intensity of the residual OH absorption to the intensity of the C-H stretch absorption at 2925 cm^{-1}, the order of alcoholic character of the five reduced kerogens can be determined. It is as follows: OC > CH2 > CH1 > KC >JC. Since LAH reduction forms hydroxyl groups, this order may not reflect the alcoholic content of the original kerogens. However, this information can be used with other structural parameters in the elucidation of kerogen structures.

The C-H stretching frequency of the added methyl group is located at 2960 cm^{-1} but is not well resolved from other alkyl group absorptions in that area. This is also true for the methyl ether sym. deformation absorption which occurs at 1440-1455 cm^{-1}. By comparing the spectra a and c for both samples (Figures. 5.1 and 5.2), we can see the addition of the perdeutero methyl group into the kerogen. The same reduction in the OH absorption is seen as with the normal methyl iodide but in addition the C-D stretches at 2060-2280 cm^{-1} are clearly seen. Also the CD_3 symmetrical deformation absorption at 1070-1110 cm^{-1} can be seen. These absorptions, especially the C-D stretches, occur in regions of the spectra that are largely devoid of other absorptions. This helps us to 'see' more clearly whether O-methylation has taken place when the effect on the hydroxyl absorbance is less marked.

The fine structure of the C-D stretches (maxima at 2248, 2226, 2124 and 2067 cm^{-1}) of both O-perdeutero methylated kerogens is very similar to that for a,a,a d_3 anisole. However the methoxy group of an ester has essentially the same absorptions as the methoxy group in anisole [222]. Nonetheless we can attribute the C-D stretches to those of the anisole type because the kerogens were reduced before O-perdeutero methylation and therefore carboxylic acids would not be present in significant concentrations.

In the work by Liotta[207] and Liotta, Rose and Hippo[215] the presence of

carboxylic acids in the coals under study was suggested. They found that after O-methylation/O-perdeuteromethylation a carbonyl absorption developed sharply at 1720 cm^{-1}. This they attributed to the formation of methyl esters from carboxylic acids.

In our reactions we also see the development of a carbonyl absorption, but since the kerogens had been previously reduced it can not be due to the formation of methyl esters from carboxylic acids. In contrast to Liotta's et al. work we find the carbonyl absorption developing at 1700 cm^{-1}. This is outside the range quoted for methyl esters[223] (1750-1717 cm^{-1}) and is nearer the absorptions due to aryl carboxylic acids.

We explain the presence of these carboxylic acids via oxidation of the O-methylated kerogens during their work-up. It was noticed that the extent of oxidation taking place during the work-up of these PTC-assisted reactions was greater than for any other reaction involving the same kerogens. This suggests that either the O-methylated kerogens are more prone to oxidation or that the presence of the PTC enhances the rate of oxidation. Since O-methylation of phenols is used to protect them during permanganate oxidations it is likely that the presence of PTC is responsible for this rapid oxidation. Further work is needed to substantiate these observations.

5.2.2.3 Solid State ^{13}C NMR Analysis.

Each O-methylated kerogen, after it had been extracted, was examined by solid state ^{13}C NMR. It was hoped that the added methyl groups would 'show up' in the spectra and hence provide a way of measuring their relative concentration in each kerogen. However, the absorption in the 50-60 ppm region of the spectra of the O-methylated kerogens (characteristic of the methoxyl group) showed only very small increases when compared with the unmethylated kerogens. This is despite the attenuation of the OH peak seen in the IR spectra of the methylated kerogens. Thus it would appear that the numbers

of acidic hydroxyl groups in these kerogens are small - certainly not high enough to cause the development of a clear methoxy peak in their NMR spectra.

5.2.3 Analysis of Soluble Materials Resulting From O-Methylation.

Both the chloroform and pyridine extracts obtained after O-methylation and O-perdeutero methylation were examined by FTIR spectroscopy. In addition all chloroform extracts were analysed by GLC. Selected chloroform extracts were then analysed by GC-MS.

5.2.3.1 FTIR analysis.

In all cases FTIR analysis revealed that the PTC (tetrabutyl ammonium hydroxide/iodide) had been removed from the extracts. This can be seen quite clearly by consulting the fingerprint region (1600-400 cm^{-1}) in Figure 5.3. This figure shows the spectra of: a) tetrabutyl ammonium iodide, b) the chloroform extract and c) the pyridine extract obtained after the O-perdeutero methylation of the JC sample. (These spectra are representative of all of the O-methylated kerogen extracts).

As usual the chloroform extracts appear to be predominantly aliphatic and significantly less aromatic than the corresponding pyridine extracts. This is apparent from the 1600 cm^{-1} absorptions in these spectra. These spectra also have very weak OH absorptions which might be expected after O-methylation. However, the unusual feature of these spectra is the fact that no C-D absorption can be seen in the chloroform extract and only a very small absorption in the pyridine extract. Thus the spectra of the soluble materials (both chloroform and pyridine) obtained after O-perdeutero methylation are essentially the same as those isolated after ordinary O-methylation. This finding is consistent in all cases where CD_3I was used in place of CH_3I. This indicates that O-methylation of the extractable material, especially the chloroform extractable, does not take place to a significant extent.

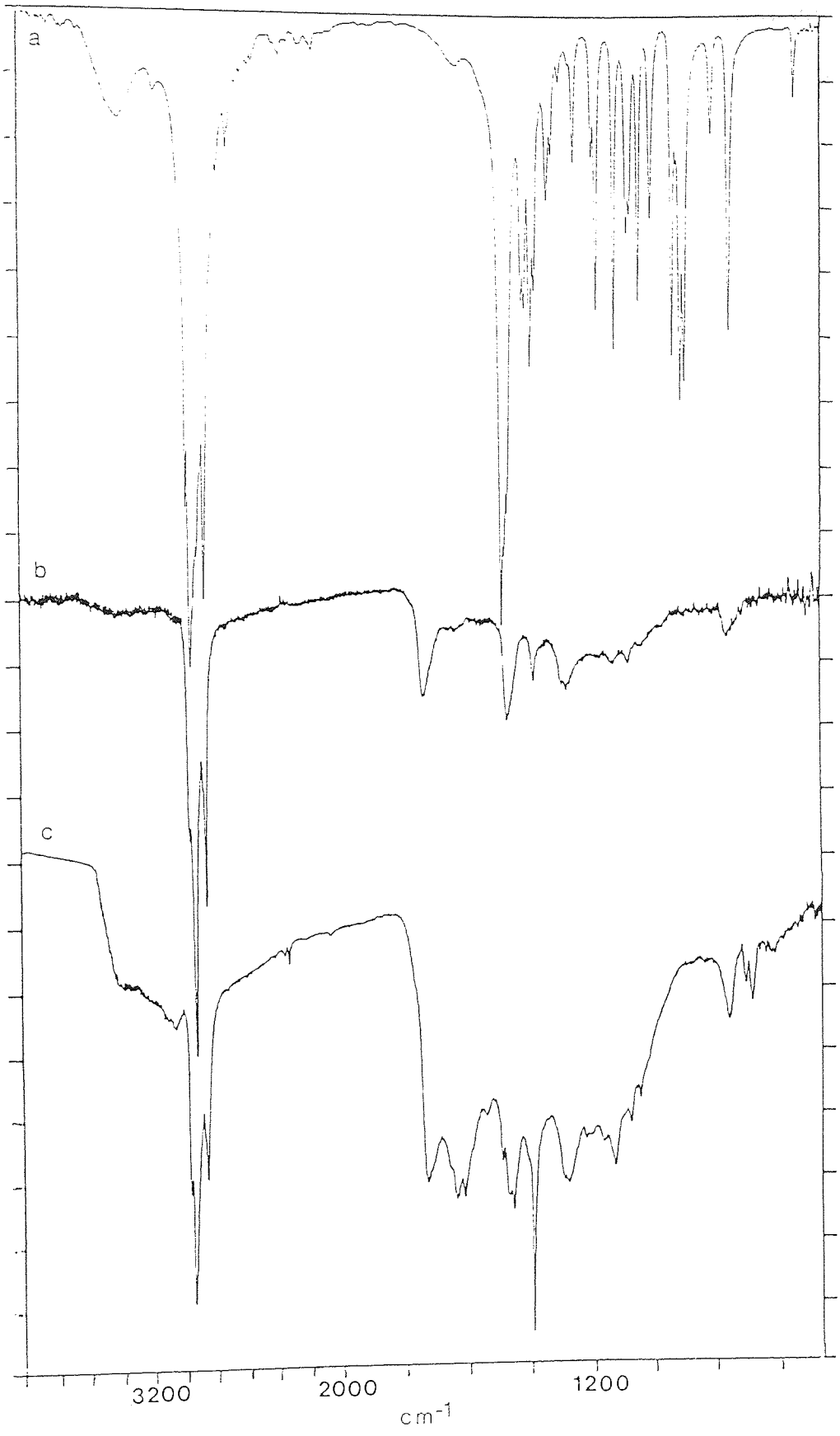

Figure 5.3 FTIR spectra of a) TBAI, b) chloroform extract and c) pyridine extract of O-perdeutero methylated JC kerogen.

In previous work[207], analysis of the material extractable after O-methylation did show the inclusion of added methyl groups in substantial quantities. However these results relate to coals which had not been extracted before O-methylation and therefore a direct comparison cannot be made.

We believe that extraction prior to O-methylation is an essential step because it separates the material originally soluble from that released by O-methylation. This prevents the original soluble material from interfering with or complicating the analysis of the material soluble after O-methylation.

Our results are somewhat surprising because they indicate that the extractable materials possess very few acidic hydroxyl groups. Also since the extractable materials do not have substantial numbers of alcoholic groups, (Figure 5.3 b,c), the participation of these extractable materials in hydrogen bonding and their association with the insoluble matrix is brought into question.

In the context of hydrogen bonding one can imagine the possibility of there being three ways that the extractable and the insoluble matrix components of these kerogens can interact. Firstly there can be a matrix/matrix interaction, secondly an extractable component/matrix interaction, or thirdly, an extractable component/extractable component interaction.

All three types of interaction mentioned above could involve either phenols or alcohols. Since the extracts from O-perdeutero methylation have very few perdeutero methyl groups, the presence of phenols in these extracts is ruled out. Also since these extracts do not have significant OH absorptions in their IR spectra, the presence of alcoholic hydroxyls is ruled out. Thus if both alcohols and phenols are largely absent from these extractable materials they cannot significantly form hydrogen bonds. Therefore we can say that extractable component/extractable component interactions and extractable component/matrix interactions are not common in our systems. We must

therefore conclude that most of the strong hydrogen bonding in our kerogens takes place between various parts of the insoluble matrix itself.

Thus if the extractable materials do not or can not hydrogen bond to the insoluble matrix, why are they only extractable after O-methyaltion and not before? At present we believe the answer involves a physical process whereby the extractable material is trapped or entangled within the insoluble matrix. Only by 'opening-up' the insoluble matrix by O-methylation can these trapped materials be subsequently extracted.

5.2.3.2 GLC and GC-MS Analysis of Soluble O-Methylation Products.

Preliminary examination of all five chloroform extracts by GLC analysis gave a rather disappointing result. The traces that were obtained showed rather broad unresolved peaks, but at least something was coming through the column. One point to note was the absence of any tributylamine in the GLC traces. This is formed by the thermal degradation of tetrabutylammonium salts and its absence indicates that all of the PTC had been removed by our work-up procedure.

In spite of the poor quality of the GLC traces two chloroform extracts (those of OC and KC) were analysed by capillary colomn GC-MS. Again relatively poor traces were obtained but as expected better resolution was achieved with the capillary column. The TIC's gave only small peaks and it is suspected that only a small proportion of the injected sample was volatile in our system. Nonetheless using the software available and selective data handling we were able to test for the presence of certain classes of compound.

From the stored data specific ion chromatograms (SIC's) were reconstructed for ions characteristic of certain compounds. (See section 2.). These compounds were alkanes, alkylbenzenes, dialkylbenzenes, phenyl derivatives, phenols, anisole type derivatives, phthalates, esters, alkylnaphthalenes and naphtholic derivatives.

The chromatograms of both samples showed a series of n-chain alkanes, (see Figure 5.4 a) OC b) KC.), ranging from C_{15}-C_{29} with maxima in this range at C_{18} for KC and C_{19} for OC. Alkylbenzenes and dialkylbenzenes were present in the KC sample but not in the OC sample. Other phenyl derivatives were present in both samples but only in small amounts. Alkylphthalates were detected in both samples but contamination from rubber tubing is thought responsible. There were no esters, anisole derivatives, alkylnaphthalenes, phenols or methylated naphtholic derivatives detected in either sample. The absence of anisole and methylated naphtholic derivatives supports the IR analysis of these extracts which showed that very little O-methylation of the extracts had taken place.

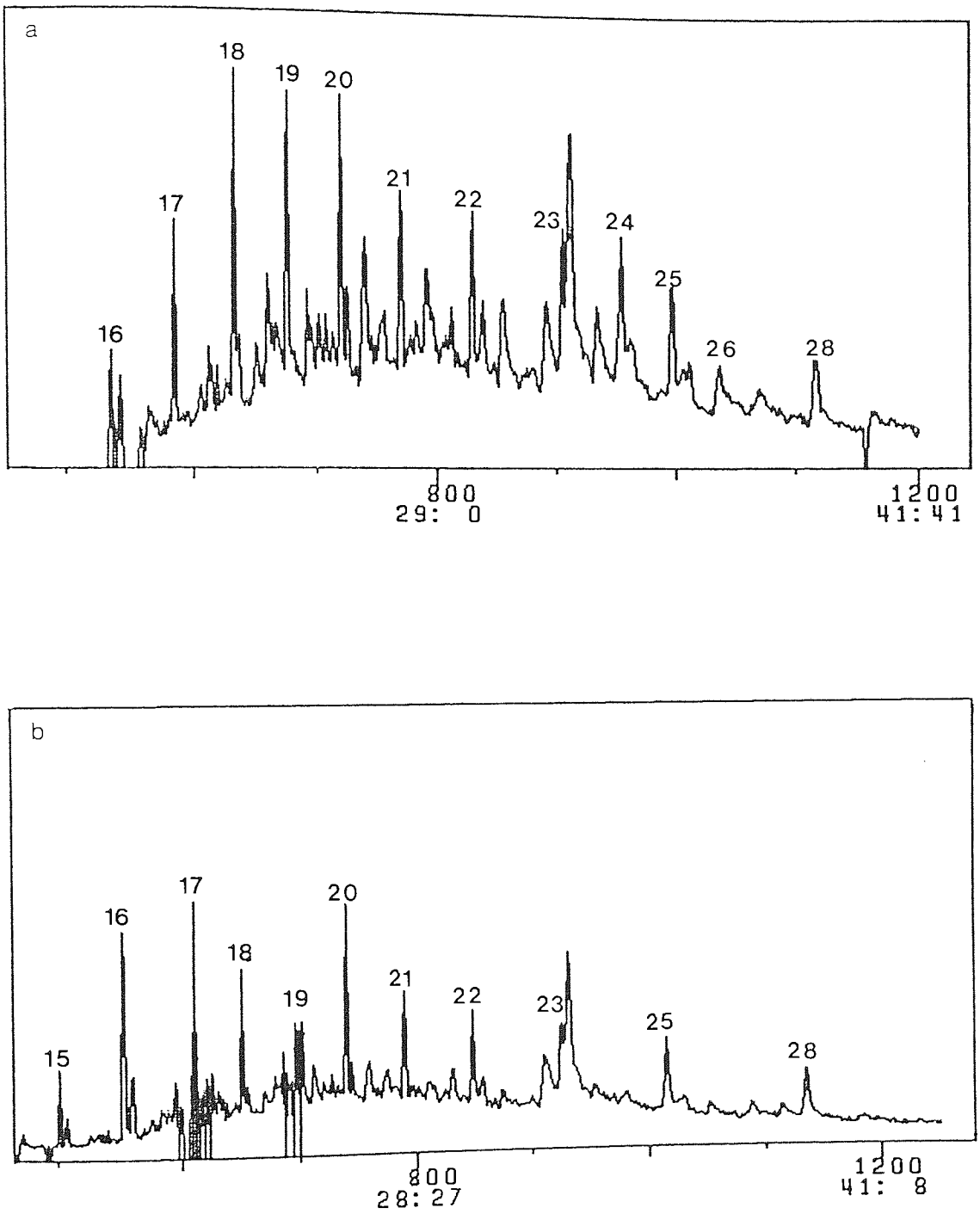

Figure 5.4 Alkanes in extracts of O-methylated kerogens detected by GC-MS using the SIC technique.

5.3 Conclusions.

The five reduced and pyridine extracted kerogens under study can be O-methylated using Liotta's phase transfer method. However a modified work-up procedure is required to remove all traces of the phase transfer catalyst from the products. The extent of O-methylation is low in these samples as shown by solid state NMR and indicates that there are few acidic hydroxyl groups in them. Also the O-methylation does not go to completion, a condition we attribute to the presence of alcoholic hydroxyls which are not acidic enough to react.

The solubility of the kerogens after O-methylation is only slightly improved by this treatment. In addition FTIR and GC-MS analysis of the material soluble after O-methylation suggests that this material does not hydrogen bond to itself or to the kerogen matrix. The extraction of this material after O-methylation, but not before, is explained in terms of the 'opening-up' of the kerogen matrix upon O-methylation, thereby releasing trapped or entangled materials.

Chapter 6

The Oxidation of Kerogens.

(PerTFA vs Permanganate Oxidation).

6.1 Introduction.

Oxidation is the degradative technique that has been most widely used in the study of the chemical structure of coals and kerogens. This is reflected in the wealth of information in the literature relating to this topic, most of which has been very well reviewed[224,225]. Many different reagents have been applied to the oxidation of kerogens; air, oxygen, ozone, hydrogen peroxide, potassium permanganate, chromic acid and nitric acid are among those most commonly used. These oxidants are active over different pH ranges and differ in their mechanism of degradation. Consequently the degradation products and their yields may differ depending on the oxidant and the conditions of its use.

Early workers used rather harsh conditions and powerful oxidising reagents which led to a high conversion of the kerogen but with very unselective degradation into simple, stable molecules such as carbon dioxide, short chain aliphatic carboxylic acids and benzenecarboxylic acids. In addition, the oxidation products were generally studied using very limited classical methods for separation and characterisation. As a result only very limited structural information was obtained. However, if an oxidation is too mild then insufficient degradation of the kerogen occurs and again little structural information is obtained. It is therefore important to get a balance between the severity of an oxidation and its selectivity.

Alkaline permanganate oxidation is probably the most frequently used oxidant for the structural analysis of carbonaceous materials. It belongs to a group of the more traditional oxidants (permanganate, chromate, oxygen and nitric acid etc) which attack at the benzylic position of alkyl aromatics. PerTFA on the other hand, can selectively attack at the aromatic position in such molecules, hence leaving their benzylic positions intact.

These two oxidants therefore complement each other and provide two of the most effective methods for investigating the chemical structure of kerogens. Although alkaline potassium permanganate oxidation of kerogens has been extensively studied, very little work has been done using the perTFA reagent. Since very useful information has been obtained from the use of the perTFA reagent on coals, it was thought worthwhile to carry out a comparative study of the perTFA and permanganate oxidation of kerogens.

Both a mild, stepwise alkaline potassium permanganate and a mild perTFA oxidative procedure have been employed in the investigation of the structure of our five reduced and pyridine extracted kerogens. Our oxidation procedures (whether permanganate or perTFA) are such that each oxidised kerogen forms a base insoluble residue (Residue), a methylated humic acid-like fraction (MHA) and a dichloromethane soluble fraction (Solubles). The distribution and analysis of these product fractions allows, not only the chemical structure of kerogens to be probed, but also allows for a direct comparison between the two oxidation procedures to be made. As a consequence of our work-up procedures carbon dioxide and highly polar water soluble acids are lost.

The soluble fractions were analysed by many analytical techniques including GC-MS, FTIR spectroscopy, ^{1}H and ^{13}C NMR spectroscopy and some UV/vis spectroscopy. Residues and MHA were analysed by elemental analysis, FTIR spectroscopy and ^{13}C solid state NMR spectroscopy where possible. Analysis of residual organic material is something which is often overlooked in oxidation studies. It is believed that analysis of the residual material is just as important as that of the solubilised material. This is because it is highly likely that such residues contain structural information that is absent in the soluble products. Thus to this end, in addition to their spectroscopic analysis, selected residues from the perTFA oxidation were re-oxidised using the permanganate procedure. This resulted in the formation of a secondary set of residues,

MHA's and solubles, which were then amenable to further detailed analysis.

The history and development of the alkaline potassium permanganate and the perTFA oxidation reactions are discussed below.

A) Potassium permanganate oxidation.

Oxidation with alkaline potassium permanganate was one of the first degradants to be used for the investigation of coal structures[226,227]. In these early studies coals of different rank plus lignin were totally oxidised into various soluble products. This oxidative procedure developed two different approaches, the carbon balance and the bulk oxidation techniques, each of which were later applied to oil shales[48,228].

The original carbon balance technique[48] consisted of exhaustive oxidation of an amount of sample equivalent to 1g of organic carbon with alkaline (1.6% solution of KOH) potassium permanganate. When the oxidation was complete the distribution of the original carbon was determined in the following oxidation products:

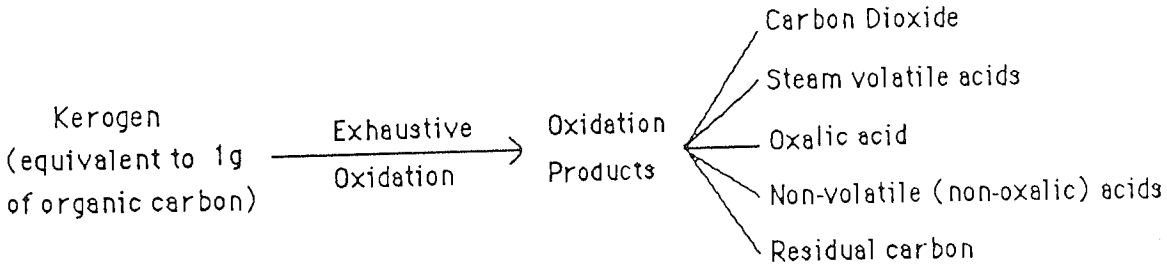

Since many organic materials , upon exhaustive oxidation, yield large amounts of carbon dioxide and oxalic acid, it was obvious that the carbon balance oxidation products were not truly representative of the kerogen structures. Nevertheless, it was suggested that the yield of non-volatile acids, consisting mainly of benzenecarboxylic acids, reflected the aromaticity of the starting materials. Comparison of the results of these oxidations with those obtained from known compounds as model substances[229,230] and

coals[226,227] gave information about the structure of kerogens. In other words the carbon balance oxidation was a method to show structural similarities or differences among materials under investigation.

The bulk oxidation technique involves the degradation of larger samples (0.5 - 1.0 kg) by the addition of solid potassium permanganate. The soluble oxidation products were separated and identified as carbon dioxide and various volatile and non-volatile acids including benzenecarboxylic acids[48,231]. It was found that in the first stages of kerogen oxidation, acids were frequently formed which were subsequently oxidised, largely to carbon dioxide and oxalic acid. In order to prevent this over oxidation, ie further degradation of the primary products, stepwise oxidation was introduced. This technique involves the addition of the potassium permanganate in small portions and then separating the oxidation products from the unreacted kerogen prior to each new addition of the permanganate. This approach gave relatively high yields of degradation products[232,233] and produced more information for the reconstruction of the original kerogen as compared with the carbon balance or bulk oxidation techniques. It was this approach that we used in our work.

B) <u>Peroxytrifluoroacetic acid (perTFA) Oxidation.</u>

The use of perTFA (30% H_2O_2 - CF_3COOH with or without the addition of 96% H_2SO_4) in structural studies was initially applied to the oxidation of lignite and bituminous coals[234,235]. Since these first studies this reagent has received considerable attention as a coal oxidant [236,237,238,239,240] and has been used to determine the sulphur functionality of some coals[241]. The addition of H_2SO_4 to the reaction mixture was found to prevent the formation of large amounts of acetic acid, formed by hydrogen migrations from the coals and model compounds. The exact

mechanism of such migrations and the role played by H_2SO_4 in suppressing them is not as yet fully understood. The reaction mixture is reported to generate the hydroxyl cation (OH^+)[242]. This is apparently formed via the protonation and subsequent cleavage of the peroxide bond. The OH^+ species is a very powerful electrophile and as such will attack the electron-rich aromatic ring system. Its advantage over other oxidants is that it can destroy aromatic centres whilst leaving the benzylic positions of any alkyl aromatics intact. The nature of the oxidation was illustrated using model compounds such as toluene, ethylbenzene, n-propylbenzene and isopropylbenzene[243]. The major oxidation products were acetic, propionic, butyric and isobutyric acids respectively. In contrast, common oxidants such as HNO_3, O_2, permanganate and chromate, attack the benzylic hydrogen yielding benzoic acid for all four of these aromatic compounds. In general, H_2O_2-CF_3COOH-H_2SO_4 oxidation of alkylbenzenes leads to degradation of the benzene ring to a carbonyl group and preservation of over 70% of the aliphatic structure.

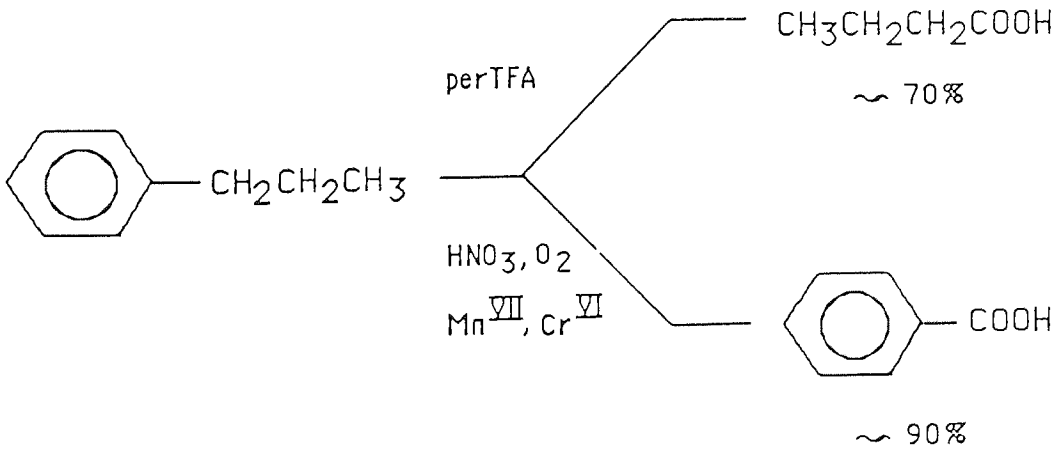

These model compound results suggested that this might be a good technique for examining the aliphatic structure of coals/kerogens.

However, it has now been shown that some aromatic rings can survive the action of this reagent. Oxidation of Monterey bituminous coal was found to give benzene

carboxylic acids in its oxidation products. These products were also obtained in model compound studies from the oxidation of 5,12 dihydronaphthacene[244], and led to the postulation of such structures existing in coals. In addition benzenecarboxylic acids were produced from naphthalene, anthracene, chrysene and benzanthracene in model compound studies[237]. Further criticism of this reaction procedure was forthcoming after the expected oxidation products from perTFA oxidation were tested for their stability to this oxidant[245]. It was concluded that secondary oxidation of initial oxidation products could result if there was insufficient control of the reaction temperature. To overcome this problem, a low boiling point, inert solvent (typically chloroform B.pt 61°C) was added to limit the temperature of the reaction and therefore restrict its severity[246,247].

Despite the fact that we now know that this reagent has many shortcomings, the perTFA reagent remains one of the few that can selectively degrade aromatic centres in the presence of aliphatic material whilst leaving the benzylic positions intact. It is therefore considered to be a very useful degradant, especially if used in conjunction with alternative modes of degradation , eg. permanganate.

6.2 Results and Discussion.

6.2.1 Product Recovery and Distribution.

The total product recovery from the perTFA oxidations, ie. the combined weights of the residues, MHA and solubles, together with the distributions between the residues, MHA and soluble fractions for each kerogen, are shown in table 6.1. Those from the permanganate oxidation are shown in Table 6.2.

Table.6.1 Distribution of oxidation products from perTFA oxidation.

sample	Product Distribution (wt%)*			total product
	Residue	Insolubles	Soluble	recovery (Wt%)*
KC	36.5	14.1	13.5	64.1
JC	53.0	8.7	16.6	79.3
OC	19.0	30.4	26.6	76.0
CH1	37.5	44.7	9.3	101.5
CH2	61.3	8.1	46.3	115.7

* All weight percentages are expressed in terms of the dry parent kerogen.

Table.6.2 Distribution of oxidation products from permanganate oxidation.

sample	Product Distribution (wt%)*			total product
	Residue	Insolubles	Soluble	recovery (Wt%)*
KC	49.2	11.1	12.0	72.3
JC	29.3	19.8	22.3	71.4
OC	2.2	13.1	30.7	46.0
CH1	32.5	25.5	8.3	66.3
CH2	44.2	9.7	20.8	74.7

* All weight percentages are expressed in terms of the dry parent kerogen.

a) Total product recovery.

The total product recovery after perTFA oxidation of each of the five kerogens shows considerable variation. This can be explained by the different reactivities of each kerogen towards the perTFA reagent which in turn can be explained by differences in

their structures. Total product recoveries or yields are seen to vary from above 100% to well below this (64.1%) (% based on weight of the dry parent kerogen). Yields below 100% indicate the degradation of the kerogen into carbon dioxide and water soluble acids which are lost, whilst yields above 100% can be accounted for by the addition of oxygen to the kerogen upon its oxidation. This can be visualized by considering the following reactions.

i) Yields below 100% Eg.(weight loss)

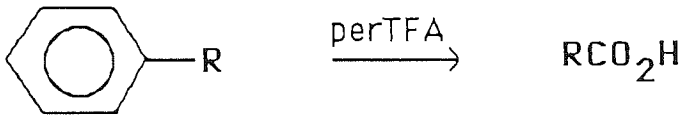

R + 77 R + 45 ie. loss of 12 amu.

ii) Yields above 100%. Eg.(weight gain)

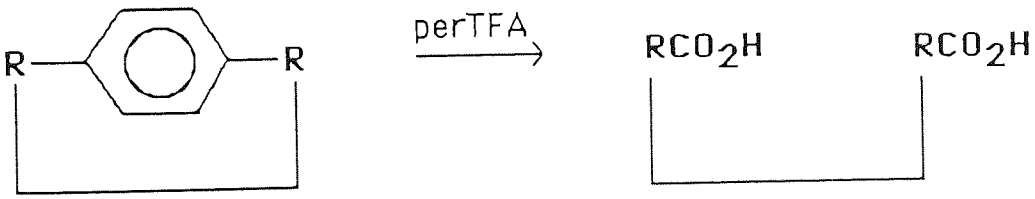

2R + 76 2R + 90 ie. a gain of 14 amu.

Clearly both processes are likely to operate in all five kerogens but it is apparent that one process dominates the other in different kerogens.

Since perTFA can oxidise aromatic rings to carbon dioxide[234] it would appear probable that those kerogens having low product yields are those with higher aromatic contents. Indeed from Fig. 6.1a. we can see that as the fa value of the kerogen increases so the total product yield decreases. Although this trend is erratic, it indicates that the

aromatic units of the kerogens are being oxidised by the perTFA.

Figure 6.1a Plot of total product yield vs fa value (perTFA oxidation).

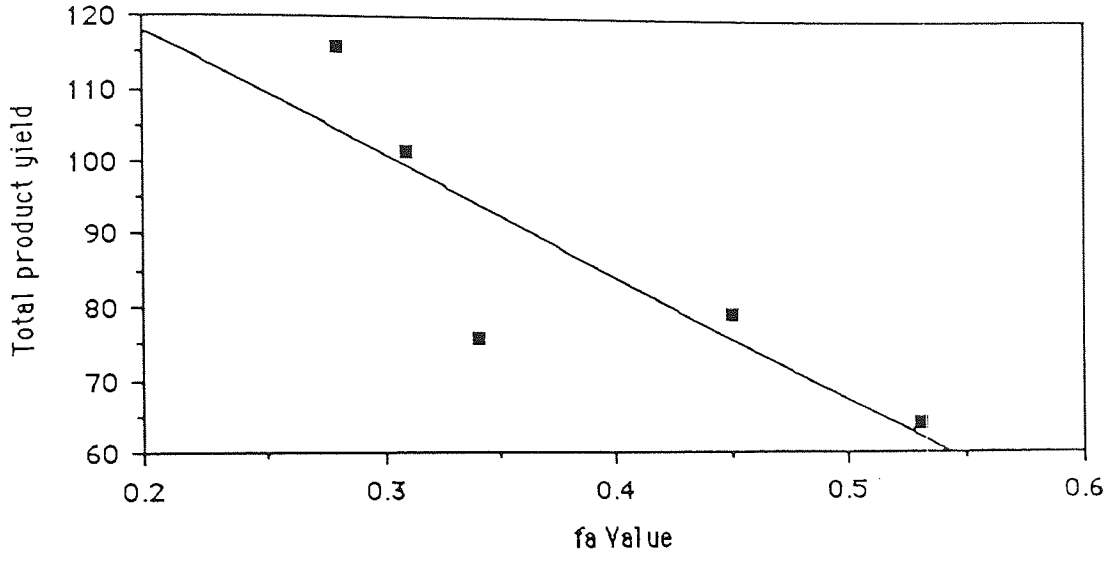

The total product recovery from the permanganate oxidations also shows considerable variation, but with this oxidant no yields above 75% were obtained. In contrast to the perTFA oxidation, there appears to be no correlation between the fa value of the parent kerogen and the total product yield obtained via permanganate oxidation. (See Fig 6.1b).

Figure 6.1b Plot of total product yield vs fa value ($kMnO_4$ oxidation).

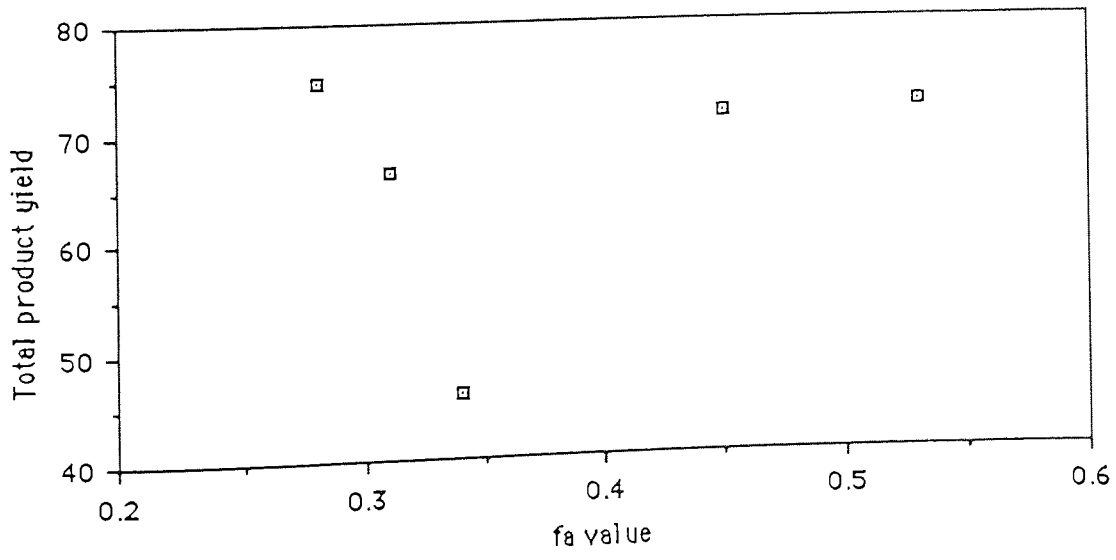

In other words the degree to which the kerogen is degraded by permanganate, (whether by conversion to carbon dioxide and water soluble acids or by oxygen addition), seems largely independent of its aromatic content.

b) **Product fraction distribution.**

The residue , MHA and soluble product distributions for each kerogen are plotted against the fa value in Figure 6.2a (perTFA oxidation) and Figure 6.2b (permanganate oxidation).

Figure 6.2a Product distribution vs fa value (perTFA oxidation).

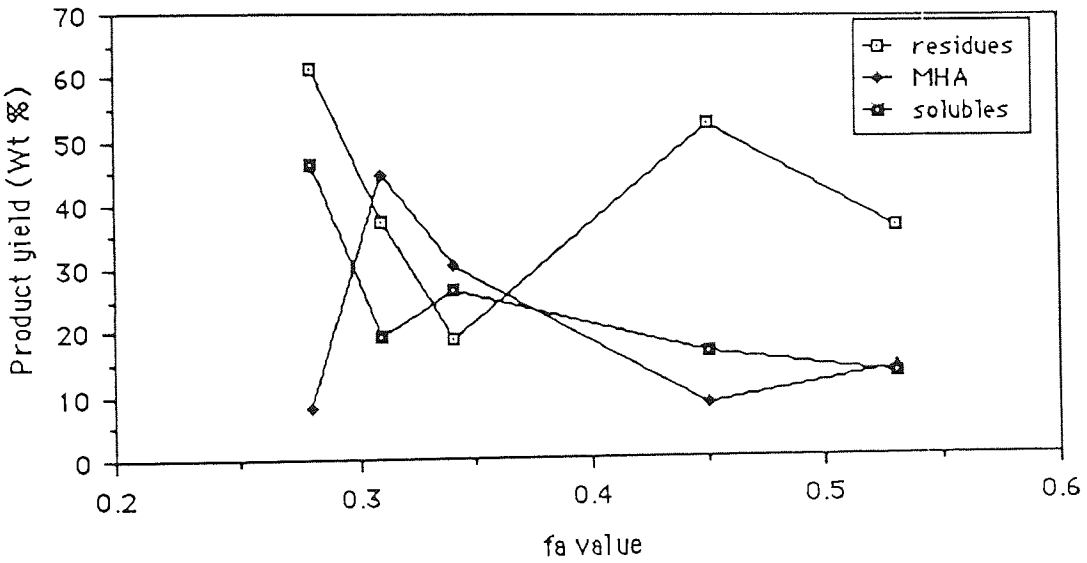

Figure 6.2b Product distribution vs fa value (KMnO4 oxidation).

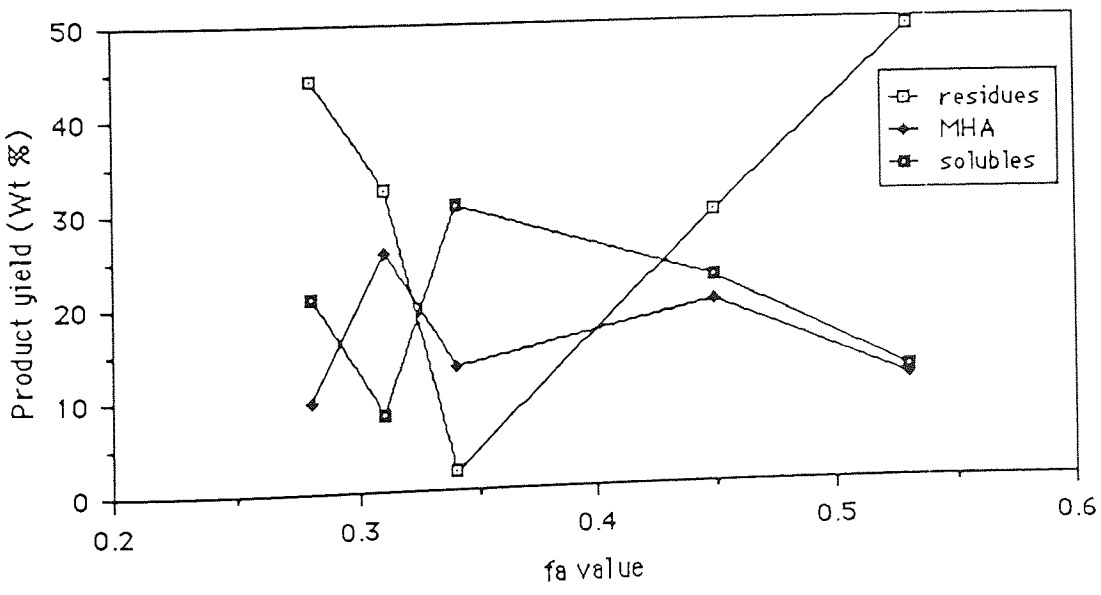

As we can see from these graphs there appears to be little correlation between the amount of each product fraction formed (whether by perTFA or permanganate oxidation) and the fa value of the unoxidised kerogen. This is somewhat unexpected because both reagents are supposed to attack aromatic centres, albeit in a different way, and therefore one might have expected for instance, that the amount of soluble material produced would be a function of kerogen aromaticity. Similarly, we may have expected the amount of residue from perTFA oxidation to increase with increasing aliphatic content (since aliphatic material is supposed to survive this oxidation). However, in a recent study on a series of Australian coals[239] Verheyen et al noted that as the rank and therefore aromaticity[248] of the coal increased so did the quantity of residue remaining after oxidation. We see neither this nor the expected trend in our kerogens.

However we still see considerable quantities of residue from both oxidation procedures, indicating a marked resistance to degradation. This resistance can be due to either i) the lack of a reactive site (eg an alkyl benzene or similar alkyl aromatic), ii) insufficient penetration by the oxidant or iii) deactivation of the substrate by highly carboxylated materials. It is a combination of the last two explanations which Verheyen et al use to justify the occurrence of residues in their perTFA oxidation studies. However reoxidation of a residue with perTFA yielded no further dissolution suggesting that the lack of reagent penetration was not a problem.

6.2.2 Analysis of Solubles.

Soluble product fractions were analysed by FTIR spectroscopy, GC-MS analysis and ^{1}H and ^{13}C solution state NMR.

6.2.2.1. FTIR Analysis.

The FTIR spectra of all solubles, (whether generated by the perTFA or the permanganate oxidant), look very similar despite originating from different kerogens. (The FTIR spectrum of the perTFA JC solubles is shown in Figure 6.3 as an example together with its corresponding parent kerogen, residue and MHA spectra). In general the solubles show strong absorptions from aliphatic groups and only weak absorptions due to aromatic groups. Each spectra is dominated by a very intense absorption at 1735 cm^{-1} which is due to the carbonyl stretch of an ester. These ester groups obviously result from the methylation of carboxylic acids produced during the oxidation procedures. This methylation also explains why the OH peaks are relatively small and sharp.

6.2.2.2 GC-MS Analysis.

The dominating feature of all the GC-MS traces of the soluble fractions, both those from perTFA and stepwise permanganate oxidations, is a series of saturated mono methyl esters (m/z 74 and 87). The GC-MS traces for perTFA (Fig. 6.4a) and permanganate oxidation of the CH2 sample both showed a series of saturated isoprenoid chain monomethyl esters as the dominant volatile species. In all other samples a series of n-chain monomethyl esters dominates. The GC-MS trace for the perTFA oxidation of OC is shown (Fig. 6.4b) as an example.

From perTFA oxidation studies on model compounds such as toluene, ethylbenzene, n-propylbenzene and iso-propylbenzene[249] it is clear that the alkyl chain esters are likely to have been produced from alkyl aromatic species present within the kerogen. Since the fatty acids (which give rise to the methyl esters) have been proven to be relatively stable towards further oxidation by perTFA[250], it is reasonable

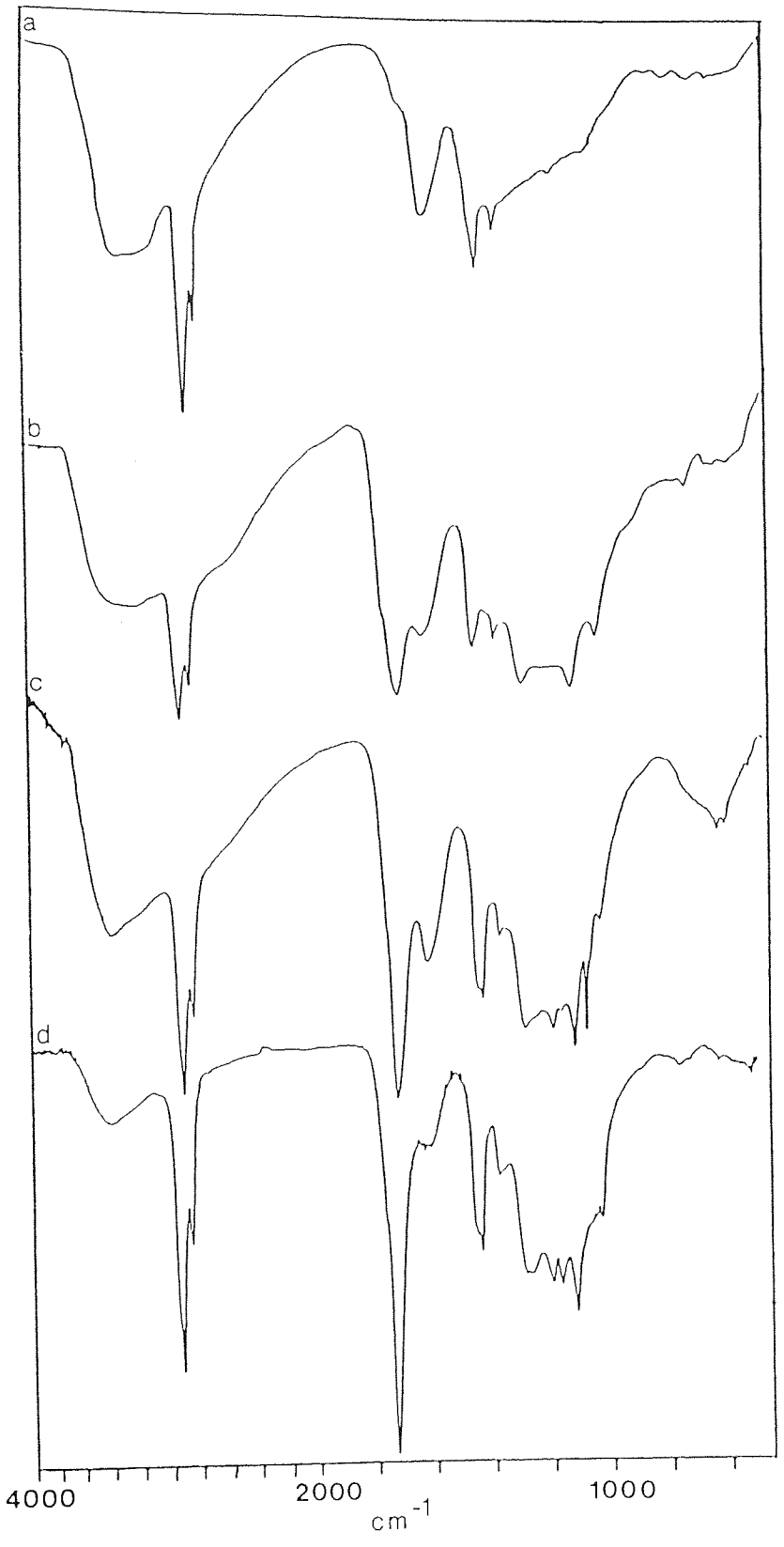

Figure 6.3 FTIR spectra of the perTFA oxidation products from the JC kerogen.

a) parent reduced extracted kerogen

b) residue

c) MHA

d) Solubles

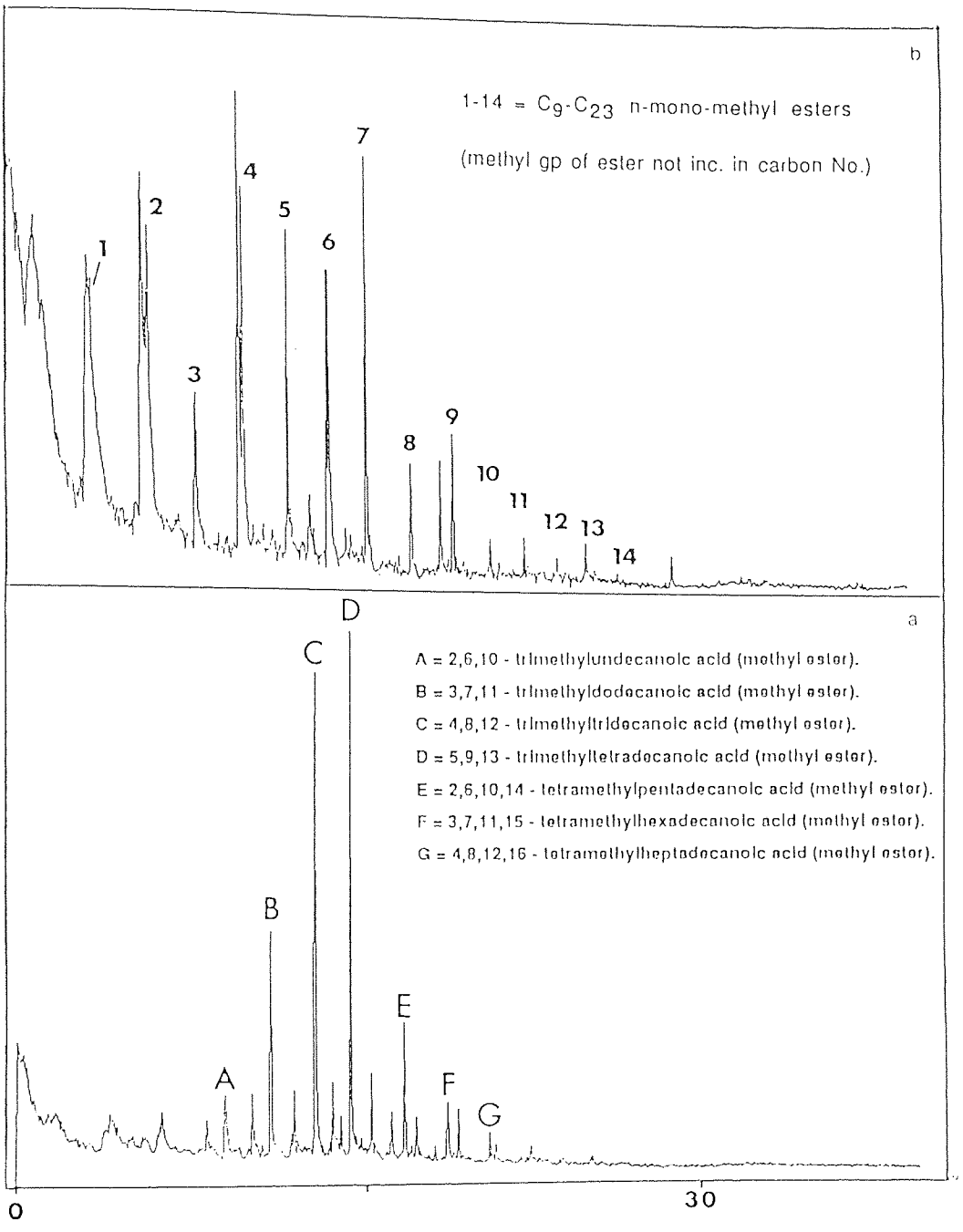

Figure 6.4 GC-MS TIC traces for perTFA oxidation solubles.

a) from the CH2 kerogen

b) from the OC kerogen

to assume that their carboxyl group marks the position of linkage between the alkyl chain and the aromatic unit. Therefore the distribution of fatty acids represents the distribution of the respective alkyl chains within that part of the kerogen which is solubilised.

As mentioned earlier the CH2 sample is different from the other four in that it produces saturated isoprenoid chain monoesters as the most prominant volatile products.

The distributions of the n-chain methyl esters produced by perTFA and permanganate oxidation of each kerogen are shown in Figure. 6.5. It is clear from these plots of relative intensity vs carbon number that permanganate oxidation produces a shorter range of acids and shifts the maxima in their distribution to shorter carbon chain lengths.

It would be expected that the maxima in the distribution of the permanganate oxidation products would be one carbon atom lower than those from the perTFA oxidation because permanganate oxidises the benzylic position of alkyl aromatics whereas the perTFA leaves it intact. This is represented below;

PerTFA Ox:

$$Ar\text{-}CH_2CH_2CH_2CH_3 \longrightarrow CH_3CH_2CH_2CH_2CO_2H$$

Permanganate:

$$Ar\text{-}CH_2CH_2CH_2CH_3 \longrightarrow CH_3CH_2CH_2CO_2H$$

However, the maxima shifts much more than one position and this can be explained by the secondary oxidation of primary oxidation products by the permanganate. Thus here we can see a major benefit to be gained by using perTFA instead of alkaline

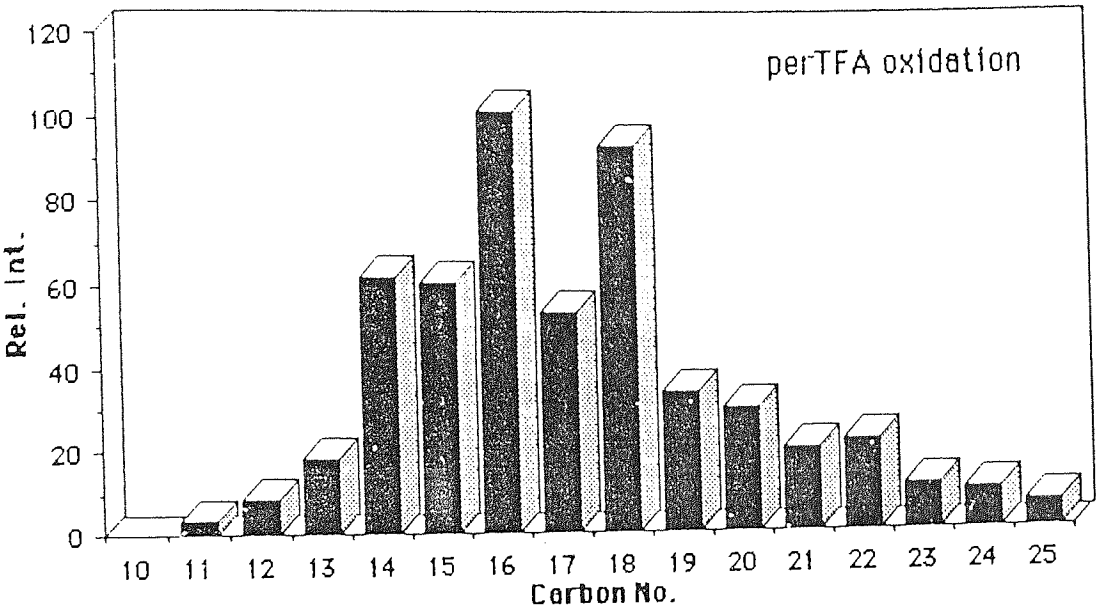

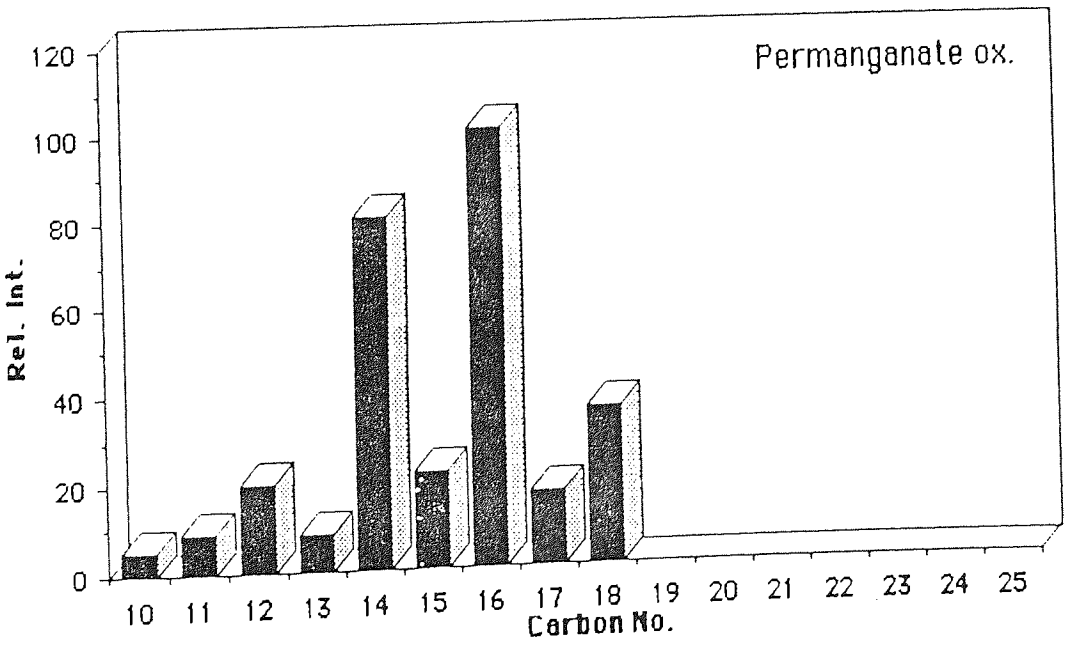

Figure 6.5a Distribution of n-chain methyl esters produced by perTFA and permanganate oxidation of the KC kerogen.

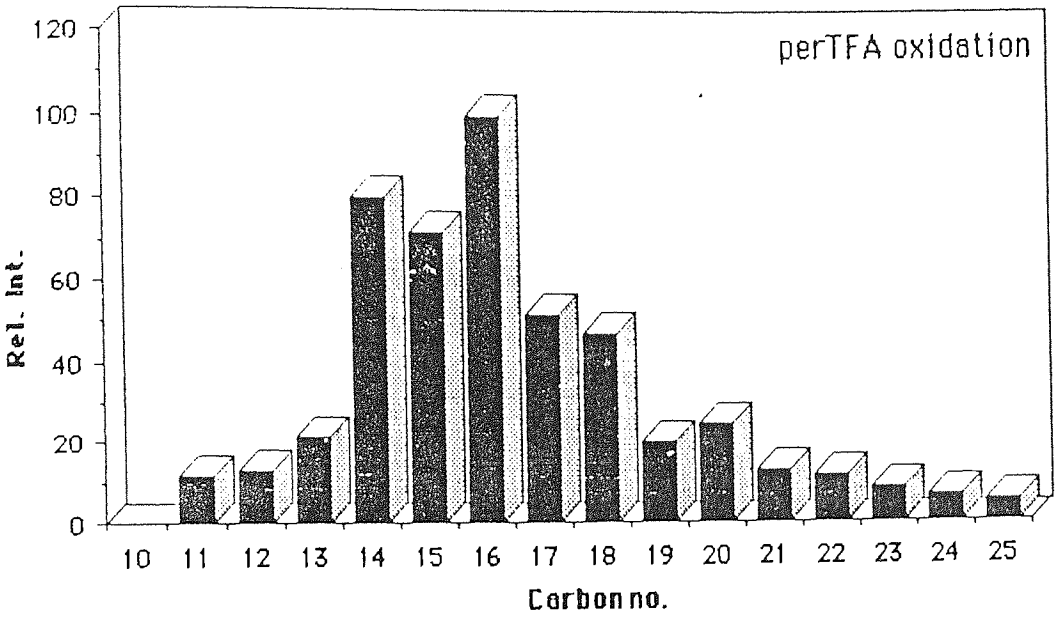

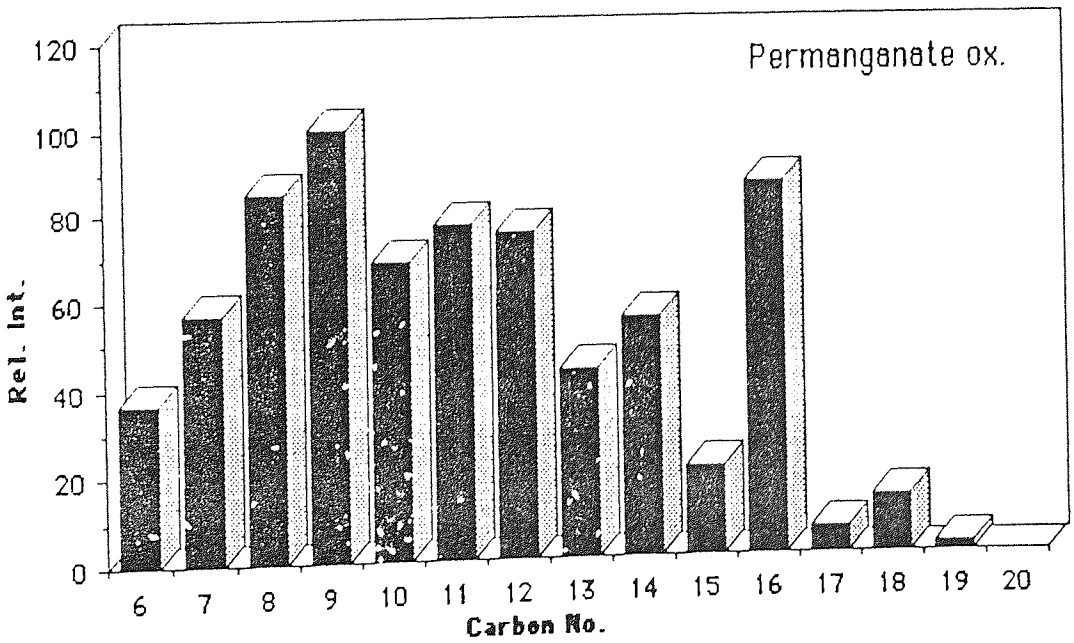

Figure 6.5b Distribution of n-chain methyl esters produced by perTFA and permanganate oxidation of the JC kerogen.

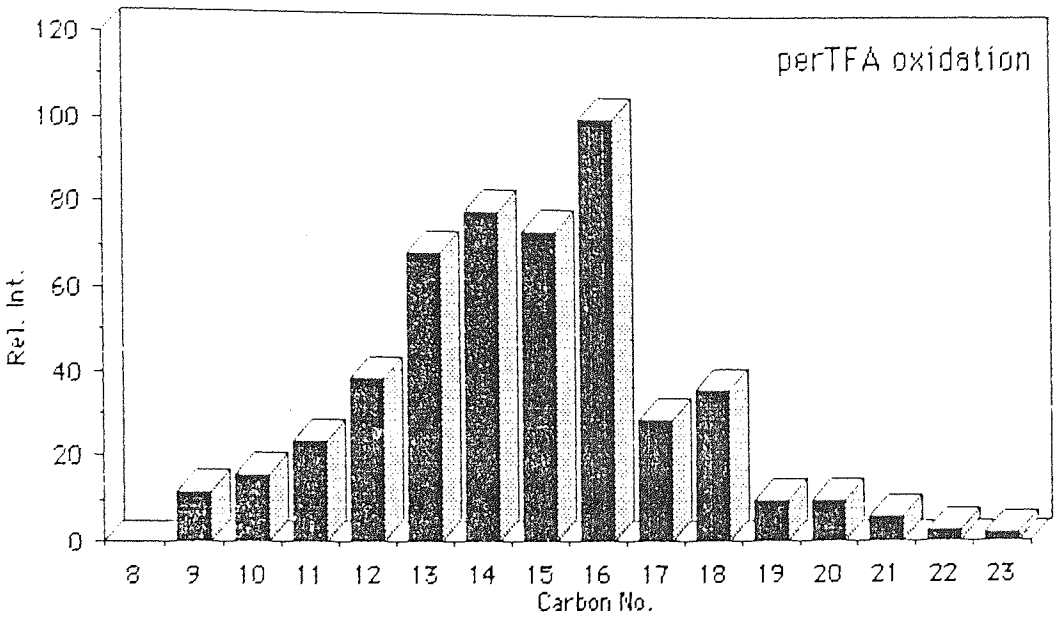

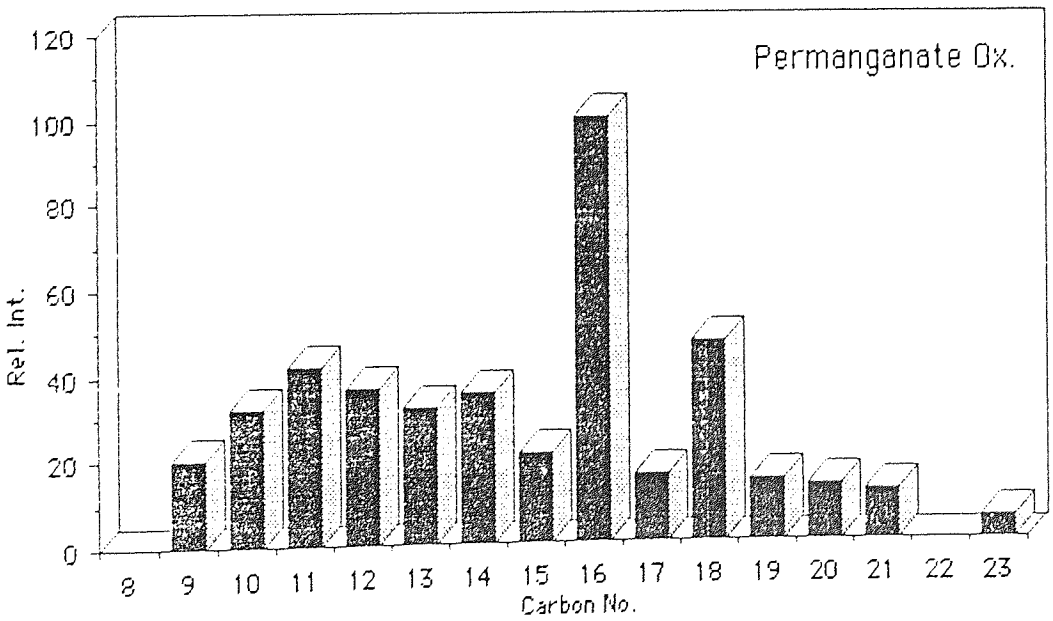

Figure 6.5c Distribution of n-chain methyl esters produced by perTFA and permanganate oxidation of the OC kerogen.

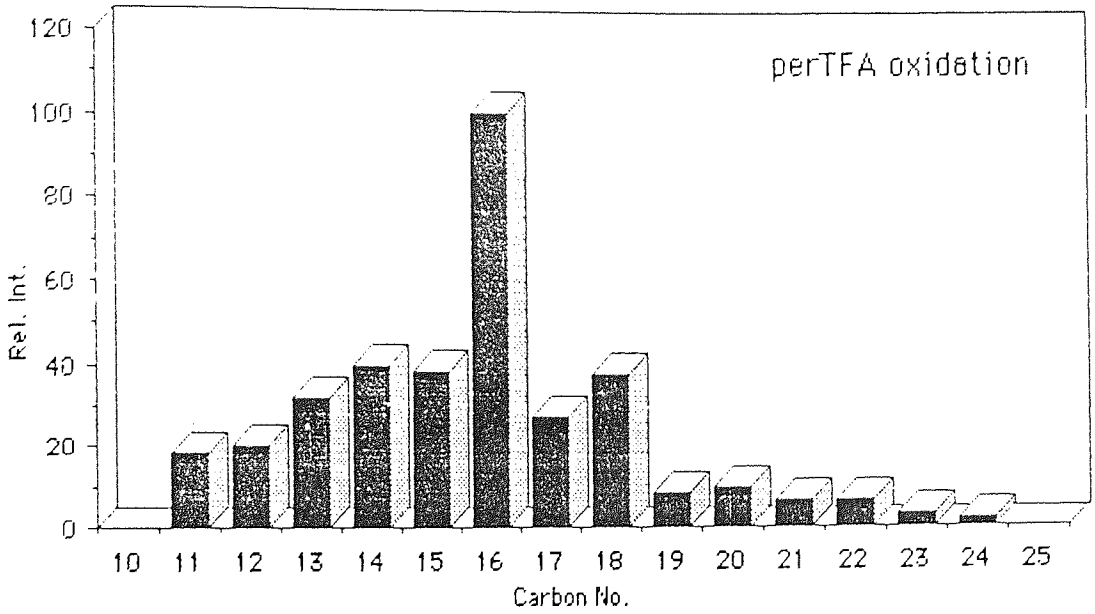

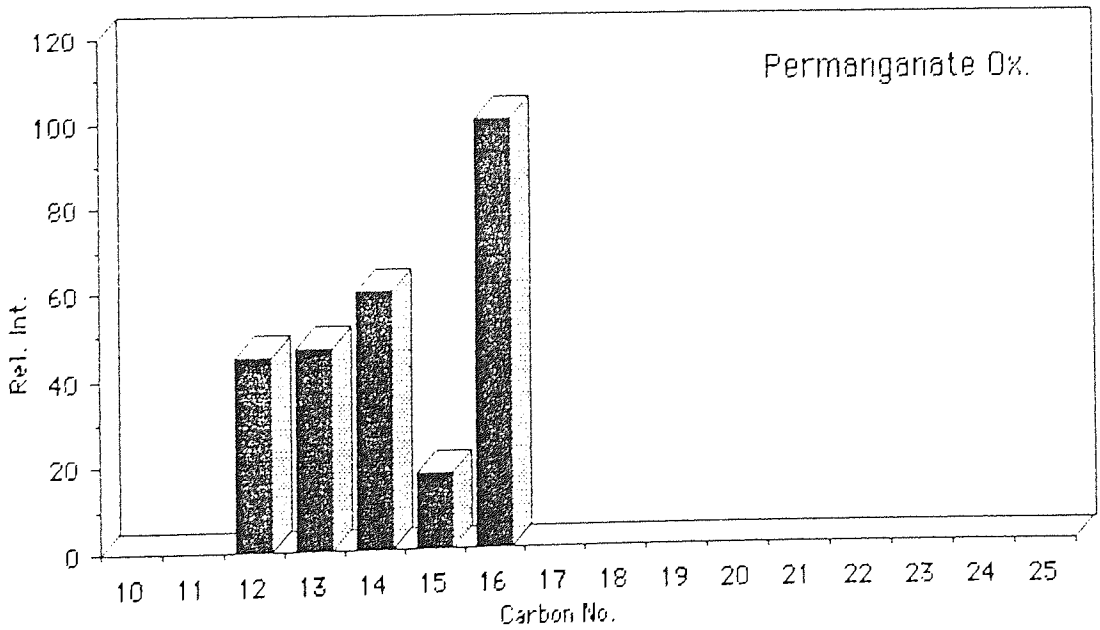

Figure 6.5d Distribution of n-chain methyl esters produced by perTFA and permanganate oxidation of the CH1 kerogen.

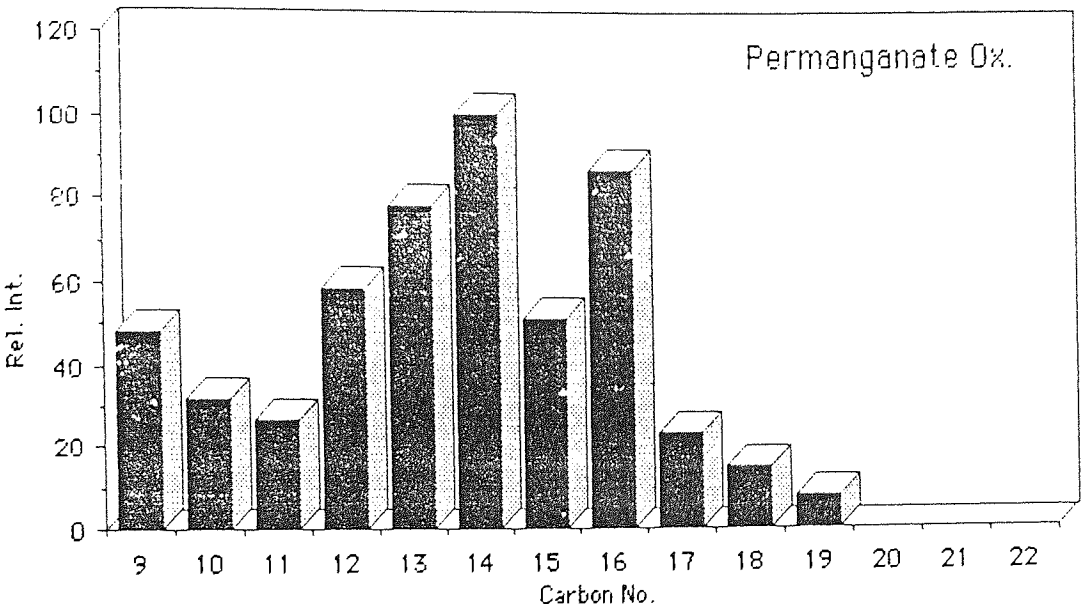

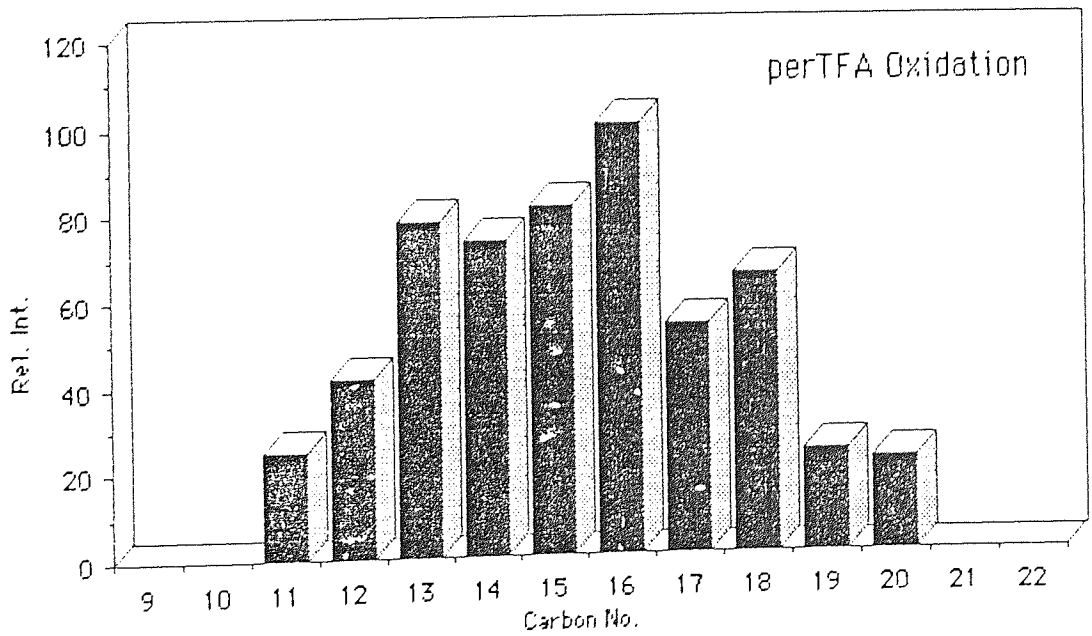

Figure 6.5e Distribution of n-chain methyl esters produced by perTFA and permanganate oxidation of the CH2 kerogen.

permanganate. It is interesting to note that the range and distribution of the n-chain mono-methyl esters derived from each kerogen is very similar to that of the n-chain alkanes identified in the original bitumens isolated from the corresponding kerogens (see table 3.7 page 96). This similarity suggests that the bitumens are formed in a similar way to the mono-methyl esters, ie. via the cleavage of alkyl chains from aromatic units within the kerogen.

By generating a SIC for m/z 98 we detected a series of n-chain dicarboxylic acids in each of the five samples oxidised by perTFA. The relative concentrations of these dicarboxylic acids are low and this indicates that long alkyl chain bridges between two aromatic units are rare in these kerogens. We can make this observation because recent work[251] has shown that, although short chain dicarboxylic acids (C3 - C6) do oxidise further, longer chain ones are relatively stable to perTFA. Therefore the low concentrations of these acids is not due to their destruction by secondary oxidation.

The relative concentrations of dicarboxylic acids produced by permanganate oxidation of each kerogen are compared with those from the perTFA oxidation in table 6.4. As this shows, relatively more dicarboxylic acids are formed via permanganate oxidation than by perTFA oxidation. This again is due to secondary oxidation of primary oxidation products, such as fatty acids[252], to dicarboxylic acids by permanganate.

GC-MS analysis also revealed the presence of 1,2-benzene dicarboxylic acid (dimethyl ester) and 1,4-benzene dicarboxylic acid (dimethyl ester) in all of the five samples. These demonstrate that some aromatic compounds can survive the perTFA reagent. These were also found in the permanganate oxidation products. The formation of these compounds in the perTFA oxidation of coals has been attributed to the presence of dihydrobenzene ring systems, such as 5,12-dihydronaphthacene[244]. Presumably such structures are also present in our kerogens.

The fact that these benzene dicarboxylic acids are present, indicates that they are stable to oxidation by the perTFA reagent. This is probably a result of the electron withdrawing effects of the two carboxyl groups. This would deactivate the benzene rings towards further electrophilic attack by the OH^+ species present in the reaction mixture[238,242]. It is probable that this effect helps to deactivate the residues during oxidation.

In each of the soluble product fractions produced by oxidation (perTFA and permanganate) were found a series of n-chain alkanes. These materials are unreactive towards perTFA and permanganate, and it is proposed that they result from the release of trapped materials via the break-up of the kerogen network, which once prevented their dissolution. This has been observed in the degradation of coals and has led to the description of a mobile phase in these materials[253]. The presence of a mobile phase in kerogens has also been observed[23], and has been discussed previously in chapters 4 and 5.

6.2.2.3 . NMR of the Soluble perTFA Fractions.

The ^1H and ^{13}C spectra of the perTFA solubles from KC are shown in Figure. 6.6a and 6.6b respectively. These spectra can be considered to be representative of all the five kerogens studied for there are only minor differences between them.

From these spectra it is evident that these soluble fractions are highly aliphatic. Peaks due to aromatic protons normally resonate at 6.5 - 8.0 ppm in ^1H spectra, whilst aromatic carbon resonances occur predominantly in the range 115 - 140 ppm in ^{13}C spectra. Only weak peaks are observed in these areas. In the spectra shown (KC), the fraction of aromatic protons is only 1.2% as calculated from the integrals of the peaks. In the spectra of the other samples the aromatic proton absorptions are virtually non-

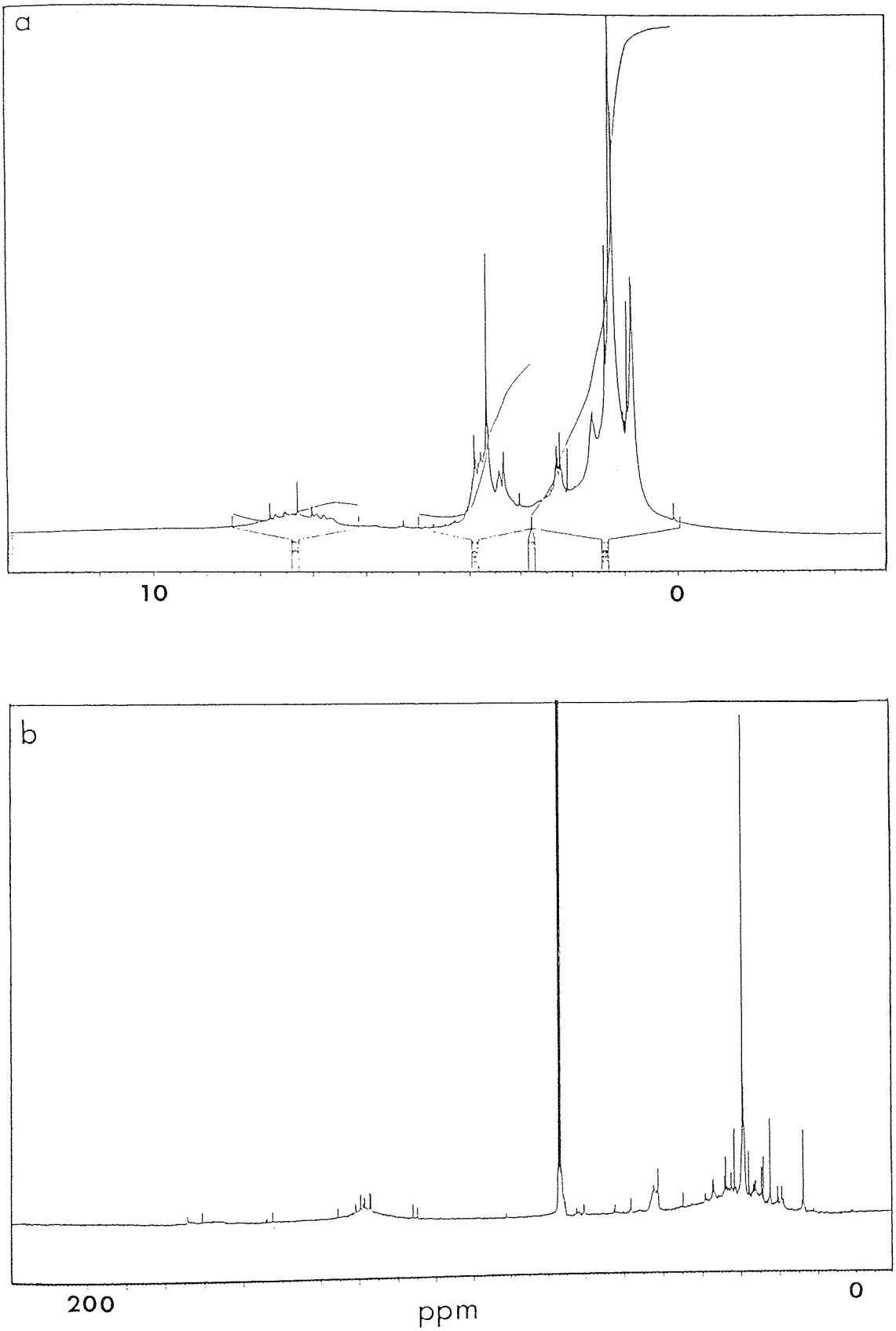

Figure 6.6 NMR spectra of the perTFA oxidation solubles from the KC kerogen.

a) ^{1}H NMR b) ^{13}C NMR

existent and it was not possible to integrate them.

The largest peaks in both the ^{1}H and the ^{13}C spectra of all samples are due to long methylene chains. In this respect they are very similar to the original chloroform bitumens isolated from the kerogens before reduction/oxidation. The protons of this group resonate at 1.15 - 1.30 ppm whilst the ^{13}C nucleus resonates at approximately 29.8 ppm. There are many peaks in the aliphatic region of the spectra in addition to the large CH_2 peaks. For instance the resonances due to methyl groups of aliphatic chains are prominent. These resonate at 0.7 - 0.9 ppm in proton NMR and from 10 - 22 ppm in ^{13}C NMR spectroscopy. The relative size of these peaks measured against that of the methylene units is a comparative measure of the degree of branching along the paraffinic chain of each sample. Those samples with a higher CH_3/CH_2 peak ratio will have a higher degree of branching. This high ratio for the CH2 sample supports the GC-MS analysis results from this sample. Further support for this is provided by the ^{13}C NMR spectra. When compared with the other samples the spectrum of the CH2 sample shows stronger resonances in the region 32 - 40 ppm region which are due to carbon atoms at and next to the sites of branching. This is also a strong feature of the chloroform bitumens of this particular sample and shows that the material solubilised by oxidation has a great deal in common with the naturally soluble material.

Other peaks which have been assigned are those resonating at 2.0 - 2.5 ppm in all proton NMR spectra. These are probably due to methylene units next to carbonyl groups of methyl esters. This assignment is supported by the peaks at approximately 32.0 ppm in the ^{13}C NMR spectra which can also be due to this group.

Several peaks due to different methoxy groups in both proton and ^{13}C NMR spectra can be clearly seen. These peaks are mainly due to methyl esters in various chemical environments which were formed via the methylation of the carboxylic acids

produced in the oxidation. Methyl ether groups are another possibility. The region 3.0 - 4.3 ppm in proton NMR is attributed to these groups as is the 50 - 60 ppm region in the ^{13}C NMR. Small peaks at 160-180 ppm in the ^{13}C spectra of these products can be attributed to carbonyl groups of esters. In some instances a small peak is resolved at 167-169 ppm which can be attributed to the carbonyl absorption of aromatic methyl esters - probably the benzene carboxylic acid methyl esters detected by GC-MS analysis. The NMR spectra of the solubles generated via permanganate oxidation are virtually the same as those obtained for the perTFA solubles. Slight differences were apparent however, the aromatic peaks being slightly larger in the permanganate soluble spectra.

6.2.3. Analysis of Residues and MHA.

All residues and MHA were analysed by elemental analysis and FTIR spectroscopy. Selected residues and MHA were also analysed by solid state ^{13}C NMR.

6.2.3.1. Elemental Analysis.

The H/C ratios of the residues and MHA's derived from each kerogen by perTFA and permanganate oxidation are shown in table 6.3.

As we can see from this table, the H/C ratios vary from kerogen to kerogen and depend on which oxidant is used. There is one underlying trend however. It is apparent that the H/C ratios of these oxidation products are generally lower than those of their parent kerogens. There are only a few exceptions to this pattern; the residues and MHA derived from the OC kerogen by perTFA oxidation and the residue derived from the KC kerogen by permanganate oxidation.

Table 6.3. H/C ratios of residues and MHA's.

sample	parent kerogen	H/C Ratio residue		MHA	
		perTFA	$KMnO_4$	perTFA	$KMnO_4$
KC	0.99	0.97	1.02	0.66	0.82
JC	1.31	1.19	1.19	0.97	1.10
OC	1.30	1.33	1.14	1.40	1.23
CH1	1.33	1.17	1.25	1.28	0.99
CH2	1.32	1.21	1.30	1.26	1.21

The fall in the H/C ratio for these oxidation products suggests that they have relatively fewer CH_3 and CH_2 groups and relatively more non-protonated carbon sites than their parent kerogens. Thus these results can be interpreted as showing that the residues and MHA's possess fewer methylene chains than their corresponding unoxidised kerogens. However, the results do not necessarily indicate that the residues and MHA are more aromatic than their parent kerogens. This is because it has been demonstrated that there is no correlation between aromaticity and H/C values[254] - a low H/C ratio being equally well explained by a condensed aromatic structure on the one hand and a totally aliphatic polyadamantane structure on the other. The solution to this dilemma rests with the application of solid state NMR analysis to these products.

6.2.3.2. FTIR Analysis.

Examination of all five perTFA oxidation residues, MHA and solubles together with the five parent kerogens via FTIR spectroscopy revealed that in all cases extensive oxidation had taken place. (Figure 6.3 shows the FTIR spectra of the three oxidation product fractions from the perTFA oxidation of the reduced extracted JC kerogen. These can be taken as representative of all the other corresponding product fractions, since

there are only minor differences between them). The similarity between the oxidation products from different kerogens is surprising, especially in the light of the elemental analyses of these products. The spectra of the residues (Figure 6.3b) have large absorptions at 1714 cm^{-1} coupled with broad peaks at 3500 to 2500 cm^{-1}, which indicate the presence of the C=O and OH units of a carboxylic acid respectively. These peaks are present in the parent kerogen but at much lower intensities. Other absorbances which appear in the residues but not in the parent kerogen occur in the region 1300 - 1000 cm^{-1} and can be attributed to various types of C - O linkages, both hydroxyl and ether. The IR spectra of the residues also contain an absorption in the 1600 - 1630 cm^{-1} region which has been shown to be due to aromatic moieties in coals and similar materials. From this it is clear that, under the condition we have used, aromatic units can survive perTFA oxidation. The size of this peak appears unchanged when compared to the parent kerogen, but this is difficult to interpret because it is very likely that the strong carbonyl peak that is introduced upon oxidation, interferes with it.

All perTFA MHA's also give similar IR spectra. These contain similar peaks to those of the residues but there are some differences. The OH peaks at 3500 -3000 cm^{-1} are sharper indicating the success of the methylation, which has also caused the carbonyl absorption to shift to that of an ester (1735 cm-1). Again we see the presence of the 1600 - 1630 cm^{-1} peak, but in these MHA spectra it is slightly weaker than in the residues. The spectra of the perTFA solubles show the same peaks as the MHA but the OH absorption is much weaker, the carbonyl absorption much stronger and the the aromatic peaks also much weaker. They appear very aliphatic in character.

Analysis by FTIR of permanganate oxidation products yielded much the same information.

6.2.3.3. Solid State ^{13}C NMR Analysis.

The ^{13}C NMR spectra of the perTFA oxidation residues and MHA's of both KC and CH2 samples are compared with those of their parent kerogens in Figures. 6.7 and 6.8 respectively. These two samples were chosen because they have the highest and lowest aromatic contents respectively.

As we can see from these figures both perTFA residue spectra have a considerably attenuated aromatic character. This is reflected in the fall in their fa values from 0.53 to 0.24 for the KC sample and from 0.28 to 0.12 for the CH2 sample. This result does not agree with those of Verheyen et al[239] for Australian coals, but it is to be expected if the perTFA reagent preferentially destroys aromatic rings. Hence, it would appear that perTFA oxidation of these kerogens yields an insoluble residue which is predominantly aliphatic, not aromatic as found for coals. The residual aromatic character of these residues may be due to either i) insufficient penetration by the oxidant or ii) deactivation of the aromatic rings especially by electron-withdrawing carboxyl groups and/or the lack of a reactive site for attack. This second possibility is supported by the presence of carbonyl peaks in these spectra which resonate between 170 and 182 ppm with a maximum at 175 ppm. However, due to SSB once again, it is very difficult to see if there are sufficient numbers of carbonyl groups to deactivate all of the aromatic rings.

The spectra of the perTFA MHA are very interesting for they show considerable residual aromatic character (especially that MHA derived from the KC kerogen). This is somewhat surprising bearing in mind that the residues have a much lower aromatic character. For the MHA materials to dissolve in base (before methylation) they must have had a higher carboxyl content than the residues, otherwise the residues would have dissolved as well. This is supported by the carbonyl absorptions for these MHA, which are stronger than for the residue spectra. This indicates that the materials giving rise to

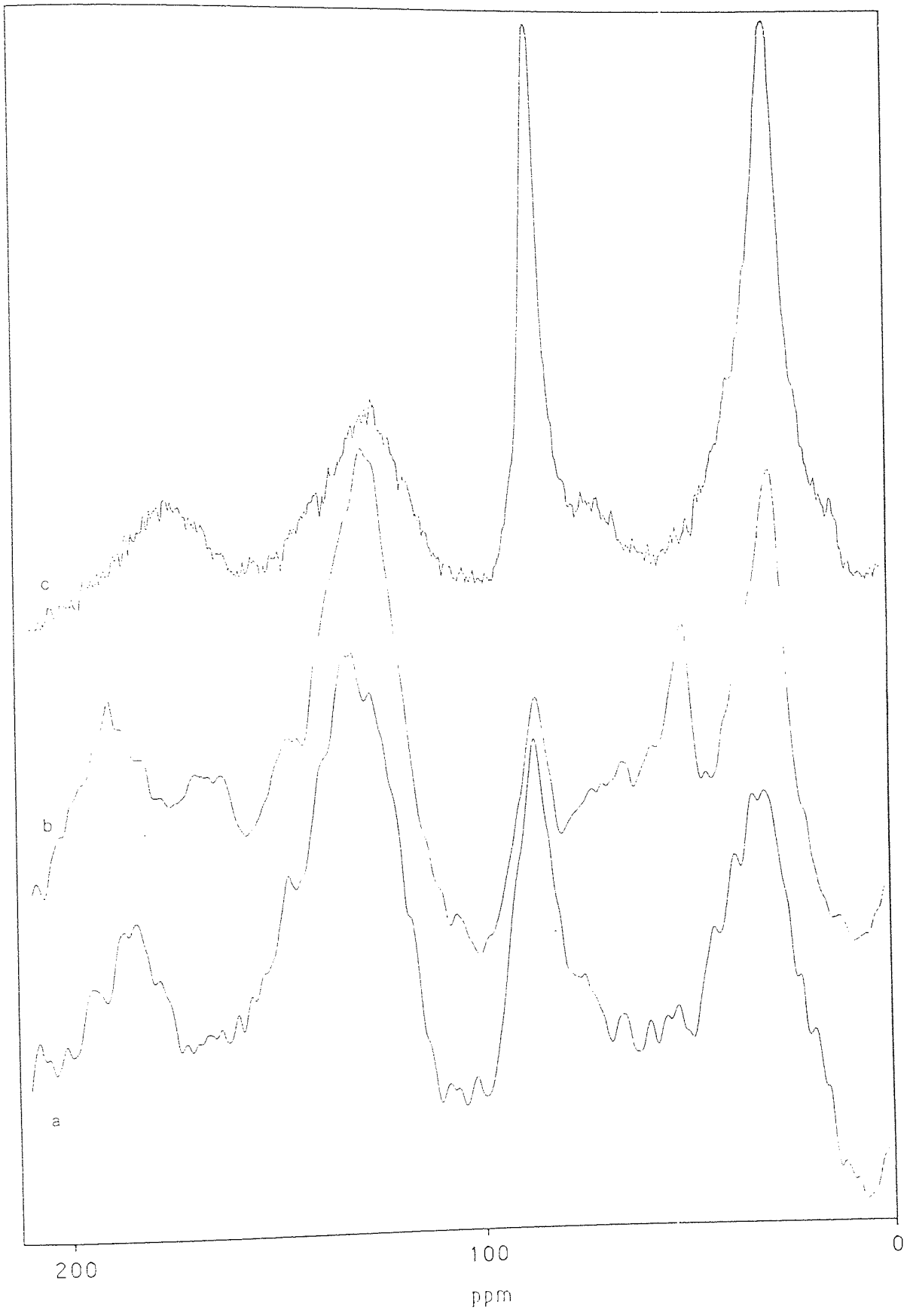

Figure 6.7 Solid state 13C NMR spectra of a) Reduced extraced KC kerogen
b) MHA from perTFA oxidation of a
c) Residue from the perTFA oxidation of a

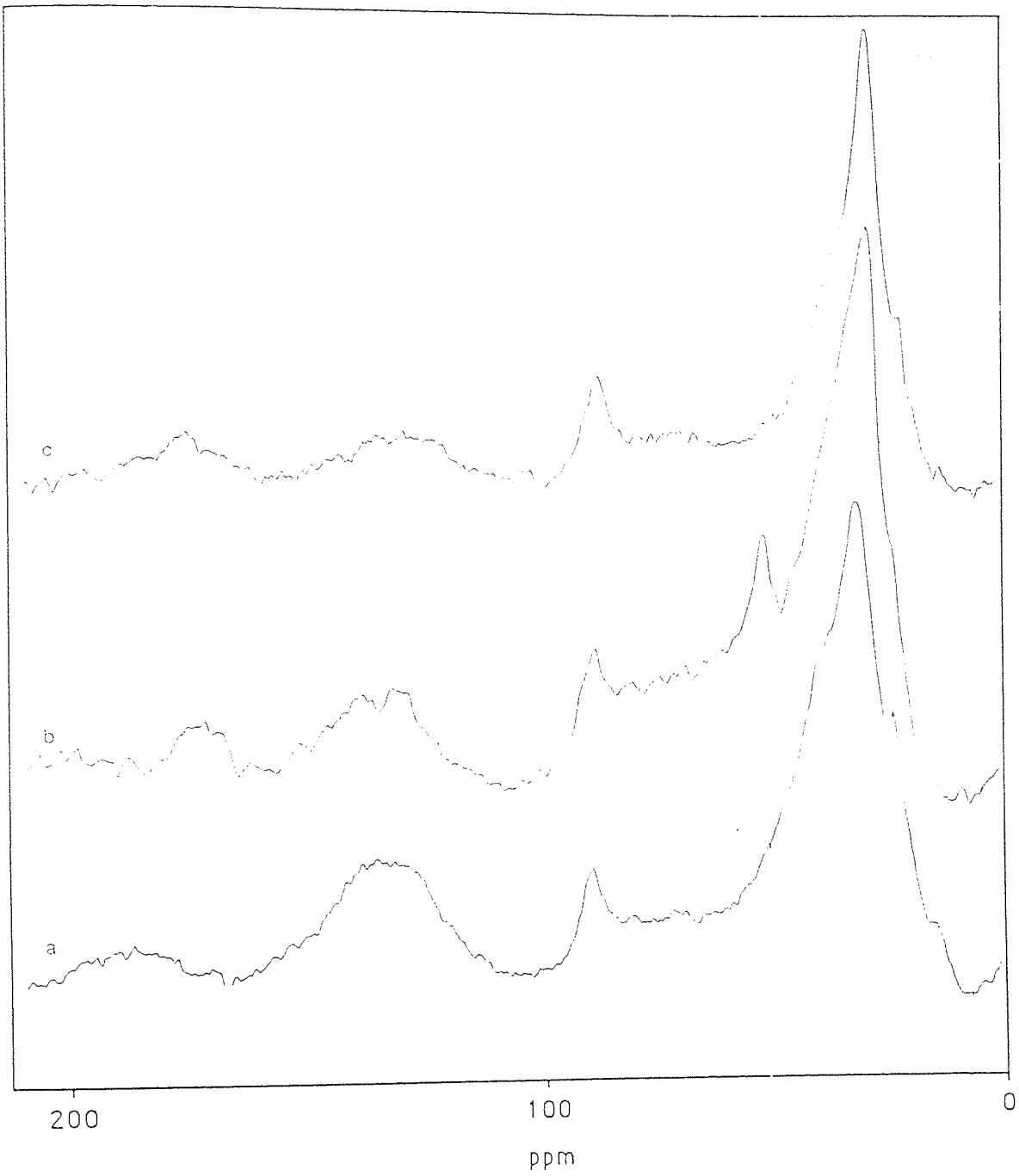

Figure 6.8 Solid state 13C NMR spectra of a) Reduced extraced CH2 kerogen

b) MHA from perTFA oxidation of a

c) Residue from perTFA oxidation of a

the MHA were more oxidised than the residues, but yet they contain more aromatic character. The presence of this resistant aromatic material can once again be explained either by insufficient reagent penetration or deactivation by carboxyl groups. Lack of reagent penetration seems unlikely in view of the continued resistance of the residues to perTFA and the closer examination of the carbonyl resonances which reveals that they are slightly shifted to lower ppm values indicating the presence of aromatic methyl esters of the type Ar-CO_2CH_3. This would suggest the deactivation theory is correct. The presence of methyl esters is confirmed by the strong absorptions in the 50-60 ppm area which are due the the methyl groups of such structures.

The two MHA's derived from the two different kerogens have widely different aromaticities, but then so do the two kerogens studied. The aromatic part of the MHA's may therefore reflect some aromatic unit in the parent kerogen, but conclusions cannot be drawn from just two samples. Further work is required before elaboration of this theory is possible.

Analysis by solid state NMR of the residues obtained by permanganate oxidation of the KC and CH2 kerogen gave spectra similar to those obtained from the perTFA oxidation. However the permanganate residues were more aromatic than the perTFA ones.

NB. Once again it must be remembered that doubts exist as to the quantitative reliability of solid state ^{13}C NMR spectra. Since it was not possible to measure the relaxation times needed to optimise the cross-polarisation experiment (for reasons explained earleir), the results presented above must be treated with some caution.

6.2.3.4. <u>Further oxidation of a PerTFA residue.</u>

It was decided to oxidise the perTFA CH2 residue further in an attempt to

solublise this material and therefore to obtain more detailed information about it. The CH2 residue was chosen for this because, throughout the analysis of this kerogen, isoprenoid structures had been detected. It would therefore be of interest to see if such structures were still present in the residue of the perTFA oxidation. Initially reoxidation with perTFA was tried but this was found to be ineffective. From this it is apparent that the residues result from a resistance to perTFA oxidation and not the lack of perTFA penetration. For this reason stepwise permanganate oxidation was performed on the perTFA CH2 residue.

This CH2 perTFA residue when oxidised in this way gave only small amounts of a secondary residue, some 10-15% of the starting weight, virtually no MHA material and a soluble fraction. The secondary residue was analysed by solid state NMR and was found to have a very strong aromatic peak, a strong carbonyl peak and a relatively weak aliphatic peak. This suggests a heavily carboxylated aromatic structure with a few aliphatic groups attached. From a mass balance consideration it would appear that virtually all of the aromatic material present in the perTFA residue is present in this second residue. This indicates that the permanganate oxidation has cleaved the aromatic/aliphatic bonds that the perTFA left intact.

GC-MS analysis of the soluble material derived from this perTFA residue showed an abundance of mono-methyl esters of carboxylic acids. Prominant were a set of isoprenoid chain mono-methyl esters similar to those found in the original perTFA solubles from this kerogen. In addition, a set of n-chain mono-methyl esters C_{12}-C_{26} and a set of dicarboxylic acids as methyl esters were detected (C_{10}-C_{24}). [Carbon number includes the carbonyl of the ester group but not that of the methyl group]. In addition phthalates were detected as was 1,2-benzenedicarboxylic acid (as the dimethyl ester). Also a significant single component was detected which could not be identified

fully but whose fragmentation pattern was similar to that for polycyclic aliphatic structures such as the triterpanes. It did not have the characteristic m/z peaks at 191 or 217 but instead there were peaks at 171, 201 and 215 in this region. The predominance of the isoprenoid and n-chain esters in this fraction suggests that the aliphatic composition of the perTFA residue is somewhat similar to the aliphatic material already dissolved from it, ie. the initial perTFA solubles.

6.3 Conclusions.

We have used a mild perTFA oxidative procedure to degrade each of five kerogens into a base insoluble residue (Residue), a methylated humic acid-like fraction (MHA) and a dichloromethane-soluble fraction (Solubles). We have found that the combined product yield of these three fractions decreases as the fa values, hence aromaticity of the parent kerogens, increase. This we explain via the oxidation of the aromatic units within the kerogens into carbon dioxide and water-soluble acids, which escape determination. Indeed solid state ^{13}C NMR of oxidation residues reveals a considerable reduction in aromatic character when compared to their parent kerogens. The residual aromatic carbon that survives oxidation may be due to either i) the insufficient penetration of the perTFA reagent into the kerogen or ii) deactivation of the aromatic rings by carboxylation and/or their lack of a reactive site. The lack of reagent penetration does not appear to be the problem with this system and it is believed that each product fraction results from the oxidation of different structural units in our kerogens. It is proposed that solubles result from those units in the kerogens that have a relatively high concentration of oxidisable sites. These units therefore degrade into relatively low molecular weight compounds which are soluble. Likewise the residues are derived from units within the kerogens that have relatively few oxidisable sites, hence they remain largely undegraded and therefore still insoluble. The methylated humic acid fraction

would then represent structural units in the kerogens which had more oxidisable sites than the residues but not as many as the solubles.

Detailed analysis by GC-MS of the soluble oxidation products from each kerogen suggested that the CH2 kerogen alone contained structural units having a high composition of isoprenoid chains. This is confirmed by both proton and ^{13}C NMR of this particular sample. This indicates that this kerogen may well have a different source material composition than the others. The release of trapped molecules upon the degradation of the kerogen network was noted throughout.

Comparing alkyl chain distributions in the soluble products produced by both perTFA and alkaline permanganate oxidation has shown that permanganate oxidises primary oxidation products into lower molecular weight products. This outlines a significant benefit to be gained by using perTFA as the oxidative degradant in oxidation studies and that perhaps permanganate oxidation is not best suited for the study of structures in kerogens.

CHAPTER 7

CONCLUSIONS

7.1 Conclusions.

In this study we have attempted to address some of the many problems that are encountered in the determination of the molecular structure of the organic matter in oil shales. Central to the approach used was the development of mild and selective degradative procedures for the solubilisation and hence eventual characterisation of this particularly complex material.

Three oil shales from the Kimmeridge Clay sequence were investigated together with one from the Oxford Clay sequence and one from the Julia Creek deposits in Australia. The organic matter in these samples was isolated by acid demineralisation and then separated into its kerogens and bitumens by solvent extraction.

Analysis of these bitumens and kerogens before their degradation showed that these materials were extremely complex and heterogeneous. Fractionation of the original pyridine extracts into chloroform-soluble bitumens and chloroform-insoluble but pyridine-soluble bitumens was found necessary to facilitate their analysis. Chloroform bitumens were largely aliphatic in character and GC-MS showed the presence of normal and branched chain alkanes whose distribution indicated that algae were the main source organisms for the organic matter in these oil shales. A contribution from lower land plants was possible in some samples. Pyridine soluble/chloroform insoluble bitumens were much more aromatic than their chloroform soluble counterparts and yielded no volatile components when analysed by GC-MS.

Only solid state techniques could be used for the analysis of the kerogens of which solid state ^{13}C NMR was probably the most useful. It was possible to show from solid state ^{13}C NMR that the aromatic content of the five kerogens varied considerably. It was interesting to note that the KC sample (Kimmeridge Clay from North Yorkshire) is much more aromatic than the CH1 and CH2 samples (Kimmeridge Clay from Dorset), which suggests that the northern Kimmeridge Clay is much more mature than that of the south

and indicates that it has been exposed to higher temperatures via deeper burial. Elemental analysis of these kerogens showed them to be highly heterogeneous.

Treatment of the insoluble kerogens with lithium aluminium hydride was found to i) remove residual pyrite, ii) reduce their labile functional groups, and iii) to increase their solubility in common organic solvents. Workers in this area are constantly seeking mild solubilising agents and LAH would appear to fulfill this purpose. Despite the confirmation by FTIR that the kerogens were reduced by LAH, it was shown that the most important factor in the dissolution of the kerogens was the solubilisation of the pyrite and not cleavage of the kerogen backbone. This suggests a very close association between pyrite and the organic matter concerned.

The O-methylation of reduced and extracted kerogens increased their solubility only slightly, indicating that H-bonding did not play a significant role in holding these kerogens together. Although the O-methylation reaction was not quantitative, considerable attenuation of the OH absorptions in the IR spectra of O-methylated kerogens was observed. In addition the incorporation of the CD_3 group into the kerogen was observed when CD_3I was used for methylation. However solid state NMR of the O-methylated products detected only a slight increase in the methoxy group concentration. Much of the material that was rendered soluble by the O-methylation process could not have been H-bonded with the insoluble matrix and therefore must have been derived from trapped materials released through the opening up the the kerogen matrix. Problems with the oxidation and purification of products were encountered in reactions using phase transfer catalysts.

Permanganate oxidation of the reduced extracted kerogens had a significant solubilising effect on them. Comparison of the soluble oxidation products produced by permanganate oxidation with those produced by peroxytrifluoroacetic acid oxidation however, showed that permanganate produces much higher yields of secondary oxidation

products. Hence permanganate would not appear to be best suited to the analysis of kerogen structures.

Peroxytrifluoroacetic acid oxidation on the other hand does not produce secondary oxidation of this kind and the integrity of the initial oxidation products is maintained. This oxidant would seem therefore to be a much more useful degradant than permanganate. Residual material from the perTFA oxidation showed enhanced aliphatic character when compared with the unoxidised material. This suggests that an aliphatic core is present in each kerogen which is largely inert to this reagent. The preferential destruction of aromatic rings is demonstrated by the correlation of the total product yield with the fa values of these kerogens and is further indicated by the residue analysis. However it is evident that not all aromatic rings are destroyed by this reagent, which may be explained either by the lack of a reactive site and/or the deactivation of the rings by carboxyl groups. It is suggested that the different product fractions produced by this oxidation represent different structural units within the kerogen. For instance it is suggested that the residues represent structural units in the kerogens which have low concentrations of oxidisable sites and which therefore remain largely undegraded and insoluble. Assuming the validity of this argument, soluble oxidation products must come from structural units possessing a high concentration of oxidisable sites whose degradation leads to a low molecular weight, hence more soluble, product.

It has been noted throughout the analysis of the organic material derived from the CH2 sample (bitumens, kerogens and their degradation products) that isoprenoid chain aliphatic structures are present in much greater abundance than n-chain aliphatic structures. The CH2 sample is alone in this behaviour which suggests its structure is significantly different from those of the other samples and perhaps therefore its organic matter has come from a different source.

The fact that these isoprenoid chains are predominant in the bitumens as well as

the kerogen degradation products (especially the oxidation products) suggests that structures in the bitumens may well be used as models for at least part of the kerogen structure. Indeed, in all cases there was striking similarity between bitumens and the soluble materials isolated after perTFA oxidation of the corresponding kerogen. For instance the distributions of the alkyl chains, as alkanes in the bitumens and as mono-methyl esters in the oxidation products, are almost identical, which not only confirms the similarity between the bitumens and portions of their corresponding kerogens, but indicates that the natural bitumens were formed in much the same way by diagenesis, as the soluble oxidation products, ie. through cleavage at or near the sites where aromatic and aliphatic units bond together

In addition to these findings it has been noted that kerogens do not totally consist of insoluble materials as their definition implies. We have found that kerogens, when degraded by chemical reagents, release soluble products that can not be derived through the reactions of the degradant. For instance, after lithium aluminium hydride reduction, O-methylation and even the oxidation with permanganate and perTFA of the kerogens, a series of n-chain alkanes were detected in the soluble products. These inert alkanes cannot be formed via the actions of these degradants and consequently they must have been trapped within the kerogen and subsequently released as the kerogen matrix was broken down. The variation of proton relaxation times of these materials is further confirmation of a mobile or trapped phase. Similar measurements have identified such a mobile phase in coals. These observations are consistent with the view that kerogens are highly crosslinked sponge-like materials which, when broken up by degradation, release trapped compounds.

As a consequence of these investigations a great deal of information regarding the molecular structure of these materials has been obtained. Although much work is still required in this area before the elucidation of these materials can be even considered

near complete, it is felt that significant progress has been made towards this objective.

Chapter 8.

Experimental.

8. Experimental.

8.1. Sample Origin.

8.2. Sample Preparation.

8.3. Acid Demineralisation.

8.4. Soxhlet Extraction.

8.5. $LiAlH_4/D_4$ Reduction.

8.6. Methylation. 8.6.1 PTC/CH_3I or CD_3I.

8.6.2 BF_3/MeOH.

8.7. Alkaline Potassium Permanganate Oxidation.

8.8. PerTFA Oxidation.

8.9. Sulphur Determination by Eschka Method.

8.10. Instrumentation. 8.10.1 Elemental Analysis.

8.10.2 IR Analysis.

8.10.3 GLC and GC-MS Analysis.

8.10.4 UV/VIS Analysis.

8.10.5 ^{1}H , ^{13}C and Solid State NMR.

8.10.6 GPC Analysis.

8. Experimental

The procedures described in this chapter are summarised in schemes 1-4 at the end of this chapter and are those used throughout the project unless stated otherwise. All reagents used were of general purpose grade unless stated otherwise. Where possible the exposed surfaces of each oil shale deposit were removed to a depth of several inches before samples were taken. This was done to avoid inclusion of the more severely weathered material.

8.1. Sample Origin.

OC	Oxford Clay	Taken from the bottom of No. 2 pit of the London Brick Company at Calvert, Buckinghamshire. (Grid Ref. SP 680 240).
KC	Kimmeridge Clay	Taken from the base of the cliff at Port Mulgrave. North Yorkshire (Grid Ref. NZ 790 170).
CH1	Kimmeridge Clay	Taken at 120cm below Rope Lake Headstone Band from the cliff at Clavell's Hard, 1.5 km east of Kimmeridge Bay, Dorset (Grid Ref. SY 920 777).
CH2	Kimmeridge Clay	Taken at 60cm above Rope Lake Headstone Band from the cliff at Clavell's Hard, 1.5km east of Kimmeridge Bay, Dorset (Grid Ref. SY 920 777).
JC	Julia Creek	This sample was supplied by Dr. H Stephenson at Marquarie University, New South Wales, Australia.

The Kimmeridge Clay outcrop in the British Isles is shown in fig 8.1 and a more detailed map of the Kimmeridge Bay area in fig 8.2(a+b).

8.2. Sample Preparation.

Rock samples obtained from the source locations were washed and scrubbed in distilled water in order to remove surface debris and possible contaminants. These cleaned rocks were then broken into small lumps (1 - 2 cm) and then crushed using a Sibertechnic Tema disc mill to below 200 mesh. Samples ground in this way were then stored under nitrogen for subsequent analysis.

8.3. Acid Demineralisation.

Powdered samples (100g) were suspended in concentrated HCl and warmed to 70°C for 1 hr. The residues from this treatment were added to cold 40% w/v HF, and the medium was agitated from time to time. The spent acid was replaced daily, and the extent of demineralisation measured by combustion. After about 1 week, when there was no further change in the organic/inorganic ratio, the residues were washed free from HF, heated to 70°C with concentrated HCl to decompose insoluble fluorides, filtered and finally washed with distilled water before drying and storage in a vacuum desiccator. These methods have been used extensively[23,57,58,170,173]. Kerogens and bitumens were separated from these acid demineralised organic concentrates by extraction with pyridine as described below. These procedures are summarised in scheme 1.

8.4. Soxhlet Extraction.

Samples to be extracted, unless otherwise stated, were exhaustively extracted with pyridine using soxhlet apparatus under a nitrogen atmosphere. Extraction residues were then extracted with methanol or acetone to remove all traces of pyridine, dried in a

Figure 8.1 The Kimmeridge Clay outcrop in the British Isles.[145]

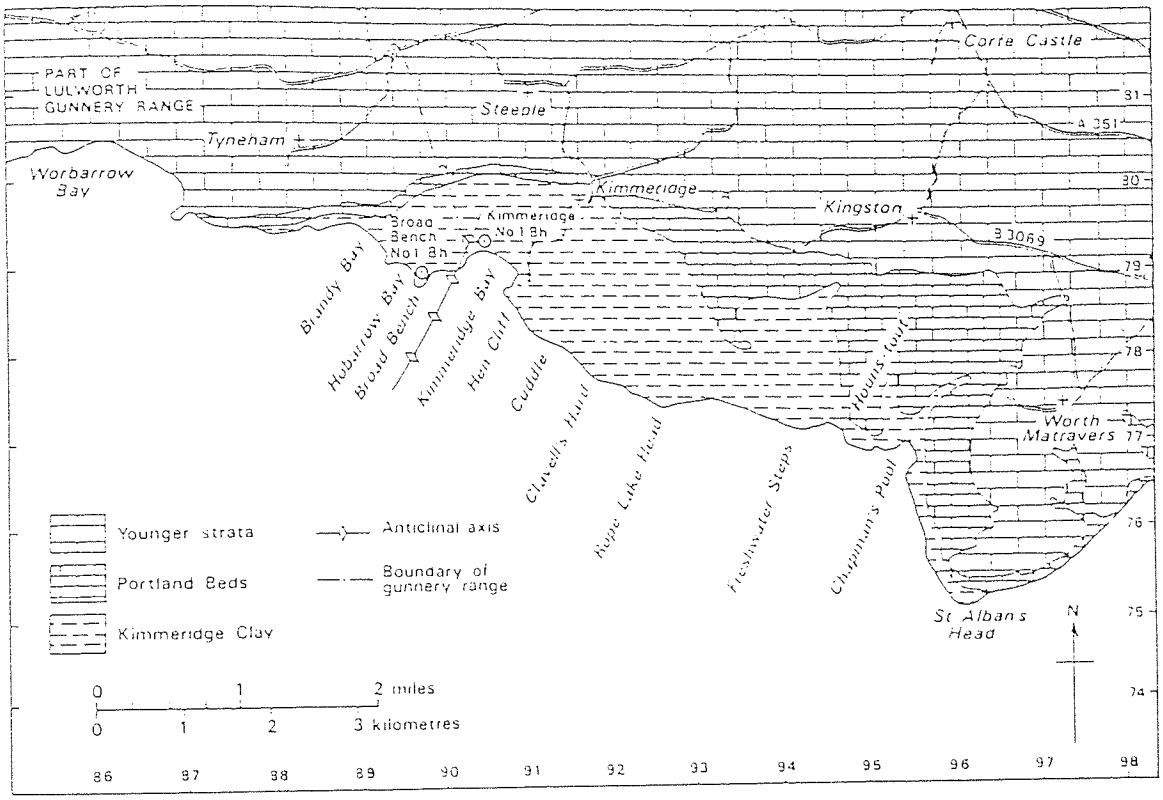

Figure 8.2a Sketch of the Kimmeridge Bay area Dorset.[37]

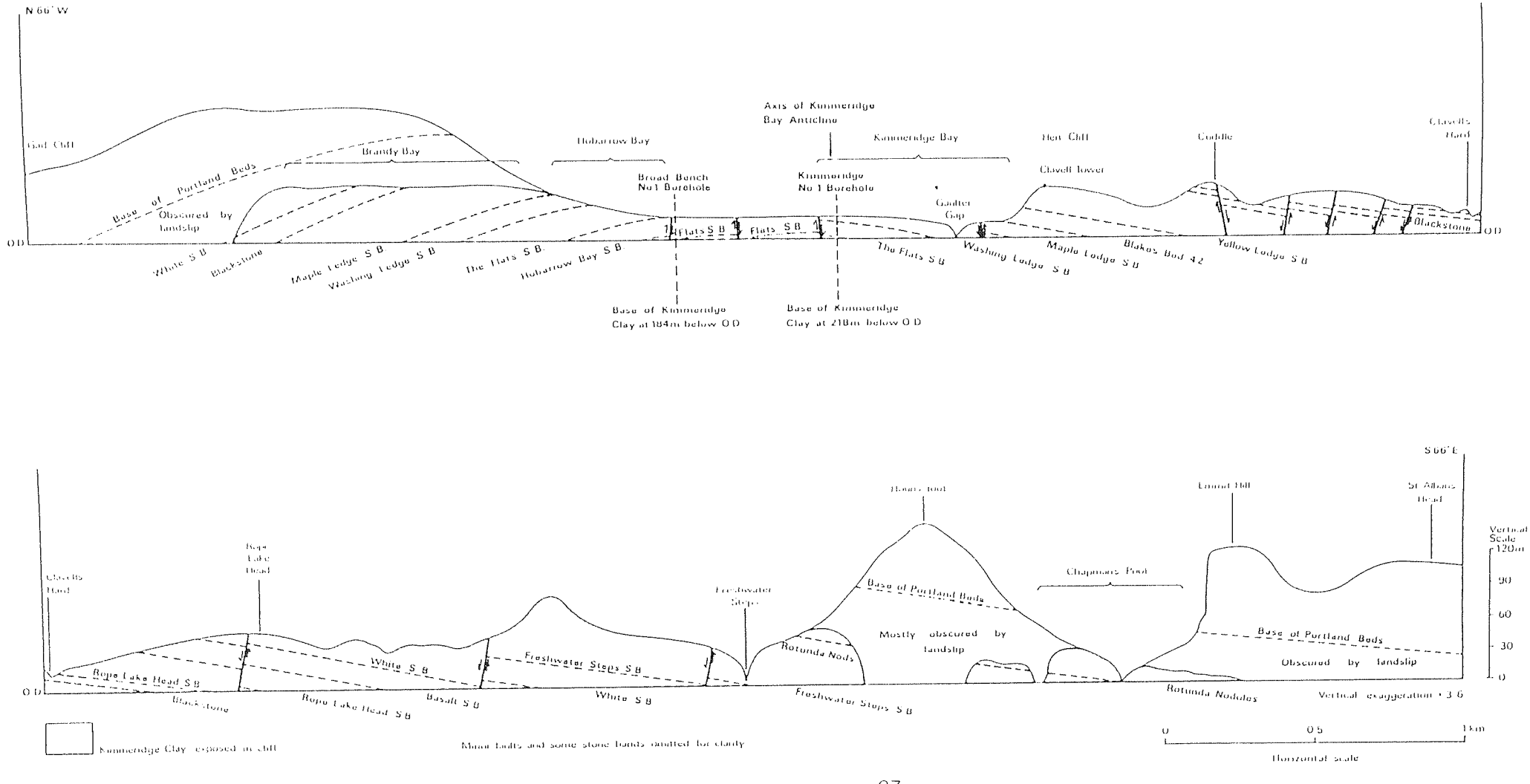

Figure 8.2b Geological sketch sections of the Kimmeridge Clay exposed in the cliffs between Brandy Bay and Chapman's Pool

vacuum oven (80 °C for 6 hrs) and stored in a vacuum desiccator.

The pyridine extract was evaporated to dryness on a rotary evaporator and chloroform added to dissolve any chloroform soluble material. The resulting mixture was filtered to separate the chloroform solubles from the insolubles (pyridine soluble but not chloroform soluble).

It was found necessary to extract the chloroform solubles with dilute HCl in order to remove the last traces of pyridine. These solutions then required drying over magnesium sulphate before being isolated on the rotary evaporator. All isolated extracts were stored under nitrogen until required.

8.5. $LiAlH_4/D_4$ Reduction - Removal of Pyrite.

The pyridine extracted, acid demineralised organic residues (kerogens) and $LiAlH_4$ in a ratio of 4:1 by weight were refluxed in dry tetrahydrofuran (THF) for a period of 3 - 5 days[23,170,173]. Excess $LiAlH_4$ was then quenched with distilled water, and the reaction mixture acidified to pH 1 with conc. HCl before heating to 70° C for 2 hrs. Throughout this time nitrogen was bubbled through the mixture in an attempt to minimize any oxidation of the substrate. After filtration of the reaction mixture the reduced and pyrite-free kerogen was washed with distilled water, dried and stored under nitrogen. Extraction of the reduced kerogens was performed as already described. However, in addition to this, the water used to quench the excess $LiAlH_4$ was also extracted with chloroform in order to collect any water-soluble reduction products. This is summarised in scheme 1.

An identical procedure was adopted for both reduction of other kerogen-derived products and the reductions with $LiAlD_4$, although this was done on a smaller scale.

8.6. Methylation.

8.6.1 PTC/CH_3I or CD_3I.

Kerogen or kerogen derivatives (10g), tetrabutylammonium hydroxide ($30cm^3$ 40% aqueous solution), methyl iodide ($10cm^3$) and freshly distilled THF ($150cm^3$) were stirred for 2 days under a nitrogen atmosphere following the procedure of Liotta[207]. Excess methyl iodide and solvent were removed using a rotary evaporator. To the residues, containing methylated kerogen and tetrabutylammonium iodide / hydroxide, were added pyridine ($50cm^3$). This mixture was transferred to a tared extraction thimble and extracted with pyridine. This pyridine extraction was found necessary in order to remove the PTC from the kerogens. The extraction residue was treated as before but the pyridine extract was isolated on the rotary evaporator and to it added 5% aqueous HCl ($200cm^3$) to dissolve the PTC and remaining pyridine. This mixture was then filtered at the pump and the filtrate washed with boiling distilled water ($1000cm^3$). The filter cake (the true pyridine extract free from PTC) was then dried and treated as before. These procedures are summarised in scheme 2.

An identical procedure was adopted for methylations using d^3 methyl iodide but on a smaller scale.

8.6.2 Methylation using BF_3/MeOH.

Oxidation products, whether as precipitated acids, solutions in organic solvents or as a combination of both, were dried and then refluxed with $20cm^3$ of 14% BF_3 in methanol for three days[240]. Preliminary experiments had shown that this extended reaction time was necessary for complete reaction to occur. The resulting mixture was then extracted with CH_2Cl_2 and the insoluble material (MHA) isolated and dried. The CH_2Cl_2 solution was washed with sat. NaCl solution ($100cm^3$). The aqueous phase was then extracted with CH_2Cl_2 ($2x35cm^3$). The combined CH_2Cl_2 solutions were then

washed with 10% Aq Na_2CO_3 ($100cm^3$) and finally with sat. NaCl solution ($100cm^3$). The remaining solution was dried over $MgSO_4$ before isolation on the rotary evaporator to give the 'Solubles' fraction.

8.7. Stepwise Alkaline Potassium permanganate Oxidation.

Pyridine-extracted kerogens / kerogen derivatives (0.5g), distilled water ($20cm^3$) and 20 cm^3 of potassium permanganate stock solution (4.5g $KMnO_4$ + 6.4g KOH in 1000 cm^3 distilled water) were reacted together. When all colour of permanganate had gone from the reaction mixture it was filtered and the filter cake treated with a further 20 cm^3 of distilled water and $20cm^3$ of stock solution[23,232]. This was repeated until reduction of the permanganate (measured by the loss of colour) was found to be extremely slow even upon heating to 60°C. After this final oxidation step excess permanganate and residual manganese dioxide were removed using sodium sulphite and sulphuric acid. Residual organic material not solubilised by oxidation (Permanganate Residue) was collected at the pump, dried and retained for analysis. All filtrates were combined and then acidified to precipitate the oxidised materials which were collected at the pump. The remaining filtrate was then extracted with $CHCl_3$. This $CHCl_3$ extract was isolated and combined with the precipitated acids ready for methylation as described in section 8.6.2. The remaining aqueous solution was discarded. These procedures are summarised in scheme 3.

8.8. perTFA Oxidation.

The oxidation mixture (CF_3COOH, 30% Aq H_2O_2 and H_2SO_4 in a volume ratio of 8:10:5) ($80cm^3$) was added over a period of 15 minutes, to the kerogen / kerogen derivative (2g) suspended in distilled $CHCl_3$ ($100cm^3$). This mixture was refluxed for 5hrs[247]. NaOH solution (20% w/v) was then added to the cooled reaction mixture to

give pH 14 and then filtered at the pump. The filter cake (perTFA Residue) was then washed with distilled water and dried in a vacuum oven. The $CHCl_3$ and the aqueous alkaline layers of the filtrate were then acidified with c.HCL to pH 1 and, after cooling overnight, filtered at the pump. The precipitate was washed and dried as before and retained for methylation. The remaining filtrate was then extracted with $CHCl_3$. This $CHCl_3$ extract was isolated and combined with the precipitated acids ready for methylation. The remaining aqueous solution was discarded. These procedures are summarised in scheme 4.

8.9. Sulphur Determination by Eschka Method.[255]

The kerogen sample (1g accurately weighed) was mixed with the Eschka mixture (2 parts magnesium oxide and 1 part anhydrous sodium carbonate) (3g) in a porcelain crucible. This mixture was then covered by further Eschka mixture (1g). The crucible was then heated electrically, slowly at first (30 mins) and then more vigorously until no black particles were revealed by careful stirring of the crucible contents.

After heating, the crucible contents are digested in dil hydrochloroic acid (1N, $100cm^3$) and filtered. After repeated washings of the filter cake with hot distilled water the combined filtrate was neutralised with NaOH solution. Then dilute HCl ($1cm^3$) was added and $BaCl_2$ solution ($10cm^3$) added with stirring. This was then left to cool for 2hrs. The precipitate was then collected on ashless filter paper and the amount of $BaSO_4$ determined by smoking off the filter paper and then heating to 800°C and constant weight. Blanks were also taken.

8.10. Instrumentation.

8.10.1 Elemental analysis.

Carbon, hydrogen, nitrogen and some sulphur determinations were carried out using a Carlo Erba auto analyser model 1106. Oxygen contents were calculated by

difference, taking account of mineral contents whenever possible. Vanadium pentoxide was added to assist combustion. Each sample was analysed 10 times and the average values and standard deviation calculated. This was done to help minimise the effects of the inherent heterogeneity of these materials.

8.10.2 Infra-Red Analysis.

Infra red spectra were obtained using a Perkin Elmer 1710 fourier transform infra-red spectrometer fitted with a 3600 Perkin Elmer data station running M1700 software. Solids were examined by the KBr disc method whilst extracts were examined as thin films on KBr plates. It was found necessary to dry KBr discs in a vacuum oven (1hr at 80°C) and then to store them in a vacuum desiccator to prevent ingress of moisture and therefore distortion of the IR spectra in the 3500-3000 and 1630 cm-1 region. In all cases blank KBr discs and plates were used to generate the background spectra which were subsequently subtracted from the spectra of interest.

8.10.3 GLC and GC-MS Analysis.

Preliminary GLC examinations of bitumens and soluble degradation products were carried out on a Pye Unicam 304 gas chromatograph fitted with a 1m x 0.5cm (ID) SE30 glass column and flame ionisation detector.

All GC-MS analyses were performed on a VG Micro Mass 12000 series quadrupole mass spectrometer fitted with a 30m x 0.3mm (ID) bonded phase fused silica column.

Unless otherwise stated the column temperature was programmed from 80°C to 300°C with a 2min delay and a 20min hold at 300°C. The helium flow rate in the GC-MS work was approximately $5cm^3/min$. Components separated on the column were fed into the source of the mass spectrometer (maintained at 200°C) where they were ionised by

a 70eV electron beam.

Mass spectra were generated and recorded every 2 seconds on a Digital PdP8a mini computer running VG Release 8 (MS1 2000) software.

8.10.4 UV/Visible Spectroscopy.

The ultra violet/visible spectra of bitumens and selected extracts were obtained using a Pye Unicam SP 800B spectrometer. Glass cells of 1cm pathlength were used throughout.

8.10.5 ^{1}H, ^{13}C Solution and Solid State NMR.

^{1}H and ^{13}C solution state NMR spectroscopy of soluble bitumens and degradation products was carried out on two instruments. Firstly a Jeol FX90Q instrument was used which studied proton and carbon 13 nuclei at 90MHz and 22.5MHz respectively. Using this instrument proton spectra typically required at least 1000 pulses with up to a 4 second repetition time. Carbon 13 spectra usually required at least 100,000 pulses for a reasonable result.

In addition to the Jeol instrument a Bruker AC series 300 MHz NMR spectrometer, fitted with an Aspect 3000 NMR data system and accessory for CP MAS, was used. Proton and carbon 13 nuclei were studied at 300Mhz and 75MHz respectively. Using this instrument better resolution was obtained and more advanced pulse programs were available. Subsequently some samples were examined using the DEPT pulse sequences.

$CDCl_3$ was the most common solvent used but on occasions d^6 DMSO and d^5 pyridine were used. In all cases TMS was used as internal reference. Ultra-sonic agitation was often used to aid the swift dissolution of the samples.

Solid state ^{13}C CPMAS NMR spectra were also obtained on two instruments. Some

spectra were recorded at 50.3MHz using a Bruker 200MHz instrument at the University of East Anglia. On this instrument spectra were obtained using magic angle spinning (3KHz), proton decoupling (60KHz) and cross-polarisation (proton enhancement) with a contact time of 3ms. Spectra were also recorded at East Anglia using a pulse program that introduced a dipolar dephasing technique. Between 26,000 and 90,000 pulses with a repetition time of 0.75 seconds were required for a reasonable result.

Other solid state spectra were recorded within the department of Molecular Sciences at Aston University using a Bruker AC series 300MHz NMR spectrometer. Pulse sequences used were similar to those used at East Anglia.

8.10.6. Gel permeation chromatography.

Solutions made up in chloroform (2% Wt) were examined by gel permeation chromatography using a Perkin Elmer series 10 liquid chromatograph fitted with a Perkin Elmer LC-85B spectrophotometric variable wavelength detector. The column was calibrated with n-alkanes as the low molecular weight calibrant and polystyrene fractions with a maximum molecular weight of 6×10^6 as the high molecular weight calibrant.

Scheme 1. Procedures for the acid demineralisation and $LiAlH_4$ reduction of organic matter in oil shales and their extraction.

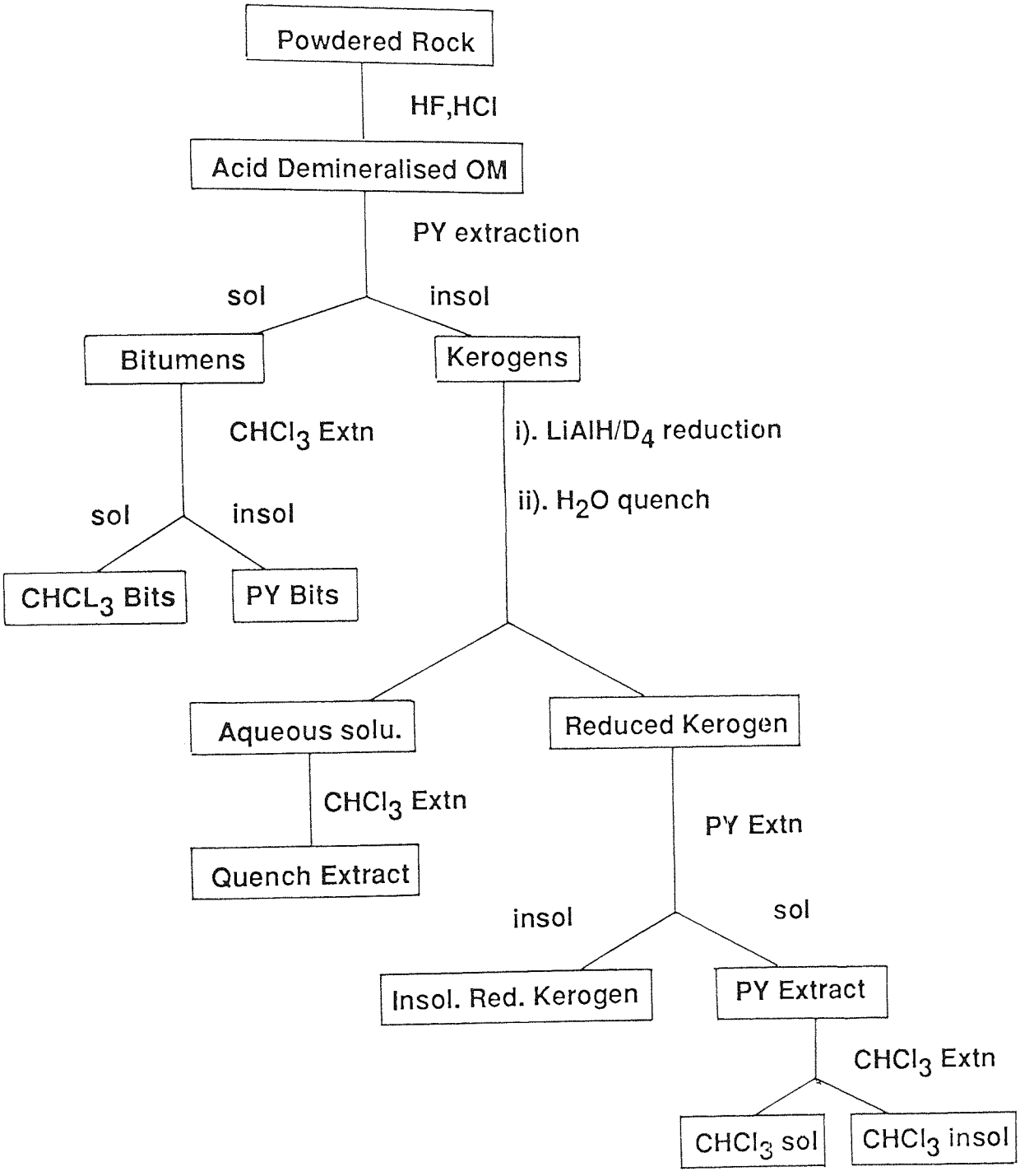

Where OM = Organic Matter

PY = Pyridine

Scheme 2. Procedures used for the O-Methylation and subsequent extraction of reduced extracted kerogens.

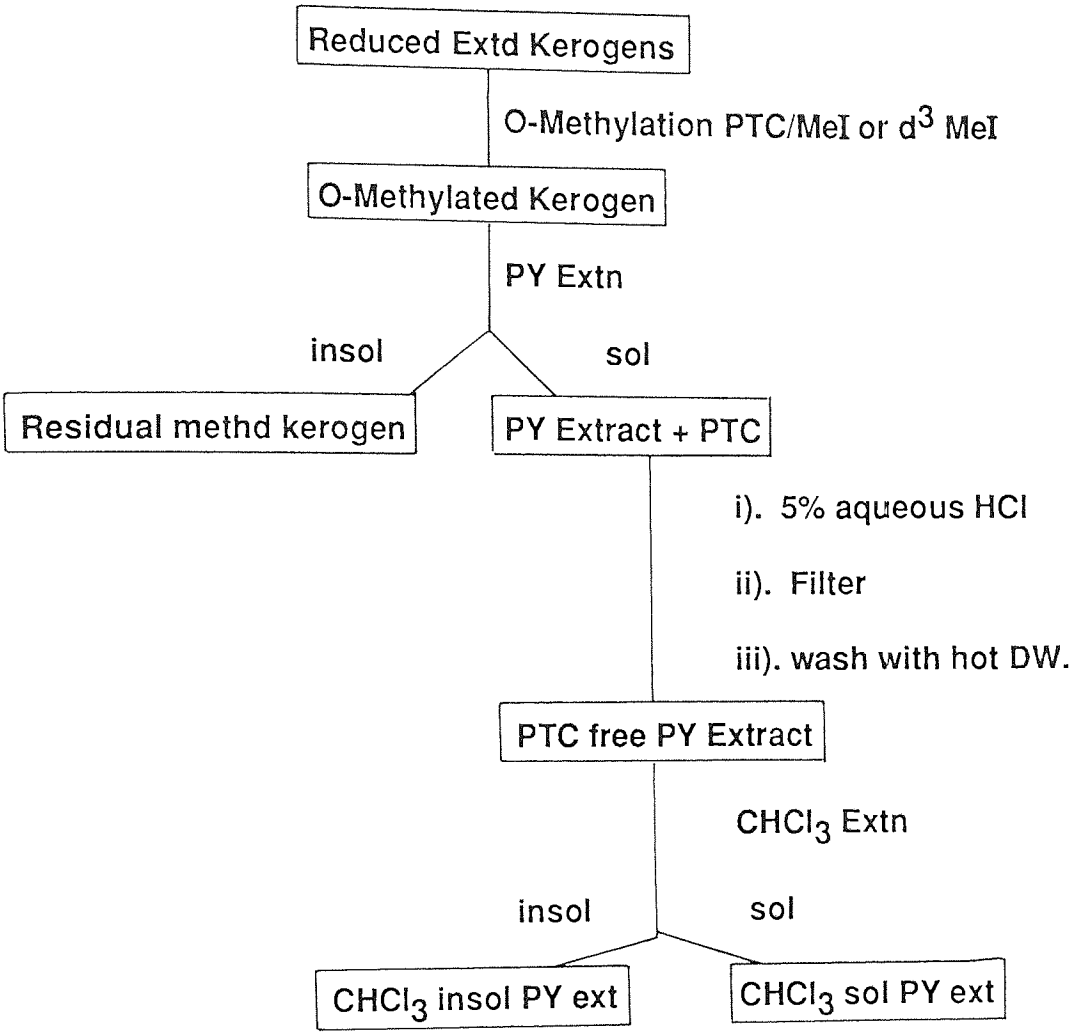

Where PTC = Phase Transfer Catalyst

DW = Distilled Water

PY = Pyridine

Scheme 3. Procedures involved in the stepwise alkaline potassium permanganate oxidation.

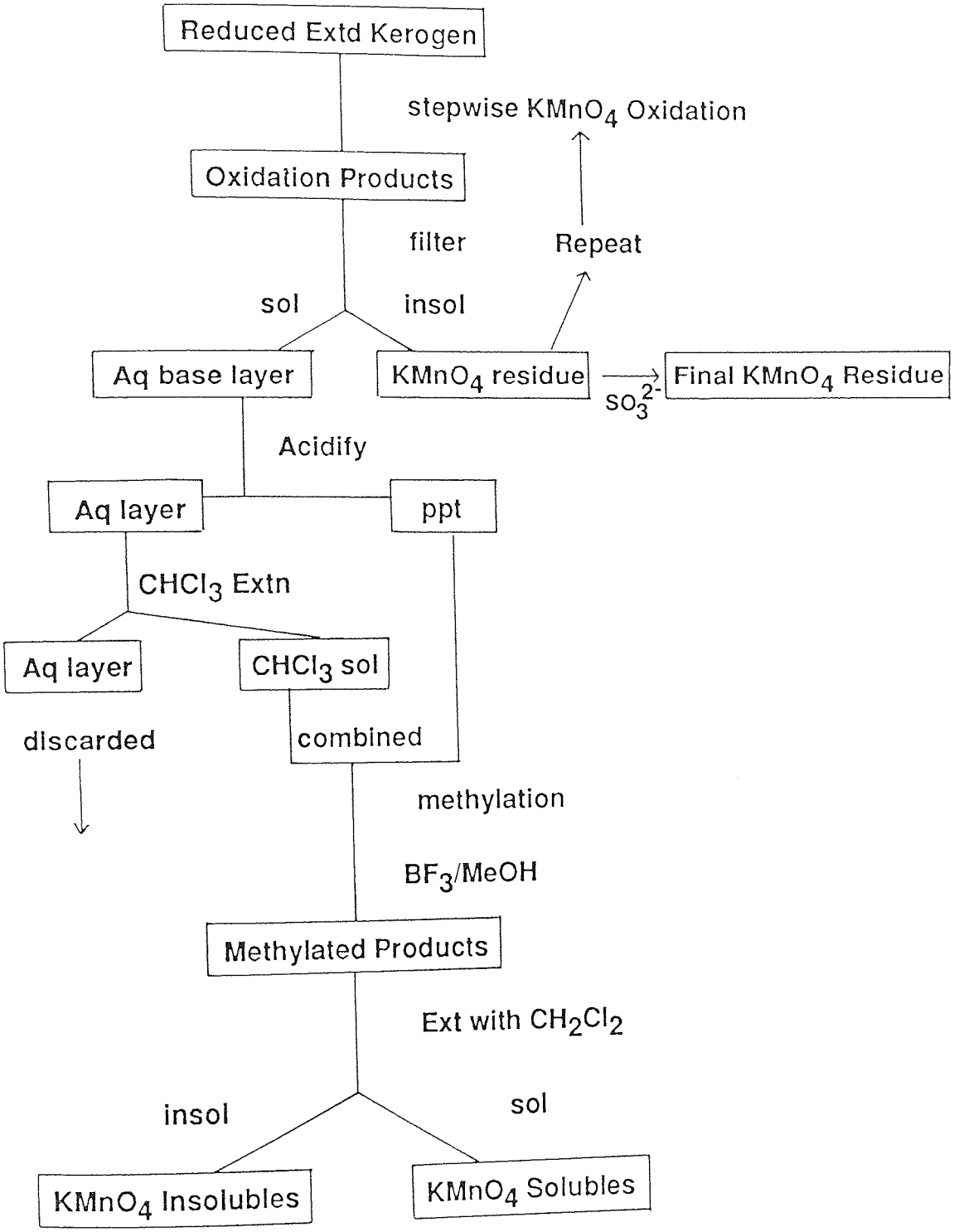

Scheme 4. Procedures involved in perTFA oxidation.

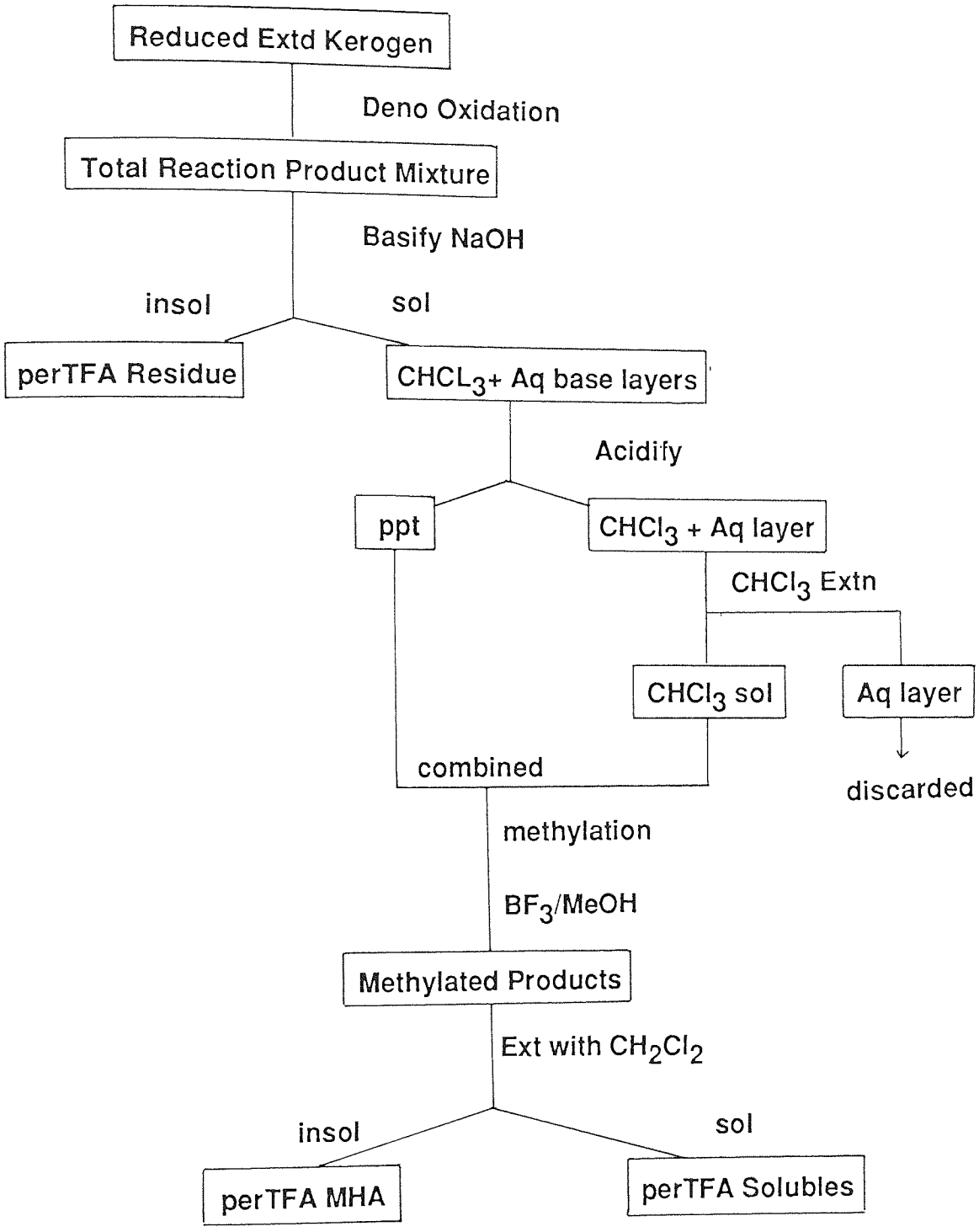

Appendix 1

GC-MS Analysis of Bitumens.

Appendix 1a. GC-MS data from KC chloroform bitumens.

Peak No	Scan No.	Intens	Mol. Wt	Peak Assignment	Principal peaks m/e
1	230	45	212	2,6,10-trimethyldodecane	57,71,43,41,85
2	242	170	198	n-chain alkane $C_{14}H_{30}$	57,43,73,41,29
3	276	236	226	2,6,10-trimethyltridecane	43,57,71,41,85
4	294	959	212	n-chain alkane $C_{15}H_{32}$	43,57,71,85,41
5	319	114	-	cyclohexyl derivative	83,41,43,55,82
6	323	91	-	branched alkane deriv.	43,71,57,41,70
7	326	115	240	2,6,10-trimethyltetradecane	43,57,71,41,85
8	329	41	-	alkyl derivative	57,28,41,71,43
9	335	165	-	cyclohexanol derivative	71,43,28,41,82
10	344	1848	226	n-chain alkane $C_{16}H_{34}$	43,57,71,41,85
11	370	700	254	2,6,10-trimethylpentadecane	57,43,71,41,85
12	377	148	-	alkyl derivative	43,57,71,41,85
13	380	78	-	alkyl derivative	57,71,43,56,41
14	397	1940	240	n-chain alkane $C_{17}H_{36}$	43,57,71,85,41
15	402	1987	268	pristane	43,57,71,85,41,
16	420	136	-	alkyl derivative	57,43,71,41,85
17	425	175	-	cyclohexane derivative	83,82,43,41,55
18	429	79	-	alkyl derivative	43,57,71,28,85
19	423	66	-	mix. alkane + alkyl toluene	57,43,71,105,41
20	448	1963	254	n-chain alkane $C_{18}H_{38}$	43,57,71,85,41
21	454	1224	282	phytane	43,57,71,85,41
22	465	218	-	alkyl phthalate	149,57,41,29,28
23	468	43	-	branched alkane	71,43,57,85,32

24	477	150	-	cyclohexyl derivative	83,82,43,41,55
25	482	53	-	mix. alkane + alkyl benzene	57,43,92,91,71
26	496	2159	268	n-chain alkane $C_{19}H_{40}$	43,57,71,85,41
27	509	1093	-	alkyl phthalate	149,29,41,28,57
28	515	55	-	branched alkane	57,43,71,85,41
29	525	132	-	cyclohexyl derivative	43,83,82,28,41
30	541	2009	282	n-chain alkane $C_{20}H_{42}$	43,57,71,85,41
31	570	181	-	cycloalkane/alkane ?	43,57,41,83,28
32	583	1832	296	n-chain alkane $C_{21}H_{44}$	43,57,71,41,85
33	598	161	-	alkyl derivative	28,57,43,71,85
34	611	113	-	cyclohexyl derivative	43,57,41,83,82
35	622	1409	310	n-chain alkane $C_{22}H_{46}$	43,57,71,85,41
36	656	145	-	alkyl derivative	43,57,41,83,82
37	663	924	324	n-chain alkane $C_{23}H_{48}$	43,57,71,41,85
38	698	245	-	alkyl indan/indene	129,57,43,41,55
39	712	544	338	n-chain alkane $C_{24}H_{50}$	43,57,71,85,41
40	734	329	-	alkyl derivative	43,57,71,85,41
41	770	348	352	n-chain alkane $C_{25}H_{52}$	43,57,71,85,41
42	779	84	-	alkyl phthalate	149,41,43,57,70
43	818	198	-	alkyl derivative	43,57,71,85,41
44	842	142	366	n-chain alkane $C_{26}H_{54}$	43,57,71,85,41
45	918	217	-	alkyl derivative	43,57,71,85,28
46	934	80	380	n-chain alkane	43,57,71,85,41

Appendix 1b. GC-MS data from JC chloroform bitumens.

Peak No	Scan No.	Intens	Mol. Wt	Peak Assignment	Principal peaks m/e
1	87	221	156	n-chain alkane $C_{11}H_{24}$	43,57,71,40,85
2	145	383	170	n-chain alkane $C_{12}H_{26}$	68,43,139,57,71
3	154	727	184	2,6-dimethylundecane	41,57,29,68,71
4	179	139	-	alkyl derivative	40,41,43,71,119
5	186	287	142	methylnaphthalene	141,43,115,70,57
6	188	335	198	2,6,10-trimethylundecane	71,57,43,40,29
7	193	304		alkylnaphthalene	141,115,70,131,160
8	202	1019	184	n-chain alkane $C_{13}H_{28}$	57,43,71,41,85
9	213	208		alkyl derivative	57,43,159,119,71
10	223	697	174	ionene	159,174,130,44,116
11	240	234	156	dimethylnaphthalene or iso.	141,156,115,147,69
12	246	532	212	2,6,10-trimethyldodecane	57,71,43,56,85
13	257	1607	198	n-chain alkane $C_{14}H_{30}$	57,43,71,41,85
14	263	106	156	dimethylnaphthalene or iso.	141,156,43,40,56
15	270	117	156	dimethylnaphthalene or iso.	141,156,115,128,63
16	288	117	176	hydroaromatic $C_{13}H_{20}$	71,43,147,161,141
17	291	1070	226	2,6,10-trimethyltridecane	57,43,71,41,85
18	298	294	197	unknown	161,176,155,128,69
19	304	161	176	cycloalkane derivative	56,161,176,29,82
20	306	315	188	unknown	174,69,188,142,158
21	309	2092	212	n-chain alkane $C_{15}H_{32}$	57,43,71,41,85
22	313	176	176	hydrocarbon $C_{13}H_{20}$	69,161,176,71,45
23	327	114	170	trimethylnaphthalene or iso.	155,170,133,85,97
24	337	186	190	mix arom H/C + alkyl deriv.	43,175,57,70,155

25	342	177	240	2,6,10-trimethyltetradecane	43,71,57,161,148
26	357	1519	226	n-chain alkane $C_{16}H_{34}$	57,43,71,41,85
27	364	136	204	$C_{16}H_{12}$ or $C_{15}H_{24}$ H/C	189,204,40,161
28	374	97	190	$C_{14}H_{22}$ H/C	175,147,40,56,29
29	381	928	254	2,6,10-trimethylpentadecane	57,43,71,41,85
30	385	48	-	alkylbenzene/aromatic H/C	169,184,43,91,153
31	390	173	-	alkyl derivative	57,43,71,85
32	398	68	-	alkylbenzene/aromatic H/C	169,184,40,189
33	403	1725	240	n-chain alkane $C_{17}H_{40}$	57,43,71,41,85
34	407	2309	268	pristane	57,71,43,41,85
35	424	153	-	alkyl derivative	43,40,57,71,83
36	428	132	-	alkyl derivative	43,57,71,85,99
37	431	225	-	alkyl derivative	43,57,71,85,99
38	446	515	254	n-chain alkane $C_{18}H_{38}$	57,43,71,41,56
39	452	2312	282	phytane	57,71,43,41,85
40	457	215	-	alkyl phthalate	149,29,57,105
41	459	127	-	alkylbenzene/alkane mix.	43,40,91,128,196
42	469	107	198	$C_{15}H_{18}$ H/C suggested	198,145,40,165
43	493	542	268	n-chain alkane $C_{19}H_{40}$	57,43,71,85,29
44	541	225	282	n-chain alkane $C_{20}H_{42}$	43,57,71,85,41
45	585	220	296	n-chain alkane $C_{21}H_{44}$	43,57,71,85,41
46	626	108	310	n-chain alkane $C_{22}H_{46}$	43,57,71,85,41
47	664	100	324	n-chain alkane $C_{23}H_{48}$	43,57,71,85,41
48	690	127	338	alkyl indene	43,129,57,70,55
49	700	81	352	n-chain alkane $C_{24}H_{50}$	43,57,71,85,41
50	737	83	366	alkyl phthalate + alkane mix.	57,71,85,149

Appendix 1c. GC-MS data from OC chloroform bitumens.

Peak No	Scan No.	Intens	Mol. Wt	Peak Assignment	Principal peaks m/e
1	89	99	-	carboxylic acid or ester	73,88,43,28
2	101	99	-	unknown	
3	143	48	-	unknown	
4	203	78	-	carboxylic acid or ester	73,88,41,32,44
5	210	83	-	carboxylic acid or ester	73,88,44,41,28
6	225	74	-	alkyl derivative	43,41.57,71,45
7	280	101	-	carboxylic acid or ester	73,88,111,83
8	321	33	-	unknown	
9	330	81	198	n-chain alkane $C_{14}H_{30}$	57,43,71,85.41
10	335	66	-	carboxylic acid or ester	73,88,111,97
11	371	69	226	2,6,10-trimethyltridecane	43,57,71,85,41
12	401	81	212	n-chain alkane $C_{15}H_{32}$	57,43,71,85.41
13	437	121	-	carboxylic acid or ester	73,88,111,97
14	440	150	240	2,6,10-trimethyltetradecane	57,43,71,41,85
15	453	165	226	n-chain alkane $C_{16}H_{34}$	57,43,71,85,41
16	480	580	-	alkyl derivative	43,71,85,57
17	485	240	254	2,6,10-trimethylpentadecane	57,43,71,41,85
18	500	110	-	cyclohexyl derivative	82,83,56,67,43
19	510	1907	240	n-chain alkane $C_{17}H_{36}$	57,71,43,85,41
20	514	796	268	pristane	43,57,71,85,41
21	537	281	178	anthracene	178,56
22	563	1824	254	n-chain alkane $C_{18}H_{38}$	57,43,71,85,41
23	567	1211	282	phytane	43,57,71,85,41

24	578	1626	-	alkyl phthalate	149,93
25	600	231	-	alkyl benzene	91,77,57,43,41
26	605	132	-	alkyl methylnaphthalene	155,141,77,56,43
27	613	1244	268	n-chain alkane $C_{19}H_{40}$	57,43,71,85,41
28	628	1144	-	alkyl phthalate	149,77
29	646	663	-	alkyl benzene	91
30	660	962	282	n-chain alkane $C_{20}H_{42}$	57,43,71,85,41
31	683	199	-	polyalkyl naphthalene	155,169,141,77,41
32	704	1161	296	n-chain alkane $C_{21}H_{44}$	57,43,71,85,41
33	728	232	-	cyclohexyl derivative	82,83,56,57,41
34	746	696	310	n-chain alkane $C_{22}H_{46}$	57,43,71,85,41
35	801	1011	324	n-chain alkane $C_{23}H_{48}$	57,43,71,85,41
36	840	530	-	alkyl indane/indene	129,57,43,41,55
37	863	729	338	n-chain alkane $C_{24}H_{50}$	57,43,71,85,41
38	948	945	-	alkyl phthalate	149,77,93
39	952	531	352	n-chain alkane $C_{25}H_{52}$	57,43,71,85,41
40	1036	448	366	n-chain alkane $C_{26}H_{54}$	57,43,71,85,41
41	1163	381	380	n-chain alkane $C_{27}H_{56}$	57,43,71,85,41

Appendix 1d. GC-MS data from CH1 chloroform bitumens.

Peak No	Scan No.	Intens	Mol. Wt	Peak Assignment	Principal peaks m/e
1	2	-	-	solvent	
2	88	4095	79	pyridine	79,52,52,50,39
3	133	261	120	ethylmethyl benzene	105,120,44,77,26
4	145	495	144	unknown	40,84,129,82,61
5	151	479	120	iso-propyl benzene	105,120,77,79,119
6	174	252	158	unknown	39,36,52,51,143
7	180	212	134	dimethylethyl benzene or iso.	115,119,74,134,38
8	193	523	134	As No. 7 or $C_{10}H_{14}$ H/C	39,119,79,101,117
9	211	206	134	As No. 8 + alkyl derivative	29,43,119,41,105
10	221	529	134	As No. 8	29,119,134,129,79
11	232	687	146	methyl tetralin or iso.	131,117,91,115,146
12	238	520	132	methyl dihydro indene	117,132,91,115,119
13	241	1121	134	dimethylethyl benzene	119,134,91,41,65
14	245	208	-	unknown	115,41,101,69,133
15	258	471	128	naphthalene	128,115,52,81,27
16	261	297	146	methyltetralin or iso.	131,101,27,146,41
17	264	591	146	methyltetralin or iso.	131,39,146,129,115
18	269	557	146	methyltetralin or iso.	131,146,27,41,129
19	274	244	-	unknown	27,41,88,73,29
20	283	712	148	polyalkyl benzene $C_{11}H_{16}$	133,148,27,119,105
21	285	1380	170	n-chain alkane $C_{12}H_{26}$	57,43,71,27,39
22	294	1048	139	mix. 2,6-dimethylundecane + ?	67,139,53,27,39
23	300	767	160	dimethyl tetralin	145, 160, 115, 131 ,91

24	302	571	146	methyltetralin/dimethylindan	131, 146, 64, 43, 115
25	309	616	146	methyltetralin/dimethylindan	131, 146, 115, 27, 129
26	315	435	162	pentane, 2-methyl, 2-phenyl	119, 105, 27, 131, 162
27	319	343	160	ethyl tetralin	131, 117, 27, 145, 115
28	325	1215	142	methylnaphthalene	142, 141, 115, 101, 70
29	330	457	198	2,6,10-trimethylundecane	57,43,71,145,41
30	333	2639	142	methyl naphthalene	142,141,115,63
31	344	1261	184	n-chain alkane $C_{13}H_{28}$	57,43,71,41,85
32	348	539	158	hydroxymethylnaphthalene	129,115,130,158,39
33	355	282	160	ethyl tetralin or indan isomer	118,145,160,119,91
34	364	2208	174	lonene	159,174,160,128,131
35	369	113	184	mix. aromatic/hydroaromatic	115,55,105,43,145
36	381	1112	156	ethyl naphthalene	141,156,115,128,69
37	385	860	-	cyclic sulphide or di acid ?	41,101,67,69,55,
38	389	977	212	2,6,10-trimethyldodecane +?	133,88,162,161,29
39	394	1647	156	1,4-dimethyl naphthalene	156,141,155,115,64
40	396	543	162	poly alkyl benzene	162,147,70,76
41	399	1343	198	n-chain alkane $C_{14}H_{30}$	57,43,77,85,29
42	405	890	156	1,8-dimethyl naphthalene	156,141,143,155,115
43	411	504	156	1,2-dimethyl naphthalene	141,156,115,128,101
44	415	495	186	cycloalkane derivative	43,27,69,97,81
45	417	505	204	polyalkyl benzene	119,128,41,164,121
46	422	726	190	trimethylpentyl benzene or iso	133,36,27,134,41
47	429	477	176	dipropylmethylbenzene or iso	161,176,147,143,69.
48	433	2336	226	2,6,10-trimethyltridecane	57,43,71,41,85
49	439	1655	176	di iso propyl methyl benzene or iso.	161,176,155,153,128

Appendix 1e. GC-MS data from CH2 chloroform bitumens.

Peak No	Scan No.	Intens	Mol. Wt	Peak Assignment	Principal peaks m/e
1	48	112	142	n-chain alkane $C_{10}H_{22}$	57,71
2	88	91	156	n-chain alkane $C_{11}H_{24}$	57,71
3	145	222	170	n-chain alkane $C_{12}H_{26}$	57,71
4	154	3692	184	2,6-dimethylundecane	57,43,71,41,56
5	188	2642	198	2,6,10-trimethylundecane	57,71,43,41,56
6	194	48	142	methyl naphthalene	40,142,141,131,69
7	202	98	184	n-chain alkane $C_{13}H_{28}$	57,71
8	210	48	-	alkane or alkene	57,71
9	213	75	-	branched alkane	57,71
10	220	58	180	unknown	81,69,95,109,180
11	223	127	174	lonene	159,43,83,55,174
12	246	3341	212	2,6,10-trimethyldodecane	57,71,43,29,41
13	251	907	-	methyl ketone possibly	58,43,70,56,41
14	257	662	198	n-chain alkane $C_{14}H_{30}$	57,71
15	290	4028	226	2,6,10-trimethyltridecane	71,57,43,41,85
16	309	651	212	n-chain alkane $C_{15}H_{32}$	57,71
17	331	81	-	cyclohexyl derivative	83,55,41,71,67
18	337	1200	240	2,6,10-trimethyltetradecane	57,43,71,85,41
19	342	52	-	alkyl derivative	44,57,71,70,85
20	357	750	226	n-chain alkane $C_{16}H_{34}$	57,71
21	369	124	-	alkyl derivative	57,29,43,71,85
22	381	4043	254	2,6,10-trimethylpentadecane	57,71,43,29,85
23	402	410	240	n-chain alkane $C_{17}H_{36}$	57,71

50	447	1115	188	unknown	173,188,155,115,145
51	450	2911	212	n-chain alkane $C_{15}H_{32}$	57,43,71,41,85
52	459	608	170	trimethyl naphthalene or iso	155,170,69,153,152
53	468	405	170	trimethyl naphthalene or iso	155,170,41,82,67
54	478	631	190	dimethyl dipropyl benzene	175,169,155,190,115
55	484	730	190	trimethyethyl isopropyl benzene	161,190,81,115,128
56	489	752	-	ethyl ester of carboxylic acid	88,43,41,70,101
57	498	1889	226	n-chain alkane $C_{16}H_{34}$	57,43,71,41,85
58	510	464	210	unknown	39,193,210,180,165
59	519	468	218	polyalkyl benzene	133,134,27,189,119
60	523	1220	254	2,6,10-trimethylpentadecane	57,43,71,40,41,29
61	535	703	-	ethyl ester of carboxylic acid	88,101,41,43,29
62	544	3923	240	n-chain alkane $C_{17}H_{36}$	57,43,71,41,85
63	549	3902	268	pristane	71,57,43,41,85
64	572	240	252	unknown	237,43,57,209,252
65	578	375	242	ethyl ester of carboxylic acid	88,101,41,43,29
66	587	1670	254	n-chain alkane $C_{18}H_{38}$	57,43,71,41,85
67	593	3895	282	phytane	71,57,43,85,41
68	600	424	-	phthalate/α ketone	43,58,27,55,41
69	620	450	-	ethyl ester of carboxylic acid	88,101,43,27,55
70	629	1852	268	n-chain alkane $C_{19}H_{40}$	57,71
71	636	1450	248	alkyl phthalate	149,41,27,29,223
72	666	604	-	ethyl ester of carboxylic acid	88,101,43,41,29
73	677	872	282	n-chain alkane $C_{20}H_{42}$	57,71
74	723	1417	296	n-chain alkane $C_{21}H_{44}$	57,71
75	792			alkyl phthalate	149,36,43,57,70,167

24	407	4044	268	pristane	57,71,43,85,41
25	424	465	-	branched alkane	57,71
26	435	479	-	unknown	29,70,111,57,55
27	446	320	254	n-chain alkane $C_{18}H_{38}$	57,71
28	452	4065	282	phytane	71,57,43,85,41
29	458	509	-	unknown	43,59,70,56,57
30	464	50	-	cycloalkyl derivative	57,43,29,55,133,
31	491	410	268	n-chain alkane $C_{19}H_{40}$	57,71
32	535	101	-	branched alkane	57,71
33	540	110	282	n-chain alkane $C_{20}H_{42}$	57,71
34	584	112	296	n-chain alkane $C_{21}H_{44}$	57,71
35	625	60	310	n-chain alkane $C_{22}H_{46}$	57,71
36	663	50	324	n-chain alkane $C_{23}H_{48}$	57,71

References.

1. J.G.Speight. "The chemistry and technology of coal.' (1983). Marcel Dekker Inc.

2. T.F.Yen. 'Structural aspects of organic components in oil shales.' in Oil shale. T.F.Yen and G.V.Chilingarian (Eds). (1976). Elsevier.

3. J.M.Hunt. in: Petroleum geochemistry and geology. (1979) pp 551. Freeman.

4. T.F.Yen. 'Terrestrial and extraterrestrial organic molecules'. in: Chemistry in Space Research. R.F.Landel and A. Rembaum. (Eds). (1972). Am Elsevier. New York. pp 105-152.

5. D.R.Stuart. 'The chemistry of the oil shales ' in: The oil shales of the Lothians Part III. (2nd Ed). (1912). Memoirs of the geological survey, Scotland. pp 143.

6. J.P.Forsmann and J.M Hunt. 'Insoluble organic matter (kerogen) in sedimentary rocks of marine origin'. (1958) in: Habitat of oil. L.G.Weeks (Ed). AAPG pp 747.

7. D.H.Welte. 'Oganischer Kohlenstoff und die entwicklung der photosynthese auf der erde.' Naturwissenschaften. 57. (1970). pp 17-23.

8. R.F.Cane. 'The origin and formation of oil shale.' in: Oil shales. T.F.Yen and G.V.Chiligarian. (Eds). (1976). pp 27-60. Elsevier.

9. J.Bimer, P.H.Given and S.Raj. 'Phenols as chemical fossils in coal.' Prepr. Am. Chem. Soc. Div. Fuel Chem. 22 (1977) pp 169.

10 W.Bergmann. 'Geochemistry of lipids.' in: International series of monographs on earth science. I.A.Breger. (Ed). (1963) Chapter 12 pp503-542. Pergamon Press.

11. J.Krey. 'Die urproduktion des meeres.' in: Erforschung des meeres. G.Dietrich (Ed). (1970). pp 183-195. Umschan, Frankfurt.

12. H.T.Clark and A.Mazur. 'The lipids of diatoms'. J.Biol Chem. 126 (1941) pp 283-289.

13. R.F.Cane. 'The constitution and synthesis of oil shale.' Proc. 7th World Pet. Congress III. (1967). pp 681-689. Elsevier.

14. H.G.Schlegel. 'Allgemeine mikrobiologie Stllgart. Thesis. (1969).

15. R.F.Lee, J.G.Nevenzei and G.A.Pfaffenhafer. 'Wax esters in marine copepods.'

Science 167 (1970). pp1510-1511.

16. B.Tissot and D.H.Welte. (1978). Petroleum formation and occurence. Springer Verlag.

17. M.Schnitzer and S.U.Khan. 'Humic substances in the environment.' (1972). Dekker.

18. P.F.V.Williams. 'Oil shales and their analysis.' Fuel (1983). 62 pp 756-771

19. D.M Fenton, H.Henning and R.L.Ryden. 'The chemistry of shale oil and its refined products.' in: Oil shale, tar sands and related amaterials. H.Stauffer (Ed). Am. Chem. Soc. Symp. Ser. 163. Am Chem Soc. Washington DC. (1981) pp 315.

20. D.Vitorovic. 'Structure elucidation of kerogen by chemical methods.' in: Kerogen. Insoluble organic matter in sedimentary rocks. B.Durand. (Ed). (1980) pp Editions Technip. Paris.

21. C.W.McGowan, R.C.Pearce and H.Diehl. 'A comparison of the dissolution of model compounds and the kerogen of Green River oil shale by oxidation with perchloric acid. Fuel Process Technol. (1985) 10. pp 195-204.

22. J.Solash, D.C.Cronear and T.P.Kobylinski. 'Reduction and phenol acid depolymerisation of Western US oil shale kerogen.' Prepr. Pap .Am. Chem. Soc. Div. Fuel Chem.(1983) 28 . pp 185-265.

23. S.R.Palmer, A.F.Gaines and A.W.P.Jarvie. 'Analysis of the structures of the organic materials in Kimmeridge and Oxford Clays.' Fuel (1987). 66 pp 499-504.

24. S.Brown, T.A.Baillie and A.L.Burlingame. 'Analytical approaches to the investigation of kerogen structures by mass spectrometric techniques.' in: Advances in organic geochemistry 1979.' A.G.Douglas and J.R.Maxwell (Eds). (1980) pp 475-484.

25. A.O.Barakat and T.F.Yen. 'Kerogen structures by stepwise oxidation. Use of sodium dichromate in glacial acetic acid.' Fuel (1987). 66 pp 587.

26. P.H.Given. 'The distribution of hydrogen in coals and its relation to coal structure.' Fuel (1960) 39. pp 147-153.

27. H.W.Sternburg. In: Research in coal technology. The universities role. (1975) CONF - 741091 pp 11-57.

28. T.F.Yen, J.C.Erdman and S.S.Pollock. "Investigation of the structure of petroleum

asphaltenes by X-ray diffraction.' Anal. Chem. (1962). 34. pp 694-700.

29. T.I.Balkas, O.Basturk, A.F.Gaines, I.Salihoglu and A.Yilmaz. 'Comparison of five humic acids.' Fuel (1983) 62 pp373.

30. F.E.Brauns and D.A.Brauns. 'The chemistry of lignin'. (1960) pp616-629. Academic Press.

31. A.L.Burlingame, P.A.Haug, H.K.Schnoes and B.R.Simoneit. 'Fatty acids derived from the Green River formation oil shale by extraction and oxidation. Review.' in: Advances in organic geochemistry 1968. P.A.Schenck and I.Havenar. (Eds). (1969). pp 85-129. Pergamon Press.

32. R.C.Murphy, K.Biemann, M.Djuricic and D.Vitorovic. 'Organic acids obtained by alkaline permanganate oxidation of kerogen from the Green River (Colorado) shale. Geochimica et Cosmochimica Acta (1971) 35 pp 1201-1207.

33. A.Oberlin, J.L.Boulmeir and M.Villey. 'Electron microscopic study of kerogen microtexture. Selected criteria for determining the evolution path and evolution stage of kerogen.' In: Kerogen-The insoluble organic matter from sedimentary rocks. B.Durand (Ed). (1980). pp 191-241. Editions Technip. Paris.

34. J.J.Schmidt-Collerus and C.H.Prien. 'Investigation of the hydrocarbon structure of kerogen from oil shale of the Green River formation.' ACSA Div. Fuel Chem.(1974). 19. pp 100-108.

35. A.L.Burlingame and B.R.Simoneit. 'High resolution mass spectroscopy of Green River formation kerogen oxidation.' Nature (1969). 222. pp 741-747.

36. T.F.Yen. 'A new structural model of oil shale kerogen.' ACS Div. Fuel Chem. (1974). 19. pp 109-114.

37. R.W.Gallois. 'A pilot study of oil shale occurrences in the Kimmeridge Clay.' (1978) Institute of Geological Sciences. Report No. 78/13.

38. B.M.Cox and R.W.Gallois. 'The stratigraphy of the Kimmeridge Clay of the Dorset type area and its correlation with other Kimmeridgeian sequences.' (1980). Institute of Geological Sciences. Report No. 80/4.

39. K.L.Duff. 'Palaeoecology of a bituminous shale: The lower Oxford Clay of central England.' Palaeontology (1975). 18 pp 443-482.

40. S.Holloway. 'Upper Jurassic early Callovian to Middle Oxfordian.' In: Atlas of onshore sedimentary basins in England and Wales. (1985). pp 47-48. Blackie.

41. K.L.Duff. 'Bivalva from the English lower Oxford Clay (Middle Jurassic).' (1978). Palaeontographical Society.

42. A.Hallam. Jurassic Environments. (1975). Cambridge University Press.

43. B.Durand (Ed). 'Kerogen'. (1980). Editions Technip Paris.

44. P.F.V.Williams and A.G.Douglas. 'Organic geochemistry of the British Kimmeridge Clay. 1. Composition of shale oils produced from Kimmeridge sediments.' Fuel (1985). 64 pp 1062-1069.

45. P.F.V.Williams and A.G.Douglas. 'Organic geochemistry of the British Kimmeridge Clay. 2. Acyclic isoprenoid alkanes in Kimmeridge shale oils.' Fuel (1986). 65 pp 1728-1734.

46. P.F.V. Williams. 'Organic geochemistry of the british Kimmeridge Clay 3. The occurrence and distribution of acyclic C-19 alkenes in Kimmeridge Clay shale oil.' Fuel (1987). 66. pp 87-91.

47. P.F.V.William and A.G.Douglas. 'A preliminary organic geochemical investigation of the Kimmeridgian oil shales'. In: Advances in organic geochemistry (1979). A.G.Douglas and J.R.Maxwell (Eds). pp 531-545. Pergamon Press.

48. A.L.Down and G.V.Himus. 'A preliminary study of the chemical constitution of kerogen.' J. Inst. Petroleum (1941).27. pp 426.

49. A.R.Atkins, C.J.R.Fookes, A.Muradian and L.Stephenson. 'Upgrading strategies for Julia Creek shale oil.' Fuel (1987) 66 pp 392-395.

50. T.Noon. 'Oil shale exploration activity in Queensland during 1985/86.' Fuel (1987). 66 pp295-297.

51. C.J.R.Fookes and A.R.Atkins. Proceedings of the second Australian workshop on oil shale, Brisbane. December (1984). pp 245.

52. E.Evans, B.Batts and N.Cant. 'The yield of Australian oil shales as determined by nuclear magnetic resonanace and IR spectroscopy.' Fuel (1987). 66 pp 327-330.

53. J.D.Saxby, D.E.Lambert and K.W.Riley. 'Simulated weathering of oil shales from Rundle, Julia Creek and Green River. Effects on oil yields and kerogen composition.' Fuel (1987). 66 pp 365-368.

54. I.A. Breger. (Ed) 'Origin and classification of naturally occurring carbonaceous

substances'. in: "Organic Geochemistry". (1963) Ch 5. pp 50-86. Pergamon, Oxford.

55. J.P. Forsman. 'Geochemistry of kerogen' in: "Organic Geochemistry". I.A. Breger (Ed) (1963) Ch 5. pp 148-182. Pergamon ,Oxford.

56. W.W. Robinson. 'Isolation procedures for kerogen and associated soluble organic materials'. in: "Organic Geochemistry". G. Eglinton and M.T.J. Murphy. (Eds). (1969), Ch 6. pp 181-195. Springer, Berlin.

57. J.D. Saxby. 'Chemical Separation and Characterisation of Kerogen from Oil Shale'. in: "Oil shale". T.F.Yen (Ed) (1976), pp 103 . Elsevier, Amsterdam.

58. B. Durand (Ed) and G.Nicaise.'Procedures for Kerogen Isolation' in: "Kerogen" (1980), pp 35 . Editions Technip. Paris.

59. R.D. McIver. 'Ultrasonics- A Rapid Method for Removing Soluble Organic Matter From Sediments'. Geochimica et Cosmochimica Acta. (1962), 26 pp 343-345.

60. D.K. Vitorovic and P.A. Pfendt.' Investigation of the kerogen of a Yugoslav (Aleksinac) Oil Shale' Proceedinds 7th World Petroleum Congress. (1967), 3 pp 691-694.

61. W.R. Thompson and C.H. Prien.'Thermal extraction and solution of oil-shale kerogen.' Industrial and Engineering Chemistry, (1958), 50 pp 359-364.

62. B. Durand, G. Nicaise, J. Roucache, M. Vandenbroucke and H.W. Hagemann, in: "Advances in Organic Geochemistry". R. Campos and J. Coni (Eds). (1975) Enadimsa, Madrid. pp 601 .

63. D.W. vanKrevelen, in: "Coal". (1961) pp514. Elsevier, Amsterdam.

64. B. Durand and J.C. Monin. Elemental analysis of kerogens in: "Kerogen" (Ed) B.Durand. (1980) pp 113- . Editions Technip. Paris.

65. J. Brooks. 'Petroleum geochemistry and fossil fuel exploration'. Chemistry in Britain. (1983). pp 390.

66. J.K. Brown.' The infra-red spectra of coal'. J. Chem. Soc. (1955) pp 744 and 752.

67. R.A. Friedel. in: "Applied Infrared Spectroscopy". D.N. Kendall (Ed). (1966), pp 312. Reinhold.

68. R.A. Friedel and G.L. Carlso. 'Difficult carbonaceous materials and their infra-red and Raman spectra. Reassignment for coal spectra'. Fuel. (1972), 51, pp 194.

69. P.L. Robin, P.G. Rouxhet. 'Contribution of molecular water in the infrared spectra of kerogens and coals.' Fuel (1976) 55 pp 177-83.

70. M. Schnitzer and S.U.Khan. "Humic Substances in the Environment". (1972), Marcel Decker.

71. J.G. Speight. 'Apllication of spectroscopic techniques to the structural analysis of coal and petroleum.' Applied Spectroscopy Reviews. (1971), 5, pp 211-264 .

72. M. Avram and G. Mateescu. "Infrared Spectrscopy". (1972). Wiley.

73. L.J. Bellamy. "Advances in Infrared Group frequencies". (1968). Chapman and Hall.

74. L.J. Bellamy. "The Infrared Spectra of Complex Molecules" (1958 and 1975) . 2nd + 3rd editions. Chapman and Hall.

75. H.N.S. Schafer.' Factors affecting the equilibrium moisture contents of low rank coals.' Fuel. (1972), 51 pp 4.

76. P.L. Robin and P.G. Rouxhet. 'Contribution of different chemical functions in the 1710, 1630 and 3420cm^{-1} infrared absorption bands of kerogens.' Rev. Inst. Franc du Petrole. (1976) XXXI pp 955.

77. H.S.Rao, P.L.Gupta, F.Kaiser and A. Lahiri.' The assignment of the 1600 cm^{-1} band in the infra-red spectra of coals.' Fuel. (1962), 41 pp 417.

78. Y.Osawa, H. Sugimura and S. Fuji. 'The infra-red spectra of Japanese coals. The absorption bands at 3030, 2920 and 1600 cm^{-1}.' Fuel(1970) 49 pp 68.

79. P.C.Painter, R.W.Snyder, M.Stansinic, M.M.Coleman, D.W.Kuehn and A. Davis.'Concerning the application of FT-IR to the study of coal. A practical assessment of band assignments and the application of spectral analysis programs'. Applied Spectrroscopy. (1981), 35 pp 475 .

80. P.L. Robin. and P.G. Rouxhet.' Characterisation of kerogens and study of their evolution by infra-red spectroscopy: Carbonyl and carboxyl groups.' Geochimica et Cosmochimica Acta. (1978). 42 pp 1341.

81. L. Petrakis and J.P.Fraissard (Eds) in: Magnetic Resources Introduction.

Advanced Topics and Application to Fossil Energy (1984). NATO ASI Series C, Vol 124.

82. R.M. Davidson in: Nuclear Magnetic Studies of Coal. (1986) IEA Coal Research. London.

83. I.V.Aleksandrov. 'The theory of nuclear magnetic resonanace.' (1966). Academic Press.

84. J.A.Pople, W.G.Schneider and H.J.Berstein. 'High resolution nuclear magnetic resonance.' (1959). McGraw-Hill.

85. H.D. Schultz. (Ed). 'Analysis of Coal-Tar Pitch Oils' in: Coal Liquefaction Products, Vol 1. (1983) pp 139-166. John Wiley and Sons.

86. A.A. Herod, W.R. Ladner, C.E. Snape.' Structural studies of coal extracts.' Philisophical Transactions of the Royal Society of London. (1981) Series A.

87. P.J. Collin, R.J. Tyler, M.A. Wilson. 'Structural characterisation of coal tars derived by flash pyrolysis'. In: Coal Liquefaction products Vol 1. H.D.Schultz (Ed). (1983). John Wiley and Sons.

88. C.E. Snape, K.D. Bartle. 'Application of silylation to the characterisation of benzene-insoluble coal extract fractions.'(1979). Fuel. 58 pp 898-900.

89. D.L. Vanderhart and H.L. Retcofsky .'Estimation of coal aromaticities by proton-decoupled carbon-13 magnetic resonance spectra of whole coals'. Fuel.(1976) 55 pp 202-204.

90. V.J. Bartuska, G.E. Maciel, J. Schaefer and E.V. Stejskal.' Prospects for carbon - 13 nuclear magnetic resonance analysis of solid fossil fuel materials.'Fuel. (1977). 56 pp 354.

91. H.A.Resing, A.N. Garrowary and R.N. Hazlett . 'Determination of aromatic hydrocarbon fractions of oil shales by ^{13}C NMR with MAS.' Fuel.(1978) 57 pp 450-454.

92. G.E. Maciel, V.J. Bartuska and F.P. Miknis .'Correlation between oil yields of oil shales and ^{13}C nuclear magnetic resonance spectra.'.' Fuel.(1978) 57 pp 505-506.

93. F.P. Miknis, M.J. Sullivan, V.J. Bartuska, and G.E. Maciel. ' Cross polarisation magic angle spinning carbon 13 NMR spectra of coals of varying rank.' Organic Geochemistry.(1981). 3 pp19-28.

94. N.J. Russell, M.A. Wilson, R.J.Pugmire and D.M. Grant. 'Preliminary studies on the aromaticity of Australian coal: solid state NMR techniques.'. Fuel.(1983) 62 pp 601-605.

95. R.H. Newman, S.J. Davenport, R.H. Meinhold .' An assessment of carbom 13 solid state NMR spectroscopy for the characterisation of New Zealand Coals'. DSIR-CD-2346. Lower Hutt. New Zealand. Department of Scientific and Industrial Research. (1984).58pp.

96. B.G. Gerstein. 'Coal Aromaticity' In: Magnetic Resonance. Introduction to Advanced Topics and Application to Fossil Energy. L.Petrakis and J.P. Fraissard (Eds). (1984). NATO ASI Series C Vol. 124.

97. F.P. Miknis, G.E. Maciel and V.J. Bartuska. 'Characterisation of organic material in coal by proton-decoupled carbon 13 nuclear magnetic resonance with MAS.' Organic Geochemistry. (1979). 1. pp 169.

98. D. Vucelic, N.Juranic and D.Vitorovic. 'Potential of proton enhanced ^{13}C NMR for the classification of kerogens.' Fuel. (1979). 58 pp759.

99. F.P. Mlknis, D.A. Netzel, J.W.Smith, M.A. Mast and G.E. Maciel. '^{13}C NMR measurement of the genetic potential of oil shales.' Geochimica et Cosmochimica Acta. (1982). 46 pp 977-984.

100. K.W. Zilm, R.J. Pugmire, S.R. Larter, J. Allan and D.M. Grant 'Carbon 13 CP/MAS spectroscopy of coal macerals.' Fuel. (1981) 60 pp 717-722.

101. R.J.Pugmire, K.W. Zilm, D.M. Grant, S.R. Larters, J. Allen, J.T. Senftle, A. Davis and W. Spackman. 'Carbon 13 CP/MAS study of coal macerals of varying rank.' (1981) ACS Symposium Series (169). pp 23-42.

102. G.E.Maciel, M.J.Sullivan, L. Petrakis and D.W. Grundy. '^{13}C nuclear magnetic resonance characterisation of coal macerals by magic-angle spinning.' (1982). Fuel. 61 pp 411-414.

103. R.E. Winans and J.C. Crelling (Eds). In: Chemistry and Characterisation of Coal Macerals. (1984). ACS Symposium Series 252. American Chemical Society.

104. A. Marzec.' Molecular structure of coal investigated by solvent extraction, mass spectroscopy and pulse nuclear magnetic resonance.' (1981). In: Proceedings of the International Conference on Coal Science. Dusseldorf FRG. 7-9 Sept (1981) Essen FRG. pp 98-103. Verlag Glueckauf.

105. A. Jurkiewicz, A. Marzec and S. Idziak 'Immobile and mobile phases of

bituminous coal detectable by pulse nuclear magnetic resonance and their chemical nature.'. Fuel (1981) 60 pp1167-1168.

106. M.A. Wilson, R.J. Pugmire, J. Karas, L.B. Alemany, W.r. Woolfenden, D.M. Grant amd P.H. Given. Carbon distribution in coals and coal macerals by cross-polarisation/magic angle spinning carbon-13 nuclear magnetic resonance spectroscopy.'. Analytical Chemistry. (1984) 56 pp 933-943.

107. M.J. Sullivan, G.E. Maciel. 'Spin dynamics in the carbon-13 nuclear magnetic resonance spectrometric analysis of coal by cross-polarisation and magic angle spinning.', Analytical Chemistry. (1982) 54 pp1615-1623.

108. P.G. Hatcher, I.A. Breger, G.E. Maciel and N.M. Szeverenyi. ' Chemical structures in coal: geochemical evidence for the presence of mixed structural components.'(1983). In: proceedings of the 1983 International Conference on Coal Science. Pittsburg PA. USA. pp 310-313.

109. R.M. Davidson (1980).'Molecular Structure of Coal.' ICTIS/TR08, London UK. IEA Coal Research. 86pp.

110. D.E. Wemmer, A. Pines, D.D. Whitehurst.'^{13}C NMR studies of coal and coal extracts.' (1981). Philosophical Transactions of the Royal Society of London, Series A :300 (1453);pp 15-41.

111. R.L. Dudley and C.A .Fyfe.' Evaluation of the quantitative reliability of the ^{13}C CP/MAS technique for the analysis of coals and related materials'. Fuel (1982) 61 pp 651-657.

112. W.Jennings. 'Gas chromatography with glass capillary columns.' 2nd Ed. (1980). Academic Press.

113. W.H.McFadden. 'Techniques of combined gas chromatography mass spectroscopy.' (1973) J.Wiley.

114. B.G. Rohrback. 'Crude oil geochemistry of the Gulf of Suez.' Advances in Organic Geochemistry. M.Bjoroy (Ed) (1981). pp39-48. Wiley.

115. M. Bjoroy, P.W.Brooks and K. Hall .'An oil/oil correlation study utilizing high resolution GC-MS.' In: Advances in Organic Geochemistry. M. Bjoroy (Ed) (1981), pp 87-93. Wiley.

116. M. Bjoroy, A. Monk, J.O. Vigram. 'Organic geochemical studies of the Devonian to Triassic succession on Bjornoya and the implications for the Barent Shelf.'In: Advances in Organic Geochemistry. M. Bjoroy (Ed). (1981). pp 49-59. Wiley.

117. D.M. McKirdy, A.K.Aldridge, P.J.M. Ypma. 'A geochemical comparison of some crude oils from pre-Ordovician carbonate rocks.' In: Advances in Organic Geochemistry. M. Bjoroy. (Ed). (1981). pp 99-107. Wiley.

118. G. vanGraas, T.C. Viets, J.W. deLeear and P.A. Schenck. 'Origins of the organic matter in a Cretaceous black shale deposit in the central Apennines (Italy).' Advances in Organic Geochemistry. M.Bjoroy.(Ed). (1981). pp 471-476. Wiley.

119. J. Allan and S.R. Larter. 'Aromatic structures in coal maceral extracts and kerogens.' Advances in Oganic Geochemistry. M.Bjoroy. (Ed). (1981). pp 534-545. Wiley.

120. P.F.V. Williams and A.G. Douglas. 'The effects of lithologic variation on organic geochemistry in the Kimmeridge Clay of Britain.' Advances in organic Geochemistry. M.Bjoroy. (Ed). (1981). pp 568-575. Wiley.

121. C.E. Rovere, P.T. Crisp, J. Ellis and P.D. Bolton. 'Chemical characterisation of shale oil from Condor, Australia.' Fuel (1983). 62 pp 1274-1281.

122. A. Ambles, M.V. Djuric, L. Djoidjevic and D. Vitorovic. 'Nature of kerogen from the Green River shale based on the character of the products of a forty-step alkaline permanganate oxidation.' In `Advances in Organic Geochemistry. M.Bjoroy. (Ed) (1981). pp. Wiley.

123. D. Vitorovic, A. Ambles and M. Djoidjevic. 'Relationships between kerogens of various structural types and the products of their multi-step oxidative degradation.' Advances in Organic Geochemistry. E.W.Baker. (Ed). (1983). pp 333-342.

124. J.H.Beynon, R.A.Saunders and A.E.Williams. 'The mass spectra of organic molecules.' (1968). Elsevier. Amsterdam.

125. R.P.Philp. 'Fossil Fuel Biomarkers' (1985). Elsevier. Amsterdam.

126. R.P.Philp. 'Geochemistry in the search for oil.' Chemical and Engineering News. (1986), pp28-43.

127. G.H. Draffan, R.N.Stillwell, J.A.McCloskey. Organic Mass Spectroscopy. (1968). Vol 1 pp 669-685.

128. F.T.Gillan, R.B.Johns, T.V.Verheyen and P.D.Nichols. 'Monounsaturated fatty acids as specific bacterial markers in marine sediments.' Advances In Organic Geochemistry. M. Bjoroy (Ed). (1981) pp 198-206. Wiley.

129. J.F. Johnson and R.S.Porter. Analytical GPC. (1968). Wiley New York.

130. H. Determan. Gel Permeation Chromatography. (1968). Springer Verlag. New York.

131. D.S.Big. Physical Methods in Macromolecular Chemistry. B.Carroll (Ed).Vol 2. (1972). Dekker. New York.

132. N.Evans, T.M. Haley, M.J.Mulligan and K.M. Thomas. 'An Investigation of the use of Size Exclusion Chromatography for the Determination of Molar Mass Distributions and fractionation of coal tars.' Fuel (1986). 65 pp 694-703.

133. B.S.Ignasiak, S.K.Chakrabartty and N. Berkowitz. 'Molecular weights of solubilised coal products' Fuel (1978). 57 pp 507-508.

134. K.D.Bartle, M.J.Mulligan, N. Taylor, T.G. Martin and C.E.Snape. 'Molecular mass calibration in size exclusion chromatography of coal derivatives.' Fuel (1984). 63 pp 1556.

135. M.G.Strachan and R.B. Johns.'Determination of Molecular weights of Coal Derived Liquids by Gel Permeation Chromatography- High-Performance Liquid Chromatography. J. Chromatography. (1985). pp 65-80.

136. K.D. Bartle, G. Collin, J.W.Stadelhofer and M.J.Zander. 'Recent advances in the analysis of coal derived products.' J Chem .Tech. Biotechnol. (1979).29. pp 531-551.

137. R.B. Meiris. 'Gel-permeation for analysis of tarbitumens mixtures.' Chem. Ind. (London). (1973). 642 pp11.

138. D.L.Wooton, W.M.Coleman. L.T.Taylor and H.C.Dorn. 'Characterisation of organic fractions in solvent refined coal by quantitative NMR spectra.' Fuel (1976). 57. pp17.

139. C.Cockram and R.V.Wheeler. 'Composition of coal- resolution of coal by extraction.' J.Chem Soc (1927) 119. pp700.

140. T.G.Squires, C.G.Venier, J.D.Hunt, J.C.Shei and B.F.Smith. 'Supercritical solvents. Carbon dioxide extraction of retained pyridine from pyridine extracts of coal.' Fuel (1982). 61. pp1170-1172.

141. I.Schwager, P.A.Farnanian and T.F.Yen. 'Structural characterisation of solvent fractions from five major coal liquids by proton magnetic resonance.' In:

Analytical chemistry of liquid fuel sources: tar sands, oil shale, coal and petroleum. Advances in chemistry series 170. (1978). pp 66-77.

142. G.C.Levy. 'Topics in carbon 13 NMR spectroscopy.' (1979). Wiley.

143. D.A.Netzel, D.R.McKay, R.A.Heppner, F.D.Guffey, S.D.Cooke, D.L.Varie and D.E Linn. '^{1}H and ^{13}C NMR studies on naptha and light distillate saturate hydrocarbon fractions obtained from in situ shale oil.' Fuel (1981) 60. pp 307-319

144 J.K.Brown and W.R.Ladner. 'A study of the hydrogen distribution in coal like materials by high resolution nuclear magnetic resonance spectroscopy. A comparison with infra red measurement and the conversion to carbon structure.' Fuel (1960) 39. pp 87-96.

145. P.Farrimond, P.Comet, G.Eglinton, R.P.Evershed, M.A.Hall, D.W.Park and A.M.K.Wardroper. 'Organic geochemical study of the Upper Kimmeridge Clay of the Dorset type area.' Marine and petroleum geology (1984) 1. pp 340-354.

146. E.E.Bray and E.D.Evans. 'Distribution of n-alkanes as a clue to recognition of source beds.' Geochimica et Cosmochimica Acta. (1961). 22. pp 2-22.

147. M.Blumer, R.R.L.Guillard and T.Chase. 'Hydrocarbons of marine phyto-plankton.' Marine Biology. (1971) pp 183.

148. E.Gelpi, H.Schneider, J.Mann and T.Oro. 'Hydrocarbons of geochemical significance in microscopic algea.' Phytochemistry. (1970). 9. pp 603-612.

149. W.H.Youngblood and M.Blumer. 'Alkanes and alkenes in marine benthic algea.' Marine biology. (1973). 21. pp 163.

150. W.H.Youngblood, M.Blumer, R.R.L.Guillard and F.Fiorc. 'Saturated and unsaturated hydrocarbons in marine benthic algea.' Marine biology (1971). 8. pp 190.

151. G.Eglinton and R.J.Hamilton. 'The distribution of alkanes.' In: Chemical plant taxonomy. T.Swain. (Ed). (1963). pp 187-205. Academic press.

152. A.B.Caldicott and G.Eglinton. 'Surface waxes.' In: Phytochemistry 3. Inorganic elements and special groups of chemicals. L.P.Miller. (Ed). (1973). pp 162. Van Nostrand Reinhold.

153. D.Corrigan, C.Loos, S.S.O'Cconnor and R.F.Tomoney. 'Alkanes from four species of sphagnum moss.' Phytochemistry. (1973). 12. pp 213-214.

154. R.I.Morrison and W.Bick. 'The wax fraction of soils; separation and determination of some components.' J. Science Food Agriculture. (1967). 18. pp 352-355.

155. J.R.Maxwell, R.E.Cox, R.G.Ackman and S.N.Hooper. 'The diagenesis and maturation of phytol. The stereochemistry of 2,6,10,14-tetramethylpentadecane from an ancient sediment.' In: Advances in organic geochemistry (1971). H.R.von Caertner and H.Wehner. (Eds). (1972). pp 177-291. Pergamon Press.

156. G.Deroo, B.Tissot, R.G.McCrossan and F.Der. 'Geochemistry of heavy oils of Alberta.' In: Oil sands. Fuel of the future. Memoir 3. Can. Soc. Pet. Geol. (1974). pp148-167 and pp184-189.

157. J.Connan, K.LeTran and B.van der Weide. 'Alteration of petroleum in reservoirs.' Proc. 9th World Pet. Congr. Tokyo. London. Applied Science Publications. (1975). 2. pp 171-178.

158. T.Powell and D.M.McKirdy. 'Relationship between ratio of pristane to phytane, crude oil composition and geological environments in Australia.' Nature (1973). 203. pp 37-39.

159. C.N.R.Rao. 'Ultraviolet and visible spectroscopy chemical applications.' 3rd Ed. (1985). Butterworth.

160 A.G.Sharkey and J.T.McCatney. 'Physical properties of coal.' In: Chemistry and utilisation of coal. 2nd supplementarty volume . M.A.Elliot (Ed). (1981) Chapter 4 . Section 4.15. pp261-164. Wiley.

161. A.Ekstrom, H.Loeh and L.Dale. 'Petroporphyrins found in oil shale from the Julia Creek deposit of the Toolebuc Formation.' In: Geochemistry and chemistry of oil shales. F.P.Miknis and J.F.McKay. (Eds). (1983) ACS Symposium series 230. pp 411-422.

162. G.E.Maciel. 'Line broadening influences and line narrowing techniques in solid state NMR.' In: Magnetic resonance-Introduction, advanced topics and application to fossil energy. L.Petrakis and J.P.Fraissoid. (Eds). (1984). NATO ASI Series C Vol 124 pp 71-110. Dordrecht. the Netherlands, D. Reidel.

163. R.Gerhards and I.Kasueschke. 'Qualitative aspects of solid state NMR spectrosopy for the analysis of coal and coal products.' In: Proceedings international conference on coal science (1985). Sydney NSW. Australia. pp 838-841. Pergamon Press.

164. R.E.Botto and R.E.Winans. 'Characterisation of whole coals by ^{13}C CP/MAS spectroscopy at high field.' Fuel (1983) 62. pp 271-273.

165. T.E.Dancy and V.Giedroyc. 'Further investigation of the chemical constitution of the kerogen of oil shales.' J.Inst.Petroleum. (1950). 36. pp 593.

166. A.L.Down. 'Analysis of the kerogen of oil shales.' J.Inst. Petroleum. (1939). 25 pp 813.

167. L.Reggel, R.Raymond, I.Wender and B.D.Blaustein. 'Preparation of ash free pyrite free coal by mild chemical treatment.' Abstracts 164th Nat. Meet Am.Chem Soc. Fuel division. (1972). pp 10.

168. J.W.Hamersma, M.L.Kraft, E.P.Koutsoukos and R.A.Meyers. 'Chemical removal of pyritic sulphur from coal.' Abstracts of the 164th Nat. Meet. Am. Chem. Soc. Fuel Division. (1972). pp16.

169. J.P.Forsman and J.M.Hunt. 'Insoluble organic matter (kerogen) in sedimentary rocks of marine origin.' In: Habitat of oil. (1958). pp747-778.

170. D.L.Lawlor, J.I.Fester and W.E.Robinson. 'Pyrite removal from oil shale concentrates using $LiAlH_4$.' Fuel (1963). 42 pp 239-244.

171. J.D.Saxby. 'Isolation of kerogen in sediments by chemical methods.' Chemical geology. (1970). 6 pp173-184.

172. R.D.McIver. 'Composition of kerogen - clue to its role in the origin of petroleum.' Proc. 7th world pet. cong. (1967) 2 pp25-36.

173. D.G.Jones and J.J.Dickert. 'Composition and reactions of oil shale of the Green River formation.' Chem. Eng. Progr. Symp. Ser. (1965). 61 pp 33-41.

174. I.P.Fedina and A.I.Danyusherskaya. 'Extraction of pyrite from residual organic matter (kerogen) in sedimentary rocks.' Nov. Metody. Issled. Osad. Porod. Tseliyu. Poiskov. Blagopriyatnykh. Neffe-Gazoobrazovaniu. Usoviy. (1971). pp37-43.

175. J.Solash, D.C.Croneour and T.P.Kobylinski. 'Reduction and phenol acid depolymerisation of western US oil shale kerogen.' Prep. Pap. Am. Chem. Soc. Div. Fuel Chem. (1983). 28 pp 158-165.

176 L.M.Stock. 'The reductive alkylation reaction.' In: Coal Science 1. M.L.Gorbaty, L.W.Larsen and I.Wender. (Eds). (1982). pp 161-279. Academic Press.

177. A.B.Hubbard and J.I.Fester. 'A hydrogenolysis study of the kerogen in Colorado oil shales.' US Bur. Mines. Rep. Inest. 5458. (1969).

178. T.C.Hoering. 'The organic geochemistry of precambrian rocks.' In: Reseaches in geochemistry. 2nd Ed. (1967). P.H.Abelson (Ed). Wiley.

179. A.Y.Aarna and E.T.Lippmaa. 'Cleavage of ether bonds in kerogens from Estonian oil shale.' Zhur. Priklad. Khim. (1957). 30. pp312-315.

180. M.V.Cheshire, P.A.Cranwell, C.P.Falshaw, A.J.Floyd and R.D.Haworth. 'Humic acids II - structure of humic acids.' Tetrahedron (1967). 23 pp 1669.

181 N.A.Burges, H.M.Hurst and B.Walkden. 'The phenolic constituents of humic acids and their relation to the lignin of the plant cover.' Geochimica et Cosmochimica Acta. (1964). 28 pp 1547.

182. A.Al-Ahmadi. 'Structural analysis of humic acids.' (1986) PhD Thesis University of Aston in Birmingham . England.

183. L.F.Fieser and M.Fieser. Reagents for organic synthesis. (1967) pp 581-595 Wiley.

184. A.Combaz. 'Les kerogenes vus au microscope.' In: Kerogen (1980). B.Durand (Ed). pp55-112. Editions Technip.

185. Love.L.G. and G.G.Amstutz. 'Framboidal pyrite in two andesites.' Fortschr Mineral (1966). 43 pp 273.

186. G.H.Draffan, R.N.Stillwell and J.A.McCloskey. 'Electron impact induced rearrangement of trimethyl silyl groups in long chain compounds.' Organic mass spectroscopy. (1968). 1. pp 669-685.

187. A.Streitwieser and C.H.Heathcock. 'Introduction to organic chemistry.' 2nd Ed. (1981). pp 699. Collier Macmillan.

188 C.Kroeger and H.A.W.deVries. 'Alkylation of lignite.' Ann. (1962) 625 pp 35.

189 C.Kroeger, J.G.Rabe and B.Rabe. 'Alkylation of bituminous coal.' Erdoel Kohle. Erdgas. Petrochem. (1963). 16 pp 21.

190 J.Solash, D.C.Cronauer and T.P.Kobylinski. 'Reduction and phenol acid depolymerisation of Western US oil shale kerogen.' Prepr. Pap. Am. Chem. Soc. Div. Fuel Chem. (1983) pp158.

191 L.A.Heredy and M.B.Neuworth. 'Low temperature depolymerisation of bituminous coal.' Fuel (1962). 41 pp 221.

192 R.M.Roberts and K.M.Sweeney. 'Aluminium bromide catalysed transalkylations of a Texan lignite coal.' Fuel (1985). 64 pp 321.

193. R.A.Flores, M.A.Geigel and F.R.Mayo. 'Hydrogen fluoride catalysed alkylations of Pittsburg seam Chvb coal.' Fuel (1978). 57 pp697.

194. L.Reggel, R.Raymond, S.Friedman, R.A.Friedel and I.Wender. 'Reduction of coal by lithium ethylenediamine.' Fuel (1958) 37 pp 126.

195. H.W.Sternburg. 'Solubiliisation of an lvb coal by reductive alkylation.' Fuel (1971). 50 pp 432.

196. J.Solash and D.C.Cronauer. 'Reduction of eastern US oil shale kerogen using dissolving metals.' Symp. Pap. Synth Fuels. Oil Shale. Tar Sands (1983) pp 267-78.

197. H.W.Sternburg and C.L.DelleDonne. 'Solubilisation of coals by reductive alkylation.' Fuel (1974) 53 pp 172.

198. C.G.Screttas. ' Stoichiometry and synthetic utility of the reaction of alkyl halides with lithium dihydronaphthylide.' J.Chem. Soc. Chem. Commun. (1972). pp 869-870.

199. H.O.House and V.Kramar, 'The chemistry of carbanions 1. The reaction of triphenylmethane with potassium.' J. Organic Chemistry. (1962). 27 pp 4146.

200. L.B.Erbert. 'Reductive alkylation of aromatic hydrocarbons.' Fuel (1986). 65 pp 144-145.

201. B.S.Ignasiak, S.K.Chakrabartty and N.Berkowitz. 'Molecular weights of solubilised coal products.' Fuel (1978) 57 pp 507-511.

202. J.W.Larsen and L.O.Urban. 'Incorporation of naphthalene and THF during the reductive alkylation of Illinois No. 6 coal.' J.Organic Chemistry. (1979). 44 pp 3219.

203. D.Carson and B.S.Ignasiak. 'Evolution of hydrogen alkylation of coal.' Fuel (1979). 58 pp72.

204. S.Friedman, M.L.Kaufman, W.A Steinger and I.Wender. 'Determination of hydroxyl content of vitrains by formation of trmethylsilyl ethers.' Fuel (1961). 40 pp 33.

205. L.Blom, L.Edelhausen and D.W.VanKrevelen. 'Chemical structure and properties of coal XVIII- Oxygen groups in coal and related products.' Fuel (1957) 36 pp

135.

206. G.C.Briggs and G.J.Lawson. 'Chemical constitution of coal: 16. Methylation studies on humic acids.' Fuel (1970) 49 pp 39.

207. R.Liotta. 'Selective alkylation of acidic hydroxyl groups in coal.' Fuel (1978) 58 pp 724.

208. I.Mochida, T.Shimohura, Y.Korai and H.Fijitsu. 'Carbonisation of coals to produce anisotropic cokes.' Fuel (1984). 63 pp 849.

209. T.R.Gouker and R.Liotta. 'Caustic oxidation as a pretreatment to high pressure bituminous coal gasification.' Fuel (1985). 64 pp200.

210. D.Brenner. 'The macromolecular nature of bituminous coal.' Fuel (1985). 64 pp 167.

211. J.W.Larsen, T.K.Green and J.Kovac. 'The nature of the macromolecular network structure of bituminous coals.' J. Organic Chemistry. (1986). 50 pp 4729.

212. G.W.Gokel and W.P.Weber. 'Phase transfer catalysts. Part 1. general principles: Part 2. Synthetic applications.' J. Chemical Education. (1978). 55 pp350 and 429.

213. W.P.Weber and G.W.Gokel. Phase transfer catalysis in organic synthesis. (1977). Springer-Verlag Berlin.

214. C.M.Starks and C.Liotta. Phase transfer catalysis. Principles and techniques. (1978). Academic Press.

215. R.Liotta, K.Rose and E.Hippo. 'O-alkylation of coal and its implications for the chemical and physical structure of coal.' J.Organic Chemistry. (1981). 46 pp 271.

216. M.G.Matturo, R.Liotta and J.J.Isaacs. 'Coal swelling and neutralisation. Reactions within a three dimensional organic matrix.' J. Organic Chemistry. (1985). 50. pp 5560.

217. R.Liotta and G.Brons. 'Coal. Kinetics of O-alkylation.' J. American Chemical Society. (1981) 103 pp 1735.

218. N.Mallya and L.M.Stock. 'The alkylation of high rank coals. Non-covalent bonding interaction.' Fuel (1986) 65 pp 736.

219. F.Cassani and G.Eglinton. 'Organic geochemistry of Venezuelan Extra-heavy oils.' Chemical Geology. (1986). 56 pp 167.

220. M.Ettinger, R.Nardin, S.R.Mahassay and L.M.Stock. 'An investigation of the O and C alkylation of coal.' J.Organic Chemistry. (1986). 51 pp 2841.

221. S.Burke. 'The use of phase transfer catayst in the characterisation of coal.' Thesis in preparation. University of Aston in Birmingham England (1988).

222. A.R.Katritzky and N.A.Coats. 'Infrared absorption of substituents in aromatic systems. Part 1 Methoxy and ethoxy compounds.' J.Chemical Society. (1959) pp 2062.

223. L.J.Bellamy. The infrared spectra of complex molecules. (1962). pp 179. J.Wiley.

224. R.Hayatsu, R.G.Scott and R.E.Winans. 'Oxidation of coal'. In: Oxidation in organic chemistry. W.S.Trahonovsky (Ed) Part D. (1982). Academic Press.

225. D.Vitorovic. 'Structure elucidation of kerogen by chemical methods.' In: Kerogen Chapter 10. B.Durand (Ed). (1980). pp 301-338. Editions Technip.

226. W.A.Bone, L.Horton, S.G.Ward. 'Chemistry of coal (VI) its benzenoid constitution shown by its oxidation with alkaline permanganate.' (1930). Proc. Roy. Soc. London. 127 A. PP 480.

227. W.A.Bone, L.G.B.Parsons, R.H.Sapiro and C.M.Groocock. 'Chemistry of coal (VIII) benzenoid constitution in the lignite-peat-coal series.' (1935). Proc. Roy. Soc. London. 148 A pp492.

228. P.Kogerman. "Oil shale and Cannel coal". In: Proceedings of the conference. Scotland (1938). Published by the Institute of petroleum London. pp115.

229. R.B.Randall, M.Benger and C.M.Groocock. 'Alkaline potassium permanganate oxidation of organic substances selected for their bearing on the chemical constitution of coal.' (1938). Proc. Roy. Soc. London. 165 A pp 432.

230. W.E.Robinson, D.L.Lawlor, J.J.Cummins and J.I.Fester. 'Oxidation of a Colorado oil shale.' (1963) U.S. Bureau of mines rep. Invest 6166.

231. W.E.Robinson, H.H.Heady and A.B.Hubbard. 'Alkaline permanganate oxidation of oil shale kerogen.' Ind. Chem. Eng. (1953). 45. pp 788.

232. M.V.Djuricic, R.C.Murphy, D.Vitorovic and K.Biemann. 'Organic acids obtained by alkaline potassium permanganate oxidation of kerogen from the Green River

(Colorado) shale.' Geochimica et Cosmochimica Acta. (1971). 35. pp 1201.

233. M.V.Djuricic, D.Vitorovic, B.D.Andresen and H.S.Hertz. 'Acids obtained by oxidation of kerogens of ancient sediments of different geographic origin.' In: Advances in organic geochemistry. (1972). H.R.vonGaertner. (Ed). pp 305. Pergamon Press.

234. N.C.Deno, B.A.Greigger and S.G.Stroud. 'The aliphatic structure of coal.' Preprint No.23 (2). Div. of Fuel Chem. Am. Chem. Soc. (1978).

235 N.C.Deno, B.A.Greigger and S.G.Stroud. 'New method for elucidating the structures of coal.' Fuel (1978). 57. pp 455.

236. N.C.Deno, B.A.Greigger, A.D.Jones, W.G.Rakitsky, K.A.Smith and R.D.Minard. 'Chemical structure of Wyodak coal.' Fuel (1980). 59. pp 699.

237. N.C.Deno, B.A.Greigger, A.D.Jones, W.G.Rakitsky, D.D.Whitehurst and T.O Mitchell. 'Structural changes occurring in coal liquifraction.' Fuel (1980) 59. pp 701.

238. S.K.Sobocenski. "A study of the structure of coal using oxidative degradation with trifluoro peroxy acetic acid." PhD Thesis Penn State Univ. USA. (1984).

239. T.V.Verheyen, A.G.Pandolfo, R.B.Johns and G.H.Mackey. 'Structural investigation of Australian coals VI. The effect of rank as elucidated by per trifluoroacetic acid oxidation.' Geochimica et Cosmochimica Acta. (1985). 49. pp 1603-1614.

240. T.V.Verheyen and R.B.Johns. 'Analysis of peroxy trifluoroacetic acid oxidation products from Victorian brown coal.' Anal. Chem. (1983). 55. pp 1564-1568.

241. C.G.Vernier, T.G.Squires and Chen Y.Ying. 'The fate of sulphur functional groups on oxidation with peroxytrifluoroacetic acid

242. D.H.Derbyshire. 'An oxidation involving the hydroxyl cation $(OH)^+$.' Nature (1950). 165 pp 401-402.

243. N.C.Deno, B.A.Greigger, L.A.Messer. M.D.Meyer and S.G.Stroud. 'Aromatic ring oxidation of alkylbenzenes.' Tetrahedron letters. (1977). pp 1703.

244. N.C.Deno, B.A.Greigger, A.D.Jones, W.G.Rakitsky, K.A.Smith and R.D.Minard. 'Dihydroaromatic structure of Illinois No. 6 Monterey coal.' Fuel (1980). 59. pp 694.

245. D.Dumay, G.Kirsch, R.Gruber and D.Cagniant. 'Deno's oxidation - analysis of

oxidation products from model compounds.'. Fuel. (1984). 63 pp 1544-1546.

246. L.J.Shadle and P.H.Given. 'Dependance of liquefaction behaviour on coal characterisation. Part VIII.' Report DOE/PC/40784-T6. pp 246.

247. L.J.Shadle, A.D.Jones, N.C.Deno and P.H.Given. 'Multi faceted study of a cretaceous coal with algal affinities.3. Asphaltenes from liquefaction and a comparison with some hydrogen rich Texan coals.' Fuel (1986). 65. pp 611-619.

248. P.H.Given and M.E.Peover. 'Polarographic and electrolytic reduction of the aromatic systems in solvent extracts of coals.' Fuel. (1960). 39 pp 463.

249. R.Hessey, B.M.Benjamin and J.W,Larsen. 'Deno's oxidation. Isolation of high molecular weight aliphatic material from coals and further model compound studies.' Fuel. (1982). 61 pp 1085.

250. N.C.Deno,B.A.Greigger, A.S.Jones, W.G.Rakitisky and S.G.Stroud. 'Coal structure and coal liqurefaction.' Report Elect Power Res. (1979) No. AF-960. Energy Research Abs. Abs No. 42216.

251. P.C.Painter, R.W Snyder, M.Starsinic, M.M.Coleman, D.W.Kuehn and A.Davis. 'Concerning the application of FT-IR to the study of coal: A critical asssment of band assignment and the application of spectral analysis programmes.' Applied Spectroscopy. (1981). 35 pp 475.

252. M.R.Davis, J.M.Abbott and A.F.Gaines. 'Chemical structure of tellocolinites and sporinites. ' Fuel (1985). 64 pp 1362.

253. D.D.Whitehurst. 'Organic chemistry of coal.' (1978). J.W.Larsen. (Ed).ASC Washington.

254. L.B.Alemany, D.M.Grant, R.J.Pugmire, T.D.Alger and K.W.Zilm. J.Am. Chem. Soc. (9183). 105 pp 2142.

255. N.F.Shimp, J.K.Kuhn and R.J.Helkinite. Energy Sources. (1977). 3 pp 93-109.